TOWARDS

advanced therapy guidance in the failing heart

CHEYENNE
TSENG

Towards advanced therapy guidance in the failing heart

Op weg naar geavanceerde begeleiding van therapie in het falende hart

(met een samenvatting in het Nederlands)

Proefschrift

ter verkrijging van de graad van doctor aan de Universiteit Utrecht op gezag van de rector magnificus, prof.dr. G.J. van der Zwaan, ingevolge het besluit van het college voor promoties in het openbaar te verdedigen op donderdag 24 mei 2018 des middags te 4.15 uur

door

Cheyenne Charissa Sandra Tseng

geboren op 2 maart 1987
te Amsterdam

CONTENTS

1

Introduction

Heart Failure

Heart failure (HF) is a progressive disease with a significant socio-economic impact on healthcare. This clinical syndrome is characterized by structural or functional ventricular impairment(1). Most patients with HF suffer from symptoms due to impaired function of the left ventricle (LV), typically caused by initial injury that leads to a maladaptive process of the ventricle, known as ventricular remodeling(2). Although pharmacological and non-pharmacological treatment options have significantly improved, the prevalence of patients with HF is rising(3). Clinical manifestations of HF are dyspnea, fatigue, exercise tolerance and fluid retention(1). In patients with severe symptoms of HF, intractable angina or arrhythmia's, without any alternative form of treatment and a poor prognosis, heart transplantation should be considered(4). However, an increasing mismatch between the supply and demand of donor hearts is reported(5). The scarcity in treatment options for end-stage HF patients calls for novel therapeutic approaches for this patient population. Understanding pathophysiological processes that are important in ventricular remodeling may help to unravel novel therapeutic targets and aid therapy guidance. A long-standing therapeutic aim in experimental cardiology is repair and regeneration of the damaged heart(6–11).

Cardiac regenerative therapy

Current status

Regenerative therapies for the damaged heart have been investigated vigorously in the last 15 years(6–13). The ultimate aim of cardiac regenerative medicine is to replace damaged myocardium with newly formed, functional tissue. A way to achieve this is through direct differentiation from transplanted cells into myocardial cells(14,15). A more plausible mechanism of action is the paracrine hypothesis. Different important processes for cardiac repair and regeneration like inflammation, fibrosis, metabolism and contractility may be influenced in a paracrine fashion(14). Since the existence and regenerative capacity of resident stem cells in the heart have been discovered, stimulation of these endogenous cardiac stem cells has become an additional strategy for cardiac regeneration(12,16,17). Multiple tactics to activate proliferation and transdifferentiation of endogenous cardiac stem cells have been studied. Examples of these strategies are growth factors, stem cells,

exosomes and biomaterials(18–21). From bench to bedside most experience is gained with stem cell therapy in ischemic heart disease. Cell therapy has been used in patients with an acute myocardial infarction (AMI), refractory angina pectoris and chronic ischemic HF(7,22,23). Less experience and no conclusive therapeutic efficacy exist on cell therapy for dilated cardiomyopathy(24,25). The success of cell therapy for ischemic heart disease has been significant, but debatable with regard to clinical relevance. Nonetheless results are encouraging(26,27). In patients with chronic ischemic HF cell therapy is usually injected in the myocardial wall(28). Besides existing issues with regard to optimal cell type, dose, route and frequency(29), there are two important factors that are proposed to limit the success of cell therapy, i.e. retention and delivery accuracy of therapeutics.

How to improve cell retention

With regard to retention of cells, the majority of cells after intramyocardial injection is washed out of the myocardium into the venous system within 3 heart beats(30). Not more than 10% of injected cells are found back in the heart after 4 hours regardless of the used delivery strategy(30). Furthermore, the environment that cells are transplanted in has to be considered. The hostile milieu of the ischemic and/or overloaded heart is not hospitable for cell survival and engraftment(9,29).

For optimization of retention research has focused on biomaterials as carriers of therapeutics as to reduce wash out. Different applications, e.g. gelatin microspheres, gelatin/hyaluronic acid patches and hydrogels, for sustained delivery of cells and growth factors have been reported(20,31). For clinical applicability, percutaneous delivery is preferable to more invasive delivery techniques. Therefore, biomaterials should also be catheter-compatible while gelation should occur fast once it is in contact with cardiac tissue. A very interesting biomaterial that fulfills these requirements is the ureido-pyrimidinone (UPy)-modified polyethylene glycol (PEG) hydrogel(32). Beneficial effects of UPy-gel have already been reported in combination with growth factors(20). However, retention of the hydrogel after intramyocardial injection has not yet been visualized.

A different approach to increase retention is by changing the local environment in a more favorable milieu for cells. In patients with HF this could be established by unloading of the heart. Although mechanical circulatory support is only recommended in a selected patient

population(33), in advanced HF patients who need mechanical circulatory support, additional cell therapy may improve retention and the combination might even synergistically improve efficacy(34). Another approach that might effect retention of cells is pretreatment of the local host tissue(28).

How to improve delivery accuracy of therapy

Regarding the delivery of regenerative therapies in ischemic heart disease, the target area is viable tissue in the infarct borderzone. In AMI patients cell therapy is usually infused in the coronary artery post-PCI. As patients with chronic ischemic HF often suffer from occluded coronary arteries, intramyocardial cell injection with an electromechanical mapping (EMM) system (NOGA®XP, Biosense Webster, Cordis, Johnson & Johnson, version 1.1.43) is typically used in the clinical setting. For identification of the infarct borderzone with this method, a special mapping catheter measures both electrical voltages and local linear shortening on the endocardium of the left ventricle(35). This approach appears reproducible if both unipolar and bipolar maps are used(36). The NOGA method also seems to be able to accurately differentiate between totally infarcted and viable tissue, but not to discriminate between the different degrees of infarct transmurality(37). As this region is very important in treatment planning, implementation of detailed and accurate viability assessment is imperative.

The second subject of regenerative therapy that needs improvement is the delivery accuracy. Although EMM seems to be able to accurately distinguish between infarcted and viable tissue, a mismatch between EMM and the infarct borderzone assessed by late gadolinium enhanced (LGE)-MRI has been reported(37). Feasibility of additional MRI, the gold standard for infarct assessment, has been shown for image-guided intramyocardial injections(38). Whether targeting of the infarct borderzone is substantially more accurate with additional LGE-MRI and leads to improved functional outcome needs to be investigated. LGE-MRI could benefit accuracy of treatment planning. In order to prevent data loss and radiation, performing the injection procedure in the MR environment would be the ultimate goal. Fundamental hurdles, e.g. compatible catheters, have to be overcome for this aim. Feasibility of such a state-of-the-art injection technique has to be evaluated.

Figure 1. The route towards advanced therapy guidance and response assessment
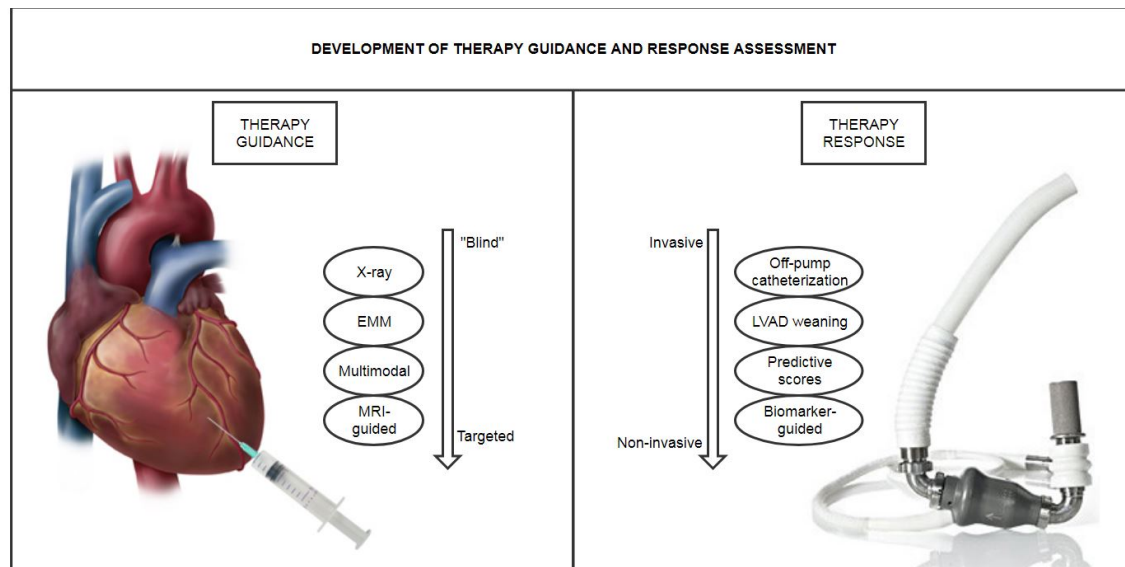
EMM, Electromechanical mapping; LVAD, left ventricular assist device

Exploring opportunities in end-stage heart failure

Cardiac recovery in the LVAD population

Besides the exploration of new HF therapies, the shortage of donor hearts has also led to an increased use of left ventricular assist devices (LVADs)(39,40). These mechanical pumps warrant circulation by taking over the left ventricular function and can thereby act as a bridge to transplantation in patients that are waiting for a donor heart. The introduction of LVADs in clinical practice has dramatically improved survival and quality of life in end-stage HF patients(41). While LVADs were initially used as a bridge to transplantation, LVADs are currently also widely used as destination (permanent) therapy (DT) for patients ineligible for heart transplantation(40,42). However, long-term complications caused by LVADs still hamper mechanical circulatory support as true replacement for heart transplantation(40,41). As the duration of LVAD support increased with the expanding waiting list, it became evident that in some patients reverse remodeling of the LV occurred during unloading with an LVAD. In some patients this manifested in cardiac recovery to the extent that the pump could be successfully removed(43–46). Although sustained cardiac recovery does not occur frequently(41,43,47–51), the phenomenon of reverse remodeling and recovery has been researched extensively in LVAD patients(46,48–50,52–56). With regard to patient characteristics, the majority of patients in which myocardial recovery occurs during LV unloading suffer from non-ischemic cardiomyopathy. In particular those

with an acute onset of HF symptoms and potentially reversible causes of HF (i.e. acute myocarditis and peripartum cardiomyopathy) have the highest recovery rates(43,57). In patients with chronic ischemic HF cardiac recovery occurs the least(46,52).

How to improve the assessment of cardiac recovery

Clinical factors that are related to cardiac recovery have been described, as well as criteria for LVAD explant(53,58). Nonetheless, the decision to explant is still challenging. The unpredictability of recurrent HF and the lack of clinical markers to select candidates for successful pump removal restrict clinical decision-making(48,55). A predictive score system (like I-CARS) may help to predict individual odds of cardiac recovery(59). However, myocardial changes during unloading do not only occur in functional and clinical parameters, but also on cellular, molecular and genomic level(50,53,55,60–62). Studies addressing the connection between clinical and biological outcomes are indispensable to gain mechanistic insights in the phenomenon of (sustained) recovery(53). The impact of LVAD support on neurohormones, cytokines, apoptosis, extracellular matrix, calcium cycling and other properties has been reported(49). Conversely, the exact role of these different characteristics in the process of reverse remodeling and recovery is not yet established(49,50). There are signs that recovery can be stimulated actively with a specific pharmacological regiment(63). Prospective studies that include protocols to monitor and stimulate clinical improvement are essential in this regard. In addition, novel methods that are suitable to recognize, monitor and predict sustained cardiac recovery should be developed to identify the appropriate individuals for pump removal(48).

How to improve the prediction of cardiac recovery

For clinical practice, non-invasive, fast and easy methods to predict cardiac recovery are required. Biomarkers might be valuable in this regard since an ideal biomarker reflects abnormal physiology and is prognostic and usable to guide and monitor therapy(64). In addition, most biomarkers can be simply measured in serum or plasma. In this way biomarkers may help to monitor and to predict reverse remodeling and recovery in individual patients and thereby personalize medical treatment. There are some attractive biomarkers that might be able to predict reverse remodeling and cardiac recovery, for

example BNP, galactin-3, sST2, BMP-1 and osteopontin(64–68). Existing data, however, are not (yet) sufficient for recommendations in clinical practice with regard to predicting reverse remodeling(68). Biomarkers of specific interest in LVAD patients include those that represent processes like inflammation, fibrosis and myocardial stress(65,67,68). Osteopontin and GDF-15 are both involved in the process of fibrosis, and expression and plasma levels have been assessed in LVAD patients(69,70). Osteopontin is suggested to be a valuable tool in the determination of cardiac recovery while GDF-15 does not seem to be able to identify those patients(69,70). With regard to more cardio-specific markers that fulfill the criteria of a good biomarker, soluble ST2 (sST2) is of interest as it is involved in inflammation and fibrosis(71). Many studies have investigated the prognostic value of this novel biomarker. In summary, these studies show that increased sST2 is associated with poor outcome in both acute and chronic heart failure(72,73). Besides predicting all-cause mortality in heart failure, sST2 also seems to predict reverse remodeling after acute myocardial infarction, hospitalizations for worsening heart failure and cardiovascular events(74–76). Also, the prognostic value of sST2 is not related to kidney function, in contrast to for example BNP(77). Abovementioned results led to the adaptation of sST2 by the ACCF/AHA guidelines for risk prediction in acute and chronic heart failure(1). In contrast to acute HF and the NYHA I-III population, not so much is known about sST2 in end stage HF. Also, the value of sST2 as a biomarker to benefit clinical decision-making needs to be explored.

Thesis outline:

This thesis, "Towards advanced therapy guidance in the failing heart", presents and discusses the pathway from limitations in cardiac regenerative therapies and mechanical circulatory support towards advanced and guided approaches to improve chronic heart failure therapy (**Figure 1**).

Part one illustrates the road from current to novel application strategies for cardiac regenerative therapy with a focus on improving retention and optimizing therapeutic delivery. **Chapter 2** deliberates on stem cell therapy for the injured heart so far with the possibilities and limitations. The results of a clinical study with autologous bone marrow mononuclear cells in chronic HF patients are presented and discussed in **chapter 3**. The

delivery technique for intramyocardial cell injection (NOGA) that is used in this chapter is elucidated (and visualized) in **chapter 4**. Here, intramyocardial injections are performed with a supramolecular hydrogel to increase retention. In **chapter 5** the supramolecular hydrogel is chemically bound to a MR-visible molecule (DOTA) to gain insights in retention using magnetic resonance imaging. This chapter describes the synthesis and validation of the novel hydrogel. The feasibility of MR-guided intramyocardial injections of the newly developed hydrogel is described in a first-in-pig study in **chapter 6**.

In part two of this thesis opportunities towards biomarker-guided therapy are explored in the failing heart. The LVAD population is the backbone of this part as these patients offer profound research possibilities in both the failing heart in the end-stage as well as in the reverse remodeled heart. **Chapter 7** reviews the combination of regenerative therapies with LVAD as a potential new treatment strategy for HF. A promising biomarker of cardiac fibrosis, soluble ST2, in end-stage HF patients is the focus of **chapter 8 and 9**. In **chapter 8** the association of sST2 and clinical factors in end-stage HF patients before LVAD support are studied. The response of sST2 levels to left ventricular unloading is also evaluated in **chapter 8**. In the final chapter of this thesis, **chapter 9,** the relation between the IL-33/ST2 pathway and fibrosis is studied by quantification of fibrosis and mRNA expression of the IL-33/ST2 pathway and pro-fibrotic markers in cardiac tissue.

References

1. Yancy CW, Jessup M, Bozkurt B, Butler J, Casey DE, Drazner MH, et al. 2013 ACCF/AHA guideline for the management of heart failure: a report of the American College of Cardiology Foundation/American Heart Association Task Force on Practice Guidelines. J Am Coll Cardiol. 2013;62(16):e147-239.

2. Mann DL. Mechanisms and Models in Heart Failure : A Combinatorial Approach. Circulation. 1999 Aug 31;100(9):999–1008.

3. Koopman C, Van Dis I, Bots M, Vaartjes I. Feiten en cijfers Hartfalen. Vol. Juni, Nederlandse Hartstichting. 2012.

4. de Jonge N, Kirkels JH, Klöpping C, Lahpor JR, Caliskan K, Maat a PWM, et al. Guidelines for heart transplantation. Neth Heart J. 2008 Jan;16(3):79–87.

5. Foundation EI. Eurotransplant Annual Report 2015. 2015.

6. Orlic D, Kajstura J, Chimenti S, Bodine DM, Leri A, Anversa P. Bone marrow stem cells regenerate infarcted myocardium. Nature. 2001;410:701–5.

7. Dimmeler S, Burchfield J, Zeiher AM. Cell-based therapy of myocardial infarction. Arterioscler Thromb Vasc Biol. 2008;28(2):208–16.

8. Janssens S. Stem cells in the treatment of heart disease. Annu Rev Med. 2010 Jan;61:287–300.

9. Menasché P. Cardiac cell therapy: lessons from clinical trials. J Mol Cell Cardiol. 2011;50(2):258–65.

10. Koudstaal S. Stamceltherapie voor ischemische hartziekten. Cordiaal. 2013;2:40–4.

11. Dimmeler S, Zeiher AM, Schneider MD. Review series Unchain my heart : the scientific foundations of cardiac repair. J Clin Invest. 2005;115(3):572–83.

12. Laflamme MA, Murry CE. Heart regeneration. Nature. 2011;473(7347):326–35.

13. Doppler SA, Deutsch M-A, Serpooshan V, Li G, Dzilic E, Lange R, et al. Mammalian Heart Regeneration. Circ Res. 2017;120(4):630–2.

14. Gnecchi M, Zhang Z, Ni A, Dzau VJ. Paracrine mechanisms in adult stem cell signaling and therapy. Circ Res. 2008;103(11):1204–19.

15. Chimenti I, Smith RR, Li TS, Gerstenblith G, Messina E, Giacomello A, et al. Relative roles of direct regeneration versus paracrine effects of human cardiosphere-derived cells transplanted into infarcted mice. Circ Res. 2010;106(5):971–80.

16. Bergmann O, Bhardwaj RD, Bernard S, Zdunek S, Barnabé-Heider F, Walsh S, et al. Evidence for cardiomyocyte renewal in humans. Science (80-). 2009;324(5923):98–102.

17. Ellison GM, Nadal-Ginard B, Torella D. Optimizing cardiac repair and regeneration through activation of the endogenous cardiac stem cell compartment. J Cardiovasc Transl Res. 2012;5(5):667–77.

18. Ellison GM, Torella D, Dellegrottaglie S, Perez-Martinez C, Perez de Prado A, Vicinanza C, et al. Endogenous cardiac stem cell activation by insulin-like growth factor-1/hepatocyte growth factor intracoronary injection fosters survival and regeneration of the infarcted pig heart. J Am Coll Cardiol. 2011;58(9):977–86.

19. Vrijsen KR, Sluijter JPG, Schuchardt MWL, van Balkom BWM, Noort WA, Chamuleau SAJ, et al. Cardiomyocyte progenitor cell-derived exosomes stimulate migration of endothelial cells. J Cell Mol Med. 2010;14(5):1064–70.

20. Koudstaal S, Bastings MMC, Feyen DA, Waring CD, van Slochteren FJ, Dankers PYW, et al. Sustained delivery of insulin-like growth factor-1/hepatocyte growth factor stimulates endogenous cardiac repair in the chronic infarcted pig heart. J Cardiovasc Transl Res. 2014;7(2):232–41.

21. Sahoo S, Losordo DW. Exosomes and cardiac repair after myocardial infarction. Circ Res. 2014 Jan 17;114(2):333–44.

22. Clifford DM, Fisher SA, Brunskill SJ, Doree C, Mathur A, Watt S, et al. Stem cell treatment for acute myocardial

infarction (Review). Cochrane database Syst Rev. 2012;(2).

23. Saramipoor Behbahan I, Keating A, Gale RP. Bone Marrow Therapies for Chronic Heart Disease. Stem Cells. 2015;33(11):3212–27.

24. Gho JMIH, Kummeling GJM, Koudstaal S, Jansen Of Lorkeers SJ, Doevendans PA, Asselbergs FW, et al. Cell therapy, a novel remedy for dilated cardiomyopathy? A systematic review. J Card Fail. 2013;19(7):494–502.

25. Marquis-Gravel G, Stevens L-M, Mansour S, Avram R, Noiseux N. Stem Cell Therapy for the Treatment of Nonischemic Cardiomyopathy: A Systematic Review of the Literature and Meta-analysis of Randomized Controlled Trials. Can J Cardiol. 2014;

26. Afzal MR, Samanta A, Shah ZI, Jeevanantham V, Abdel-Latif A, Zuba-Surma EK, et al. Adult Bone Marrow Cell Therapy for Ischemic Heart Disease: Evidence and Insights from Randomized Controlled Trials. Circ Res. 2015;117(6):558–75.

27. Fisher SA, Doree C, Mathur A, Martin-Rendon E. Meta-Analysis of Cell Therapy Trials for Patients with Heart Failure - An Update. Circ Res. 2015;116:1361–77.

28. Sanganalmath SK, Bolli R. Cell therapy for heart failure: a comprehensive overview of experimental and clinical studies, current challenges, and future directions. Circ Res. 2013;113(6):810–34.

29. Wu R, Hu X, Wang J. Concise Review: Optimized Strategies for Stem Cell-based Therapy in Myocardial Repair: Clinical Translatability and Potential Limitation. Stem Cells. 2018

30. van den Akker F, Feyen D a M, van den Hoogen P, van Laake LW, van Eeuwijk ECM, Hoefer I, et al. Intramyocardial stem cell injection: go(ne) with the flow. Eur Heart J. 2016;ehw056.

31. Gaetani R, Feyen DAM, Verhage V, Slaats R, Messina E, Christman KL, et al. Epicardial application of cardiac progenitor cells in a 3D-printed gelatin/hyaluronic acid patch preserves cardiac function after myocardial infarction. Biomaterials. 2015;61:339–48.

32. Bastings MMC, Koudstaal S, Kieltyka RE, Nakano Y, Pape ACH, Feyen DAM, et al. A fast pH-switchable and self-healing supramolecular hydrogel carrier for guided, local catheter injection in the infarcted myocardium. Adv Healthc Mater. 2014;3(1):70–8.

33. McMurray JJ V, Adamopoulos S, Anker SD, Auricchio A, Böhm M, Dickstein K, et al. ESC guidelines for the diagnosis and treatment of acute and chronic heart failure 2012: The Task Force for the Diagnosis and Treatment of Acute and Chronic Heart Failure 2012 of the European Society of Cardiology. Developed in collaboration with the Heart. Eur J Heart Fail. 2012 Aug;14(8):803–69.

34. Ibrahim M, Rao C, Athanasiou T, Yacoub MH, Terracciano CM. Mechanical unloading and cell therapy have a synergistic role in the recovery and regeneration of the failing heart. Eur J Cardiothorac Surg. 2012 Aug;42(2):312–8.

35. Gyöngyösi M, Dib N. Diagnostic and prognostic value of 3D NOGA mapping in ischemic heart disease. Nat Rev Cardiol. 2011;8(7):393–404.

36. Pavo N, Jakab A, Emmert MY, Strebinger G, Wolint P, Zimmermann M, et al. Comparison of NOGA Endocardial Mapping and Cardiac Magnetic Resonance Imaging for Determining Infarct Size and Infarct Transmurality for Intramyocardial Injection Therapy Using Experimental Data. PLoS One. 2014;9(11):e113245.

37. van Slochteren FJ, van Es R, Gyöngyösi M, van der Spoel TIG, Koudstaal S, Leiner T, et al. Three dimensional fusion of electromechanical mapping and magnetic resonance imaging for real-time navigation of intramyocardial cell injections in a porcine model of chronic myocardial infarction. Int J Cardiovasc Imaging. 2016;32(5):833–43.

38. van Slochteren FJ, van Es R, Koudstaal S, van der Spoel TIG, Sluijter JPG, Verbree J, et al. Multimodality infarct identification for optimal image-guided intramyocardial cell injections. Netherlands Hear J. 2014;22(11):493–500.

39.   Lahpor J, Khaghani A, Hetzer R, Pavie A, Friedrich I, Sander K, et al. European results with a continuous-flow ventricular assist device for advanced heart-failure patients. Eur J cardio-thoracic Surg. 2010;37(2):357–61.

40.   Kirklin JK, Cantor R, Mohacsi P, Gummert J, De By T, Hannan MM, et al. First Annual IMACS Report: A global International Society for Heart and Lung Transplantation Registry for Mechanical Circulatory Support. J Hear lung Transplant. 2016;35(4):407–12.

41.   Hunt SA, Rose EA. The REMATCH trial: Long-term use of a left ventricular assist device for end-stage heart failure. J Card Fail. 2002;8(2):59–60.

42.   Birks EJ. A Changing Trend Toward Destination Therapy. Texas Hear Insitute J. 2011;38(5):552–4.

43.   Simon MA, Kormos RL, Murali S, Nair P, Heffernan M, Gorcsan J, et al. Myocardial recovery using ventricular assist devices: prevalence, clinical characteristics, and outcomes. Circulation. 2005 Aug 30;112(9 Suppl):I32-6.

44.   Birks EJ, Tansley PD, Hardy J, George RS, Bowles CT, Burke M, et al. Left ventricular assist device and drug therapy for the reversal of heart failure. N Engl J Med. 2006 Nov;355(18):1873–84.

45.   Butler CR, Jugdutt BI. The paradox of left ventricular assist device unloading and myocardial recovery in end-stage dilated cardiomyopathy: Implications for heart failure in the elderly. Heart Fail Rev. 2012;17(4–5):615–33.

46.   Birks EJ, George RS, Firouzi A, Wright G, Bahrami T, Yacoub MH, et al. Long-term outcomes of patients bridged to recovery versus patients bridged to transplantation. J Thorac Cardiovasc Surg. 2012;144(1):190–6.

47.   Lee SH, Doliba N, Osbakken M, Oz M, Mancini D. Improvement of myocardial mitochondrial function after hemodynamic support with left ventricular assist devices in patients with heart failure. J Thorac Cardiovasc Surg. 1998;116(2):344–9.

48.   Simon MA, Primack BA, Teuteberg J, Kormos RL, Bermudez C, Toyoda Y, et al. Left ventricular remodeling and myocardial recovery on mechanical circulatory support. J Card Fail. 2010;16(2):99–105.

49.   Burkhoff D, Klotz S, Mancini DM. LVAD-induced reverse remodeling: basic and clinical implications for myocardial recovery. J Card Fail. 2006;12(3):227–39.

50.   Klotz S, Jan Danser a H, Burkhoff D. Impact of left ventricular assist device (LVAD) support on the cardiac reverse remodeling process. Prog Biophys Mol Biol. 2008;97(2–3):479–96.

51.   Kato TS, Chokshi A, Singh P, Khawaja T, Cheema F, Akashi H, et al. Effects of continuous-flow versus pulsatile-flow left ventricular assist devices on myocardial unloading and remodeling. Circ Heart Fail. 2011 Sep;4(5):546–53.

52.   Maybaum S, Mancini D, Xydas S, Starling RC, Aaronson K, Pagani FD, et al. Cardiac improvement during mechanical circulatory support: a prospective multicenter study of the LVAD Working Group. Circulation. 2007;115(19):2497–505.

53.   Drakos SG, Kfoury AG, Stehlik J, Craig H. Bridge to Recovery: Understanding the Disconnect Between Clinical and Biological Outcomes. Circulation. 2012;126(2):230–41.

54.   Drakos SG, Wever-pinzon O, Selzman CH, Gilbert M, Alharethi R, Reid BB, et al. Magnitude and Time Course of Changes Induced by Continuous-Flow Left Ventricular Assist Device Unloading in Chronic Heart Failure: Insights into Cardiac Recovery. J Am Coll Cardiol. 2013;61(19):1–21.

55.   Miyagawa S, Toda K, Nakamura T, Yoshikawa Y, Fukushima S, Saito S, et al. Building a bridge to recovery: the pathophysiology of LVAD-induced reverse modeling in heart failure. Surg Today. 2015;

56.   Marinescu KK, Uriel N, Mann DL, Burkhoff D. Left ventricula assist device-induced reverse remodeling: it's not just about myocardial recovery. Expert Rev Med Devices. 2017;14(1):15–26.

57.   Mancini DM, Beniaminovitz A, Levin H, Catanese K, Flannery M, DiTullio M, et al. Low Incidence of Myocardial Recovery After Left Ventricular Assist Device Implantation in Patients With Chronic Heart Failure. Circulation. 1998 Dec 1;98(22):2383–9.

20

58. Dandel M, Weng Y, Siniawski H, Stepanenko A, Krabatsch T, Potapov E, et al. Heart failure reversal by ventricular unloading in patients with chronic cardiomyopathy: criteria for weaning from ventricular assist devices. Eur Heart J. 2011;32(9):1148–60.

59. Wever-Pinzon O, Drakos SG, McKellar SH, Horne BD, Caine WT, Kfoury AG, et al. Cardiac Recovery During Long-Term Left Ventricular Assist Device Support. J Am Coll Cardiol. 2016;68(14):1540–53.

60. Hall JL, Birks EJ, Grindle S, Cullen ME, Barton PJ, Rider JE, et al. Molecular signature of recovery following combination left ventricular assist device (LVAD) support and pharmacologic therapy. Eur Heart J. 2007;28(5):613–27.

61. Ibrahim M, Terracciano C, Yacoub MH. Can bridge to recovery help to reveal the secrets of the failing heart? Curr Cardiol Rep. 2012 Aug;14(4):392–6.

62. Dandel M, Hetzer R. Myocardial recovery during mechanical circulatory support : cellular, molecular, genomic and organ levels. Hear lung Vessel. 2015;7(2):110–20.

63. Birks EJ, George RS, Hedger M, Bahrami T, Wilton P, Bowles CT, et al. Reversal of severe heart failure with a continuous-flow left ventricular assist device and pharmacological therapy: a prospective study. Circulation. 2011;123(4):381–90.

64. Wettersten N, Maisel AS. Biomarkers for Heart Failure : An Update for Practitioners of Internal Medicine. Am J Med. 2016;

65. Milting H, Ellinghaus P, Seewald M, Cakar H, Bohms B, Kassner A, et al. Plasma biomarkers of myocardial fibrosis and remodeling in terminal heart failure patients supported by mechanical circulatory support devices. J Heart Lung Transplant. 2008;27(6):589–96.

66. Boer RA De, Daniels LB, Maisel AS, Januzzi Jr JL. State of the Art : Newer biomarkers in heart failure. Eur J Heart Fail. 2015;17:559–69.

67. Ahmad T, Wang T, O'Brien EC, Samsky MD, Pura J a., Lokhnygina Y, et al. Effects of Left Ventricular Assist Device Support on Biomarkers of Cardiovascular Stress, Fibrosis, Fluid Homeostasis, Inflammation, and Renal Injury. JACC Hear Fail. 2015;3(1):30–9.

68. Motiwala SR, Gaggin HK. Biomarkers to Predict Reverse Remodeling and Myocardial Recovery in Heart Failure. Curr Heart Fail Rep. 2016;13(5):207–18.

69. Schipper MEI, Scheenstra MR, van Kuik J, van Wichen DF, van der Weide P, Dullens HFJ, et al. Osteopontin: a potential biomarker for heart failure and reverse remodeling after left ventricular assist device support. J Heart Lung Transplant. 2011;30(7):805–10.

70. Lok SI, Winkens B, Goldschmeding R, van Geffen AJP, Nous FM a, van Kuik J, et al. Circulating growth differentiation factor-15 correlates with myocardial fibrosis in patients with non-ischaemic dilated cardiomyopathy and decreases rapidly after left ventricular assist device support. Eur J Heart Fail. 2012;14(11):1249–56.

71. Pascual-Figal DA, Januzzi JL. The biology of ST2: The international ST2 consensus panel. Am J Cardiol. 2015;115(7):3B–7B.

72. Dieplinger B, Mueller T. Soluble ST2 in heart failure. Clin Chim Acta. 2015;443:57–70.

73. McCarthy CP, Januzzi JL. Soluble ST2 in Heart Failure. Hear Fail Clin. 2018;14(1):41–8.

74. Weir RAP, Miller AM, Murphy GEJ, Clements S, Steedman T, Connell JMC, et al. Serum Soluble ST2. A Potential Novel Mediator in Left Ventricular and Infarct Remodeling After Acute Myocardial Infarction. J Am Coll Cardiol. 2010;55(3):243–50.

75. Januzzi JL, Pascual-Figal D, Daniels LB. ST2 Testing for Chronic Heart Failure Therapy Monitoring: The International

ST2 Consensus Panel. Am J Cardiol. 2015;115(7):70B–75B.

76. Bayes-Genis A, Nunez J, Lupon J. Soluble ST2 for prognosis and monitoring in failure: The new gold standard? JACC. 2017;70(19):2389–92.

77. Bayes-Genis A, Zamora E, de Antonio M, Galán A, Vila J, Urrutia A, et al. Soluble ST2 serum concentration and renal function in heart failure. J Card Fail. 2013;19(11):768–75.
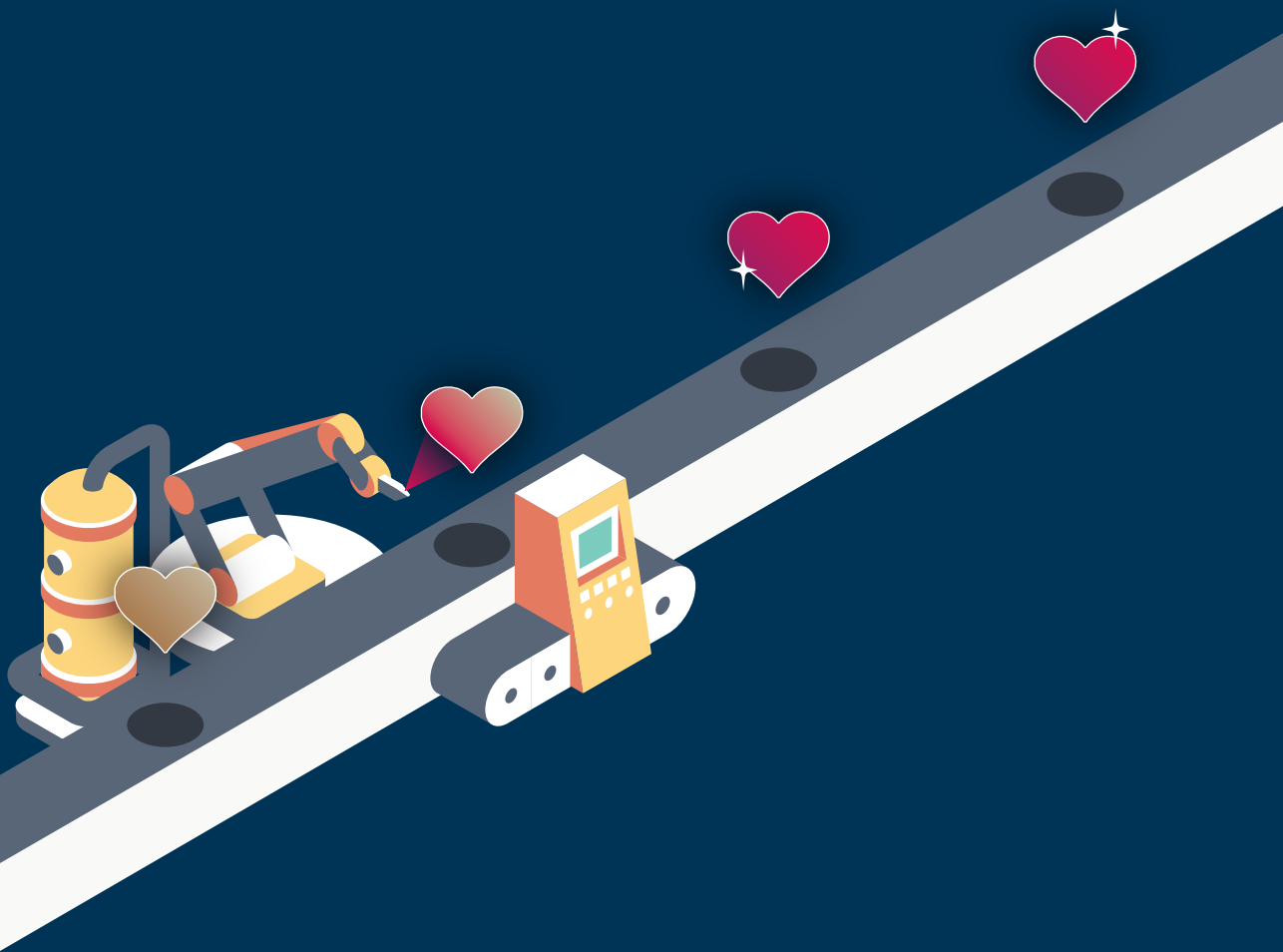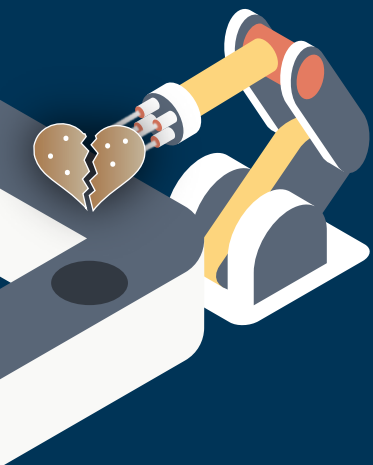
PART ONE

IMPROVING CARDIAC REGENERATIVE THERAPY

2

Stem cell therapy for the damaged heart

M. van der Naald*, C.C.S. Tseng*, P.A. Doevendans, S.A.J. Chamuleau

* These authors contributed equally to this work

Abstract

Current therapies for ischemic heart failure are not sufficient. Regenerative therapy is a promising strategy that has rapidly developed into a clinical phase. Although the exact mechanism of action is not entirely understood, clinical results show a significant effect of stem cells in ischemic heart diseases. At this moment there is no consensus on the clinical relevance of stem cell therapy. In this review the rationale for stem cell therapy is discussed. We will focus on autologous bone marrow cells in clinical setting. Finally, we will give an overview of new developments that will optimize future cell therapy.

Introduction

Ischemic heart disease is one of the main causes of mortality in the Netherlands. More than 5.000 people suffered from a fatal acute myocardial infarction (AMI) in the Netherlands in 2014 and another 3500 patients died of other coronary vessel diseases, such as ischemic heart failure (IHF) and angina pectoris (AP). Mortality of AMI has decreased the last decades(1). This trend is seen internationally and can be explained by improved prevention and treatment, partly due to the introduction of primary coronary interventions (PCI) and stents(2). However, the heart failure population is growing progressively(3). The only curative treatment for end stage heart failure is heart transplantation, but the demand of donor hearts is exceeding the availability. Therefore, the development of novel therapies is essential. Stimulating cardiac regeneration is a potential strategy. In this review we discuss the rationale of cell therapy for the damaged heart and clinical experience, focused on bone marrow-derived cells.

Rationale of stem cell therapy

In the 1990s differentiative plasticity of specialized cells has been shown. These studies mainly concern bone marrow cells. Initially, the capacity of bone marrow cells to migrate to the brain and remain in the parenchyma was demonstrated(4). Circulating extrahepatic stem cells, probably derived from bone marrow, were also found to differentiate to de novo hepatocytes and cholangiocytes(5). Moreover, bone marrow-derived progenitor cells were shown to migrate to degenerated muscle and produce fully differentiated muscle fibers(6). Hereafter, it was hypothesized that bone marrow cells might migrate to the myocardium and differentiate to new cardiomyocytes. To examine this hypothesis, Lin$^-$ c-kit$^+$- bone marrow cells of transgenic mice were injected in the border of infarcted myocardium. The study demonstrated 50% newly formed myocardium in 40% of mice. This result was explained by transdifferentiation of bone marrow cells into de novo myocardium(7). However, other research groups have not been able to demonstrate transdifferentiation of transplanted bone marrow cells in an ischemic mouse model(8,9).

In the human heart, proliferation of cardiomyocytes was considered impossible, since the heart was assumed to be a postmitotic organ. This concept was recently questioned by intruiging research. In the zebrafish heart, total regeneration based on increased cardiomyocyte proliferation is seen (from 3% in the healthy heart to maximum 34% after

injury) after 20% resection of the ventricle(10). In another study, regeneration in the heart was demonstrated by determining the age of cardiomyocytes. The basis of this analysis was ^{14}C integration in DNA, since the atmospherical ^{14}C concentration suddenly rose and exponentially fell due to nuclear atom bomb tests during the Cold War. Cell turnover of cardiomyocytes was demonstrated, annualy 1% at the age of 25 and 0.45% at the age of 75(11). It is not known whether the cell renewal was caused by proliferation of cardiomyocytes or differentiation of stem cells into cardiomyocytes.

An alternative mechanism of action of stem cells is the paracrine hypothesis. Stem cells produce cytokines and growth factors that can lead to neovascularisation, decreased apoptosis and inflammation, improved metabolism, increased contractility and reduced remodeling. This hypothesis is supported by similar effects of conditioned medium of stem cells compared to cell therapy(12).

Translational studies

The promising hypothesis of cardiac regeneration led to a rapid translation to the clinic. Many developments in the preclinical setting were directly translated to clinical studies. In 2001 formation of de novo cardiomycytes was described in a mouse model and in 2002 the first clinical trial with mononucleair bone marrow cells was published(7,13). Meanwhile, various cell types have been tested preclinically for their capacity of repairing and regenerating the damaged heart. The majority of large animal studies has been performed in pigs due to the large anatomical similarity to the human coronary arteries. A significant effect of cell therapy is seen in large animals (n=1.415)(14). Left ventricular ejection fraction (LVEF) (the amount of blood pumped out per beat) increases with 8.3%. This is a functional parameter for the pump function of the heart that is use in clinical care with an important prognostic value.

Table 1. Clinical trials in the Netherlands

Study	Cell	Patient	Administration	Primary endpoint	Status
Registry	BM-MNC	AP	IM	Perfusion	Enrolling
AMICI	allogeneic MSC	AMI	IC	Safety & feasibility	Enrolling
BAMI	BM-MNC	AMI	IC	Mortality	Starts 2016
REPEAT	BM-MNC	IHF	IC	Mortality	Starts 2016
SCIENCE	allogeneic MSC	IHF	IM	LV systolic volume	Expected 2016

BM-MNC, bone marrow mononuclear cell; MSC, mesenchymal stem cell; AMI, acute myocardial infarction; HF, heart failure; IHF, ischemisch heart failure; AP, angina pectoris; IC, intracoronary; IM, intramyocardial; LV, left ventricle.

Clinical trials

More than 50 clinical studies have been performed in which over 2.600 patients have been treated. Many studies did not have enough "power" to demonstrate a reduction in mortality as an endpoint. Meta-analyses do not show an important mortality reduction(15). A more frequently used endpoint is LVEF. The most recent systematic review and meta-analysis of randomized clinical trials with bone marrow cells for ischemic heart disease shows an increase in ejection fraction (2.92%), smaller infarct size (2.25%) and decreased left ventricular end-systolic volume (LVESV) (6.37ml) compared to standard therapy(16). Although the reported differences are statistically significant, clinical relevance varies. Some studies show a relevant improvement in exercise tolerance and quality of life, while other studies do not confirm this. Consequently, there is no consensus on the value of stem cell therapy.

The effect size of primary studies varies a lot. This finding cannot be explained by the diversity in patient populations (AMI, chronic IHF and AP). A possible explanation is the variation in cell type, cell treatment protocol and administration route. No consensus exists on the best strategy. An overview of clinical trials in the Netherlands is summarized in **Table 1**.

Cell type

Bone marrow

The most frequently used cells in clinical setting are the undifferentiated mononuclear bone marrow cells (BM-MNCs), amongst others consisting of hematopoietic, mesenchymal and endothelial stem- and progenitor cells. Other cell types that have been used for clinical studies are flow cytometry selected CD34^{+} (hematopoietic) and CD133^{+} (hematopoietic and

endothelial) cell populations(17). Mesenchymal stromal cells (MSCs), selected (by attachment to plastic) from the mononuclear fraction and then cultured, have been examined to a lesser degree in clinical setting(17,18). MSCs are of interested due to their strong paracrine effects(19). A 6.2% increase in LVEF is reported in a clinical study with heart failure patients(18). G-CSF ('granulocyte colony stimulating factor') is a routine therapy to mobilize stem cells for transplantation from peripheral blood. No significant functional improvement is seen after G-CSF-treatment in AMI patients(20).

Adipose tissue

Stem cells can also be isolated from other tissues. Limited results are available concerning adiposed tissue-derived cells. Improvements in wall motions, but not in LVEF, have been reported(21).

Heart

The discovery of endogenous cardiac stem cells, that have the potential to differentiate into cardiomyocytes, gave rise to a novel therapeutic aim: stimulating regeneration through already existing cardiac stem cells(22). These c-kit[+] endogenous stem cells were isolated from the right atrial appendage and administered as autologous therapy after expansion in the SCIPIO trial(23). Cardiosphere-derived cells (CDCs) were used in the CADUCEUS trial(24). Both studies were phase 1/2a trials showing feasibility and safety.

Autologous versus allogeneic

Quality of stem cells is hypothesized to be influenced by cardiovascular risk factors and chronic disease. Allogeneic stem cells might benefit treatment. In addition, allogeneic cells can be used 'off-the-shelf' in an acute situation. MSCs can be used as an allogeneic product without a immune reaction. The difference between autologous and allogeneic cells has not been clinically investigated properly(25). No difference in efficacy is seen in large animals(14).

Cell treatment

Various methods of cell treatment have been applied in clinical trials. Different density gradient media, Ficoll or Lymphoprep, are used for cell isolation. Furthermore, washing

media, e.g. NaCl-heparin-plasma or phosphate buffer, vary. A couple of research groups have applied different protocols in the same cell population. It is unknown which protocol leads to the most optimal results(26).

Administration method

Multiple techniques to transplant cells into the heart exist. In this paragraph we will focus on the most clinically relevant methods (**Figure 1**).

Epicardial injection

The epicardial technique (**Figure 1A**) is the gold standard for cell application since injections in the target area take place under direct visualization. This approach is only used in combination with another cardiac surgery in clinical setting, as an open chest is necessary for this route.

Figure 1. Adminstration methods

A) epicardial, *B) intracoronary,* *C) intramyocardial*
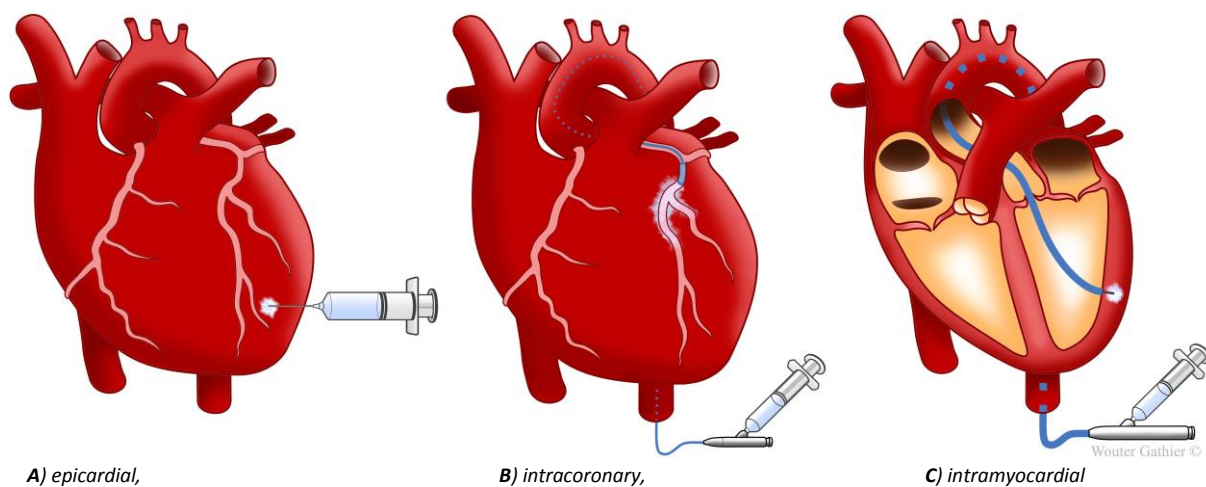
Intracoronary infusion

During a heart catheterization cells can be infused in a coronary artery through the central lumen of a balloon catheter (**Figure 1B**). This method is especially suitable for cell therapy after an AMI, and can be performed right after the percutaneous coronary intervention (PCI). Another advantage of this approach is that is concerns a well-known technique for interventional cardiologists. The main disadvantage of this method is that is not applicable in case of occluded coronary arteries(27).

Intramyocardial injection

For this percutaneous injection method (**Figure 1C**) an electromechanical mapping system (NOGA, Biosense Webster) is most frequently used. This means both electrical and mechanical activity of the left ventricle is measured in the endocardium with a dedicated catheter and a 3D-model of the endocard is made. With this system the target area for injections can be defined accurately and can thereafter be used to navigate an injection catheter to the target area and finally injection. This application route can also be used in occluded coronary arteries. However, this procedure is time consuming, expensive and demands specific expertise(27).

Clues for the future

Potential cells

As described earlier, multipotent cells (BM- and cardiac derived) have not been able to truly regenerate the human heart. For real regeneration pluripotent cells theoretically propose a better possibility than the so far used multipotent stem cells (see Table 2). Pluripotent stem cells have the property of differentiating to cells from all germ layers (ecto-, meso- and endoderm). With that that have the potential to regenerate the heart, but also to potentially form teratomas. Moreover, functional properties of newly formed cardiomyocytes are unknown(28). A new strategy of improving the effect of cell therapy is to combine different cell types (NCT02501881, NCT02503280). There is also research performed on repeated cell administrations (NCT01693042).

Cell-less therapy

In combination with the paracrine hypothesis, various experimental regenerative strategies with only cytokines are possible; "cell-less therapy". Examples are growth factors (IGF-1/HGF) and exosomes. Gene therapy that influences cardiogenic activity, like micro-RNA and follistatin-like 1 (FSTL-1), is studied in striving true regeneration. These therapies are promising in preclinical research, but not yet clinically applicable due to unknown systemic effect(29,30).

Optimizing cell retention

Although the epicardial injection method is the reference for cell transplantation, efficiency with this method varies considerably. The intramyocardial and intracoronary method are comparable with regard to cell retention(31). Less than 4% of cells is found back in the heart after an hour of administration(32). Hence, the success of cardiac cell therapy (and other regenerative therapies) is importantly limited by insufficient retention and survival of cells. The use of biomaterials, especially hydrogels, is an approach to stimulate cell retention. While translation to clinical setting is ongoing, results in small and large animals with several hydrogels (fibrin, gelatin, hyaluronic acid, poly ethylene glycol (PEG)) are promising(33,34). For example, in a large animal model of chronic myocardial infarction a better functional effect was seen after treatment with growth factors in a (UPy) PEG-gel compared to only growth factors(34). In addition to an increase in cell retention and survival, biomaterials can also be used to support thinned myocardial wall (after infarction or in dilated cardiomyopathy), of even better to prevent remodeling post-infarction. This was recently shown in a mice study, where a 3D-printed patch of hyaluronic acid/gelatin and human cardiac progenitor cells (hCMPCs) was transplanted after a myocardial infarction(33).

Conclusion

Indications for proliferation and transdifferentiation of stem cells to cardiomyocytes are present. This theory has led to rapid development of cardiac stem cell therapy resulting in years of clinical experience, proving safety of the therapy. Until now, true regeneration has not been shown successfully in clinical setting. A significant but modest functional improvement is seen, likely based on paracrine effects. Promising results in animal models have not yet been translated to a clinically relevant effect. To enhance the results of cell therapy innovations in the basal and technical field are essential. Not only different cell types and cell products, but also biomaterials might play an important role. In addition, optimizing current administration methods is crucial. The ultimate goal, true regeneration, is searched in combining cell(-less) therapies. It is a dynamic research field in a large patient population that craves novel therapies.

References

1. Centraal Bureau voor de Statistiek [Internet]. Available from: http://www.cbs.nl/nl-NL/menu/themas/gezondheid-welzijn/cijfers/default.htm

2. Keeley EC, Boura JA, Grines CL. Primary angioplasty versus intravenous thrombolytic therapy for acute myocardial infarction: a quantitative review of 23 randomised trials. Lancet. 2003;361(9351):13–20.

3. Koopman C, Van Dis I, Bots M, Vaartjes I. Feiten en cijfers Hartfalen. Vol. Juni, Nederlandse Hartstichting. 2012.

4. Eglitis MA, Mezey E. Hematopoietic cells differentiate into both microglia and macroglia in the brains of adult mice. Proc Natl Acad Sci U S A. 1997;94(8):4080–5.

5. Theise ND, Nimmakayalu M, Gardner R, Illei PB, Morgan G, Teperman L, et al. Liver from bone marrow in humans. Hepatology. 2000;32(1):11–6.

6. Ferrari G, Angelis GC De, Coletta M, Paolucci E, Stornaiuolo A, Cossu G, et al. Muscle Regeneration by Bone Marrow – Derived Myogenic Progenitors. Science (80-). 1998;279(6):1–4.

7. Orlic D, Kajstura J, Chimenti S, Bodine DM, Leri A, Anversa P. Bone marrow stem cells regenerate infarcted myocardium. Nature. 2001;410:701–5.

8. Balsam LB, Wagers AJ, Christensen JL, Kofidis T, Weissman IL, Robbins RC. Haematopoietic stem cells adopt mature haematopoietic fates in ischaemic myocardium. Nature. 2004;428:668–73.

9. Murry CE, Soonpa MH, Reinecke H, Nakajima H, Nakajima HO, Rubart M, et al. Haematopoietic stem cells do not transdifferentiate into cardiac mycocytes in myocardial infarcts. Nature. 2004;428(6983):664–8.

10. Poss KD, Wilson LG, Keating MT. Heart regeneration in zebrafish. Science (80-). 2002;298(5601):2188–90.

11. Bergmann O, Bhardwaj RD, Bernard S, Zdunek S, Barnabé-Heider F, Walsh S, et al. Evidence for cardiomyocyte renewal in humans. Science (80-). 2009;324(5923):98–102.

12. Gnecchi M, Zhang Z, Ni A, Dzau VJ. Paracrine mechanisms in adult stem cell signaling and therapy. Circ Res. 2008;103(11):1204–19.

13. Strauer BE. Repair of Infarcted Myocardium by Autologous Intracoronary Mononuclear Bone Marrow Cell Transplantation in Humans. Circulation. 2002;106(15):1913–8.

14. Jansen of Lorkeers SJJ, Eding JEC, Vesterinen HM, van der Spoel TIG Van Der, Sena ES, Duckers HJ, et al. Similar Effect of Autologous and Allogeneic Cell Therapy for Ischemic Heart Disease : Systematic Review and Meta-Analysis of Large Animal Studies. Circ Res. 2015;116:80–6.

15. Martin-Rendon E, Brunskill S, Dorée C, Hyde C, Watt S, Mathur A, et al. Stem cell treatment for acute myocardial infarction. Cochrane Database Syst Rev. 2008;(4):CD006536.

16. Afzal MR, Samanta A, Shah ZI, Jeevanantham V, Abdel-Latif A, Zuba-Surma EK, et al. Adult Bone Marrow Cell Therapy for Ischemic Heart Disease: Evidence and Insights from Randomized Controlled Trials. Circ Res. 2015;117(6):558–75.

17. Chavakis E, Koyanagi M, Dimmeler S. Enhancing the outcome of cell therapy for cardiac repair: Progress from bench to bedside and back. Circulation. 2010;121(2):325–35.

18. Mathiasen AB, Qayyum AA, Jørgensen E, Helqvist S, Fischer-Nielsen A, Kofoed KF, et al. Bone-marrow derived mesenchymal stromal cell treatment in patients with severe ischemic heart failure : a randomised placebo-controlled trial (MSC-HF trial). Eur Heart J. 2015;36:1744–53.

19. Hatzistergos KE, Quevedo H, Oskouei BN, Hu Q, Feigenbaum GS, Margitich IS, et al. Bone Marrow Mesenchymal Stem Cells Stimulate Cardiac Stem Cell Proliferation and Differentiation. Circ Res. 2010;107:913–22.

20. Abdel-Latif A, Bolli R, Zuba-Surma EK, Tleyjeh IM, Hornung CA, Dawn B. Granulocyte colony-stimulating factor therapy for cardiac repair after acute myocardial infarction: A systematic review and meta-analysis of randomized

36

controlled trials. Am Heart J. 2008;156(2):218–226.e9.

21. Perin EC, Sanz-Ruiz R, Sánchez PL, Lasso J, Pérez-Cano R, Alonso-Farto JC, et al. Adipose-derived regenerative cells in patients with ischemic cardiomyopathy: The PRECISE Trial. Am Heart J. 2014;168(1):88–95.e2.

22. Senyo S, Wang M, Wu T, Lechene CP. Mammalian heart renewal by preexisting cardiomyocytes. Nature. 2013;493(7432):433–6.

23. Chugh AR, Beache GM, Loughran JH, Mewton N, Elmore JB, Kajstura J, et al. Administration of cardiac stem cells in patients with ischemic cardiomyopathy: the SCIPIO trial: surgical aspects and interim analysis of myocardial function and viability by magnetic resonance. Circulation. 2012;126(11 Suppl 1):S54-64.

24. Malliaras K, Makkar RR, Smith RR, Cheng K, Wu E, Bonow RO, et al. Intracoronary Cardiosphere-Derived Cells After Myocardial Infarction: Evidence of Therapeutic Regeneration in the Final 1-Year Results of the CADUCEUS Trial (CArdiosphere-Derived aUtologous stem CElls to reverse ventricUlar dySfunction). J Am Coll Cardiol. 2014;63(2):110–22.

25. Hare JM, Fishman JE, Gerstenblith G, DiFede Velazquez DL, Zambrano JP, Suncion VY, et al. Comparison of allogeneic vs autologous bone marrow–derived mesenchymal stem cells delivered by transendocardial injection in patients with ischemic cardiomyopathy: the POSEIDON randomized trial. JAMA. 2012;308(22):2369–79.

26. Yeo C, Saunders N, Locca D, Flett A, Preston M, Brookman P, et al. Ficoll-Paque^{TM} versus Lymphoprep^{TM}: a comparative study of two density gradient media for therapeutic bone marrow mononuclear cell preparations. Regen Med. 2009;4(5):689–96.

27. van der Spoel TIG, Lee JC-T, Vrijsen K, Sluijter JPG, Cramer MJM, Doevendans PA, et al. Non-surgical stem cell delivery strategies and in vivo cell tracking to injured myocardium. Int J Cardiovasc Imaging. 2011;27(3):367–83.

28. du Pré BC, Doevendans PA, van Laake LW. Stem cells for cardiac repair: an introduction. J Geriatr Cardiol. 2013;10(2):186–97.

29. van Rooij E, Olson EN. MicroRNA therapeutics for cardiovascular disease: opportunities and obstacles. Nat Rev Drug Discov. 2012;11(11):860–72.

30. Wei K, Serpooshan V, Hurtado C, Diez-Cuñado M, Zhao M, Maruyama S, et al. Epicardial FSTL1 reconstitution regenerates the adult mammalian heart. Nature. 2015;

31. van der Spoel TIG, Vrijsen KR, Koudstaal S, Sluijter JPG, Nijsen JFW, de Jong HW, et al. Transendocardial cell injection is not superior to intracoronary infusion in a porcine model of ischaemic cardiomyopathy: a study on delivery efficiency. J Cell Mol Med. 2012;16(11):2768–76.

32. Hou D, Youssef EAS, Brinton TJ, Zhang P, Rogers P, Price ET, et al. Radiolabeled cell distribution after intramyocardial, intracoronary, and interstitial retrograde coronary venous delivery: Implications for current clinical trials. Circulation. 2005;112(9 SUPPL.):150–7.

33. Gaetani R, Feyen DAM, Verhage V, Slaats R, Messina E, Christman KL, et al. Epicardial application of cardiac progenitor cells in a 3D-printed gelatin/hyaluronic acid patch preserves cardiac function after myocardial infarction. Biomaterials. 2015;61:339–48.

34. Koudstaal S, Bastings MMC, Feyen DA, Waring CD, van Slochteren FJ, Dankers PYW, et al. Sustained delivery of insulin-like growth factor-1/hepatocyte growth factor stimulates endogenous cardiac repair in the chronic infarcted pig heart. J Cardiovasc Transl Res. 2014;7(2):232–41.

3

Intramyocardial mononuclear bone marrow cell injection does not lead to functional improvement in patients with chronic ischemic heart failure without considerable ischemia

I. Mann*, C.C.S. Tseng*, S.F. Rodrigo, S.Koudstaal, J. van Ramshorst, S.L. Beeres, P. Dibbets-Schneider, H. Lamb, R. Wolterbeek, J.J Zwaginga , W.E. Fibbe, K. Westinga, J.J. Bax, P.A. Doevendans, M.J. Schalij, S.A.J. Chamuleau, D.E. Atsma

* These authors contributed equally to this work

Abstract

Background

Mononuclear bone marrow cell injection has beneficial effects in patients with refractory angina pectoris. However, previous trials have led to discrepant results of bone marrow cell therapy in patients with chronic heart failure. The aim of this study was to evaluate the efficacy of intramyocardial injection of mononuclear bone marrow cells in patients with chronic ischemic heart failure with limited stress-inducible myocardial ischemia.

Methods and Results

This multicenter, randomized, placebo controlled trial included 39 patients with no-option chronic ischemic heart failure with a follow-up of 12 months. A total of 19 patients were randomized to autologous intramyocardial bone marrow cell injection (cell group) and 20 patients received a placebo injection (placebo group). The primary endpoint was the group difference in change of left ventricle ejection fraction, as determined by single photon emission tomography. At 3 and at 12 months follow-up, change of left ventricular ejection fraction in the cell group was comparable with change in the placebo group. Also secondary endpoints, including left ventricle volumes, myocardial perfusion, functional and clinical parameters did not significantly change in the cell group, as compared to placebo. No improvement was demonstrated in a subgroup of patients with stress-inducible ischemia.

Conclusion

Intramyocardial mononuclear bone marrow cell injection does not improve cardiac function, nor functional and clinical parameters in patients with severe chronic ischemic heart failure with limited stress-inducible ischemia.

Introduction

In patients with ischemic heart disease, myocardial damage can lead to remodelling of the left ventricle (LV) and progress towards end stage heart failure (HF)(1). Despite major advances in medical and surgical options for the management of ischemic heart disease no definite cure is available for heart failure. Moreover, severe chronic heart failure has a poor prognosis with a one-year mortality rate of 50% in patients with severe heart failure symptoms (New York Heart Association (NYHA) score 4)(2,3). Many chronic heart failure patients remain symptomatic, causing a large burden on day-to-day activities, as well as on health care. Therefore, there is a need for new therapeutic strategies to treat chronic ischemic heart failure.

Bone marrow cells have emerged as a potential therapy since they were hypothesized to stimulate angiogenesis by the release of growth factors and/or by direct incorporation of cells into new capillaries(4–6). Extrapolated from this hypothesis, bone marrow cell treatment might benefit ischemic myocardium and lead to improvement in cardiac function and complaints/symptoms. The first clinical trials with bone marrow cells were performed in patients after an acute myocardial infarction(7,8) and showed contradictory results with regard to beneficial effects. Bone marrow cells have also been evaluated in no-option patients with chronic ischemia and refractory angina pectoris(9–11). These latter trials demonstrated that intramyocardial injections with bone marrow cells are safe and result in improvement of cardiac function, myocardial perfusion and anginal symptoms(9–11). Intramyocardial bone marrow cell injection in patients with chronic heart failure has been demonstrated to be safe and feasible(12–14). However, since most of these trials included patients with complaints of angina pectoris and/or (objectified) ischemia, the efficacy in patients without (chronic) stress-inducible ischemia is unclear(14–17). Up till now, there are no clinical studies that have evaluated whether the presence or absence of stress-inducible ischemia influences the outcome of bone marrow cell treatment in patients with ischemic heart failure. In patients with dilated cardiomyopathy, the majority of studies show a significant increase in left ventricular function after cell treatment, although no solid evidence exists(18).

As there is still a need for novel therapies in no-option heart failure patients, the aim of the current randomized, double-blind, placebo-controlled study is to evaluate the efficacy of intramyocardial bone marrow cell injection in patients with chronic ischemic heart failure

regardless of the presence of stress-inducible ischemia. Furthermore this study aimed to investigate whether the presence of stress-inducible myocardial ischemia influences the outcome of bone marrow cell treatment in these patients.

Methods

Study overview

The present study is a phase 2, randomized, double-blind, placebo-controlled multicenter trial. The participating centers were the Leiden University Medical Center (LUMC) and the University Medical Center of Utrecht (UMCU). The LUMC has been the coordinating center that provided trial management and data analysis. The study protocol was in accordance with the declaration of Helsinki and complied with the Guideline for Good Clinical Practice (CMPP/ICH/135/95 – 17th July 1996). The protocol was approved by the institutional ethical committees of both research centers and the Dutch Central Committee on Research Involving Human Subjects (CCMO). Overall safety examination was performed by an independent data monitoring safety board (DSMB), as well as by independent institutional safety review boards of each clinical center. The study has been registered at the Dutch trial registry (www.trialregister.nl, no. NTR2516)

Population

The study population consisted of patients with coronary artery disease and chronic heart failure (New York Heart Association (NYHA) class 2, 3 or 4) despite optimized medical therapy, and were recruited by the 2 participating centers. Full in- and exclusion criteria are provided in **Table 1.** A 1:1 randomization has been executed by a statistician of the LUMC **(Figure 1).** The randomization was stratified by presence of stress-inducible ischemia, to assure a similar number of patients with and without stress-inducible ischemia in both treatment and placebo group, and by clinical center, to equally divide patients who underwent cell therapy versus placebo over both hospitals.

Study Protocol

At baseline, a complete medical history was obtained and laboratory tests including blood count, electrolytes, cardiac markers, hepatic and renal function, and infectious disease serology were performed. Further baseline evaluation consisted of stress-rest Tc-99m tetrofosmin gated single photon emission tomography (SPECT), fluorodeoxyglucose (FDG) SPECT, metaiodobenzylguanidine (MIGB) imaging, NYHA classification, quality of life assessment using the Dutch translation of the Minnesota Living with Heart Failure Questionnaire (MLHF), and a bicycle exercise test with volume oxygen maximum (VO2 max) measurement. Thereafter, patients were hospitalized for bone marrow aspiration and the intramyocardial injection procedure. To evaluate peri-procedural and short term safety of bone marrow cell treatment, patients were admitted to the Coronary Care Unit directly after treatment. Monitoring of vital signs, heart rhythm and biochemical cardiac markers were performed during 2 days after treatment. Before discharge, echocardiography was performed to evaluate the presence of pericardial effusion. At 3 and 12 months follow-up SPECT was repeated. NYHA class was reassessed at 3, 6 and 12 months follow-up, and MLHF and bicycle test were repeated at 3 and 6 months. Long term safety was evaluated during outpatient visits at 1.5, 3, 6 and 12 months after treatment, to ensure all adverse events including all-cause death, cardiovascular death, hospitalization for worsening heart failure, rhythm disorders and myocardial infarction, were collected. 24-hour Holter recording was obtained in patients without implantable cardioverter defibrillator (ICD) at 1.5 and 6 months to monitor the occurrence of arrhythmias.

Bone marrow aspiration and cell processing

On the day of the injection procedure, ≥80ml of bone marrow was aspirated from the posterior iliac crest under local anaesthesia. During the procedure patients were under continuous ECG and oxygen saturation registration. Bone marrow was collected in flasks containing Hanks balance salt solution and heparin. Mononuclear bone marrow cells were isolated by Ficoll density gradient centrifugation according to strict GMP conditions following Standard Operating Procedures of the Stem Cell Laboratory at the LUMC (CST-WV-2014, CST-WR 2014, CST0PF-2000.BM/MNC and CST-Do-2000). Bone marrow cells were suspended at a concentration of 40×10^6 cells/ml in a solution of 0.9% sodium chloride, 0.5% human albumin and 11.3 IU/ml heparin(9). The final cell product contained 100×10^6 cells.

The bone marrow cell population was checked for clots, stained for the presence of bacteria and analysed by fluorescence-activated cell sorting for the presence and percentage of CD14, CD34 and CD45 positive cells(9).

A blinded syringe with either bone marrow solution or placebo solution, which contained a similar sodium chloride/human albumin solution without bone marrow-derived cells, was delivered at the catheterization laboratory. Patient's allocation was only known to the stem cell laboratory assistant.

Electromechanical mapping and cell injection

During cell preparation, biplane left ventricular angiography was performed. Based on ventricular size, the mapping catheter curve (D or F) was selected. Via femoral artery access and a retrograde aortic approach, the catheter was inserted into the left ventricle (LV). A non-fluoroscopic electromechanical map of the LV was constructed using the NOGA system (NOGAStar catheter, Biosense-Webster, Waterloo, Belgium)(19). The electromechanical map was used to guide the injection catheter with a 27-gauge retractable needle (MyoStar catheter Biosense-Webster) to the target region, which is the area of stress-inducible ischemia on SPECT for the patients with ischemia,[4] and to the peri-infarction zone for patients without ischemia(20). Subsequently, 8-12 injections of approximately 0.2-0.3ml each were delivered.

SPECT

Gated SPECT imaging was performed with a triple-head SPECT camera system (GCA 9300/HG, Toshiba Corp., Tokyo, Japan). A 2-day stress-rest protocol was used for Tc-99m tetrofosmin SPECT imaging. Stress imaging was performed by injection of Tc-99m tetrofosmin (500 MBq) followed by injection of adenosine (0.14 mg/kg/min for 6 minutes) after 3.5 minutes. On the second day, rest images were obtained after injection of Tc-99m tetrofosmin (500 MBq). To obtain LV ejection fraction and LV volumes, rest imaging studies were acquired using ECG gating(9).

Quantitative assessment of LV end systolic, LV end diastolic volumes and LV ejection fraction at rest and stress were performed using the 4DM-software (Corridor 4DM, INVIA, Ann Arbor, University of Michigan Medical Center)(21). To analyse myocardial perfusion, the gated SPECT images were divided in 17 segments and segmental tracer uptake, at rest and

stress imaging, were categorized on a 4 point scale: 1= tracer activity >75%; 2= tracer activity 50-75%; 3= tracer activity 25-49%; 4= tracer activity <25%. When segmental tracer uptake during stress was >75% of maximum tracer uptake, perfusion was considered to be normal(22). The summed stress score was calculated by summation of the segmental scores at stress and summed rest score was calculated by summation of the segmental scores at rest. The summed differences score was calculated by summation of the differences in stress and rest segmental scores and reflects the extent of stress-inducible ischemia. A summed difference score of 1 was defined as presence of stress inducible ischemia.

FDG SPECT

FDG imaging was performed to assess myocardial viability (23). The plasma glucose level was assessed and regulated by an oral dose of 500mg acipimox and a low-fat carbohydrate-rich meal (23). FDG (185 MBq) was injected and 45 minutes thereafter, tracer uptake imaging was performed at rest using the same camera (with 511 keV collimators) as described for perfusion imaging. Myocardial tracer uptake was scored on a 17 segment model and scored on a 4 point scale: 1= normal tracer uptake (activity >75%); 2= mildly reduced tracer uptake (activity 50-75%); 3= moderately reduced tracer uptake (activity 25-49%); 4= severely reduced tracer uptake (activity <25%). Segments with >75% of maximum tracer uptake were considered as viable (normal) and segments with tracer uptake <75% were considered to contain some extent of scar. An increase in segmental uptake by 1 point was considered as an improvement (23).

MIBG imaging

^{123}I-MIBG imaging was performed to assess myocardial (sympathic) innervation. Patients were pre-treated with sodium iodide or potassium iodide to block uptake of free [123]Iodine by the thyroid gland. 185 MBq of ^{123}I-MIBG was injected and after 4 h late ^{123}I-MIBG planar imaging was performed in the supine position. The heart-to-mediastinum ratio was calculated for the late planar images (24).

Exercise test

Exercise capacity was assessed by a bicycle exercise test. Patients performed a symptom-limited bicycle exercise test with a 20W starting load and an increment of 10 W/min,

including VO2max measurement. Test end points were angina pectoris, physical exhaustion, dyspnea and significant decrease in systolic blood pressure (>10 mmHg), as measured every 2 minutes(9).

Statistical analysis

This trial was originally powered at 80% (α<0.05) to demonstrate a minimum of 4.1%±5.4% difference in LV ejection fraction at rest as assessed by SPECT between subjects randomized to autologous bone marrow cell therapy (28 patients) compared to placebo controlled subjects (28 patients) at 3 months of follow-up. To account for a 15% drop out rate, 32 patients in each group had to be included. However due to slow inclusion it was decided to terminate inclusion 4 years after the first included patient, regardless of the number of patients at that time point. Primary endpoint was defined as the difference in change of left ventricle ejection fraction, determined by single photon emission tomography, at follow up. A prespecified composite endpoint consisted of left ventricular ejection fraction, summed stress score (SPECT), NYHA class, MLHF score, exercise capacity, VO2 max, 6-minute walking distance, viability (FDG SPECT) and heart-to-mediastinum ratio (MIBG). Improvement per patient was quantified on a scale ranging from -9 (deterioration on every test) to +9 (improvement on every test), baseline compared to 3 months follow up. A subanalysis was performed to compare the effect of cell therapy in patients with and without stress-inducible ischemia.

Continuous data were compared using student T-test and presented as mean±SD and categorical variables were analysed using Chi-square test and presented as numbers and percentage. To analyse changes during multiple follow-up time points a repeated measure model (mixed model) with time as repeated measurement (Covariance type; toeplitz heterogeneous) is used. Taken into account similarity of both groups at baseline, the interaction between treatment allocation (factor) and follow up time points (covariate) is used to analyse the treatment effect (between-group differences at each follow-up time point). Data is presented as estimated difference with 95% confidence interval (CI) between baseline and follow-up time points within groups as well as between groups. Data were analysed following the intention-to-treat principle. P-value <0.05 is considered statistically significant.

Safety monitoring

Serious adverse events (SAE) and suspected unexpected serious adverse reactions (SUSAR) were reported to the CCMO, as well as to the DSMB. The DSMB evaluated whether adverse events in the patients included in the study were related to any of the diagnostic or therapeutic procedures used in the protocol. Furthermore, an annual safety report was submitted to the CCMO and DSMB. This provided an overview of all SUSAR and SAE, accompanied by a brief report, highlighting the main points of concern.

Table 1. Inclusion/ exclusion criteria

Inclusion criteria
- Ischemic heart failure NYHA class 2, 3 or 4 despite optimal pharmacological and non- pharmacological therapy
- No candidate for (repeat) surgery (revascularization, valve repair or ventricular reconstruction)
- No candidate for (repeat) percutaneous revascularization
- Receiving resynchronization therapy when indicated.
- Male or female > 18 years
- Life expectancy more than 6 months
- Able to perform an exercise test prior to therapy
- Able and willing to undergo all the tests used in this protocol including the traveling involved
- Written informed consent

Exclusion criteria
- Evidence of cancer in the last 5 year (except low grade and fully resolved non-melanoma skin malignancy)
- Concurrent participation in a study using an experimental drug or an experimental procedure within 2 months before randomization
- Other severe concurrent illnesses (including active infection, aortic stenosis defined as aortic valve area below $1.0cm^2$, severe renal insufficiency defined as a GFR <30 mL/min/$1.73m^2$)
- Bleeding diathesis, HIV infection or pregnancy.
- Any other condition that, in the opinion of the investigator, could pose a significant threat to the subject if the investigational therapy will be initiated
- Inability to undergo cardiac catheterization or nuclear imaging
- Inability to follow the protocol and comply with follow-up requirements
- Candidate for surgery (revascularization, valve repair or ventricular reconstruction), resynchronization therapy or percutaneous revascularization

NYHA, New York heart association; HIV, human immunodeficiency virus; GFR, glomerular filtration rate.

Figure 1. Patient flow diagram.
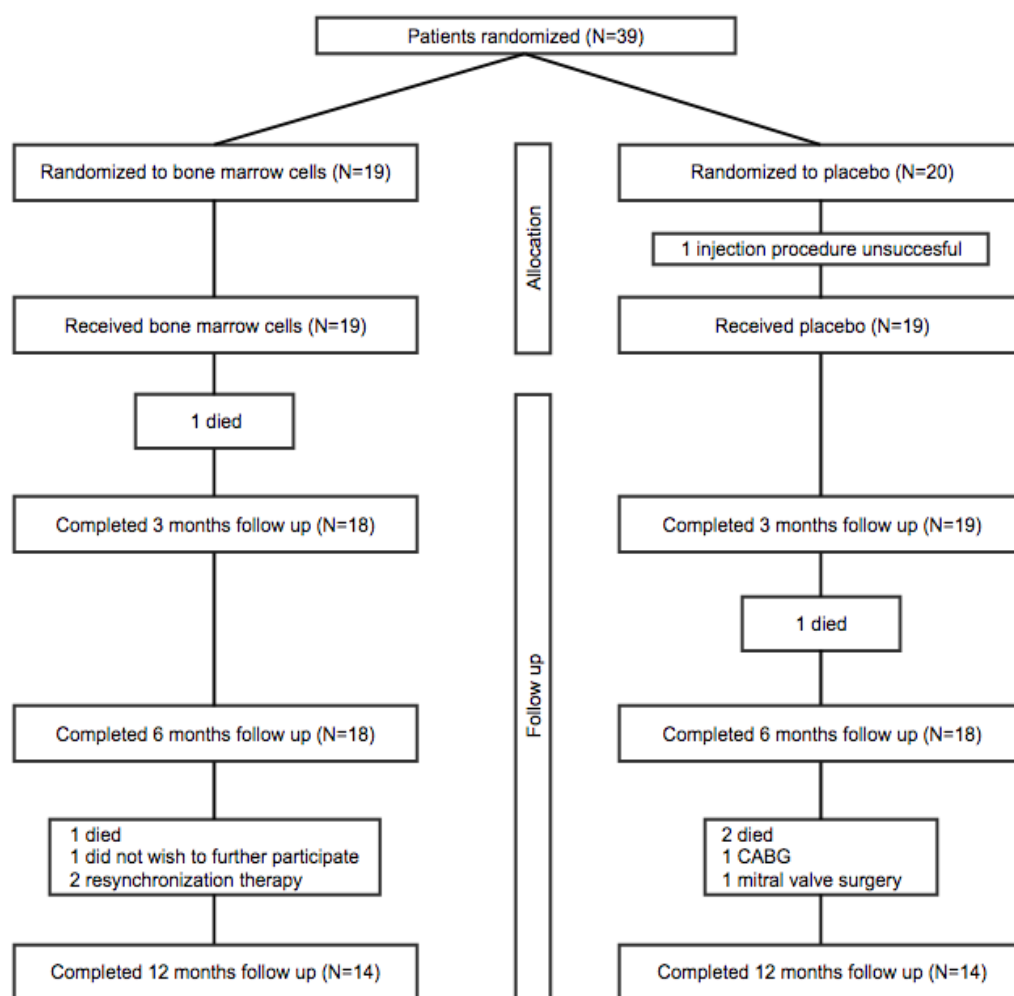
CABG, coronary artery bypass grafting.

Results

Between April 2010 and June 2014, patients were enrolled in the study. It proved not possible to include the intended number of patients fully complying with the inclusion criteria within these 4 years. A total of 39 patients, approximately 50% of all screened patients, were enrolled (**Figure 1**). The majority of screen failures were attributed to a lack of consent due to the placebo risk (20%), NYHA class I (20%) and other treatment options (15%). After randomization, 19 patients were treated with bone marrow mononuclear cells and 20 patients with a placebo suspension. Baseline characteristics of enrolled subjects are presented in **Table 2.** Patients of both groups were comparable regarding age, medical history and clinical status. A total of 21 patients were treated in the LUMC and 18 patients in the UMCU.

Safety data were collected up to 12 months in 34 patients or until death in 5 patients. Functional and clinical data were collected up to 12 months in 28 patients, until death in 5 patients, until significant medical intervention in 4 patients, or in case of 1 patient, up to the moment the patient wished to no longer participate, which was mainly determined by major comorbidities (pulmonary emphysema). In 1 patient the intramyocardial injection procedure was unsuccessful due to the inability to reach the heart with the NOGA catheter as a result from severe bilateral femoral artery stenosis. Therefore, no functional or clinical follow-up data was collected in this patient.

Table 2. Patient characteristic

	Cell injection (n=19)	Placebo (n=20)	P-value
Age, mean±SD, y	65±7	65±8	*.610*
Men	19 (100%)	18 (90%)	.487
Cardiovascular risk factors			
Current Smoking,	2 (11%)	3 (15%)	1.00
History of Smoking	16 (84%)	14 (70%)	.451
Hypertension	12 (63%)	9 (45%)	.256
Diabetes	5 (26%)	5 (25%)	1.00
Dyslipidemia	14 (74%)	14 (70%)	.798
Family history of CAD	14 (74%)	9 (45%)	.069
BMI, mean ±SD, kg/m^2	29±5	29±5	.436
Medication			
Nitrates	9 (47%)	11 (55%)	.634
Beta-blockers	17 (89%)	16 (80%)	.661
Calcium channel blockers	3 (16%)	7 (35%)	.273
Statins	17 (89%)	15 (75%)	.407
ACE inhibitors	12 (63%)	12 (60%)	.839
ATII antagonist	9 (47%)	7 (35%)	.433
Clopidogrel	2 (11%)	6 (30%)	.235
Aspirin	3 (16%)	9 (45%)	.048
OAC	16 (84%)	11 (55%)	.048
Diuretics	15 (79%)	15 (75%)	1.00
Medical history			
ICD	15 (79%)	14 (70%)	.716
PM	1 (5%)	0 (0%)	.487
Biventricular pacing	5 (26%)	6 (30%)	.798
Prior MI	18 (95%)	20 (100%)	.487
Prior CABG	12 (63%)	12 (60%)	.839
Prior PCI	11 (58%)	14 (70%)	.431
Prior CVA/TIA	2 (11%)	3 (15%)	1.00

IDDM, insulin dependent diabetes mellitus; NIDDM, non-insulin dependent diabetes mellitus; CAD coronary artery disease; BMI, body mass index; ACE, angiotensin-converting-enzyme; AT, angiotensin; OAC, oral anticoagulants; ICD, internal cardiac defibrillator; PM, pacemaker; MI, myocardial infarction; CABG, coronary artery bypass grafting; PCI percutaneous coronary intervention; CVA/TIA, cerebrovascular accident/transient ischemic attack.

Safety data

During 12 months follow-up, 2 cell-treated patients and 3 placebo-treated patients died. One of the cell-treated patients died 2.5 months after the injections. The other deceased cell treated-patient requested euthanasia at 7.5 months after the procedure because of incurable suffering from chronic pain that was not related to his cardiac disease. Of the placebo-treated patients, 1 patient died from complication of acute myocardial ischemia 7 months after the procedure, 1 patient died following an out of hospital cardiac arrest 6.5 months after the procedure, and the other patient died from cardiorespiratory insufficiency due to terminal heart failure 3.5 month after the procedure.

In 2 cell-treated and 2 placebo-treated patients a serious adverse event resulted in medical intervention and exclusion of further follow-up. Both cell-treated patients underwent cardiac resynchronization therapy (CRT). In 1 of these patients, at 6 months follow-up after a high grade-atrioventricular block and pacemaker dependency, a CRT was indicated and in 1 patient at 10 months follow-up, a CRT was indicated because of progressive intraventricular conduction delay. One placebo-treated patient had a non-ST elevated infarction 9 months after the procedure and underwent coronary artery bypass grafting. The other placebo-treated patient was admitted at 7 months follow-up because of decompensated heart failure and underwent minimal invasive mitral valve repair.

Other SAE included a monomorphic ventricular tachycardia in a cell-treated patient at 1.5 months, which was stabilized with amiodarone, and a near-collapse due to a non-sustained ventricular tachycardia in a placebo-treated patient at 6.5 months. All SAE are summarized in **Table 3.**

Table 3. Severe adverse events

Event	Cell group (N=19		Placebo group (N=20)	
Dead	2 (11%)	1 ventricular arrhythmia 1 euthanasia	3 (15%)	1 acute myocardial ischemia 1 OHCA 1 cardiorespiratory insufficiency
Medical intervention and exclusion from further follow-up	2 (11%)	2 CRT	2 (10%)	1 non-STEMI and CABG 1 minimal invasive MVR
Other	1 (5%)	1 VT	1 (5%)	1 non sustained VT

OHCA, out of hospital cardiac arrest; CRT, cardiac resynchronisation therapy; non-STEMI, non ST elevated infarction; CABG, coronary artery bypass grafting; MVR, mitral valve repair, VT, ventricular tachycardia.

Procedural data

Mean procedural time was 112±40 minutes in the bone marrow cell group and 110±44 minutes in the placebo group (P=.874). In both groups, 19 patients received intramyocardial injections. Patients in the bone marrow cell group received 9.5±0.8 injections and patients in the placebo group received 9.1±1.3 injections (P=.292). All patients from the cell group received 100×10^6 cells, with a CD34+ fraction of 1.6%±0.6%.

LV ejection fraction and volumes

At baseline all 39 patients underwent SPECT. At 3 months paired SPECT studies were available in 18 patients from both treatment groups due to previously described deaths (N=2) and unsuccessful injection procedure (N=1). At 12 months follow-up, SPECT scans of 14 cell-treated patients and 13 placebo-treated patients were available (missing scans due to previously described reasons, 1 scan unavailable due to logistics reasons).

In the cell group no improvement in LV ejection fraction at rest assessed by SPECT, was detected (P=.608 at 3 months and P=.809 at 12months follow-up). Also in the placebo group, at 3 months follow-up LV ejection fraction at rest did not change (P=.623). In the placebo group at 12 months follow-up, there was a significant increase in LV ejection fraction (P=.010). However, no significant differences were detected between both groups at 3 months and at 12 months follow-up (respectively, P=.474 and P=.078). Also, no differences between groups were observed in LV ejection fraction at stress, LV end systolic volume and LV end diastolic volume at 3 and 12 months follow-up, as shown in **Table 4 and Figure 2.**

Table 4. Left ventricular function and perfusion

Bone marrow cell group

	Baseline (N=19)	3 Months follow-up (N=18)					12 Months follow-up (N=14)				
	Absolute value (mean±SD)	Absolute change (mean±SD)	Estimated difference (mean)	95% Confidence interval		P-value	Absolute change (mean±SD)	Estimated difference (mean)	95% Confidence interval		P-value
				Lower	Upper				Lower	Upper	
EFr (%)	32.6±12.3	-1.0±7.0	-.7	-3.5	2.1	.608	.6±4.3	.2	-1.7	2.2	.809
EFs (%)	32.2±12.2	-1.9±7.6	-1.4	-4.2	1.4	.318	1.0±7.5	1.2	-2.0	4.5	.445
ESV (ml)	220±126	-3.7±23.4	-4.3	-16.8	8.2	.493	2.9±30.6	4.5	-12.9	22.0	.594
EDV (ml)	309 ±131	-6.7±26.5	-6.5	-21.4	8.4	.387	3.7±36.6	.5	-22.1	23.1	.963
SSS	46.4±7.4	-.4±1.5	-.5	-1.2	.3	.201	.2±2.5	-.1	-1.3	1.0	.856
SRS	45.1±7.6	-.1±1.9	-.1	-1.1	.9	.848	.4±2.4	-.1	-1.4	1.3	.869
SDS	1.3±2.2	-.4±1.0	-.6	-1.2	-.01	.048	-.1±1.8	-.3	-1.1	.5	.479

Placebo group

	Baseline (N=20)	3 Months follow-up (N=18)					12 Months follow-up (N=13)				
	Absolute value (mean±SD)	Absolute change (mean±SD)	Estimated difference (mean)	95% Confidence interval		P-value	Absolute change (mean±SD)	Estimated difference (mean)	95% Confidence interval		P-value
				Lower	Upper				Lower	Upper	
EFr (%)	29.0±9.7	.8±4.8	.7	-2.1	3.5	.623	2.6±2.7	2.8	.7	4.8	.010
EFs (%)	29.0±9.0	-.3±4.6	-.6	-3.3	2.2	.676	2.1±5.1	.9	-2.3	4.2	.558
ESV (ml)	221±105	-3.7±34.0	-3.8	-16.2	8.7	.548	-9.7±31.5	-6.8	-24.7	11.0	.438
EDV (ml)	299±110	-2.2±43.4	-2.0	-16.9	12.8	.784	-2.2±38.2	5.0	-18.0	28.1	.654
SSS	46.8±4.5	-.9±1.9	-.8	-1.6	-.1	.026	-.5±2.2	-.7	-1.9	.5	.225
SRS	44.0±5.1	.3±1.0	.4	-.3	1.0	.246	.4±1.5	.3	-.7	1.32	.558
SDS	2.7±3.1	-1.2±1.7	-1.1	-1.7	-.45	.001	-.8±1.9	-.9	-1.7	-.1	.036

Group difference (treatment effect)

	Baseline	3 Months follow-up					12 Months follow-up				
	Absolute difference (mean)	Absolute difference in change (mean)	Estimated difference (mean)	95% Confidence interval		P-value	Absolute difference in change (mean)	Estimated difference (mean)	95% Confidence interval		P-value
				Lower	Upper				Lower	Upper	
EFr (%)	3.7	-1.8	-1.4	-5.4	2.5	.474	-2.0	-2.5	-5.4	.3	.078
EFs (%)	3.2	-1.6	-.8	-4.6	3.0	.669	-1.1	.3	-4.1	4.7	.894
ESV (ml)	-.7	.0	-.5	18.1	17.0	.438	12.5	11.4	-13.5	36.3	.356
EDV (ml)	10.8	-4.6	-4.4	-25.5	16.6	.675	5.9	-4.5	-36.8	27.7	.773
SSS	-.3	.4	.4	-.7	1.4	.481	.7	.6	-1.0	2.2	.449
SRS	1.1	-.4	-.4	-1.3	.4	.334	.0	-.4	-1.8	1.0	.588
SDS	-1.4	.8	.4	-.3	1.2	.248	.7	.6	-.4	1.7	.244

EFr, ejection fraction at rest; EFs, ejection fraction at stress; ESV, end systolic volume; EDV, end diastolic volume; SSS, summed stress score; SRS. Summed rest score; SDS, summed difference score.

Figure 2. Change in left ventricular ejection fraction and volumes
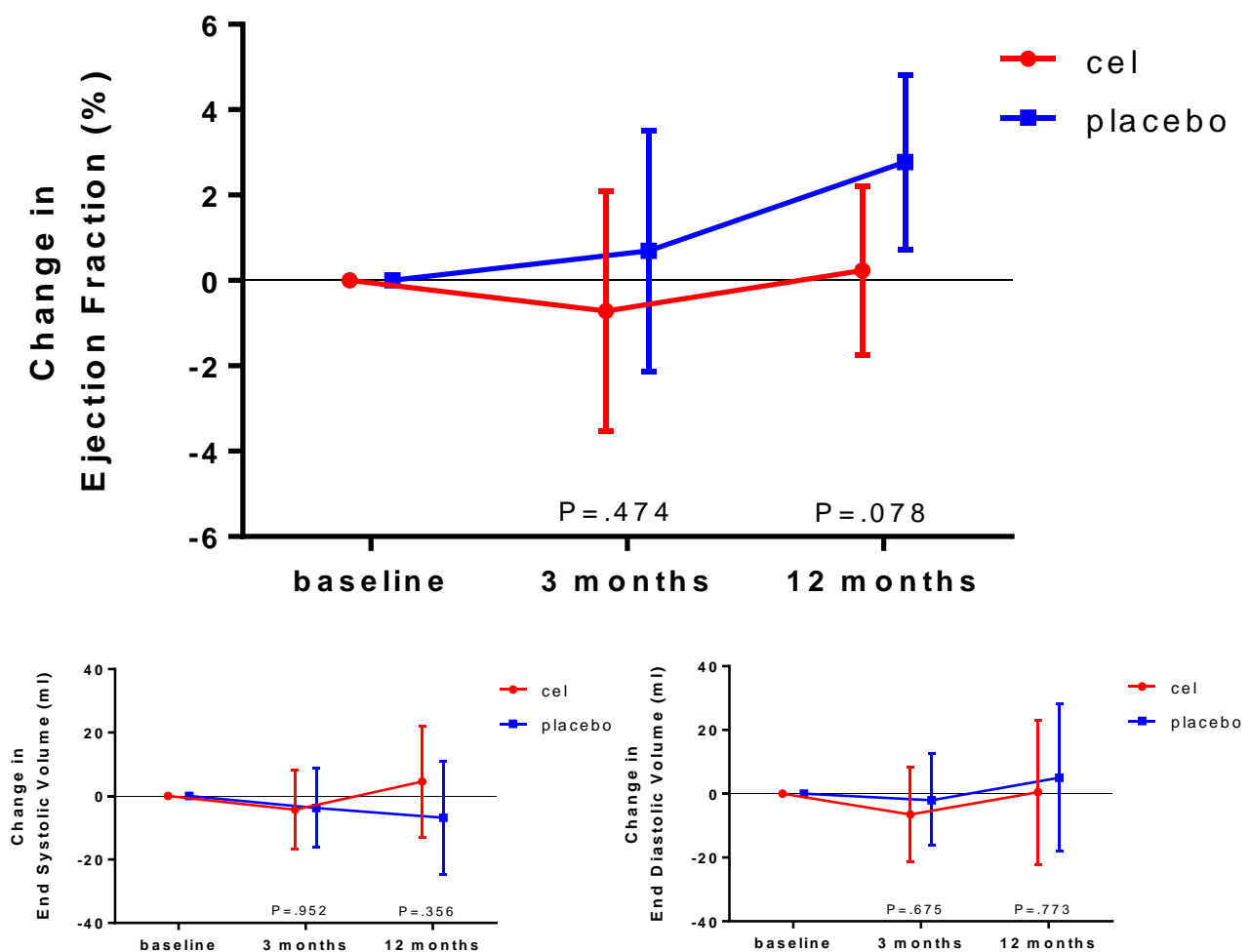
Mean estimated changes at 3 and 12 months follow-up in left ventricular ejection fraction at rest (above) and end systolic and end diastolic volumes. Bars represent 95% confidence intervals. The treatment effect (difference in changes between bone marrow cell injection group and placebo group) is not significant.

Myocardial perfusion and stress-inducible ischemia

Summed stress score did not significantly change in the cell group (P=.201 at 3 months and P=.856 at 12 months follow-up). In the placebo group at 3 months follow-up, there was a small improvement in summed stress score (P=.026). However this improvement did not

sustain up to 12 months (P=.212) and was not significantly different compared to the cell group (P=.481 at 3 months and P=.449 at 12 months follow-up).

There were no changes in summed rest score in the cell group (P=.848 at 3 months and P=.869 at 12 months follow-up) or in the placebo group(P=.246 at 3 months and P=.558 at 12 months follow-up). This was comparable between both groups (P=.334 at 3 months and P=.588 at 12 months follow-up).

There was a small but significant improvement in summed difference score in the cell group at 3 months follow-up (P=.048), which did not sustain up to 12 months(P=.479). In the placebo group there was also an improvement at 3 months, which sustained up to 12 months follow-up (respectively, P=.001 and P=.036). Importantly, no significant differences between both groups were detected (respectively, P=.248 and P=.244). Data are shown in **Table 4.**

Myocardial viability

Baseline F18-FDG SPECT images were available in all cell-treated and 17 placebo treated-patients and in 16 of both cell- and placebo- treated patients at 3 months follow-up. In the cell group at 3 months follow-up, there was a small but significant improvement in viability score (-1.2 [95%CI -2.4- -0.1]; P=.048), which was not seen after placebo treatment (-0.2 [95%CI -1.4-1.0]; P=.719). However, no significant treatment effect was observed (group difference -1.0 [95%CI -2.6-0.6]; P=.224).

Myocardial innervation

All patients underwent baseline 123-I-MIBG SPECT imaging and at 3 months follow-up, 18 scans of both groups were available for analysis. At 3 month follow-up, late heart mediastinum ratio remained unchanged in both cell and placebo group (estimated mean difference respectively, -0.01[95%CI -0.1-0.1]; P=.765 and -0.01[95%CI -0.1-0.1]; P=.754, group difference 0.001[95%CI-0.1-0.1]; P=.992).

Table 5. Clinical and Functional status

		Bone marrow cell group		Placebo group		Group difference (Treatment effect)			
						Estimated difference in change (mean)	95% Confidence interval		*P*-value
		N	Mean+SD	N	Mean+SD		lower	upper	
NYHA	Baseline	19	2.4±.5	20	2.4±.5				
	3 mth	18	2.2±.5	19	2.3±.8	-.1	-.4	.3	.727
	6 mth	18	2.3±.6	18	2.4±.6	-.2	-.5	.1	.128
	12 mth	14	2.3±.7	14	2.3±.5	-.1	-.4	.2	.523
MLHF	Baseline	16	37.6±24.4	15	49.9±19.3				
	3 mth	14	29.6±21.7	11	42.0±21.4	.01	-12.9	13.0	.992
	6 mth	13	27.9±23.7	9	45.7±19.8	-4.9	-16.3	6.5	.379
Exercise capacity (W)	Baseline	19	90.8±29.2	19	84.8±32.4				
	3 mth	17	98.5±35.5	18	88.3±36.2	2.7	-5.5	11.1	.506
	6 mth	17	95.4±35.5	14	94.0±35.5	4.5	-5.4	14.3	.364
VO2 max (ml/kg/min)	Baseline	19	14.2±3.8	17	14.0±4.4				
	3 mth	17	14.5±4.2	16	13.2±3.9	-.2	-2.2	1.7	.820
	6 mth	17	15.3±3.7	13	14.8±4.6	.9	-1.3	3.0	.419

NYHA, New York heart association; mth, month; MLHF, Minnesota living with heart failure questionnaire; VO2max, maximal oxygen

consumption; 6MWT, 6-minute walk test

Clinical outcome

Clinical status, assessed by NYHA score, did not change in both treatment groups at 3, 6 and 12 months follow-up (group difference respectively. P=.727, P=.128 and P=.523)

Improvement in quality of life MLHF score after 3 months in the cell group was not significant (estimated mean difference -5.7 [95%CI -14.5-3.0]; P=.192). However, at 6 months there was a trend to improvement (estimated mean difference -7.2 [95%CI -14.4-0.01]; P=.053). In the placebo group, improvement in quality of life score was not significant (estimated mean difference at 3 months -5.8 [95%CI -15.6-4.0]; P=.237 and at 6 months -2.2 [95%CI -11.1-6.7]; P=.605). Nevertheless, between group differences were not significant (P=.992 at 3 months and P=.379 at 6 months follow-up). Data are presented in **Table 5 and Figure 3.**

Figure 3. Change in NYHA score and quality of life
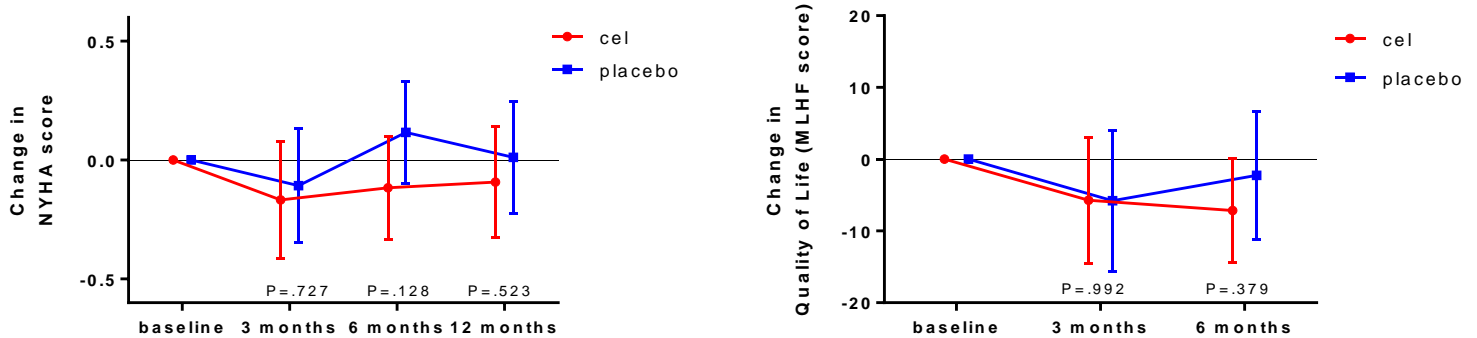
NYHA, NewYork heart association score; MLHF, Minnesota living with heart failure questionnaire.

Mean estimated changes at 3, 6 and 12 months follow-up in NYHA score and at 3 and 6 months follow-up in MLHF score. Bars represent 95% confidence intervals. The treatment effect (difference in changes between bone marrow cell injection group and placebo group) is not significant, as shown by P-values.

Exercise capacity

There were no significant changes in exercise capacity assessed by bicycle test, after cell or placebo treatment. Both groups were comparable at 3 and 6 months (respectively. P=.506 and P=.364). Similar no significant changes were found in VO2max during the bicycle test (group differences at 3 months P=.820 and at 6 months P=.419) Data are presented in **Table 5.**

Ischemia

Prespecified subgroup analysis examined the efficacy of cell therapy in patients with stress inducible ischemia. At baseline, in the cell group 8 patient had ischemia (mean summed difference score 3.1±2.4) and in the placebo group 13 patients had ischemia (mean summed difference score 4.2±3.0) Therefore, 21 patients were included in the analysis. Baseline LV ejection fraction was 29.6±11.5% in the cell group and 29.7±11.5 in the placebo group. Estimated mean difference in the cell group was -0.3% (95%CI -5.0-4.4%); P=.910 at 3 months follow-up and -0.5% (95%CI -2.9-1.8%); P=.637 at 12 months follow-up. In the placebo group estimated mean differences was 1.5% (95%CI -2.1-5.1%); P=.389 at 3 months follow-up and 1.7% (95%CI -0.5-3.9%); P=.118 at 12 months follow-up. Between group

difference at 3 months was -1.8% (95%CI -7.7-4.1%); P=. 538 at 3 months follow-up and -2.2% (95%CI -5.4-0.9%); P=.151 at 12 months follow-up. Also, no significant changes were observed between ischemic cell-treated and ischemic placebo-treated patients in secondary endpoints (data not shown).

Discussion

This multi-center, randomized, double blind, placebo controlled trial was designed to assess the efficacy of autologous bone marrow cell injection in no-option patients with severe chronic ischemic heart failure with or without stress-inducible ischemia. No beneficial effects of bone marrow cells were found in functional and clinical parameters or imaging modalities in these patients as compared to placebo.

The study population consisted of chronic heart failure patients with severe LV dysfunction (mean EF < 35%) in NYHA score/class II-IV without any treatment options. After intramyocardial injections with autologous mononuclear bone marrow cell therapy no changes were seen with regard to EF or LV volumes at 3 or 12 months. Also, no differences were found between the cell and the placebo treated group, the primary outcome. Regarding perfusion, at baseline stress-inducible ischemia measured by SPECT proved to be limited in our study population (mean SDS < 3). Although viability increased in the cell treated group after 3 months, no difference in myocardial perfusion, innervation or viability was measured between the cell and the placebo treated group during follow up. Exercise capacity and functional status remained unchanged during follow up in both the cell and the placebo treated group. These data suggest that intramyocardial injections with autologous mononuclear bone marrow cells do not improve LV function or perfusion in patients with severe chronic heart failure. These results also imply that mononuclear bone marrow cell therapy does not benefit chronic heart failure patients with limited stress-inducible ischemia.

Furthermore, we aimed to investigate whether the presence of stress-inducible myocardial ischemia influences the outcome of bone marrow cell treatment. In a prespecified subgroup analysis, only including patients with stress-inducible ischemia, no significant changes were shown between cell-treated and placebo-treated patients in primary or secondary endpoints. However, due to the low number of patients with stress-inducible ischemia and

the small extent of stress-inducible ischemia, this study was not accurately powered to answer this question.

Cell therapy has been suggested to benefit patients with ischemic heart disease. Previously performed randomized trials demonstrated that intramyocardial mononuclear bone marrow cell injection in patients with refractory angina and stress-inducible myocardial ischemia results in improvement of cardiac function, myocardial perfusion, exercise capacityand anginal symptoms(9–11). Studies with bone marrow cells in other chronic ischemic cardiac diseases including ischemic heart failure could not show beneficial effects on cardiac function(25–28). Although the majority of meta-analyses show benefit of cell therapy, inconsistencies in literature have been described(16,29–31). In a pilot study from our group, it was suggested that bone marrow cells in patients with chronic myocardial infarction and moderate LV dysfunction (mean EF 51%) lead to a decrease in heart failure symptoms and improved LV function(13). Other studies have shown that patients with a lower ejection fraction (<45%) after a myocardial infarction benefit most from cell therapy(32). It is not known whether this also holds true for patients with severe chronic heart failure (LVEF <35%). Nonetheless, the present randomized controlled trial could not confirm previous positive results. These contradictory findings might be explained by patient characteristics of the different study populations.

Sustained functional improvements were described in the cell treated group in the STAR-heart study (35). In this study bone marrow cells were infused via a coronary artery in patients with an ejection fraction below 35%. No data on myocardial perfusion were reported. Other randomized placebo-controlled clinical trials in chronic ischemic heart disease patients have reported improvements in symptoms and cardiac perfusion after bone marrow cell therapy (**Table 6**)(9,10,14).

Table 6. Effect of cell therapy on myocardial perfusion in randomized clinical trials.

Author	Year	N pts (total)	Cell type	Baseline perfusion	Outcome
Losordo(33)	2007	18 (24)	CD 34+	Not reported	-
Ramshorst(9)	2009	25 (50)	BMC	SSS 23.5, SRS 18.3	+
Tse(10)	2007	19 (28)	BMC	SDS 7.2	+
Perin (14)	2011	20 (30)	BMC	Reversible defect 18%	+
Perin (25)	2012	10 (20)	BMC	Reversible defect 9%	-
Perin (34)	2014	21 (27)	ADC	SDS 9.3	+

BMC bone marrow cell; ADC adipose-derived cells; SSS, summed stress score; SRS, summed rest score; SDS, summed difference score.

However, the patient population of these latter studies had less severe LV dysfunction (LVEF 40-55%) than our study population. Opposed to patients with refractory angina pectoris, our study population had very limited stress-inducible ischemia and therewith almost no complaints of angina pectoris. Due to inconsistent measuring methods of ischemia the extent of ischemia that is needed to profit from cell therapy is unidentified (11). With the paracrine hypothesis in mind, one could imagine that the bigger the ischemic area the more patients benefit from cell therapy(6,36). Compared to studies with a more favourable outcome, the two described dissimilarities combined in our study population, i.e. degree of LV dysfunction and extent of ischemia, may explain the results of our study. It may be that patients in our study had too severely damaged and "exhausted" myocardium to significantly increase LV function and too less ischemia to significantly improve perfusion.

Besides the results of this study, another factor needs to be addressed. As we were not able to include the intended amount of patients, the study was not sufficiently powered for our primary endpoint. Possible reasons for the inability to enroll enough patients within a realistic time frame include; exclusion of patients with other treatment options as resynchronisation therapy or revascularisation, exclusion of patients participating in other experimental studies and importantly also exclusion of heart failure patients with an ejection fraction of >35% and stress inducible ischemia. For eligible patients the 50% chance of randomization to placebo was the most common reason to not participate.. Another cause of limited patient numbers might also be due to referral bias, as physicians that do not "believe" in stem cell therapy are less likely to refer patients for screening. In the same regard, experimental therapies are competing with other emerging or standard therapies including LVADs in end-stage heart failure patients.

Because of ethical reasons to not endlessly continue a clinical trial, it was decided to prematurely terminate the study, four years after inclusion of the first patient, resulting in an inclusion of 39 patients. After terminating and deblinding the study, enrolment of 61% of the intended group was reached. Interestingly, there was no trend of improvement after cell therapy at 3 or 12 months and even more, there was a trend towards a group difference in favour of placebo treatment at 12 months follow-up (P=.078). Therefore, to demonstrate the aimed improvement of 4.1%±5.4% difference in ejection fraction between the cell and the placebo group, the 12 not included patients in the cell group should have improved >13% in ejection fraction compared to the 13 not included patients in the placebo group at 3 months follow-up and >15% at 12 months follow-up. We found this an unrealistic improvement, based on previous results(9,13,25) and the results of this study. An interim analysis would have revealed no differences between the study groups. So, our data underline the relevance of interim analyses in clinical trials to avoid unnecessary long study duration while patients might benefit more from other treatment options.

Limitations

Important limitations of this study with regard to the study design are the premature termination, resulting in a lack of power, as well as the fact that the study was not powered for secondary endpoints. Due to several secondary endpoints, including several time-point measurements, multiple testing was performed. Furthermore in this prospective trial, we had to deal with missing data, and so we had to use compensatory statistics. Another limitation is that SPECT was used instead of the gold standard, MRI to assess the ejection fraction, because of the high number of patients with an MRI-incompatible ICD or PM.

On a more conceptual level, one could deliberate on the hypothesis that the autologous cell source in chronic heart failure patients may not yield the same regenerative capacity as allogeneic cells from a healthy donor. However, in another study autologous BM derived MSCs in patients with severe LV dysfunction did give rise to significant improvements in LVEF in the cell vs placebo group (37). Unfortunately, no data on stress-inducible ischemia in this study population was reported. As other cell types, e.g. cardiac stem cells, have been suggested to be more potent during the follow up of our study, more favourable results might have been accomplished with a different cell type. Although no differences have been

described in cell retention with regard to the delivery method, the (more or less) ischemic environment may play a role in the retention and engraftment of cells after injection.

Conclusion

Intramyocardial mononuclear bone marrow cell injection does not improve cardiac function, or functional and clinical parameters in patients with severe chronic ischemic heart disease and limited stress-inducible ischemia.

References

1.   Sutton M, Sharpe N. Left ventricular remodeling after myocardial infarction: pathophysiology and therapy. Circulation. 2000;101:2981–8.

2.   Go A, Mozaffarian D, Roger V, Benjamin E, Berry J, Borden W, et al. Heart disease and stroke statistics--2013 update: a report from the American Heart Association. Circulation. 2013;127:e6–245.

3.   Lewis EF, Tsang SW, Fang JC, Mudge GH, Jarcho JA, Flavell CM, et al. Frequency and impact of delayed decisions regarding heart transplantation on long-term outcomes in patients with advanced heart failure. J Am Coll Cardiol. 2004;43:794–802.

4.   Fuchs S, Baffour R, Zhou YF, Shou M, Pierre A, Bs C, et al. Transendocardial Delivery of Autologous Bone Marrow Enhances Collateral Perfusion and Regional Function in Pigs With Chronic Experimental Myocardial Ischemia. J Am Coll Cardiol. 2001;37(6):1726–32.

5.   Kamihata H, Matsubara H, Nishiue T, Fujiyama S, Iba O, Tateishi E, et al. Implantation of Bone Marrow Mononuclear Cells Into Ischemic Myocardium Enhances Collateral Perfusion and Regional Function via Side Supply of Angioblasts, Angiogenic Ligands, and Cytokines. Circulation. 2001;104(9):1046–52.

6.   Tse H, Siu C, Zhu S, Songyan L, Zhang Q, Lai W, et al. Paracrine effects of direct intramyocardial implantation of bone marrow derived cells to enhance neovascularization in chronic ischaemic myocardium. Eur J Heart Fail. 2007;9:747–53.

7.   Strauer BE. Repair of Infarcted Myocardium by Autologous Intracoronary Mononuclear Bone Marrow Cell Transplantation in Humans. Circulation. 2002;106(15):1913–8.

8.   Schächinger V, Erbs S, Elsässer A, Haberbosch W, Hambrecht R, Hölschermann H, et al. Improved clinical outcome after intracoronary administration of bone-marrow-derived progenitor cells in acute myocardial infarction: final 1-year results of the REPAIR-AMI trial. Eur Heart J. 2006;27(23):2775–83.

9.   van Ramshorst J, Bax JJ, Beeres SL, Dibbets-Schneider P, Roes SD, Stokkel MP, et al. Intramyocardial Bone Marrow Cell Injection for Chronic Myocardial Ischemia. JAMA. 2009;301(19):1997–2004.

10.   Tse H-F, Thambar S, Kwong Y-L, Rowlings P, Bellamy G, McCrohon J, et al. Prospective randomized trial of direct endomyocardial implantation of bone marrow cells for treatment of severe coronary artery diseases (PROTECT-CAD trial). Eur Heart J. 2007;28(24):2998–3005.

11.   Fisher SA, Dorée C, Brunskill SJ, Mathur A, Martin-Rendon E. Bone Marrow Stem Cell Treatment for Ischemic Heart Disease in Patients with No Option of Revascularization: A Systematic Review and Meta-Analysis. PLoS One. 2013;8(6):e64669.

12.   Perin EC, Dohmann HFR, Borojevic R, Silva SA, Sousa ALS, Mesquita CT, et al. Transendocardial, autologous bone marrow cell transplantation for severe, chronic ischemic heart failure. Circulation. 2003;107(18):2294–302.

13.   Beeres SLMA, Bax JJ, Dibbets-Schneider P, Stokkel MPM, Fibbe WE, van der Wall EE, et al. Intramyocardial injection of autologous bone marrow mononuclear cells in patients with chronic myocardial infarction and severe

left ventricular dysfunction. Am J Cardiol. 2007 Oct 1;100(7):1094–8.

14. Perin EC, Silva G V, Henry TD, Cabreira-Hansen MG, Moore WH, Coulter S a, et al. A randomized study of transendocardial injection of autologous bone marrow mononuclear cells and cell function analysis in ischemic heart failure (FOCUS-HF). Am Heart J. 2011;161(6):1078–87.e3.

15. Pokushalov E, Romanov A, Chernyavsky A, Larionov P, Terekhov I, Artyomenko S, et al. Efficiency of intramyocardial injections of autologous bone marrow mononuclear cells in patients with ischemic heart failure: a randomized study. J Cardiovasc Transl Res. 2010;3:160–8.

16. Fisher S, Brunskill S, Doree C, Mathur A, Taggart D. Stem cell therapy for chronic ischaemic heart disease and congestive heart failure (Review). Cochrane database Syst Rev. 2014;(4).

17. Perin E, Willerson J, Pepine C, Henry T, Ellis S, Zhao D, et al. Effect of transendocardial delivery of autologous bone marrow mononuclear cells on functional capacity, left ventricular function, and perfusion in chronic heart failure: the FOCUS-CCTRN trial. JAMA. 2012;307:1717–26.

18. Gho JMIH, Kummeling GJM, Koudstaal S, Jansen Of Lorkeers SJ, Doevendans PA, Asselbergs FW, et al. Cell therapy, a novel remedy for dilated cardiomyopathy? A systematic review. J Card Fail. 2013;19(7):494–502.

19. Beeres SLMA, Bax JJ, Kaandorp TAM, Zeppenfeld K, Lamb HJ, Dibbets-Schneider P, et al. Usefulness of intramyocardial injection of autologous bone marrow-derived mononuclear cells in patients with severe angina pectoris and stress-induced myocardial ischemia. Am J Cardiol. 2006 May 1;97(9):1326–31.

20. Beeres SLMA, Bax JJ, Roes SD, Lamb HJ, Fibbe WE, De Roos A, et al. Intramyocardial bone marrow cell transplantation and the progression of coronary atherosclerosis in patients with chronic myocardial ischemia. Acute Card Care. 2007;9(4):243–51.

21. Rietbergen D, Scholte A, Al Younis I, Stokkel M. Myocardial perfusion scintigraphy before and after cardioversion for atrial fibrillation: recovery of quantitative parameters. J Nucl Cardiol. 2011;18:192–5.

22. Mann I, Rodrigo SF, van Ramshorst J, Beeres SL, Dibbets-Schneider P, de Roos A, et al. Repeated Intramyocardial Bone Marrow Cell Injection in Previously Responding Patients With Refractory Angina Again Improves Myocardial Perfusion, Anginal Complaints, and Quality of Life. Circ Cardiovasc Interv. 2015;8(8):1–8.

23. Beeres SLMA, Bax JJ, Dibbets P, Stokkel MPM, Zeppenfeld K, Fibbe WE, et al. Effect of Intramyocardial Injection of Autologous Bone Marrow – Derived Mononuclear Cells on Perfusion , Function , and Viability in Patients with Drug-Refractory Chronic Ischemia. J Nucl Med. 2006;47(4):574–81.

24. van Ramshorst J, Beeres S, Rodrigo S, Dibbets-Schneider P, Scholte A, Fibbe W, et al. Effect of intramyocardial bone marrow-derived mononuclear cell injection on cardiac sympathetic innervation in patients with chronic myocardial ischemia. internatiol J Cardiovasc imaging. 2014;30:583–9.

25. Perin EC, Silva G V, Zheng Y, Gahremanpour A, Canales J, Patel D, et al. Randomized, double-blind pilot study of transendocardial injection of autologous aldehyde dehydrogenase-bright stem cells in patients with ischemic heart failure. Am Heart J. 2012;163(3):415–421.e1.

26.   Hendrikx M, Hensen K, Clijsters C, Jongen H, Koninckx R, Bijnens E, et al. Recovery of regional but not global contractile function by the direct intramyocardial autologous bone marrow transplantation: Results from a randomized controlled clinical trial. Circulation. 2006;114(SUPPL. 1).

27.   Ang K-L, Chin D, Leyva F, Foley P, Kubal C, Chalil S, et al. Randomized, controlled trial of intramuscular or intracoronary injection of autologous bone marrow cells into scarred myocardium during CABG versus CABG alone. Nat Clin Pract Cardiovasc Med. 2008;5(10):663–70.

28.   Yao K, Huang R, Qian J, Cui J, Ge L, Li Y, et al. Administration of intracoronary bone marrow mononuclear cells on chronic myocardial infarction improves diastolic function. Heart. 2008;94(9):1147–53.

29.   Afzal MR, Samanta A, Shah ZI, Jeevanantham V, Abdel-Latif A, Zuba-Surma EK, et al. Adult Bone Marrow Cell Therapy for Ischemic Heart Disease: Evidence and Insights from Randomized Controlled Trials. Circ Res. 2015;117(6):558–75.

30.   Saramipoor Behbahan I, Keating A, Gale RP. Bone Marrow Therapies for Chronic Heart Disease. Stem Cells. 2015;33(11):3212–27.

31.   Sanganalmath SK, Bolli R. Cell therapy for heart failure: a comprehensive overview of experimental and clinical studies, current challenges, and future directions. Circ Res. 2013;113(6):810–34.

32.   Dimmeler S, Burchfield J, Zeiher AM. Cell-based therapy of myocardial infarction. Arterioscler Thromb Vasc Biol. 2008;28(2):208–16.

33.   Losordo DW, Schatz R a, White CJ, Udelson JE, Veereshwarayya V, Durgin M, et al. Intramyocardial transplantation of autologous CD34+ stem cells for intractable angina: a phase I/IIa double-blind, randomized controlled trial. Circulation. 2007;115(25):3165–72.

34.   Perin EC, Sanz-Ruiz R, Sánchez PL, Lasso J, Pérez-Cano R, Alonso-Farto JC, et al. Adipose-derived regenerative cells in patients with ischemic cardiomyopathy: The PRECISE Trial. Am Heart J. 2014;168(1):88–95.e2.

35.   Strauer B-E, Yousef M, Schannwell CM. The acute and long-term effects of intracoronary Stem cell Transplantation in 191 patients with chronic heARt failure: the STAR-heart study. Eur J Hear Fail J Work Gr Hear Fail Eur Soc Cardiol. 2010 Jul;12(7):721–9.

36.   Gnecchi M, Zhang Z, Ni A, Dzau VJ. Paracrine mechanisms in adult stem cell signaling and therapy. Circ Res. 2008;103(11):1204–19.

37.   Mathiasen AB, Qayyum AA, Jørgensen E, Helqvist S, Fischer-Nielsen A, Kofoed KF, et al. Bone-marrow derived mesenchymal stromal cell treatment in patients with severe ischemic heart failure : a randomised placebo-controlled trial (MSC-HF trial). Eur Heart J. 2015;36:1744–53.

4

An Injectable and Drug-loaded Supramolecular Hydrogel for Local Catheter Injection into the Pig Heart

A.C.H. Pape*, M.H. Bakker*, C.C.S. Tseng, M.M.C. Bastings, S. Koudstaal, P.Agostoni, S.A.J. Chamuleau, P.Y.W. Dankers

* These authors contributed equally to this work

Abstract

Although the treatment of acute myocardial infarction has significantly improved survival rates, the chronic ischemic heart failure population is a major public health problem. The increasing shortcoming of donor hearts emphasizes the need to develop new available therapies to reverse this process of remodeling. A goal for future therapies is regeneration of lost myocardium. Hydrogels are interesting materials in the field of regenerative medicine because of their biocompatibility, and their sensitivity to external triggers. Hydrogels prepared from supramolecular polymers are formed by non-covalent interactions which can be switched conveniently from a gel to a solution state, and vice versa using environmental triggers. Supramolecular transient networks in water based on poly(ethylene glycol) (PEG), end-modified with ureido-pyrimidinone groups have shown the benefits of non-covalent interactions in combination with biomedical applications and have been used as drug delivery system in the heart and under the renal capsule. Conveniently, these polymers behave as Newtonian fluid at pH 9.0 or higher but rapidly switch from a solution to a gel state at physiological pH. Here, we describe the protocol of formulation and *in vivo* injection of such a supramolecular hydrogel. Furthermore, *in vitro* experiments are described which give on forehand an indication of gel stability and drug release, which allows for tuning of the gel and release properties before application *in vivo.*

Introduction

Although the treatment of acute myocardial infarction has significantly improved survival rates, the chronic ischemic heart failure population is a major public health problem that progresses with an aging population. There are approximately 6 million heart failure patients in the US with an estimated 25% increase in prevalence in 2030(1,2). Initial loss of myocardial tissue leads to cardiac remodeling and eventually causes chronic heart failure. Except for heart transplantation, there is no real treatment for this group of patients. The increasing shortcoming of donor hearts emphasizes the need to develop new available therapies to reverse this process of remodeling. A goal for future therapies is regeneration of lost myocardium.

Hydrogels are interesting materials in the field of regenerative medicine because of their biocompatibility, and their sensitivity to external triggers(3). Injectable hydrogels offer advantages over non-switchable hydrogels in their use in minimal invasive surgery(4). These injectable hydrogels, because of their switchability within physiological conditions, can be easily applied through a syringe(5) and allow for catheter-based injection approaches(6). Moreover, several drugs can be incorporated by simply mixing the hydrogelator with the active component before injection. Different strategies have been used for injectable materials, ranging from chemical crosslinking after injection to physical crosslinking by either temperature, pH and shear-thinning behavior(4,7,8). Although several systems have shown easy injectability via a syringe(9,10), full catheter-compatibility has not been shown often(6).

Hydrogels prepared from supramolecular polymers are formed by non-covalent interactions which can be switched conveniently from a gel to a solution state, and vice versa using environmental triggers(11). Furthermore, the low molecular weight precursors allow for easy processability(12,13). The mild conditions required for switching allow the addition of various biological active components such as often difficult to handle growth factors.

Supramolecular transient networks in water based on poly(ethylene glycol) (PEG), end-modified with ureido-pyrimidinone groups(14) have shown the benefits of non-covalent interactions in combination with biomedical applications and have been used as drug delivery system in the heart(6) and under the renal capsule(15). These networks are formed by dimerization of the UPy-groups shielded from the aqueous environment by alkyl spacers forming a hydrophobic pocket. Urea hydrogen bonding facilitates subsequent stacking of these dimers into nanofibers. Due to the reversible interaction of the UPy-UPy dimer,

triggers such as pH and temperature can be used to switch from solutions to gels. The use of a synthetic motif allows for design of the molecule and gel properties by for example tuning length of the PEG-chains and alkyl spacers(14,16).

Here, we describe the protocol of formulation and injection of such a supramolecular hydrogel. Furthermore, *in vitro* experiments are described which give on forehand an indication of gel stability and drug release, which allows for tuning of the gel and release properties before application *in vivo.*

Protocol

Statement:

All in vivo experiments were conducted in accordance with the *Guide for the Care and Use of Laboratory Animals* by the Institute of Laboratory Animal Resources. Experiments were approved by the Animal Experimentation Committee of the Medicine Faculty of the Utrecht University, the Netherlands.

1. Formulation of the hydrogel

1.1) Dissolve 10 wt% of the hydrogelator in a vial in PBS pH 11.7 by stirring at 70 °C for 1 hour. Afterwards let the viscous solution cool down to room temperature. The solution should now have a pH of approximately 9.0. This solution can be stored for several days.

1.2) Pipette the appropriate amount of drug or biomolecule into the viscous solution and stir for 10 minutes to reach a uniform distribution. If the solution becomes too viscous, shortly warming it with hot water can help.

1.3) Place the solution for 1h under an UV-lamp to sterilize.

2. Analysis of hydrogel

2.1) Rheological assessment of the solution.

2.1.1) Before loading the gel, mount the 25 mm plate-plate geometry in the rheometer, set the temperature to 20 °C and load the plate with water to prevent evaporation of the gel during measurement

2.1.2) Pipette 300 L of the solution onto a 25 mm plate-plate geometry on a rheometer maintained at 20 °C and lower the plates to obtain a 0.5 mm gap distance.

2.1.3) Record shear viscosity as function of shear stress from 0.1 to 500 Pa with 10 points per decade.

2.2) Rheological assessment of the gel.

2.2.1) Load 300 L of the solution onto the plate and add a total of 4.2 L 1M HCl at different places on the gel to induce the gel-formation.

2.2.2) Lower the plates to a gap distance of 0.5 mm and let the gel cure for approximately 30 minutes. This process can be followed by measuring the storage and loss moduli at low frequency and strain, for example respectively 1 rad/s and 0.5%.

2.2.3) After the gel has cured (after approximately 30 minutes), record storage and loss moduli as function of the frequency and subsequently as function of the strain.

3. Erosion and release experiments

3.1) Transfer 100 µL of the viscous solution containing the drug or biomolecule into a poly(ethylene terephthalate) millicell hanging cell culture insert for 24-wells plate with pore size 8.0 µm. To prevent leakage of the polymer solution, cover the bottom of the inserts with parafilm (**Figure 2A**).

3.2) Immediately afterwards pipette 1.4 µL of 1 M HCl on top of the viscous solution to reduce the pH to approximately 7.0 - 7.2 and let the gel cure inside the insert for about 30 minutes.

3.3) Remove the parafilm from the inserts, place the insert in a 24-wells plate and fill the well with 800 µl PBS pH 7.4. Incubate the plate at 37 °C with moderate rocking or shaking movement. To prevent evaporation of the solvent, empty wells were filled with PBS and the 24-wells plate was sealed with parafilm (**Figure 2B**).

3.4) Periodically refresh the PBS and analyze the PBS removed, via fluorescence spectroscopy, UV/VIS-spectroscopy or ELISA for quantification of released drug/biomolecule.

4. Local injection via a catheter

4.1) Induction of myocardial infarction.

4.1.1) After accomplishing general anesthesia and mechanical ventilation occlude the LAD distal to the second diagonal branch by intracoronary balloon occlusion, for 90 minutes, in accordance to previously described protocol.[17]

4.2) NOGA mapping.

4.2.1) At four weeks after myocardial infarction NOGA procedure is planned. Prepare the NOGA system (Biosense Webster) (**Figure 4**) in the cathlab for 3D electromechanical mapping (EMM) of the left ventricle. With this system viable, hibernating and infarcted myocardium can be identified without fluoroscopic guidance. To construct such a EM-map a series of points at multiple locations on the LV endocardial surface are acquired using an ultralow magnetic-field energy source and a sensor-tipped catheter[18,19].

4.2.2) After general anesthesia place the external reference patch on the pig's back.

4.2.3) Secure vascular access (a.carotis, v.jugularis) according to protocol[17].

4.2.4) After biplane left ventricular angiography give 75U/kg of heparin.

4.2.5) Advance an 8French-mapping (D or F curve) catheter under fluoroscopic guidance to the descending aorta, aortic arch and across the aortic valve into the left ventricle (LV).

4.2.6) Orientate the tip of the catheter to the apex of the LV to acquire the first data, followed by outflow tract, lateral and posterior points to form a 3D silhouette, defining the borders of the ventricle.

4.2.7) Obtain subsequent points until all endocardial segments have been sampled by dragging the mapping catheter over the endocardium and sequentially acquiring the location of the tip while in contact with the endocardium[20,21].

4.2.8) Define the target area, that is where electrical activity is (near) normal and mechanical movement impaired, so-called hibernating myocardium (**Figure 5**).

4.3) Intramyocardial injection.

4.3.1) Replace the NOGA mapping catheter by the MyoStar (D or F curve) injection catheter which is composed of a 27-gauge needle and a core lumen inside an 8 French catheter (**Figure 6**).

4.3.2) After preparation by adjusting the needle extension at 0° and 90° flex and by placing 0.1cc of hydrogel to fill the needle dead space, place the MyoStar catheter tip across the aortic valve and into the target area.

4.3.3) Evaluate each injection site carefully before injecting the hydrogel. The following criteria have to be met: (1) perpendicular position of the catheter to the LV wall; (2) excellent loop stability (<4 mm); (3) underlying voltage >6.9 mV; and (4) presence of a premature ventricular contraction on extension of the needle into the myocardium[20]. Deliver between 6 and 10 injections of 0.1-0.3 cc.

Results

Typical results obtained from the oscillatory rheological measurements on both the solution and the gel are represented in **Figure 1**. For injection through a long catheter, a Newtonian fluid with low viscosity is desirable. Viscosity was measured as function of shear rate, showing that at pH 8.5 the solution is shear thinning but at pH 9.0 and 9.5 the solutions behave as Newtonian fluids as evidenced by the constant viscosity of respectively 0.54 and 0.36 Pa.s (**Figure 1A**). After neutralizing the samples, the samples show a solid-like response observed by a storage modulus G' which is larger than the loss modulus G'' and therefore a $\tan\delta = G''/G' < 1$ (**Figure 1B**). The gel obtains its final strength within 30 minutes. Oscillatory rheological measurements show a typical solid-like response with G' almost independent of the angular frequency and G'>G" for all frequencies measured (**Figure 1C**).

Figure 1: Rheological assessment of the solutions and gels.
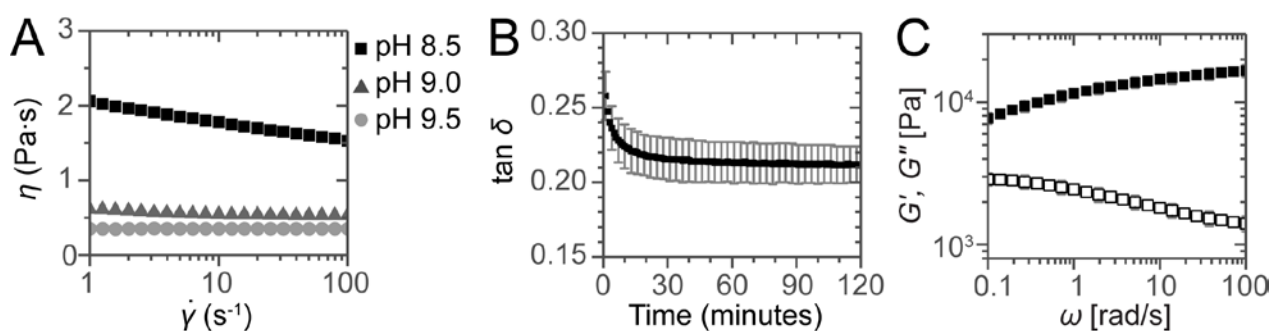
A) Viscosity as a function of shear rate for the solutions at different pH. For the sample at pH 8.5 shear thinning is observed but for the samples at pH 9.0 and 9.5 constant viscosities are obtained, showing the Newtonian behavior of these solutions. **B**) Gel curing followed by plotting tan δ as a function of time. **C**) Frequency sweep for a neutralized sample after 2 hours curing. Error bars show standard deviations of independent measurements, indicating a typical experimental error.

Essential for the use as drug delivery system is the erosion of the hydrogel over time. The supramolecular interactions are inherently dynamic and allow for a slow erosion of the gel *in vitro*. Erosion and release experiments are performed at 37 °C using porous well inserts (**Figure 2A+B**). By tuning the length of the hydrophobic and hydrophilic block(14), a gel that erodes over a period of several weeks can be obtained (**Figure 3A**). The gel erodes 25% in 2 weeks with an initial erosion of 10% in the first day, presumably due to initial swelling of the hydrogel. As example, both the release of a small molecule drug (pirfenidone), and the release of a model fluorescent protein (mRuby2) was studied. A fluorescent model protein allows for a easy readout; however, *in vitro* release experiments can also be performed on other proteins using ELISA(6). The small molecule drug is released within a day, while bigger

molecules such as proteins are gradually released over 1 week (**Figure 3B**). Fitting the release profile of mRuby up to 60% release with the semi-emperical Korsmeyer-Peppas model indicates release due to diffusion (n = 0.44)(22). The absence of an offset in the (adapted) Korsmeyer-Peppas model shows that there is no burst release present for mRuby(23). Because of the limited amount of data points with a release lower than 60% for pirfenidone, no fitting was performed on this release profile.

Figure 2: Setup for degradation and release experiments.
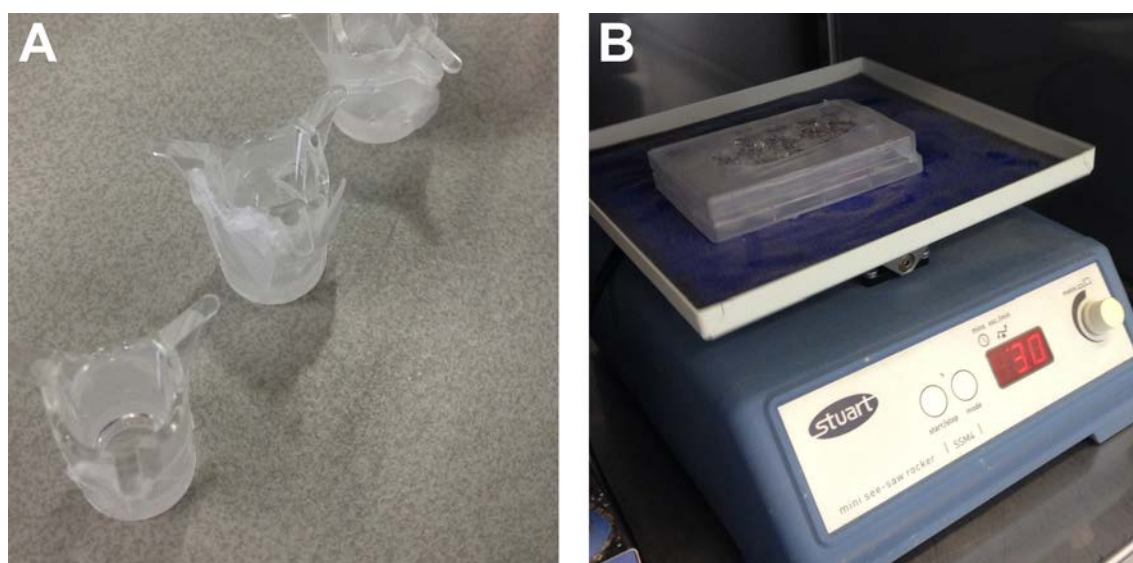
A) poly(ethylene terephthalate) millicell covered with parafilm to prevent leakage during preparation. **B**) 24-wells plate with inserts, wrapped with parafilm to prevent evaporation of the solvent.

Figure 3: Erosion and Release.
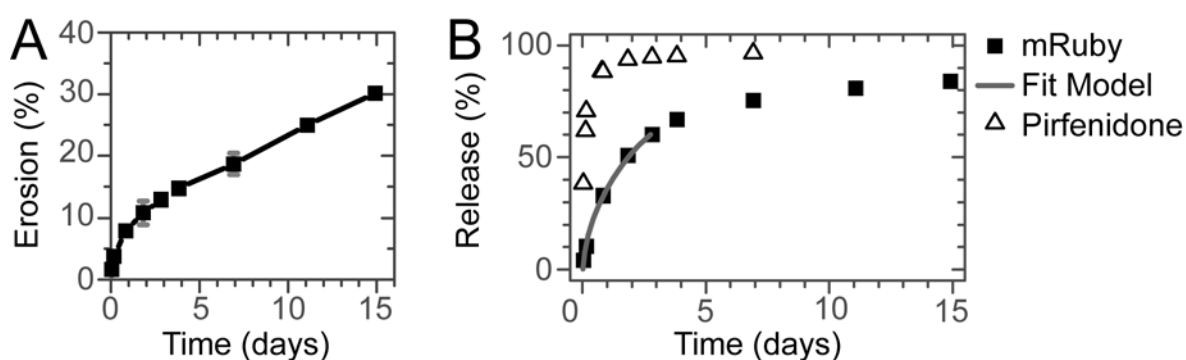
A) Erosion of the hydrogel over time. Gradual erosion of the gel for at least 2 weeks is observed. B) Release of a small molecule drug and a model protein. While the small molecule is released within a day, the model protein is gradually released over a week without a significant burst release. The line shows the fit of the Korsmeyer-Peppas model to the initial stage of the release.

The NOGA system consists of a communication unit console, a workstation **(Figure 4)**, a triangular location pad (generating a low magnetic field) with an external reference patch,

and two NOGA- catheters, the NogaStar (diagnostic) and MyoStar (injection) catheter **(Figure 6)**.

Figure 4. NOGA®System.
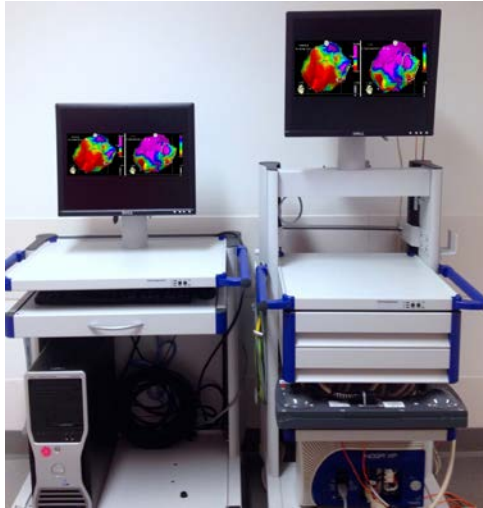
Communication unit console with NOGA® XP Cardiac Navigation System (Biosense Webster).

After postprocessing analysis has filtered unstable points the 3D endocardial reconstruction of the LV is updated in real time with the acquisition of each new data point and is continuously displayed as unipolar and bipolar voltage potentials on a graded color scale (**Figure 5A)**. The local linear shortening (LLS) function quantifies regional wall motion by obtaining the average change in distance between sample site and adjacent points at end-systole and end-diastole. The mean voltage and LLS values are calculated for each segment and displayed in the polar map. (**Figure 5B)**. The presence of an abnormal or low unipolar potential (≤6mV) and impaired mechanical activity (LLS ≤4) characterizes infarcted areas(21).

Figure 5: NOGA unipolar voltage and LLS map.
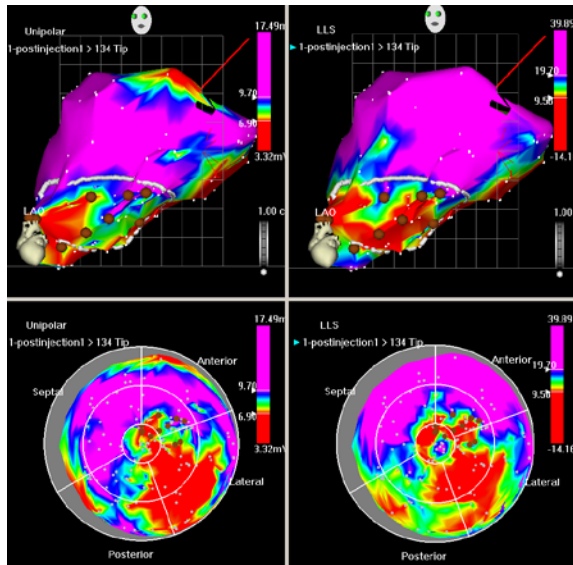
A) Unipolar map, LAO view (top) and bulls eye (below). Red color indicates low unipolar voltage values at myocardial base (normal) with loss of electrical activity posterolateral. Blue indicates normal myocardium, whilst green and yellow colors indicate decreased viability. *B*) LLS map, LAO view (top) and bulls eye (below). Red color indicates akinesia in the posterolateral wall, green and yellow indicate decreased wall motion. The mapping points are shown by white dots. The drawn white line shows the area of interest, characterized by decreased unipolar voltages and impaired wall motions. Brown points represent the injection sites.

Figure 6: NOGA MyoStar intramyocardial injection catheter (Biosense Webster)

Intramyocardial injection catheter with syringe attached and detail of injection needle.

Discussion

A key challenge is to obtain a solution, which is injectable through a long catheter while keeping the solution compatible with the bioactive compounds. Although the pH should be increased to increase injectability, bioactive compounds such as growth factors are fragile molecules that should be handled carefully. We monitor the pH of the solution closely using a pH meter after adding the hydrogelator to confirm it is pH 9.0 before adding any bioactive components. Initially, several rounds of adjusting the starting pH of the PBS were necessary to end with the right pH. For *in vitro* experiments, the solution was gelated by neutralizing the gel with HCl, while *in vivo* this is done by the natural pH of the tissue. Therefore, it is important to add the right amount of HCl to prevent an overshoot in pH. The diffusion of this acid is probably the limiting factor in the gelation of the hydrogel on the rheometer, although the gel switching is much faster with this mild procedure as compared to previously used methods (0.5 h vs 2 h)(24).

Successful release of a drug from the hydrogel largely depends on the size of the drug. As shown, the small molecule drug is released immediately while the gradual release of the model protein over 1 week shows the promise of these hydrogels as delivery systems for growth factors. In general, hydrogels are more promising as delivery tool for larger objects such as proteins and cells(25,26).

The 3-D electromechanical mapping and injection procedure with NOGA technology provides a clinically validated catheter-based delivery approach for various myocardial regenerative therapies, such as hydrogels. The added value of this technology compared to other delivery techniques is the treatment planning, making it possible to differentiate normal, infarcted and hibernating myocardium and to guide therapies in the area of interest. In the presented porcine model of myocardial infarction NOGA mapping was followed by guided intramyocardial injections with UPygel loaded with exosomes. Other combinations with regenerative therapies have to be tested *in vitro* and *in vivo* to gain more success in this emerging field.

References

1. Levy, D., et al. Long-Term Trends in the Incidence of and Survival with Heart Failure. The New England Journal of Medicine. 347 (18), 1397-402 (2002).

2. Roger, V. L., et al. Heart disease and stroke statistics—2012 update: a report from the American Heart Association. Circulation. 120 (1), 2-220 (2012).

3. Peppas, N. A., Huang, Y., Torres-Lugo, M., Ward, J. H. & Zhang, J. Physicochemical foundations and structural design of hydrogels in medicine and biology. Annual Review of Biomedical Engineering. 2 (1), 9–29 (2000).

4. Olsen, B. D., Kornfield, J. A. & Tirrell, D. A. Yielding Behavior in Injectable Hydrogels from Telechelic Proteins. Macromolecules. 43 (21), 9094–9099 (2010).

5. Guvendiren, M., Lu, H. D. & Burdick, J. A. Shear-thinning hydrogels for biomedical applications. Soft Matter. 8 (2), 260 (2012).

6. Bastings, M. & Koudstaal, S. A Fast pH-Switchable and Self-Healing Supramolecular Hydrogel Carrier for Guided, Local Catheter Injection in the Infarcted Myocardium. Advanced Healthcare Materials. 3 (1), 70–78 (2014).

7. Pawar, G. M., Koenigs, M., et al. Injectable Hydrogels from Segmented PEG-Bisurea Copolymers. Biomacromolecules. 13 (12), 3966–3976 (2012).

8. Yoon, H.-J. & Jang, W.-D. Polymeric supramolecular systems for drug delivery. Journal of Materials Chemistry. 20 (2), 211–222 (2009).

9. Christman, K. L. & Lee, R. J. Biomaterials for the treatment of myocardial infarction. Journal of the American College of Cardiology. 48 (5), 907–13 (2006).

10. Yu, L. & Ding, J. Injectable hydrogels as unique biomedical materials. Chemical Society reviews. 37 (8), 1473–81 (2008).

11. Krieg, E. & Rybtchinski, B. Noncovalent Water-Based Materials: Robust yet Adaptive. Chemistry – A European Journal. 17 (33), 9016–9026 (2011).

12. Davis, M. E., Motion, J. P. M., et al. Injectable self-assembling peptide nanofibers create intramyocardial microenvironments for endothelial cells. Circulation. 111 (4), 442–50 (2005).

13. Li, J., Ni, X. & Leong, K. W. Injectable drug-delivery systems based on supramolecular hydrogels formed by poly(ethylene oxide)s and alpha-cyclodextrin. Journal of biomedical materials research. Part A. 65 (2), 196–202 (2003).

14. Dankers, P. Y. W., Hermans, T. M., et al. Hierarchical formation of supramolecular transient networks in water: a modular injectable delivery system. Advanced materials (Deerfield Beach, Fla.). 24 (20), 2703–9 (2012).

15. Dankers, P. Y. W., van Luyn, M. J., et al. Development and in-vivo characterization of supramolecular hydrogels for intrarenal drug delivery. Biomaterials. 33 (20), 5144–55 (2012).

16. Kieltyka, R. E., Pape, A. C. H., et al. Mesoscale modulation of supramolecular ureidopyrimidinone-based poly(ethylene glycol) transient networks in water. Journal of the American Chemical Society. 135 (30), 11159–64 (2013).

17. Koudstaal, S., et al. Myocardial infarction and functional outcome assessment in pigs. Journal of Visualized Experiments. (86), (2014).

18. Koudstaal, S., et al. Sustained delivery of insulin-like growth factor-1/hepatocyte growth factor stimulates endogenous cardiac repair in the chronic infarcted pig heart. Journal of Cardiovascular Translational Research. 7 (2), 232-241 (2014).

19. van der Spoel, T. I., et al. Non-surgical stem cell delivery strategies and in vivo cell tracking to injured myocardium. International Journal of Cardiovascular Imaging. 27 (3), 367-383 (2011).

20. Gepstein, L., Hayam, G., Shpun, S., Ben-Haim, S. A. Hemodynamic evaluation of the heart with a nonfluoroscopic electromechanical mapping technique. Circulation. 96 (10), 3672-80 (1997).

21. Gyöngyösi, M., Dib, N. Diagnostic and prognostic value of 3D NOGA mapping in ischemic heart disease. Nature Reviews Cardiology. 8 (7), 393-404 (2011).

22. Siepmann, J. & Siepmann, F. Modeling of diffusion controlled drug delivery. Journal of controlled release : official journal of the Controlled Release Society. 161 (2), 351–62 (2012).

23. Kim, H. & Fassihi, R. Application of binary polymer system in drug release rate modulation. 2. Influence of formulation variables and hydrodynamic conditions on release kinetics. Journal of pharmaceutical sciences. 86 (3), 323–8 (1997).

24. Pape, A. C. H., Bastings, M. M. C., et al. Mesoscale characterization of supramolecular transient networks using SAXS and rheology. International journal of molecular sciences. 15 (1), 1096–111 (2014).

25. Peppas, N. a., Hilt, J. Z., Khademhosseini, a. & Langer, R. Hydrogels in Biology and Medicine: From Molecular Principles to Bionanotechnology. Advanced Materials. 18 (11), 1345–1360 (2006).

26. Lutolf, M. P. & Hubbell, J. A. Synthetic biomaterials as instructive extracellular microenvironments for morphogenesis in tissue engineering. Nature Biotechnology. 23 (1), 47–55 (2005).

MRI Visualization of Injectable Ureidopyrimidinone Hydrogelators by Supramolecular Contrast Agent Labeling

M.H. Bakker*, C.C.S. Tseng*, H.M. Keizer, P.R. Seevinck, H.M. Janssen, F.J. van Slochteren, S.A.J. Chamuleau, P.Y.W. Dankers

* These authors contributed equally to this work

Abstract

Information about the *in vivo* location, shape, degradation or erosion rate of injected *in situ* gelating hydrogels can be obtained with magnetic resonance imaging. Here, an injectable supramolecular ureidopyrimidinone-based hydrogel (UPy-PEG) is functionalized with a modified Gadolinium(III)-DOTA complex (UPy-Gd) for contrast enhanced MRI. The contrast agent is designed to supramolecularly interact with the hydrogel network to enable high-quality imaging of this hydrogel. The applicability of the approach is demonstrated with the successful visualization of the Gd-labeled UPy-PEG hydrogel after targeted intramyocardial catheter injection in a pig heart.

Introduction

Injectable hydrogels have been applied as delivery vehicles for various drugs in the field of regenerative medicine(1). These hydrogels are applicable via minimal invasive procedures, integrate perfectly with surrounding tissue at the injection site, and are able to enclose and deliver drugs or other bioactive compounds(2,3). To enable the further development and optimization of hydrogels for applications in the clinic where specific organs or organ regions are targeted, it would be useful to be able to non-invasively monitor the hydrogel *in vivo*. Supramolecular hydrogels are suitable drug depots owing to their inherent non-covalent nature that gives the capacity to transform *in situ* from solution to hydrogel in response to biological stimuli(4,5). Furthermore, supramolecular hydrogels do not necessarily have to degrade, as they can erode slowly by disassembly to monomeric species that can be cleared from the body(6). A promising candidate to serve as controlled drug delivery carrier is our recently developed ureidopyrimidinone (UPy) based pH-responsive catheter-injectable supramolecular hydrogel. The UPy-PEG hydrogelator comprises a telechelic 10k poly(ethylene glycol) (PEG) chain coupled via alkyl-urea spacers to two UPy end groups. In water, the UPy groups can dimerize via fourfold hydrogen-bonding interactions, as the UPy groups are shielded by a hydrophobic pocket formed by the alkyl spacers. Lateral stacking due to the additional urea functionalities results in the formation of fibers. Gel formation is proposed to be a result of interfiber crosslinking which yields a transient but robust supramolecular hydrogel network(7). At pH 9.0 the UPy-PEG behaves as a viscous liquid and can be injected, after which it quickly gelates when it comes in contact with neutral pH tissue. UPy-based hydrogels have been successfully applied as protein delivery vehicles in the injured kidney and in the heart after myocardial infarction(8-10).

Due to the growing attention in the life sciences for biomaterials and supramolecular hydrogels in particular, for *e.g.* treatments post myocardial infarction, an emerging need has developed for methods that allow monitoring various *in vivo* characteristics of hydrogels(9,11-13). Information about e.g. precise anatomical location, 3D morphology and degradation (or erosion) is crucial for analysis and fine-tuning of the *in vivo* hydrogel properties. Several imaging modalities such as US elastography, PET imaging, CT imaging and X-ray imaging have been explored for this purpose in small-animal studies(14-17). However, use of these techniques is limited by issues such as long scan times, exposure to harmful radiation or radioisotopes, and poor spatial resolution(18,19).

Magnetic resonance imaging (MRI) on the other hand is a powerful, non-invasive and non-destructive diagnostic tool which has great potential for monitoring implants *in vivo*(20-22*)*. In order to truly benefit from MRI, contrast enhancing paramagnetic species such as Gadolinium(III) (Gd(III)) complexes are necessary, which provide MRI images with superb resolution and contrast(23). MRI is also increasingly applied for guided interventional procedures, including minimal invasive therapies(24). Conveniently, this implies that contrast enhanced MRI can be employed for both the guided injection with simultaneous visualization of the hydrogel, and for post-injection imaging of the injection site giving direct feedback on the success of the procedure(25).

Several examples, of either physically mixed hydrogels and contrast agents or hydrogels chemically functionalized with a contrast agent, have been reported that could be distinguished from adjacent tissue *in vivo*(9,26-29). Physically mixing the agent with the hydrogelator beforehand is the most straightforward approach, but leakage of the agent from the hydrogel can then compromise the ability for accurate visualization of the hydrogel. A preferable method is therefore to use chemical labeling. Indeed, an excellent comparison carried out in a chitosan hydrogel system by Liu *et al.* demonstrated the superiority of chemical label incorporation over physical mixing(30).

By using supramolecular interactions between the MRI contrast agent and the hydrogelator biomaterial, one can ideally combine the ease of simply mixing both components in any desirable ratio (a favorable feature of physical mixing) with guaranteed co-localization of hydrogel and label (a favorable feature of the chemical incorporation approach). However, supramolecular contrast agent labeling is still considered particularly challenging, as too fast leakage of the MRI label or too fast erosion of the hydrogel can still occur. To the best of our knowledge only successful examples of supramolecular contrast agent incorporation based on peptide nanofibers have been reported(31-33). A shear thinning and shear recovery Gd(III)-labeled peptide hydrogel was injected in the abdominal cavity of a mouse which was successfully monitored with MRI(32).

Recently, it was shown that guest molecules can be modularly functionalized with a UPy moiety to interact in dilute solution with the aforementioned UPy-PEG hydrogelator(34). Here, we apply this modular supramolecular principle in the concentrated hydrogel regime, by design of a UPy-functionalized Gd(III)-DOTA complex (UPy-Gd) for enhanced MR imaging of the injected UPy-PEG hydrogel. First the design, synthesis and *in vitro* relaxivity

measurements of UPy-Gd are described. Retention of UPy-Gd in the UPy-PEG hydrogel was then studied with MRI, to verify its supramolecular incorporation. Furthermore, MRI imaging studies were performed to study the location of the hydrogel injected in an explanted pig heart. For comparison, experiments were performed in parallel with UPy-PEG hydrogels physically mixed with the commercially available contrast agent Gadoteridol. Finally, an *in vivo* experiment was performed to study the location of the hydrogel in the pig heart after a catheter and MRI guided intramyocardial injection.

Figure 1. Illustration of UPy-PEG hydrogel supramolecular contrast agent labeling and intramyocardial catheter injection.
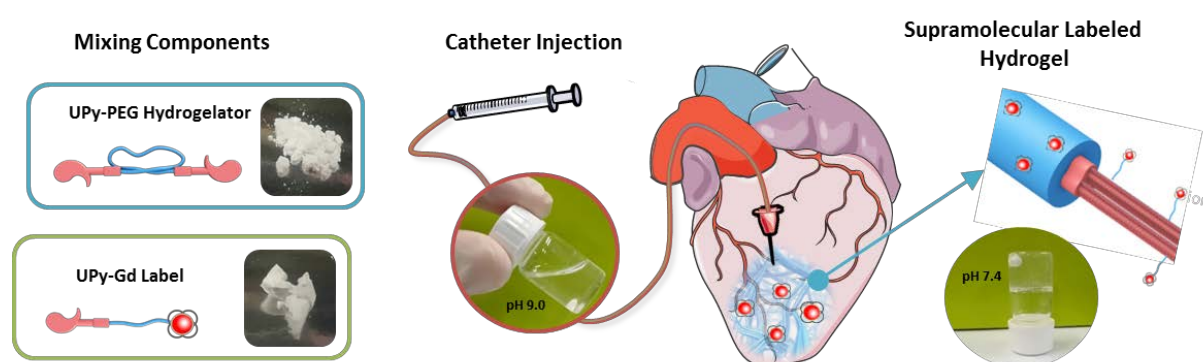
The modularity of the system enables convenient mixing of various UPy modified molecules into one supramolecular dynamic hydrogel system. At pH ≥ 9.0 the material exists as a viscous liquid which allows injection through a catheter. Servier Medical Art by Servier is licensed under a Creative Commons Attribution 3.0 Unported License.

Results & Discussion

Synthesis & Molecules

A Gd(III)-DOTA complex was conjugated to a UPy moiety via a short and discrete oligo ethylene glycol (OEG) spacer. The synthesis commenced by reaction of the N-Hydroxysuccinimide (NHS) ester and primary amine of the two precursors to form UPy-DOTA. After coupling, UPy-DOTA was complexed with $Gd(OAc)_3$ in water to produce the UPy functionalized Gd(III)-DOTA derived contrast agent UPy-Gd **I** in an overall yield of 60%. In our studies, contrast agent UPy-Gd is proposed to have an affinity via specific non-covalent interactions for the supramolecular hydrogelator UPy-PEG **II**, as both contain the same UPy-C_6-urea-C_{12}- anchoring unit. As a reference, the non-UPy-functionalized commercially available MRI contrast agent Gadoteridol **III** was used as an MRI label that can be mixed in physically (**Figure 2**).

Crucial for the paramagnetic Gd(III) based contrast agents is the stable chelation of Gd(III) into the ligand (in this case DOTA). Free Gd(III) is a toxic heavy metal similar in size to Ca(II), and this resemblance leads to competitive inhibition of biological processes and therefore severe toxicity(35). After synthesis of UPy-Gd, the absence of free Gd(III) in the product was initially confirmed with the xylenol orange test. Furthermore, a colorimetric MTT assay was performed with human vena saphena cells to determine cytotoxicity of UPy-Gd compared to the commercial Gadoteridol (**Supplementary Figure 1**). No consistent significant downregulation was measured compared to Gadoteridol, indicating that Gd(III) remains stably chelated after DOTA has been conjugated to the UPy moiety.

**Figure 2. Schematic representation of the compounds used in this study.**
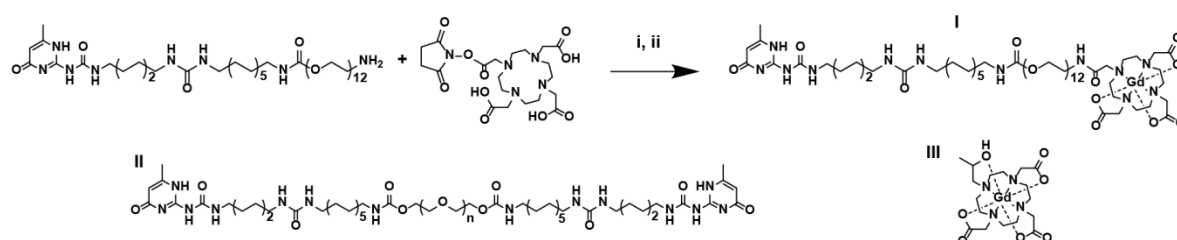
*I) UPy-Gd was synthesized by conjugation of UPy-OEG$_{12}$-NH$_2$ and DOTA-NHS ester. **i** DMF, DIPEA, room temperature, overnight, yield 94%. **ii** H$_2$O, pH~7, Gd(OAc)$_3$, room temperature, overnight, yield 63%. **II)** Bifunctional UPy-PEG hydrogelator, M$_n$ PEG = 10 kDa. **III)** Gadoteridol, a commercially available Gd(III)-DOTA contrast agent.*

Relaxivity Measurements

Water proton longitudinal and transverse relaxivities r_1 and r_2 reflect to what extent a contrast agent shortens the longitudinal and transverse relaxation times T1 and T2 of surrounding water molecules. First, it was tested whether the covalent coupling of a UPy group to the Gd(III)-DOTA complex influences its ability for water relaxation. UPy-Gd was dissolved in phosphate buffered saline (PBS) pH 7.4 and its effect on relaxation was measured at 1.4 T (60 MHz) with nuclear magnetic resonance (NMR) spectroscopy. A linear relation was found; both T1 and T2 were shortened with increasing UPy-Gd concentration resulting in an r_1 7.40 mM^{-1}s^{-1} and $r_2 \approx 9.02$ mM^{-1}s^{-1} (**Figure 3A**). Changes in pH did not have much impact, as R values measured at 1 mM were almost identical under basic or acidic conditions (**Figure 3A**).

UPy-Gd was then mixed with the UPy-PEG hydrogelator to analyze the effect of incorporation in a supramolecular polymer network. When measured in combination with 2 wt% UPy-PEG hydrogelator, no significant changes in relaxivity were observed. This applied to both r_1 and r_2 while in solution (sol) at pH 9.0 or in hydrogel form (gel) at pH 7.4 (**Figure 3B**). Furthermore, no notable changes in relaxivities were observed when varying the concentration of hydrogelator between 0 and 8 wt% (**Figure 3C**). Finally, UPy-Gd and its non-UPy-functionalized counterpart Gadoteridol were separately incorporated in a 10 wt% hydrogel and measured in a 1.5 T (64 MHz) clinical MRI scanner. Relaxivities were found to be in a similar range as observed with NMR, with r_1 4.97 mM^{-1}s^{-1} for UPy-Gd (**Figure 3D**). Furthermore, the measured r_1 4.48 mM^{-1}s^{-1} for Gadoteridol is well in line with values reported in literature(36,37).

Figure 3. Relaxivity measurements at 20 °C with relaxivities r_1 and r_2 obtained from linear fits.
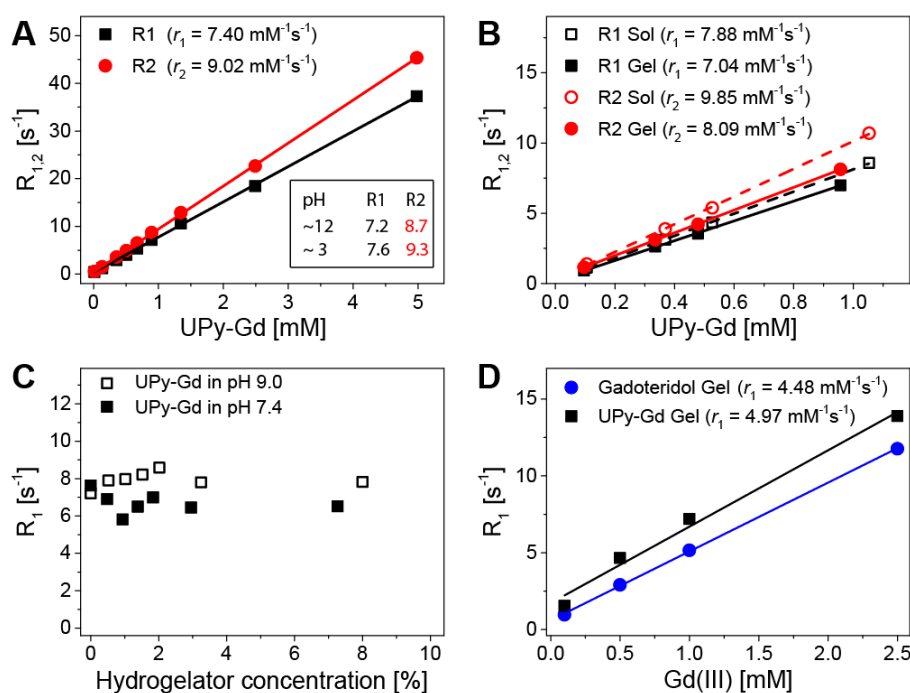
A) *Relaxation rates R_1 and R_2 for several concentrations UPy-Gd measured at 1.4 T (60 MHz) in PBS at pH 7.4, and R_1 and R_2 in PBS pH 12 and pH 3 at 1 mM UPy-Gd. B) Relaxation rates R_1 and R_2 for several concentrations UPy-Gd measured at 1.4 T (60 MHz) in PBS with 2 wt% UPy-PEG hydrogelator as solution (Sol) at pH 9.0 and as hydrogel (Gel) at pH 7.4. C) Relaxation rates R_1 for UPy-Gd measured at 1.4 T (60 MHz) in PBS pH 9.0 and pH 7.4 together with a range of UPy-PEG hydrogelator concentrations. D) Relaxation rates R_1 for UPy-Gd and Gadoteridol in PBS with 10 wt% UPy-PEG hydrogelator as hydrogel at pH 7.4, measured at 1.5 T (64 MHz).*

In view of the aggregation behavior of this supramolecular system it is surprising that neither pH changes nor incorporation in a high concentration hydrogel matrix influences the

relaxivity of the UPy-Gd. Following classic Solomon-Bloembergen-Morgan (S.B.M) theory, grafting or immobilization of the paramagnetic UPy-Gd would enhance relaxivity as a result of a decrease in molecular tumbling(38). One explanation for the absence of significant relaxivity changes could be the high exchange rates that monovalent UPy guests experience in the UPy-PEG network, as was recently disclosed with fluorescent UPy guests(34). In addition, the OEG linker may be long and flexible enough to give the Gd(III)-DOTA moiety freedom to move and tumble, despite the supramolecular anchoring interactions with the UPy-PEG hydrogelator. Another possibility is that water accessibility is reduced due to e.g. backfolding into the polymer stack, counteracting the effect of a decreased tumbling rate.

Retention of Contrast Agents in Hydrogel

A retention experiment was performed to verify the supramolecular incorporation of UPy-Gd into the UPy-PEG hydrogel. After a two week period, both the releasates and the hydrogels taken at several time points were analyzed in a 1.5 T clinical MRI scanner to quantify the amount of contrast agent. Gadoteridol was found in both the hydrogels and release samples from the first 24 hours, and correctly add up to approximately 100 % at each time point (**Figure 4A**). Release of Gadoteridol within a day occurred via an expected typical diffusion profile. In contrast, release samples from hydrogels with UPy-Gd contained almost no contrast agent, while the hydrogels itself exhibited strongly enhanced signals for the whole duration of the experiment (**Figure 4B**). The amount of UPy-Gd released from the hydrogels equates to 23 % after two weeks. This value is well in line with the previously reported rate of erosion of the hydrogel itself, which is not significantly influenced upon addition of guest molecules at this concentration(10). While dynamics at the molecular level are likely high, these retention results imply that at a macroscopic level the UPy-Gd cannot diffuse and escape from the UPy-PEG hydrogel. In fact, as a result of the supramolecular interactions, UPy-Gd is kept in place with the transient polymer network, and is only liberated by erosion of the hydrogel. Therefore, we can propose that the signal arising from the UPy-Gd MRI label serves as an accurate marker for the actual location of the UPy-PEG hydrogel carrier.

Figure 4. Pseudo-colored images from T_1-weighted 1.5 T MRI scans
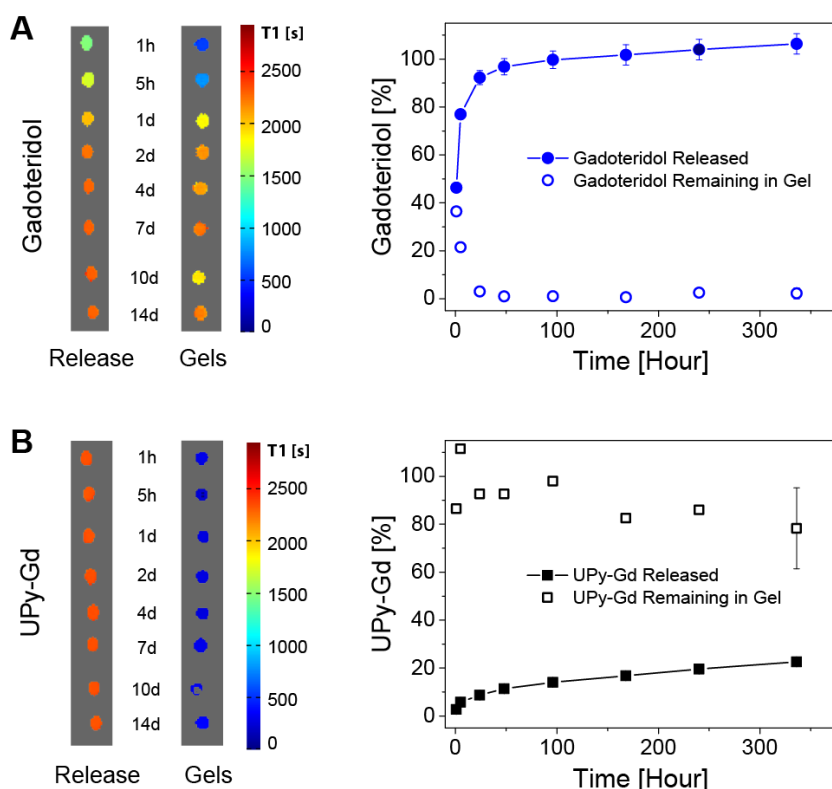
*MRI scans of release and hydrogel samples from a two week retention experiment with 10 wt% UPy-PEG hydrogels containing either (**A**) 1 mM Gadoteridol, or (**B**) 1 mM UPy-Gd. MRI data are also converted to percentage based release and retention of contrast agent in the hydrogel after that specific duration of release. The last time point of contrast agent remaining in gel represents mean ± SD, n = 2. All releasates represent mean ± SD, n = 3. The error bars of UPy-Gd released are too small to see.*

Ex Vivo Injections in Pig Heart and MRI

UPy-PEG hydrogel is under extensive investigation for delivery of therapeutics in the heart post myocardial infarction. An explanted pig heart was therefore chosen to investigate whether the supramolecular labeling technique enhances the contrast and accuracy of localization in tissue. Four injections of 10 wt% UPy-PEG hydrogels pH 9.0 functionalized with UPy-Gd and four injections of 10 wt% UPy-PEG hydrogels pH 9.0 physically mixed with Gadoteridol were performed, at 1 mM and 2.5 mM [Gd(III)]. Two 10 wt% UPy-PEG hydrogels without contrast agent were injected as control. The heart was embedded in agar 1 h after injections and stored at 4 °C. The following day T_1-weighted images were made in a 1.5 T MRI scanner. The resulting images show an enormous difference between integrated UPy-Gd and Gadoteridol with regard to intensity and location (**Figure 5A and 5B**). UPy-PEG hydrogels with integrated UPy-Gd (**1-4**) appear as hyperintense concentrated spots with easy to identify sharp borders between hydrogel and adjacent tissue. A 3D rendered image

of the complete heart illustrates this effectively (**Figure 5C**). Due to the local high content of contrast agent the T1 is shortened to such an extent that no difference in intensity between the two concentrations UPy-Gd can be seen by eye. On the contrary, injection sites of UPy-PEG hydrogel mixed with Gadoteridol (**i-iv**) are more difficult to locate. They appeared as broadened spots over an area much larger than the injected hydrogel volume. The 3D image displays all four of the Gadoteridol injections and accentuates the large, vague locations with diffuse borders (**Figure 5D**). For these formulations the higher concentration of 2.5 mM Gadoteridol improved the overall visibility as compared to that for 1 mM concentration formulations. The control injections without contrast agent were not visible.

A volume assessment on the visualized spots was performed to identify whether they match the injected volume, and to what degree the material distributes throughout the tissue (**Supplementary Figure 2**). The outcome of this analysis is determined by the (arbitrary) intensity threshold that is set to distinguish between tissue with contrast agent and normal tissue. By using a variable threshold, the volumes with signal hyperintensities were determined. Injections with high concentration UPy-Gd (**3** & **4**) show the highest signal increase, most likely caused by voxels entirely occupied with hydrogel. The two injections with lower concentration UPy-Gd (**1** & **2**) also show a very high signal increase. When lowering the threshold, an increasing number of voxels is included per region. The determined values at lower threshold are not limited to the originally injected volume of 200 uL, this is caused primarily by partial volume effects. At the edges voxels are partially filled with UPy-Gd, causing the average signal increase to be lower when compared to the signal increase of voxels entirely filled with UPY. As these voxels are at the edge of the volume, their relative contribution is substantial. These partial volume effects are amplified even more by the bio-distribution in cardiac tissue. It may be expected that injected UPy-PEG hydrogel will be distributed heterogeneously in the muscle tissue, caused by the fibrous structure. Due to this phenomenon some areas and voxels are only partially filled with hydrogel and UPy-Gd. While no difference was noticeable with the naked eye between concentrations, this observation could justify utilizing the higher concentration of UPy-Gd for optimal volume analysis.

In the injections with Gadoteridol (**i-iv**) much lower concentrations of contrast agent are present as can be concluded from the much lower maximum signal increase (**Supplementary Figure 2**). Interestingly, when reducing the threshold the volumes of the Gadoteridol

injections increase much faster, caused by the fact that the contrast agent was not confined to the location of the injection. Instead it diffused to a larger circumferential region, causing a very low concentration gradient, when compared to the steep concentration gradient in the UPy-Gd injections. No reliable hydrogel volumes could be obtained from this data.

Figure 5. MRI scans of a pig heart *ex vivo* injected with UPy-PEG and UPy-Gd.
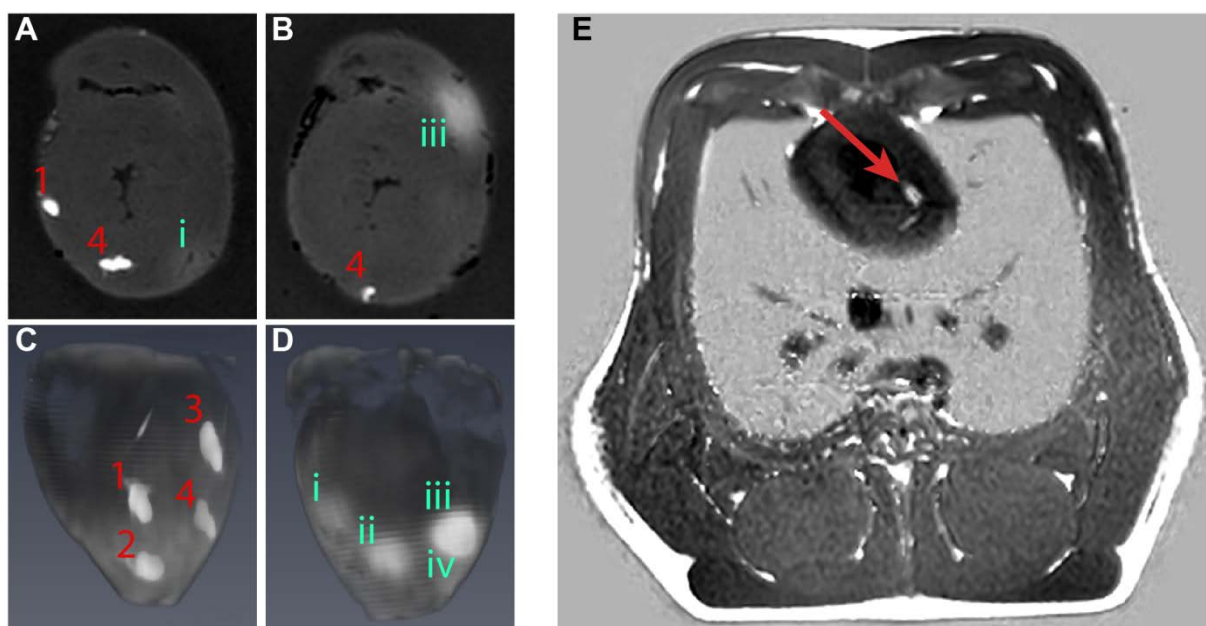
*6A-D. Selected slices of MRI scans of a pig heart ex vivo injected with 10 wt% UPy-PEG hydrogel in combination with UPy-Gd or Gadoteridol, and 3D rendered images of the whole heart. Injection spots 1 and 2 are 1 mM UPy-Gd, spots 3 and 4 are 2.5 mM UPy-Gd. Injection spots i and ii are 1 mM Gadoteridol, spots iii and iv are 2.5 mM Gadoteridol. **A)** Two clear injection sites with UPy-Gd and one with Gadoteridol. **B)** One injection site with Gadoteridol and one with UPy-Gd. C) 3D rendered image of the left side of the pig heart with four injection sites with UPy-Gd. **D)** 3D rendered image of the right side of the pig heart with four injection sites with Gadoteridol. **E)** Post-injection image of an in vivo intramyocardial injection in a pig heart with 10 wt% UPy-PEG hydrogel containing 2.5 mM UPy-Gd, applied via a catheter inside the MRI system.*

Analysis of the MRI scans supports the results from the retention experiment and demonstrates the value of supramolecular integration of the contrast agent with the hydrogel network. While the Gadoteridol injections were mostly still visible, they do not provide representative or detailed information about the location and shape of the hydrogel. Quick diffusion of Gadoteridol from the hydrogel into the surrounding tissue occurred. *In vivo* at 37 °C the diffusion rate would be even faster, and likely accelerated as a result of the high blood perfusion in the cardiac tissue and increased pressure caused by cardiac contractions(39). Also, imaging difficulty is amplified due to higher background signal, motion artifacts, and limitations in scanning time. These factors even further reduce the

feasibility and relevance of Gadoteridol for use in the imaging of hydrogels, especially when viewing the far better images obtained with the UPy-Gd contrast agent.

In Vivo MRI of Intramyocardial Catheter Injected Hydrogel

Finally, an *in vivo* feasibility study was performed by intramyocardial injection of 2.5 mM UPy-Gd in a 10 wt% UPy-PEG hydrogel formulation (this equates to a mass percentage of 4% or a molar percentage of 28% UPy-Gd relative to the used UPy-PEG) via the percutaneous approach. The injection was performed via a minimally invasive procedure through the groin using a catheter designed for injection of the viscous UPy-PEG hydrogel precursor(25). Post-injection, the hydrogel was visualized with phase sensitive inversion recovery reconstruction (PSIR) sequences (**Figure 5E**). At the intended injection site the hydrogel could be located, verifying that also *in vivo* at 37 °C the hydrogel maintained form at the injection site without immediate dispersion throughout the tissue. Furthermore, it means that contrast enhancement with the employed UPy-Gd concentration is sufficient for clear and fast *in vivo* imaging.

Conclusion

The contrast agent UPy-Gd is designed as an MRI label for supramolecular incorporation into the UPy-PEG hydrogel. At a macroscopic level the UPy-Gd retains within the hydrogel network, and provides high contrast and precise information on the 3D shape, location, and volume of the hydrogel. In contrast, physically mixed Gadoteridol does not accurately reflect the morphology or shape of injected UPy-PEG hydrogel due to rapid leakage by diffusion. We demonstrated that the UPy-Gd labeled hydrogel is perfectly visible *in vivo* after minimally invasive catheter injection in a beating heart. We foresee that this labeling and visualization method for supramolecular hydrogels can be used for sequential measurements of the same specimen to determine 3D structure, location and degradation or erosion rate of hydrogels. This crucial information is proposed to aide in the continuing development, fine-tuning and modulation of hydrogel properties for *in vivo* applications. Yet, in case alternative imaging modalities are preferred, the DOTA-Gd label is envisioned to be substitutable for other desired reporters. Finally, catheter-guided injections of viscous materials in the beating myocardium inside the MRI scanner are desired for accurate targeting of specific locations, but are not the clinical standard yet. We think that the approach presented, allowing for an

immediate post-injection feedback by MRI for confirmation of correct injection, will be particularly valuable for the future development of guided injectable therapies.

Experimental Section

Materials

All reagents and chemicals were obtained from commercial sources at the highest purity available and used without further purification unless stated otherwise. Water was purified on an EMD Millipore Milli-Q Integral Water Purification System. Phosphate buffered saline (PBS) tablets were purchased from Sigma-Aldrich. Gadoteridol was purchased from Sigma-Aldrich (1287631 USP). Millicell hanging cell culture inserts (PIEP12R48/MCEP24H48) were purchased from EMD Millipore. A fresh explanted pig heart was obtained from LifeTec Group. Data processing and analysis was performed in Excel 2010 and Origin 2015. MRI scans were processed with RadiAnt DOCIM viewer. 3D rendered images of MRI scans were made with Avizo 9.2.0.

Instrumentation: ^{1}H NMR and ^{13}C NMR spectra were recorded on a 400 MHz NMR (Varian Mercury Vx or Varian 400MR) operating at 400 MHz for ^{1}H NMR and 100 MHz for ^{13}C NMR. Proton chemical shifts are reported in ppm downfield from tetramethylsilane (TMS) and carbon chemical shifts in ppm downfield from TMS using the resonance of the deuterated solvent as internal standard. Abbreviations used are s: singlet, d: doublet, t: triplet, q: quartet, m: multiplet. Mass Spectrometry (LC-ESI-MS) was performed using a Shimadzu LC-10 AD VP series HPLC coupled to a diode array detector (Finnigan Surveyor PDA Plus detector, Thermo Electron Corporation) and an Ion-Trap (LCQ Fleet, Thermo Scientific) where ions were created via electrospray ionization (ESI). LC-analyses on precursor molecules were performed using a Alltech Alltima HP C_{18} 3 m column using an injection volume of 1-4 L, a flow rate of 0.2 mL min^{-1} and typically a gradient (5% to 100% in 10 min, held at 100% for a further 3 min) of CH_3CN/H_2O (both containing 0.1% formic acid) at 298 K. Reversed phase column chromatography was performed on a Biotage Isolera Spektra One Flash Chromatography system using Biotage KP-C18 HS SNAP cartridge.

Synthesis of UPy-Gd

The precursors UPy-C_6-U-C_{12}-C-OEG$_{12}$-NH$_2$ and N-hydroxysuccinimide activated DOTA (DOTA-NHS-xTFA) were synthesized as described elsewhere(40-42). **i:** UPy-C_6-U-C_{12}-C-OEG$_{12}$-NH$_2$ (280 mg, 0.26 mmol) was dissolved in DMF (5 mL) and DOTA-NHS-xTFA, (383 mg, 0.53 mmol) and DiPEA (0.62 mL, 3.57 mmol) were added. The reaction mixture was stirred overnight and subsequently the solvent was removed under vacuum and twice co-evaporated with toluene.

Eluting over reversed phase C18 column with a gradient ACN/water of 5/95 to 80/20 afforded the intermediate **UPy-DOTA** (360 mg, 94%) as a white powder after freeze-drying. ^{1}H NMR (400 MHz, CDCl$_3$/CD$_3$OD) 5.86 (s, 1H), 4.19 (t, J = 4.7 Hz, 2H), 3.65 (s, 44H), 3.53 (dt, J = 13.3, 6.0 Hz, 7H), 3.43 – 3.18 (m, 14H), 3.11 (q, J = 7.0 Hz, 13H), 2.25 (s, 3H), 1.58 (p, J = 6.8 Hz, 2H), 1.48 (p, J = 7.2 Hz, 6H), 1.37 (q, J = 5.9, 3.7 Hz, 4H), 1.34 – 1.17 (m, 16H) ppm. ^{13}C NMR (101 MHz, D$_2$O-NaOD)   179.94, 179.72, 175.39, 173.12, 168.35, 162.77, 159.58, 157.85, 157.34, 156.42, 104.28, 71.99, 69.80, 69.52, 69.32, 68.98, 68.83, 63.74, 58.71, 58.37, 57.16, 50.45, 40.62, 39.78, 39.25, 38.69, 30.21, 30.06, 29.66, 29.48, 29.39, 29.17, 26.89, 26.72, 26.42, 22.64 ppm.

LC-MS (ESI) R_t= 5.75 min, *m/z* calcd (C$_{66}$H$_{122}$N$_{12}$O$_{23}$) 1451.8 Da; found 484.83 [M+3H]$^{3+}$, 726.6 [M+2H]$^{2+}$, 737.5 [M+Na+H]$^{2+}$, 1452.4 [M+H]$^{+}$, 1473.9 [M+Na]$^{+}$.

ii Intermediate **UPy-DOTA** (360 mg, 0.25 mmol) was dissolved in H$_2$O (10 mL) and the pH was adjusted to 7.1 using 1 M NaOH. Gd(OAc)$_3$·4.47H$_2$O (123 mg, 0.30 mmol) in H$_2$O (4 mL, dissolved by shortly heating) was added, and the pH was again adjusted to 7.0 using 1 M NaOH. The solution was stirred at RT overnight. The solvent was removed under vacuum. Eluting over reversed phase C18 column with a gradient ACN/water of 5/95 to 80/20 first eluted free Gd and thereafter eluted the desired product. Pooling of the product fractions afforded the final product **UPy-Gd** (250 mg, 63%) as a white powder after freeze-drying. The absence of free gadolinium in the product was confirmed with the xylenol orange test.

LC-MS (ESI) R_t= 6.07 min, *m/z* calcd (C$_{66}$H$_{119}$GdN$_{12}$O$_{23}$) 1605.8 Da; found 536.6 [M+3H]$^{3+}$, 804.5 [M+2H]$^{2+}$, 1606.2 [M+H]$^{+}$, 1630.0 [M+Na]$^{+}$.

Preparation of Hydrogels and Liquid Precursors with Contrast Agents

UPy-PEG hydrogel precursor solutions were prepared by dissolving the UPy-PEG hydrogelator powder in PBS at elevated pH (e.g. 10 mg in 90 L PBS pH 11.7 for a 10 wt% hydrogel solution) and stirring at 70 °C for 1 h. Afterwards the viscous solution was cooled to RT with a resulting pH of approximately 9.0. To obtain UPy-PEG hydrogels with the desired concentration of contrast agent, the hydrogel precursor solutions were prepared at twice the intended wt%. UPy-Gd or Gadoteridol were also dissolved in PBS pH 7.4 at twice the desired concentrations. Contrast agent and hydrogel solutions were then combined in a 1 to 1 (v/v) ratio and stirred at 50 °C for 10 min to get completely dissolved homogeneous solutions with the desired wt% hydrogel and concentration of either UPy-Gd or Gadoteridol.

For gelation for *in vitro* measurements the solutions were brought back to neutral pH by addition of 1.4 µL of 1 M HCl per 100 µL hydrogel solution.

^{1}H relaxivity measurements 1.4 Tesla benchtop NMR

Longitudinal and transverse relaxation times (T1 and T2) of UPy-Gd in various formulations were determined at 1.41 Tesla (60 MHz) at 20 °C on a Bruker Minispec MQ60 (Bruker, Ettlingen, Germany) in PBS. For the pH 3 and pH 12 measurements the pH of the PBS was adjusted with HCl and NaOH, respectively. Relaxation times of samples with varying [Gd(III)] (~0.01-5.0 mM) were determined using an inversion recovery sequence for T1 and a Carr-Purcell-Meiboom-Gill (CPMG) sequence for T2 measurements. The longitudinal and transverse relaxivities r_1 and r_2 were determined from linear fits of 1/T1 and 1/T2 as a function of [Gd(III)].

^{1}H r_1 relaxivity measurements 1.5 Tesla clinical MRI scanner

Longitudinal relaxation times (T1) were determined at 1.5 Tesla (64 MHz) at 20 °C on a Philips Ingenia MR system. 10 wt% UPy-PEG hydrogels with UPy-Gd and Gadoteridol at four concentrations (0.1, 0.5, 1.0, 2.5 mM) were prepared in 1.5 mL Eppendorf tubes. The tubes were put in a green styrofoam block and the block was put in the middle of the MR scanner. Inversion recovery turbo spin echo sequences were performed with 20 different inversion times ranging from 25 to 4500 ms. Other imaging parameters included a repetition time of 6000 ms, echo time of 5 ms, and voxel size of 1 x 1 x 5 mm. T1 values were obtained by fitting the signal intensities to a mono-exponential function (non-linear Levenberg-Marquardt in Matlab). The longitudinal relaxivity r_1 was determined from linear fits of 1/T1 as a function of [Gd(III)].

Retention and Leakage of Contrast Agents from Hydrogel

Hydrogel precursor solutions with 1 mM UPy-Gd or 1 mM Gadoteridol were prepared as described above. From each solution ten hydrogels were made in Millicell inserts by transferring 100 µL into the insert and subsequently adding 1.4 µL of 1M HCl on top. The inserts were then left for incubation for 1 1. The inserts with hydrogels were placed in a 24 wells plate with 500 µL PBS per well as release medium and put in a 37 °C incubator with 95 % humidity. At set time points (1, 5, 24, 48, 96, 168, 240 and 336 h) one of the hydrogels

was removed from the setup and stored under humid conditions in the fridge to prevent drying out of the hydrogel. For all the other hydrogels the PBS was removed, stored, and replaced with fresh PBS. At the end of the experiment a minimum of three release samples and one hydrogel is obtained for each time point. After two weeks the hydrogels (still in the inserts) and release samples collected in Eppendorf tubes were put in a green styrofoam block and scanned in a Philips Ingenia MR 1.5 Tesla system. Longitudinal relaxivity measurements were performed using the same imaging parameters and data processing as just described for UPy-Gd and Gadoteridol. Furthermore, tubes with 500 µL PBS and known concentrations of Gadoteridol (0.01, 0.025, 0.05, 0.1, 0.25 mM) or UPy-Gd (0.01, 0.025, 0.05, 0.1 mM) were scanned in parallel to determine a standard curve between [Gd(III)] and T1 for the release samples. Also hydrogels in inserts with known concentrations of UPy-Gd (0.25, 0.5, 1 mM) were scanned in parallel to determine standard curves between [Gd(III)] and T1 for the hydrogels in inserts. For Gadoteridol relaxation data obtained in the previous MRI experiment was used to calculate the concentrations. Data are represented as percentage contrast agent released and percentage remaining in hydrogel. All release values are reported mean ± SD, n = 3. All values of percentage remaining in hydrogel are from single hydrogels, except the last data point at 336 h which is mean ± SD, n = 2.

Ex Vivo Injections Pig Heart and MRI

UPy-PEG hydrogel precursor solutions of pH 9.0 with UPy-Gd or Gadoteridol were prepared as described above, at 1.0 and 2.5 mM [Gd(III)]. The next morning a frozen pig heart was thawed until at room temperature. For each condition two injections of 200 µL were performed with a 1 mL syringe and 23G needle. The injection depth was approximately 4-5 mm. Injections with UPy-Gd were performed in the anterior and lateral wall of the left ventricle and the Gadoteridol injections in the infero-posterior wall and the right ventricle. As control two injections of hydrogel solution without contrast agent were injected. The heart was embedded in a 4 wt% agarose solution at 55 °C in a plastic container. This setup was cooled to 4 °C overnight for complete gelation of the agarose. The following day scans were made in a Philips Ingenia MR 1.5 Tesla system. Scans were T1-weighted 3D Turbo Field with echo times (1.93, 3.54, 5.14, 6.74, 8.34 ms) and a repetition time of 10.21 ms. The field of view was 192 x 144 x 960 mm, reconstructed to 1.25 x 1.25 x 5 mm. Two slices of the scans are presented in Figure 4 (slice 127 and 146). Furthermore a 3D image was rendered to

visualize all injections. As quantification of Gd-based contrast agents is not trivial, volumes were determined of regions expressing increased signal intensities, related to injection of Gd(III) in the heart. By defining a threshold, regions with high signal were selected that contain Gd(III). Total hydrogel volumes were determined by multiplying the number of voxels by the volume per voxel. By varying the threshold, the size of the volume per injection site changes, providing information about the (bio-)distribution.

In Vivo Intramyocardial Injection in a Pig and MRI

A 6-month old female Dalland landrace pig (70 kg) was sedated with an intramuscular injection of midazolam (0.4 mg kg^{-1}), ketamine (10 mg kg^{-1}) and atropine (0.5 mg kg^{-1}). General anesthesia was induced with intravenous infusion of sodium thiopental (5 mg kg^{-1}) and maintained with continuous intravenous infusion of midazolam (0.5 mg kg^{-1} hr^{-1}), sufentanil (2.5 µg kg^{-1} hr^{-1}) and pancuronium bromide (0.1 mg kg^{-1} hr^{-1}). Hereafter, the pig was placed in the Philips Ingenia MR 1.5 Tesla system. UPy-PEG liquid hydrogel precursor pH 9.2 with 2.5 mM UPy-Gd was prepared as just described and 200 µL of this solution was percutaneously injected in the myocardium through the groin using a catheter designed for injection of the viscous UPy-PEG hydrogel precursor(25).

Statistical Analysis

In figure 4B the 'released' samples are displayed as a simple mean ± SD from three samples. The 'remaining in gel' samples are single samples, except for the last data point which is the mean ± SD from two samples. For the MTT assay in supplementary figure 1 each condition was measured in fourfold. The mean and SD of all conditions were normalized to the mean of untreated cells (n = 4). An unpaired two-tailed *t* test was performed with GraphPad Quickcalcs to identify statistically significant differences in metabolic activity of cells treated with UPy-Gd versus Gadoteridol. P values below 0.05 are indicated with a single *, P values below 0.01 indicated with double *, P values below 0.001 with triple *. P values for concentrations that were identified as statistically different are noted in the legend.

Acknowledgements

References

1. Nguyen QV, Huynh DP, Park JH, Lee DS. Injectable polymeric hydrogels for the delivery of therapeutic agents: A Review. Eur. Polym. J. 2015;72:602-619.

2. Zhang YS, Khademhosseini A. Advances in engineering hydrogels. Science 2017; 356, eaaf3627.

3. Annabi N, Tamayol A, Uquillas JA, Akbari M, Bertassoni LE, Cha C, Camci-Unal G, Dokmeci MR, Peppas NA, Khademhosseini A. 25th anniversary article: Rational design and applications of hydrogels in regenerative medicine, Adv. Mater. 2014;26(1):85-124

4. Dong R, Pang Y, Su Y, Zhu X. Supramolecular hydrogels: synthesis, properties and their biomedical applications. Biomater. Sci. 2015;3(7):937.

5. Strandman S, Zhu XX. Self-healing supramolecular hydrogels based on reversible physical interactions. Gels 2016; 2(2):16.

6. Webber MJ, Appel EA, Meijer EW, Langer R. Supramolecular biomaterials. Nat. Mater. 2016; 15(1):13-26.

7. Dankers PYW, Hermans TM, Baughman TW, Kamikawa Y, Kieltyka RE, Bastings MMC, Janssen HM, Sommerdijk NAJM, Larsen A, van Luyn MJA, Bosman AW, Popa ER, Fytas G, Meijer EW. Hierarchical formation of supramolecular transient networks in water: a modular injectable delivery system. Adv. Mater. 2012;24(20):2703-9.

8. Dankers PYW, van Luyn MJA, Huizinga-van der Vlag A, van Gemert FML, Petersen AH, Meijer EW, Janssen HM, Bosman AW, Popa ER. Development and in-vivo characterization of supramolecular hydrogels for intrarenal drug delivery. Biomaterials 2012;33(20):5144-55.

9. Bastings MMC, Koudstaal S, Kieltyka RE, Nakano Y, Pape ACH, Feyen DAM, van Slochteren FJ, Doevendans PA, Sluijter JPG, Meijer EW, Chamuleau SAJ, Dankers PYW. A fast pH-switchable and self-healing supramolecular hydrogel carrier for guided, local catheter injection in the infarcted myocardium. Adv. Healthc. Mater. 2014;3(1): 70-8.

10. Pape ACH, Bakker MH, Tseng CCS, Bastings MMC, Koudstaal S, Agostoni P, Chamuleau SAJ, Dankers PYW. An injectable and drug-loaded supramolecular hydrogel for local catheter injection into the pig heart. J Vis Exp 2015; e52450.

11. Seif-Naraghi SB, Singelyn JM, Salvatore MA, Osborn KG, Wang JJ, Sampat U, Kwan OL, Strachan GM, Wong J, Schup-Magoffin PJ, Braden RL, Bartels K, DeQuach JA, Preul M, Kinsey AM, DeMaria AN, Dib N, Christman KL. Safety and efficacy of an injectable extracellular matrix hydrogel for treating myocardial infarction Sci. Transl. Med. 2013;5(173):5.

12. Dong R, Zhao X, Guo B, Ma PX. Self-Healing Conductive Injectable Hydrogels with Antibacterial Activity as Cell Delivery Carrier for Cardiac Cell Therapy. ACS Appl. Mater. Interfaces 2016;8(27):17138-50.

13. Serpooshan V, Zhao M, Metzler SA, Wei K, Shah PB, Wang A, Mahmoudi M, Malkovskiy AV, Rajadas J, Butte MJ, Bernstein D, Ruiz-Lozano P. The effect of bioengineered acellular collagen patch on cardiac remodeling and ventricular function post myocardial infarction. Biomaterials 2013;34(36):9048-55.

14. Yu J, Takanari K, Hong Y, Lee KW, Amoroso NJ, Wang Y, Wagner WR, Kim K. Non-invasive characterization of polyurethane-based tissue constructs in a rat abdominal repair model using high frequency ultrasound elasticity imaging. Biomaterials 2013;34(11):2701-9.

15. Tondera C, Hauser S, Krüger-Genge A, Jung F, Neffe AT, Lendlein A, Klopfleisch R, Steinbach J, Neuber C, Pietzsch J. Gelatin-based Hydrogel Degradation and Tissue Interaction in vivo: Insights from Multimodal Preclinical Imaging in Immunocompetent Nude Mice.Theranostics 2016;6(12):2114-28.

16. Hong S, Carlson J, Lee H, Weissleder R. Adv. Bioorthogonal Radiopaque Hydrogel for Endoscopic Delivery and Universal Tissue Marking. Healthc. Mater. 2016;5(4):421-6.

17. Blakely B, Hoon Lee B, Riley C, McLemore R, Pathak CP, Vernon BL. Formulation and characterization of radio-opaque conjugated in situ gelling materials. J. Biomed. Mater. Res. B Appl. Biomater. 2010;93(1):9-17.

18. Appel AA, Anastasio MA, Larson JC, Brey EM. Imaging challenges in biomaterials and tissue engineering. Biomaterials 2013;34(28):6615-30.

19. Lei K, Ma Q, Yu L, Ding J. Functional biomedical hydrogels for in vivo imaging. J. Mater. Chem. B 2016;48:7793.

20. Richardson JC, Bowtell RW, Mäder K, Melia CD. Pharmaceutical applications of magnetic resonance imaging (MRI). Adv. Drug Deliv. Rev. 2005;57(8):1191-209.

21. Lohrke J, Frenzel T, Endrikat T, Alves FC, Grist TM, Law M, Lee JM, Leiner T, Li KC, Nikolaou K, Prince MR, Schild HH, Weinreb JC, Yoshikawa K, Pietsch H. 25 Years of Contrast-Enhanced MRI: Developments, Current Challenges and Future Perspectives. Adv. Ther. 2016;33(1):1-28.

22. Mertens ME, Hermann A, Bühren A, Olde-Damink L, Möckel D, Gremse F, Ehling J, Kiessling F, Lammers T. Iron Oxide-labeled Collagen Scaffolds for Non-invasive MR Imaging in Tissue Engineering. Adv. Funct. Mater. 2014;24(6):754-62.

23. Caravan P, Ellison JJ, McMurry TJ, Lauffer RB. Gadolinium(III) Chelates as MRI Contrast Agents: Structure, Dynamics, and Applications. Chem. Rev. 1999;99(9):2293-352.

24. Sequeiros RB, Ojala R, Kariniemi J, Per l J, Niinim ki J, Reinikainen H, Tervonen. MR-guided interventional procedures: a review.Acta Radiol. 2005;46(6):576-86.

25. Tseng CCS, van Slochteren FJ, Bakker MH, Kraaijeveld AO, Dankers PYW, Seevinck PR, Smink J, Kimmel S, Chamuleau SAJ. Active tracked intramyocardial catheter injections for regenerative therapy with real-time MR guidance: feasibility in the porcine heart. In Preparation.

26. Berdichevski A, Simaan Yameen H, Dafni H, Neeman M, Seliktar D. Using bimodal MRI/fluorescence imaging to identify host angiogenic response to implants. Proc. Natl. Acad. Sci. 2015;112(16):5147-52.

27. Berdichevski A, Shachaf Y, Wechsler R, Seliktar D. Protein composition alters in vivo resorption of PEG-based hydrogels as monitored by contrast-enhanced MRI. Biomaterials 2015;42:1-10.

28. Kim JI, Kim B, Chun C, Lee SH, Song SC. MRI-monitored long-term therapeutic hydrogel system for brain tumors without surgical resection. Biomaterials 2012;33(19):4836-42.

29. Colomb J, Louie K, Massia SP, Bennett KM. Self-degrading, MRI-detectable hydrogel sensors with picomolar target sensitivity. Magn. Reson. Med. 2010;64(6):1792-9.

30. Liu J, Wang K, Luan J, Wen Z, Wang L, Liu Z, Wu G, Zhuo R. Visualization of in situ hydrogels by MRI in vivo. J. Mater. Chem. B 2016;4(7)1343.

31. Bull SR, Guler MO, Bras RE, Venkatasubramanian PN, Stupp SI, Meade TJ. Magnetic resonance imaging of self-assembled biomaterial scaffolds. Bioconjug. Chem. 2005;16(6):1343-8.

32. Bakota EL, Wang Y, Danesh FR, Hartgerink JD. Injectable multidomain peptide nanofiber hydrogel as a delivery agent for stem cell secretome. Biomacromolecules 2011;12(5):1651-7.

33. Preslar AT, Tantakitti F, Park K, Zhang S, Stupp SI, Meade TJ. (19)F Magnetic Resonance Imaging Signals from Peptide Amphiphile Nanostructures Are Strongly Affected by Their Shape. ACS Nano 2016;10(8):7376-84

34. Hendrikse SIS, Wijnands SPW, Lafleur RPM, Pouderoijen MJ, Janssen HM, Dankers PYW, Meijer EW. Controlling and tuning the dynamic nature of supramolecular polymers in aqueous solutions.Chem. Commun. 2017;53(14):2279-228.

35. Rogosnitzky M, Branch S. Gadolinium-based contrast agent toxicity: a review of known and proposed mechanisms. Biometals 2016;29(3):365-76.

36. Rohrer M, Bauer H, Mintorovitch J, Requardt M, Weinmann HJ. Comparison of magnetic properties of MRI contrast media solutions at different magnetic field strengths. Invest. Radiol. 2005;40(11):715-24..

37. Laurent S, Elst LV, Muller RN.. Comparative study of the physicochemical properties of six clinical low molecular weight gadolinium contrast agents. Contrast Media Mol. Imaging 2006;1(3):128-37.

38. Werner EJ, Datta A, Jocher CJ, Raymond KN.Raymond. High-relaxivity MRI contrast agents: where coordination chemistry meets medical imaging.Angew. Chem. Int. Ed. 2008;47(45):8568-80.

39. van den Akker F, Feyen DA, van den Hoogen P, van Laake LW, van Eeuwijk EC, Hoefer I, Pasterkamp G, Chamuleau SA, Grundeman PF, Doevendans PA, Sluijter JP. Intramyocardial stem cell injection: go(ne) with the flow. Eur. Heart J. 2017;38(3):184-186.

40. de Feijter I, Goor OJGM, Hendrikse SIS, Comellas-Aragonès M, Söntjens SHM, S. Zaccaria S, Fransen PPKH, Peeters JW, Milroy LG, Dankers PYW. Solid-Phase-Based Synthesis of Ureidopyrimidinone–Peptide Conjugates- for Supramolecular Biomaterials. Synlett 2015;26(19):2707-13.

41. Dadabhoy A, Faulkner S, Sammes PG. Long wavelength sensitizers for europium(III) luminescence based on acridone derivatives. J. Chem. Soc., Perkin Trans. 2002;2348.

42. De León-Rodríguez LM, Kovacs Z. The synthesis and chelation chemistry of DOTA-peptide conjugates. Bioconjug. Chem. 2008;19(2):391-402.

6

Active tracked intramyocardial catheter injections for regenerative therapy with real-time MR guidance: feasibility in the porcine heart

C.C.S. Tseng, F.J. van Slochteren, M.H. Bakker, A.O. Kraaijeveld, P.Y.W. Dankers, P.R. Seevinck, J. Smink, S. Kimmel, S.A.J. Chamuleau

Abstract

Background

Interventional MRI is used in multiple clinical areas. Although interventional MRI has important benefits with respect to soft tissue contrast and omits ionizing radiation, its use in interventional cardiology is limited. Because MRI is the gold standard for the assessment of infarct transmurality, MRI guided delivery of regenerative therapies into the infarct border zone of ischemic HF patients is a logical and attractive strategy. In this study we have developed a platform for MR-guided intramyocardial injections with real-time active tracking. In this study we show feasibility in a healthy porcine heart.

Method and results

Our new method for MR-guided intramyocardial injections consists of a new injection catheter with integrated coils for active tracking, in combination with the existing iSuite software platform for interventional MR. Furthermore, we use a novel supramolecular hydrogel crosslinked with MRI contrast agent, which can readily be visualized with MRI for injections. Using this approach, navigation to injection targets with real-time imaging, alternatingly using passive visualization and active tracking, was feasible and intramyocardial injections were performed successfully.

Conclusion

For the first time, we have shown that with our system it is feasible to navigate towards and inside the heart using real-time MR guidance with a combination of passive visualization and active catheter tracking. Moreover accurately targeted intramyocardial injections were performed in the heart. With this interventional MRI based platform for intramyocardial injections we aim to accelerate the development and progress of cardiac regenerative therapy. In parallel we accelerate interventional MRI towards clinical applications.

Introduction

The use of interventional magnetic resonance imaging (iMRI) has been accomplished in a variety of clinical areas(1,2). Unlike x-ray fluoroscopy, MRI lacks ionizing radiation, has superb soft tissue contrast and provides functional data. With all the aforementioned benefits MRI qualifies as a promising method to guide interventions(3). The potential of interventional cardiovascular procedures has been demonstrated in clinical research, especially for catheter ablations (1,4–6), however its applications in interventional cardiology are still limited. The MRI scanner is accepted worldwide as a diagnostic device, and for various diagnoses MRI is considered to be the gold standard technique. Multiple interventions would benefit from the direct measurement of the therapeutic effect during intervention. For example, visualization of the lesions created during the RF ablation procedure and instant feedback on the success of intramyocardial injections in the heart. For the latter purpose MRI can bring an additional advantage in terms of accurate targeting of the area of interest as a main limitation of regenerative therapies with existing delivery strategies is low accuracy and low retention of therapeutics(7–11). Despite the advancements of injection techniques from blind intramyocardial injections to targeted intramyocardial injections using electromechanical mapping (EMM)(7) the effects of regenerative therapies remain limited. Additionally, amongst users there is some debate on the reproducibility, accuracy and detailed identification of the infarct border zone by EMM. Because Late Gadolinium Enhanced (LGE) MRI is the gold standard for assessment of the infarct location and mass we hypothesize that intramyocardial injections based on the gold standard infarct assessment technique could substantially boost the effect of regenerative therapies. Currently, the infarction border zone is considered the target for cardiac regenerative therapies, but by using MRI other definitions of the target area (e.g. myocardial perfusion, deformation) can be considered.

The feasibility and value of image fusion with MRI has already been shown(7,12–14). Ultimately, to avoid ionizing radiation and the repetitive use of contrast and time-consuming procedures for image fusion, we have developed a clinically feasible system to perform MRI-guided intramyocardial injections. In this study, we report on the development process, the practical issues and the solutions for interventional cardiac MR in the field of cardiac regenerative therapy. A novel catheter was developed for retrograde passage of the aortic valve with MRI guidance and navigation in the left ventricle (LV). Finally, we show the first

guided intramyocardial injections of an MRI visible biomaterial in a healthy pig using both active tracking and live imaging interventional MRI.

Catheter tracking

In principle two methods of catheter tracking can be used: active tracking and passive visualization (**Table 1**). Passive catheter visualization relies on properties of the materials in the catheter to create a signal void. A disadvantage of passive catheter visualization is the fact that the device is only visible within the selected imaging plane(2). This means that the imaging plane must be adapted to the catheter position by the operators. For an efficient procedure, communication between the interventional cardiologist and the system operator is therefore of paramount importance. A major advantage of passive visualization is the possibility to see the trajectory of the catheter in combination with live imaging. With active tracking, receiver coils are incorporated in the tip of the catheter to measure catheter position and orientation directly in the scanner coordinate system. Navigation during active tracking is based on high-resolution anatomical imaging (roadmap scan) that is acquired just prior to the interventional procedure. Complementary to the anatomical images a 3D endomyocardial surface can be rendered in the navigational dataset to visualize anatomy and project features of cardiac pathology or function. In applications for RF ablations parameters used for projection usually are endocardial surface potentials(2). In case of cardiac regenerative therapy a color-coded infarct transmurality to target the injections to the infarction border zone will most likely be used. Because the location of the catheter tip is measured, the plane within the roadmap scan can be automatically adapted to the location of the catheter for visualization(3). With active tracking the tip and 2 cm of the shaft of the catheter are rendered during the navigation. The sampling rate of the catheter position is 3Hz. In combination with the automatic image plane updating this enables very intuitive catheter handling(6). The high catheter sampling frequency and automatic image plane adaption makes active tracking much easier and faster than passive visualization in combination with live imaging. Since the target locations for the injections are displayed on the endocardial surface mesh, active tracking allows the user to target distinct locations in the myocardium. Nonetheless, a possible advantage of passive visualization is the ability to see the complete curve of the catheter with respect to the heart in real time. This allows the physician to assess the curve of the catheter with respect to the myocardial wall and can

especially be of additional value for intramyocardial injections. An important difference between passive and active tracking is that passive tracking in fact is solely device visualization, while with active catheter tracking the device is localized in coordinates(3).

Table 1. Characteristics of active tracking vs passive visualization

Active catheter tracking	Passive catheter visualization
Based on integrated receiver coils	Based on intrinsic properties of catheter material
Catheter is visualized in high resolution pre-acquired 3D roadmap	Catheter is only visible in image plane that is acquired
Automatic updating of image plane	Image plane needs manual updating
Catheter tip is visible (rendered)	Trajectory of catheter is visible

MR-guided injection platform

One reason for the limited use of interventional MRI in the field of cardiac interventions is the lack of available and certified equipment. For catheter applications, the heating of the devices and the tendency to disturb the magnetic field and impair the image quality needs to be solved reliably. Real-time navigation and MR-guided injections with high precision and detail in the myocardium therefore require specific tools and technologies. Within this project we have combined 3 essential components:

1. An interventional MRI setup in which the catheter is connected to the MRI scanner in order to use the catheter coils for positioning of the catheter in the scanner coordinates

2. A steerable injection catheter that facilitates good maneuverability, has an extendable needle, and that can be coupled with the MRI scanner for visibility in conjunction with the images.

3. An injectable biomaterial that is coupled with an MRI contrast agent. In this way the biomaterial can be combined with biologics before injection to sustain the release of the biologics in the heart after injection, and to visualize the location of the injections immediately after the injection.

Not only the equipment but also a different procedure is developed. The most pronounced difference to previously performed cardiac MRI guided interventions is the retrograde passage through the aortic valve with the Imricor catheter to enter the LV.

Materials and method

Animals

Animal experiments were conducted in accordance with the *Guide for the Care and Use of Laboratory Animals* by the Institute of Laboratory Animal Resources. The experiments were approved by the Animal Experimentation Committee of the Medicine Faculty of the Utrecht University, the Netherlands. In this study experiments were performed in three 6-month old female Dalland landrace pigs (70kg). The experiments were performed with general anesthesia after sedation with an intramuscular injection of midazolam (0.4mg/kg), ketamine (10mg/kg) and atropine (0.5mg/kg). General anesthesia was induced with intravenous infusion of sodium thiopental 5mg/kg and maintained with continuous intravenous infusion of midazolam (0.5mg/kg/hr), sufentanil (2.5µg/kg/hr) and pancuronium bromide (0.1mg/kg/hr). Post-procedural the animals were euthanized with a bolus injection of 20ml 7.5% KCL. The heart was harvested, embedded in an agarose solution and stored at 4°C.

Interventional suite and tracking interface

The real-time image guidance platform iSuite (Philips Research, Hamburg, Germany) was installed on a 1.5 T MR scanner (Ingenia, Philips Healthcare, Best, Netherlands) in the University Utrecht (UU) veterinary radiology facility. This platform is composed of an interventional workstation that contains a real-time bi-directional interface for real-time scanner communication. The interventional MR workstation is connected to the conventional MR scanner console. Pre-acquired images from the scanner (DICOM) can then be integrated in the interventional workstation. The components and setup of the interventional suite are shown in **Figure 1**. This system has been used in clinical research applications for MR-guided EP interventions(5,17). Navigation can be done either on pre-acquired images (active tracking) or real-time images (passive visualization). For active tracking, the connection between iSuite and the catheter was implemented by using the Imricor tracking interface as used for the MRI guided ablations setup(5).

Figure 1. Schematic overview of interventional MR setup
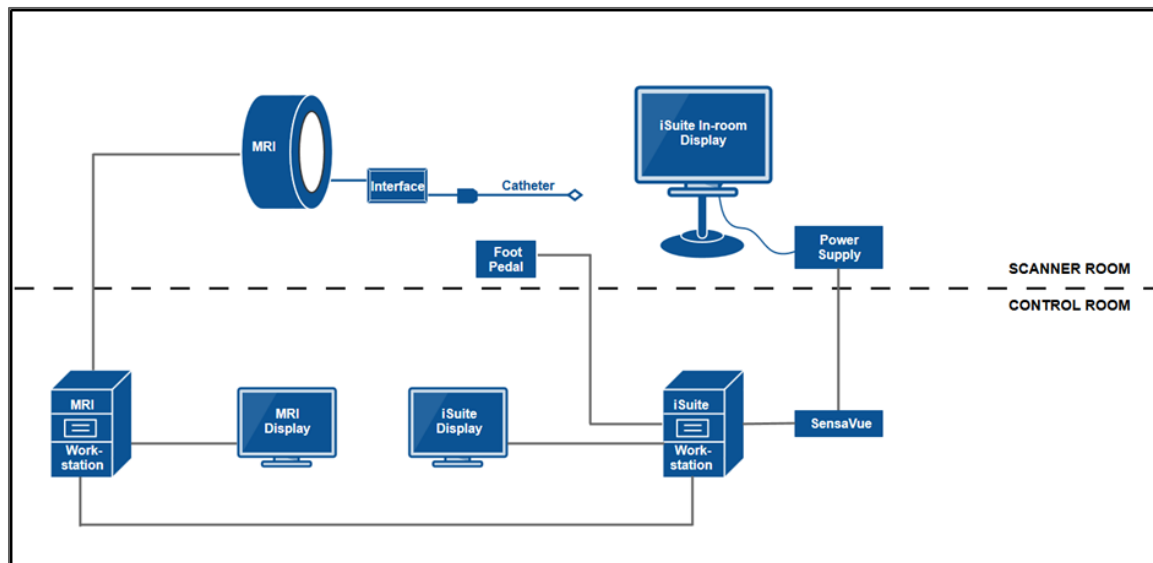
MR compatible injection catheter

A trackable and steerable injection catheter (Imricor Medical Systems, Burnsville, MN, USA) was designed and developed for use in the MR (**Figure 2A**). This catheter is adapted from a standard Imricor ablation catheter(1,6). It has a 9 French outer diameter with a length of approximately 110cm. The deflection curve is uni-directional with an inside curve diameter of 32 mm at 180 degrees of deflection. The deflection is accomplished via a polymer pull wire that is bonded at the tip distally and anchored in the handle proximally. The needle has an overall length of 145 cm and is an assembly of Nitinol (last distal 13 cm) and a polymer (proximal 132 cm) section that are bonded. The distal needle has an inner diameter of 0.25 mm (30-gauge) and an outer diameter of 0.50 mm (24-gauge) while the polymer section has an inner diameter of 0.64 mm and an outer diameter of 1.15 mm. In comparison to a NOGA catheter (27-gauge) the needle outer diameter of our developed catheter is larger, allowing easier injection of the hydrogel, with a limitation of the exerted pressure. The needle tip has an approximately 20-degree straight bevel and needle extension can be adjusted to left ventricular (LV) wall thickness. Two MR receiver coils are integrated into a support section in the catheter tip, allowing real-time imaging of the position and orientation of the catheter tip in the 1.5 T MR system. The coils are each 1.7mm long and have a space of 6 mm between them. In addition to the possibility for active catheter tracking, the signal void created by the receiver coils also allows passive visualization.

Figure 2. Injection catheter
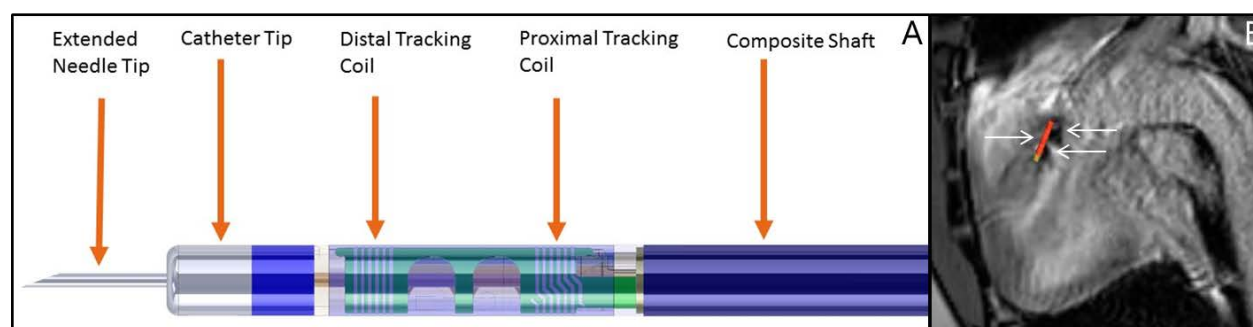
A) Translucent view of the distal catheter. B) The distal part of the catheter is demonstrated near the aortic valve with passive visualization (arrows) while the previously active tracked catheter tip is still imaged.

UPy-PEG hydrogelator

As injectable carrier material a ureido-pyrimidinone (UPy) based supramolecular pH-responsive hydrogel was chosen. This hydrogelator consists of a poly ethylene glycol (PEG, M_n 10 kDa) end-functionalized with two UPy moieties, and has been utilized effectively for the delivery of therapeutics in the heart (18). At basic pH (9.5), the UPy-PEG hydrogelator exhibits a relatively low viscosity that allows injection through a catheter; after which gelation takes place when it comes into contact with tissue of a physiological pH (7.4)(19). In order to visualize the UPy-PEG hydrogel with MR it was supramolecularly modified with the contrast-enhancing agent UPy-Gd. This contrast agent is specifically designed to interact with the UPy-PEG hydrogelator. For injections a 10wt % UPy-PEG hydrogel was used with a 2.5mM UPy-Gd concentration.

Magnetic resonance imaging

Prior to the intervention, a three-dimensional (3D) roadmap containing the heart and thoracic aorta was acquired in free-breathing by using a respiratory and cardiac gated fat-suppressed T1-weighted 3D whole heart balanced turbo field echo (bTFE) sequence. Respiratory and cardiac gating was performed using a pencil-beam navigator and ECG signal, respectively. Imaging parameters included echo time (TE)/repetition time (TR) = 2.3 ms / 4.7 ms and isotropic voxel size of 1.5 mm^3 reconstructed to 1.15 x 1.15 x 1.5 mm^3. An LV endocardial surface mesh was created based on the 3D T1-w bTFE. The LV was segmented with ITK-SNAP software and imported into iSuite (**Figure 3**) as well as a fictive infarct border zone (**Figure 4**). The 3D roadmap and surface mesh were used for catheter tracking during the procedure. During the procedure, the catheter tip position obtained using active tracking

facilitated multiplanar reformatting of the 3D T1-w bTFE roadmap data, enabling navigation in the descending aorta and LV. During injections, passive tracking was used by means of an interactive 2D balanced steady-state-free-precession (bSSFP) sequence with a 3 Hz frame rate. As such the position and orientation of the catheter was monitored in real time in the desired orientation. Post injection multiple 2D T1-w TFE late gadolinium enhancement (LGE) with phase sensitive inversion recovery reconstruction (PSIR) sequences were used to visualize the injected hydrogel immediately after the injection. Imaging parameters included TE/TR = 3.0 ms /6.1 ms; Flip angle = 25; in-plane resolution 1.6 x 2.0 mm reconstructed to 0.9 mm x 0.9 with slice thickness of 10 mm. Ex-vivo viability MRI of the embedded heart was performed one day after the injections using 3D T1-w TFE LGE with resolution 2 x 3.3 x 5 mm reconstructed to 1.23 x 1.23 x 5 mm.

Results

After the induction of anesthesia and mechanical ventilation, arterial access was gained via the femoral artery and a 10fr sheath was inserted. Hereafter the pig was placed in the MRI scanner to acquire high-resolution anatomical images in order to create a 3D whole heart roadmap.

Accessing the left ventricle

The deflectable injection catheter was placed in the LV via the femoral artery sheath using consecutive real-time MR-guided passive visualization and active tracking. When the operators switch from active tracking to passive visualization the position of the catheter tip remains visible at the last location of active tracking while passive visualization is used (**Figure 2B**). The sample frequency of 3Hz and 5-10 Hz respectively used during active tracking and passive visualization facilitates sufficient visualization of the catheter and catheter tip to allow intuitive maneuvering of the catheter within the LV.

Figure 3. Screenshot iSuite display during navigation in the ascending aorta.
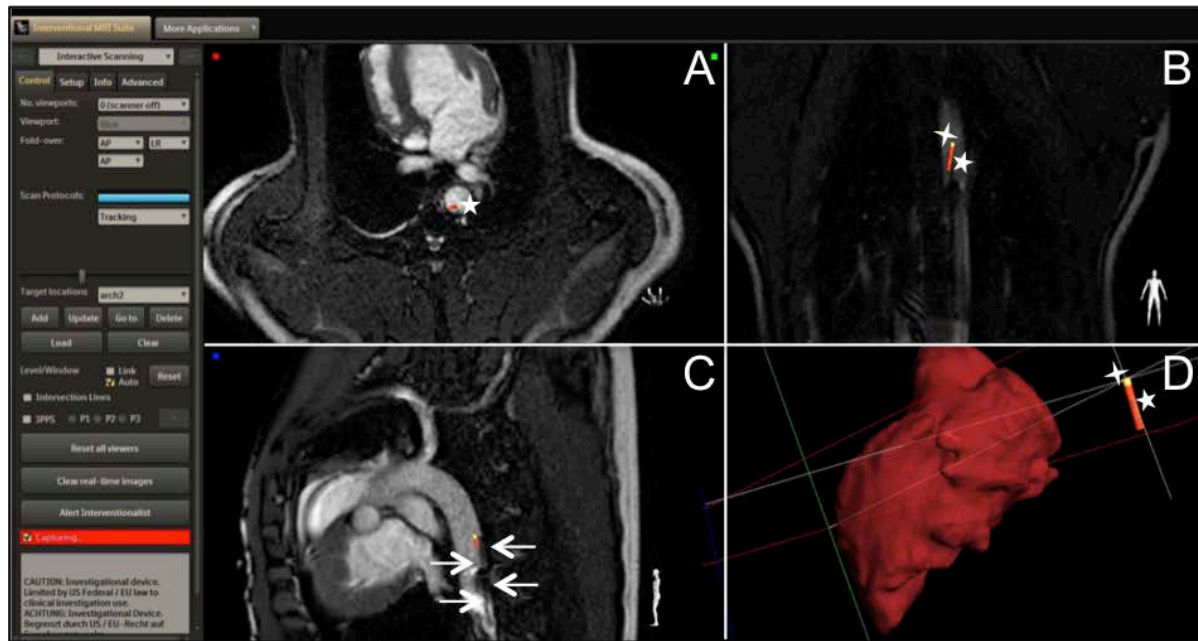
*Three orthogonal views (**A,B,C**) and 3D LV segmentation (**D**) are shown. The actively tracked injection catheter is depicted in red (★) and the catheter tip in yellow(▼). The trajectory of the catheter is passively visualized (arrows).*

Navigation and steering

To assess the navigation and steering capabilities of the system we have challenged an experienced interventional cardiologist to target a simulated infarct border zone, which was projected on the apical septum (**Figure 4**). After guidance of the catheter to the target by using active tracking, the imaging method was switched to passive visualization. When perpendicular angulation of the catheter tip with respect to the myocardial wall was confirmed (**Figure 5**), the needle was pushed into the tissue using the needle extension mechanism. When needle penetration into the myocardium was confirmed by a premature ventricular complex (PVC) on the body surface ECG, an injection was performed.

Intramyocardial injections

Targeting of the specific locations (**Figure 5**) was possible with sufficient control over the procedure. Three to five injections of 200-300μL were performed in the targeted simulated border zone.

Figure 4. LV segmentation with infarct border zone
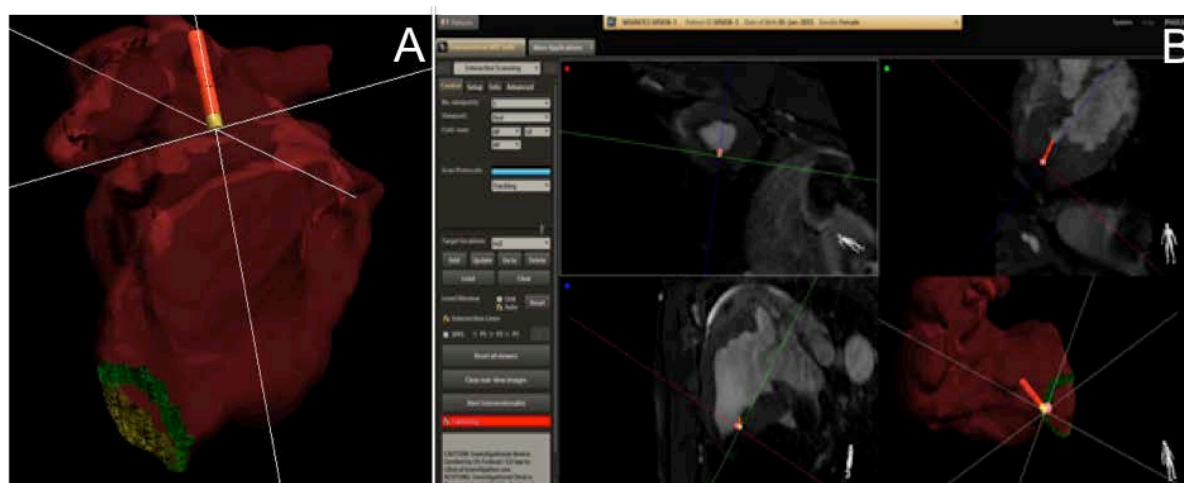
*LV segmentation with imported infarct border zone (green rim) in right anterior oblique (RAO) orientation (**A**) and screenshot of iSuite display with the catheter tip at the target location in the infarct border zone (**B**).*
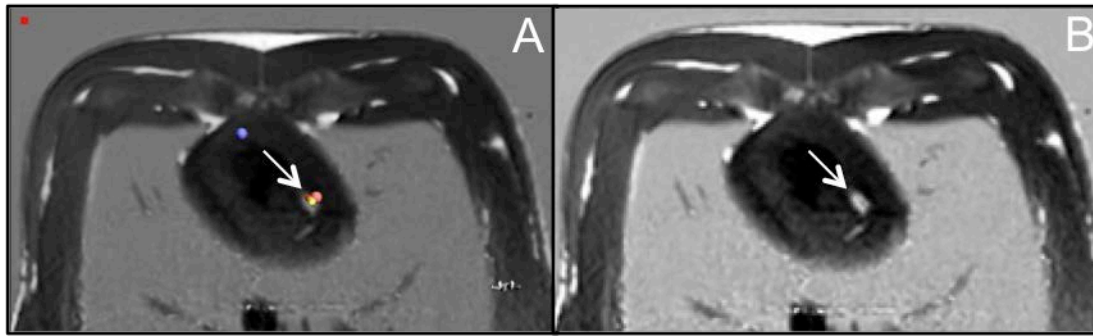
Figure 5. iSuite screenshot
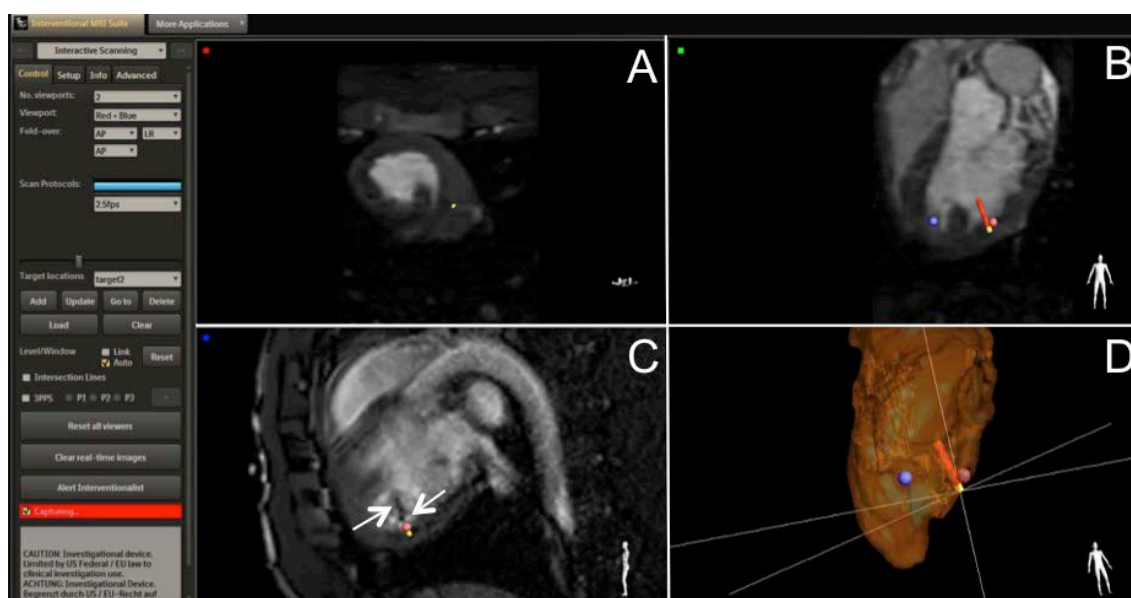
*iSuite screenshot with three orthogonal views (**A,B,C**) and 3D LV endocardial segmentation (**D**) are shown. After navigation with active tracking to the target location (red marker) the catheter is passively visualized (arrows) to confirm location and perpendicularity of the catheter tip to the myocardial wall.*

The live imaging during the injection allows the live visualization of the injected material. However, in practice an LGE-MRI scan was performed directly after an injection to visualize the injection spots in-vivo (**Figure 6 A+B**). Reconstructed post-injection images are depicted in **Figure 7**.

Figure 6. In-vivo post injection imaging.

A) iSuite screenshot of one orthogonal view. The target location (red) is depicted with actively tracked catheter (red/yellow) and the injection spot (arrow). B) MR LGE PSIR imaging of injection spot (arrow).

Figure 7. Ex-vivo imaging
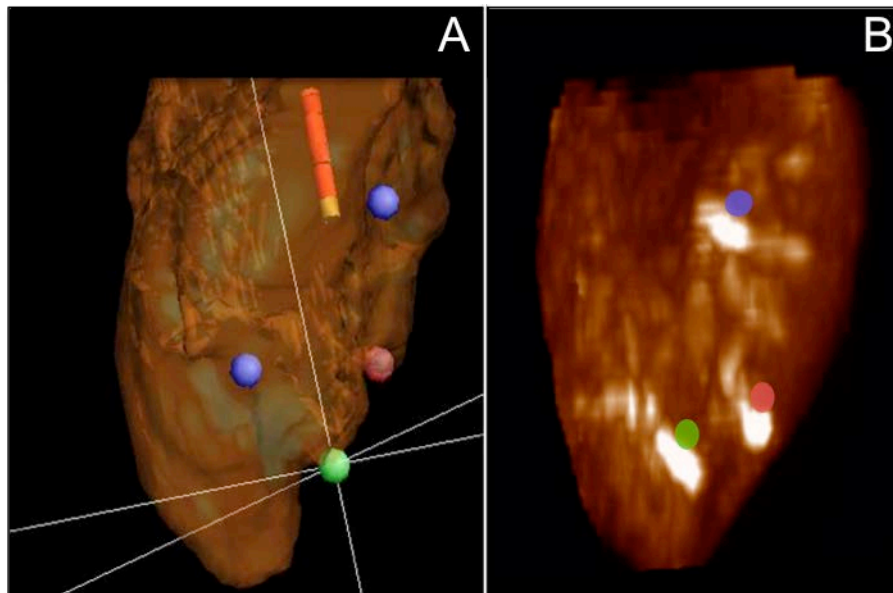
A) 3D LV model with targets in iSuite and B) 3D reconstruction of ex-vivo LGE imaging visualized from the left lateral side.

Practical aspects

The current stage of our method for MRI guided intramyocardial injections is of experimental nature and is therefore elaborate and involves a large team. A minimum of two operators in the control room and two operators in the scanner room are currently required to perform a procedure. As the team gains experience, we expect the procedure to be comparable to the current standard with regard to procedure-time. However, with respect to injection accuracy to the infarction border zone and radiation time and dose we expect to surpass the current standard.

Discussion

In this pilot study, we demonstrate for the first time the feasibility of intramyocardial injections of an MRI visible biomaterial by interventional MRI using a combination of active tracking and passive visualization.

A combined scientific and industrial consortium, MIGRATE (MrI Guided RegenerAtive ThErapy), was initiated to establish this clinically applicable MRI compatible injection strategy. By constructing the MIGRATE consortium we were able to combine state of the art technology in MRI compatible, steerable and trackable catheter design, real time in vivo catheter visualization and the MRI visible and injectable biomaterial. Hereby we extend the pallet of MR guided interventions to the field of cardiac regenerative therapy. Although the use of MRI for interventions is not entirely new some aspects of the described procedure are new. For instance the retrograde passage through the aortic valve with the Imricor catheter has been used for the first time in the described experiments. We chose to approach the LV via the aforementioned route since it is the familiar route of the current gold standard catheter injection technique that allows access to the desired locations in the LV. The retrograde route through the aortic valve with the Imricor catheter was challenging, and caused some kinking, resulting in malfunctioning catheters. Nevertheless the chosen route led to successful injections in all pigs.

By developing a clinically feasible setup we aim to introduce interventional MRI to the pallet of techniques that can be used to gain knowledge and, on the longer term, improve the effects of cardiac regenerative therapies. By using MRI to guide intramyocardial injections for cardiac regenerative therapies, an alternative is created for the endocardial mapping based techniques. Our new method is based on the gold standard LGE-MRI infarct imaging which has superb spatial resolution. Hereby we aim to reduce the inadequacy of injection techniques and maximize the effects of cardiac regenerative therapy. The additional value of MRI for the standardization of treatment planning has been reported previously(7). Target accuracy and retention with our novel injection strategy have to be studied in large animal models with and without myocardial infarction, along with the potential gain in therapeutic efficacy. Another and maybe larger benefit of iMRI is the ability to visualize the injected biomaterial directly after injection. This allows the user to increase the amount of injections until a biologically relevant deposit of the biologic is created at the optimal location. In other words, with our method for the first time real dose finding studies can be done in which the

flushing out of the myocardium is compensated for(9). Of note, the developed method is unrelated to the chosen regenerative strategy, since cells, growth factors, exosomes, or other biologics can be used as the therapeutic compound. Since the search for the most potential regenerative therapeutic is still ongoing, the future will tell which material or compound will ultimately be given to patients. The ambitions of this project have been deliberated in an interactive workshop with the Dutch cardiovascular patient association. Patients understand the power of this approach and also acknowledge the potential advantages in terms of time and risk for the patient (PULS 2016, Dutch Heart foundation).

With regard to the injectable material used in this study, UPy-PEG hydrogel was shown to be potentially beneficial for retention in the heart, however safety of this hydrogelator, with regard to embolization of the hydrogel and toxicity of the contrast agent UPy-Gd, still has to be examined. Concerning therapeutic efficacy, compatibility of UPy-PEG hydrogel with for instance cells or exosomes needs to be evaluated as well as additional effects of more accurate injections. For translational purposes, safety and procedure time of this approach have to be studied.

The first steps towards a clinical application of cardiac interventional MR are already performed in the setting of right heart catheterizations and cardiac biopsies(2,20). Eventually, the use of MR-guidance may help to shorten procedures, lower the risk (i.e. no exposure to radiation, no need for repetitive contrast injection) and improve injection accuracy of regenerative therapies. Ultimately, we envision that this optimal delivery strategy with accurate treatment planning is the next step forward to improve strategies for cardiac regeneration.

Limitations

Because not all needle penetrations into the tissue were confirmed by a PVC on the ECG, good needle insertion into the tissue could not be guaranteed at all pre-procedurally selected targets. At the locations with no confirmation of the needle insertion into the tissue, we did not perform an injection. The lack of a PVC on the ECG could be the result of inadequate wall contact with the catheter or lack of adequate needle extension. The other way around, a PVC on the ECG is not a unique requirement for needle insertion in the tissue.

Incorporation of an electrode in the catheter tip to directly measure wall contact or measure depolarization to derive wall contact might be helpful in this regard.

Conclusion

We reported for the first time that real-time MRI-guided intramyocardial injections with combined active and passive catheter tracking are feasible. The use of a pH switchable hydrogel that has MR visibility provides the opportunity to track injections in vivo directly after injection and also during follow up post-injection. Sustained contrast in the myocardium suggests that the hydrogel retains in the myocardial wall after injection. This novel delivery strategy may advance the accuracy and efficacy of cardiac regenerative therapies.

Acknowledgment

References

1. Grothoff M, Piorkowski C, Eitel C, Gaspar T, Lehmkuhl L, Lücke C, et al. MR Imaging-guided Electrophysiological Ablation Studies in Humans with Passive Catheter Tracking: Initial Results. Radiology. 2014;271(3):695–702.

2. Rogers T, Lederman RJ. Interventional CMR: Clinical Applications and Future Directions. Curr Cardiol Rep. 2015;17(5).

3. Wang W. Magnetic Resonance–guided Active Catheter Tracking. Magn Reson Imaging Clin N Am. 2015;23(4):579–89.

4. Sommer P, Grothoff M, Eitel C, Gaspar T, Piorkowski C, Gutberlet M, et al. Feasibility of real-time magnetic resonance imaging-guided electrophysiology studies in humans. Europace. 2013;15(1):101–8.

5. Hilbert S, Sommer P, Gutberlet M, Gaspar T, Foldyna B, Piorkowski C, et al. Real-time magnetic resonance-guided ablation of typical right atrial flutter using a combination of active catheter tracking and passive catheter visualization in man : initial results from a consecutive patient series. Europace. 2015;

6. Grothoff M, Gutberlet M, Hindricks G, Fleiter C, Schnackenburg B, Weiss S, et al. Magnetic resonance imaging guided transatrial electrophysiological studies in swine using active catheter tracking – experience with 14 cases. Eur Radiol. 2016;

7. van Slochteren FJ, van Es R, Koudstaal S, van der Spoel TIG, Sluijter JPG, Verbree J, et al. Multimodality infarct identification for optimal image-guided intramyocardial cell injections. Netherlands Hear J. 2014;22(11):493–500.

8. Tongers J, Losordo DW, Landmesser U. Stem and progenitor cell-based therapy in ischaemic heart disease: promise, uncertainties, and challenges. Eur Heart J. 2011 May;32(10):1197–206.

9. van den Akker F, Feyen D a M, van den Hoogen P, van Laake LW, van Eeuwijk ECM, Hoefer I, et al. Intramyocardial stem cell injection: go(ne) with the flow. Eur Heart J. 2016;ehw056.

10. van der Spoel TIG, Vrijsen KR, Koudstaal S, Sluijter JPG, Nijsen JFW, de Jong HW, et al. Transendocardial cell injection is not superior to intracoronary infusion in a porcine model of ischaemic cardiomyopathy: a study on delivery efficiency. J Cell Mol Med. 2012;16(11):2768–76.

11. Hou D, Youssef EAS, Brinton TJ, Zhang P, Rogers P, Price ET, et al. Radiolabeled cell distribution after intramyocardial, intracoronary, and interstitial retrograde coronary venous delivery: Implications for current clinical trials. Circulation. 2005;112(9 SUPPL.):150–7.

12. Dauwe DF, Nuyens D, De Buck S, Claus P, Gheysens O, Koole M, et al. Three-dimensional rotational angiography fused with multimodal imaging modalities for targeted endomyocardial injections in the ischaemic heart. Eur Heart J Cardiovasc Imaging. 2014;15(8):900–7.

13. Hatt CR, Jain AK, Parthasarathy V, Lang A, Raval AN. MRI-3D ultrasound-X-ray image fusion with electromagnetic tracking for transendocardial therapeutic injections: In-vitro validation and in-vivo feasibility. Comput Med Imaging Graph. 2013;37(2):162–73.

14. Tomkowiak MT, Klein AJ, Vigen KK, Hacker TA, Speidel MA, Vanlysel MS, et al. Targeted Transendocardial Therapeutic Delivery Guided by MRI — X-ray Image Fusion. Catheter Cardiovasc Interv. 2011;78:468–78.

15. Krombach GA, Pfeffer JG, Kinzel S, Katoh M, Günther RW, Buecker A. MR-guided percutaneous intramyocardial injection with an MR-compatible catheter: feasibility and changes in T1 values after injection of extracellular contrast medium in pigs. Radiology. 2005;235(2):487–94.

16. Corti R, Badimon J, Mizsei G, Macaluso F, Lee M, Licato P, et al. Real time magnetic resonance guided endomyocardial local delivery. Heart. 2005;91(3):348–53.

17. Chubb H, Harrison J, Williams S, Weiss S, Krueger S, Rhode K, et al. First in man: real-time magnetic resonance-guided ablation of typical right atrial flutter using active catheter tracking. Europace. 2014;

18.   Bastings MMC, Koudstaal S, Kieltyka RE, Nakano Y, Pape ACH, Feyen DAM, et al. A fast pH-switchable and self-healing supramolecular hydrogel carrier for guided, local catheter injection in the infarcted myocardium. Adv Healthc Mater. 2014;3(1):70–8.

19.   Pape ACH, Bakker MH, Tseng CCS, Bastings MMC, Koudstaal S, Agostoni P, et al. An Injectable and Drug-loaded Supramolecular Hydrogel for Local Catheter Injection into the Pig Heart. J Vis Exp. 2015;100(e52450).

20.   Rogers T, Ratnayaka K, Karmarkar P, Campbell-Washburn AE, Schenke WH, Mazal JR, et al. Real-Time Magnetic Resonance Imaging Guidance Improves the Diagnostic Yield of Endomyocardial Biopsy. JACC Basic to Transl Sci. 2016;1(5):376–83.

PART TWO

EXPLORING OPPORTUNITIES IN END-STAGE HEART FAILURE

7

Advanced strategies for end-stage heart failure: combining regenerative approaches with LVAD, a new horizon?

C.C.S. Tseng, F.Z. Ramjankhan, N. de Jonge, S.A.J. Chamuleau

Abstract

Despite the improved treatment of cardiovascular diseases the population with end-stage heart failure is progressively growing. The scarcity of the gold standard therapy, heart transplantation, demands novel therapeutic approaches. For patients awaiting transplantation ventricular assist devices have been of great benefit on survival. To allow explantation of the assist device and obviate heart transplantation, sufficient and durable myocardial recovery is necessary. However, explant rates so far are low. Combining mechanical circulatory support with regenerative therapies such as cell(-based) therapy and biomaterials might give rise to improved long-term results. Although synergistic effects are suggested with mechanical support and stem cell therapy, evidence in both preclinical and clinical setting is lacking. This review focuses on advanced and innovative strategies for the treatment of end-stage heart failure and furthermore appraises clinical experience with combined strategies.

Introduction

Heart failure (HF) is a progressive disease with an important economic burden on today's healthcare. After initial injury progressive worsening maladaptive (cellular and structural) changes result in a process called ventricular remodeling, eventually leading to diminished cardiac function(1,2). According to the Framingham study the incidence of heart failure has remained stable since the 1970s(3). Despite this unchanged incidence the population of HF patients is growing, affecting up to around 23 million patients worldwide, due to various aspects. Improvement in the acute therapy of myocardial infarction (MI) has played a major role in survival rates. Other non-pharmacological treatment options such as ICD therapy have further decreased mortality. In addition, the widespread use of ACE-inhibitors, ATII-blockers, beta-blockers, and aldosterone-antagonists, but also cardiac resynchronization therapy further enhanced survival among HF patients. These developments in combination with an aging population translate into an increase in the prevalence of chronic "end-stage HF"(4,5). Although not clearly defined, according to the guidelines for heart transplantation, heart transplantation should be considered in patients with severe symptoms of HF, intractable angina or rhythm disturbances, without any alternative form of treatment available and with a poor prognosis(6). Concerning the guidelines for HF there are different types of management approaches, which can be broadly subdivided in 3 groups, [1] general/non-pharmacological measures, [2] pharmacological therapy and [3] devices and surgery(7,8). The only current available therapy for end-stage HF is heart transplantation. Opposed to an increasing demand for donor hearts, the number of heart transplantations in Europe has diminished in recent years. In the Netherlands especially, decreasing mortality after traffic accidents, older donors and shift from heart-beating donation to non-heart-beating procedures gave rise to a further decreasing amount of donors(6). To compensate for the shortcoming of donors, novel therapeutic strategies are inevitable. Experimental regenerative therapies, intended to restore functional cardiac cells and myocardial function are of great interest(9,10). For some patients mechanical circulatory support (MCS) with a ventricular assist device (VAD) is an option. This review will focus on current and novel, advanced therapeutic strategies for end-stage HF.

Current therapies for end-stage heart failure

Heart transplantation

In European countries that are represented by the ESC there are estimated to be over 10 million patients with HF(7). For the Netherlands this number is believed to be between 100.000 and 150.000 patients, and is expected to rise to approximately 195.000 in 2025(11). These numbers are probably underestimated and lack accuracy due to the absence of a uniform definition for HF. Easier to determine is the number of patients waiting for a donor heart. Eurotransplant is the international collaborative framework responsible for allocation of donor organs in the Netherlands, Austria, Belgium, Croatia, Germany, Hungary, Luxembourg and Slovenia. Annual statistics show a rising number of patients on the waiting list, with an actual number of 1250 patients at the end of December 2013, a 2.5 fold increase compared to 2000(12). With a total of 563 heart transplantations in 2013 the scarcity of donor hearts is evident. In the Netherlands the same trend is seen. Added up with the progressive decline in the amount of donors, heart transplantation will not relieve the burden of HF on healthcare.

Mechanical support

As briefly stated in the introduction MCS with a ventricular assist device is a possibility for some patients. Ventricular assist devices can be used as a bridge to transplantation, recovery or decision, and as destination therapy. These mechanical pumps partially or completely take over ventricular function to support circulation. Either the left ventricle (LV), right ventricle (RV) or both ventricles can be unloaded. Predominantly left ventricular assist devices (LVADs) are implanted because of disappointing results of biventricular assist device (BIVAD) support(13). Since the first successful implantation of a VAD in 1966 by DeBakey(14), mechanical support has shown to be of great value in survival of patients with advanced HF. The landmark REMATCH trial(15) compared the long-term use of the first generation, pulsatile LVADs with optimal medical therapy in end-stage HF and showed significantly improved survival with an absolute reduction in mortality rate of 27 percent at one year(16). Two major factors causing a low two-year survival rate of 23 percent in the LVAD group were infection and mechanical device-failure(16). Since 2006 continuous-flow assist devices are implanted, with much better results(17). Lahpor et al(18) explored the outcomes of more than 400 patients with this second generation, continuous-flow device

and found no mechanical failure, a low incidence of neurological complications but still major infectious and bleeding complications. Although the mean duration of support was significantly higher due to the shortage of donor hearts, overall survival is comparable to other studies(17,18). Permanent mechanical support, or LVAD as destination therapy, is an option for patients with contraindications for heart transplantation, but reimbursement differs per country(19). In addition to the financial aspects, durable LVAD support as a therapy for end-stage HF is still hampered by substantial bleeding (2.69 events/pt-year) and thromboembolic events (0.31 events/pt-year), as well as inflammatory complications (2.34 events/pt-year) (16,18,20–22). The 5th INTERMACS analysis demonstrated a 6-fold increase of pump exchanges for pump thrombosis between 2011 and 2012, clinically concerning due to the associated higher mortality rates(23,24). These findings emphasize the importance of restricting long-term support only for those who really need that and stimulating myocardial recovery and device explantation in as many patients as possible. While initially ventricular remodeling in end-stage HF was held to be irreversible, multiple analyses have shown high percentages of 'reverse remodeling' but only low numbers of myocardial recovery(1,2,25). Although the influence on end-organ perfusion and unloading is similar with pulsatile versus continuous flow support, conflicting literature exists regarding their influence on recovery(26). In the current clinical setting LVADs infrequently lead to sufficient myocardial recovery to allow device explantation, i.e. function as a bridge to recovery (BTR). In a retrospective review with patients receiving MCS as a bridge to transplantation recovery occurred in less than 5 percent of patients(27). An explantation rate of 9% was described by the LVAD working group, mostly in younger patients with recent onset heart failure of non-ischemic origin(2). These results correspond to prior data showing higher percentages of myocardial recovery in patients with non-ischemic cardiomyopathy(28). Yacoub et al. aimed at the process of 'physiological hypertrophy' and 'reverse remodeling' to maximize the rate of cardiac recovery by using LVAD support in combination with a specific sequence of pharmacological therapy, including beta-2-agonist Clenbuterol(29). A small cohort of 15 patients receiving MCS for non-ischemic cardiomyopathy without acute myocarditis, were treated with the particular sequence of medication that resulted in sufficient recovery to meet explantation criteria in 11 patients (73%). In most cases improvement maintained for more than 4 years(30). Long-term outcomes of patients bridged to recovery versus bridged to transplantation were investigated(31) to review the results of an aggressive attempt at

stimulating myocardial recovery. Particularly patients with nonischemic cardiomyopathy profit from aggressively inducing reversal of HF. The rate of device explantation was 20.5%, much higher than other data so far(2,31,32).

Figure 1. Current & experimental heart failure therapy.
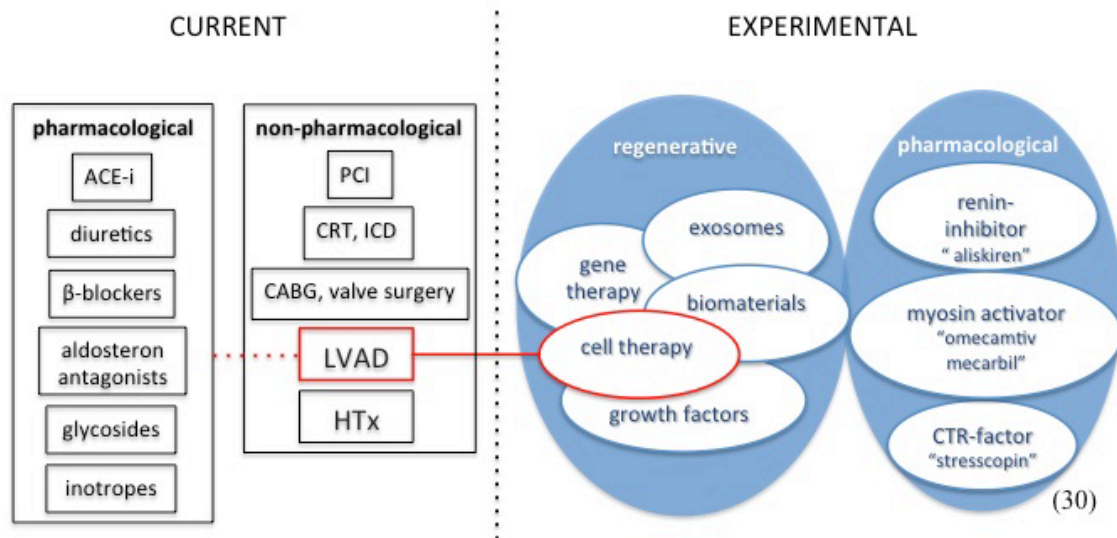
ACE-i, angiotensin-converting-enzyme inhibitor; PCI, percutaneous coronary intervention; CRT, cardiac resynchronisation therapy; ICD, implantable cardioverter defibrillator; CABG, coronary artery bypass graft; HTx, heart transplantation; CTR-factor, cortico-trophin-releasing factor.

Experimental regenerative therapies

A concise concept of different regenerative approaches, present experience and associated hurdles for clinical application will be discussed. Experimental pharmacological therapies(33) are beyond the scope of this review.

Cell therapy

Various cell populations and delivery strategies have been examined for their cardiac repair and regenerative capacity the last decades. Stem cells can derive from blood, bone marrow, skeletal muscle, adipose tissue, embryonic sources or cardiac tissue(34,35). Initially stem cells were presumed to replace damaged cardiomyocytes. Instead, currently the major mechanism of action is assumed to be trough paracrine factors leading to decreased neurohormonal activation and apoptosis, better Ca2+-handling, stimulation of neovascularization and activation of endogenous cardiac-resident cells(36–38). Most clinical experience with cell therapy is gained in ischemic heart disease with unselected bone marrow-derived mononuclear cells (BMMNCs). Results in clinical setting are modest but

132

significant with greatest improvements in the lowest LV ejection fraction (EF) at baseline(34,38–45). The discordance with preclinical data is not fully explained, but poor cell retention and survival plus possible malfunctioning of bone marrow–derived cells in patients with HF are alleged to play a role in these somewhat disappointing findings(34,46–48). The discovery of so-called endogenous cardiac stem cells (CSCs)(49) and evidence that cardiomyocytes have renewal capacity(49–51) have provided a new therapeutic approach, to stimulate the endogenous CSCs since these cells are programmed to reconstitute cardiac tissue. Encouraging results were shown in the SCIPIO trial (autologous CSCs)(52) and in the CADUCEUS trial (autologous cardiosphere-derived cells)(53). Compared to ischemic heart disease, limited clinical data is available regarding efficacy of cell therapy in dilated cardiomyopathy. Results in this population seem mostly positive, though heterogeneity of the population, procedures and outcome parameters prohibit extrapolation(54). A novel cell based technology in which somatic cells (all cells in the body except germ cells) are modified or reprogrammed into a special type of stem cell, called induced pluripotent stem cell (iPS), is in development(35,55). This technique is already applied for other purposes but is fairly unknown as therapeutic. To improve clinical success of cell therapy, better understanding of the primary mechanism and best cell type are fundamental (10,36,38,41). In addition, knowledge about optimal timing, dosing and delivery strategies, including better cell retention and survival, is essential(35,46,56).

Growth factors

Growth hormones (GH) are essential for normal myocardial and endothelium development, and for the maintenance of function(57,58). Endogenous CSCs can be activated by growth factors in the infarcted heart as shown in rodents(59) and in a porcine model(60) of acute MI(34,59–61). Vascular endothelial growth factor (VEGF) and granulocyte-macrophage colony-stimulating factor (GM-CSF) augment levels of endothelial progenitor cells (EPCs) and improve neovascularization(34). Hepatocyt growth factor (HGF) promotes cell migration, insulin-like growth factor-1 (IGF-1) is mitogenic and antiapoptotic, stimulates myocyte formation and reduces myocyte death after infarction(59). GH therapy in chronic setting seems rational since part of the neurohormonal disturbances in HF lies in the GH/insulin-like growth-factor 1 (IGF-1) signaling axis(58). Whereas animal studies demonstrate beneficial effects of growth factor therapy(34,62), clinical data about the efficacy of growth factors in

HF patients is conflicting(58). In a small group of patients (n=13) with severe coronary artery disease and refractory angina treatment with high doses of VEGF temporarily enhanced myocardial perfusion(63). A preliminary study by Fazio et al.(64) showed improved cardiac output in 7 patients with dilated cardiomyopathy treated with growth hormone, whilst other studies examining the effects of exogenous GH in HF yielded no beneficial effects on cardiac function(65–68). A more recent clinical trial(69) with granulocyte-colony stimulating factor after MI, although appearing to improve LV function, was terminated because of high incidence of in-stent restenosis in this treated group. A safety and efficacy trial with IGF-1 is currently recruiting patients with acute MI (Clinical trial info: NCT 01438086).

Gene therapy

Interest for experimental gene therapy in cardiovascular disease has grown the last ten years. The most relevant systems targeted to restore function of failing cardiomyocytes are [1] the B-adrenergic system, [2] Ca^{2+} cycling proteins, [3] homing stem cells and [4] cell death(70). The first clinical, phase 2A safety study (CUPID), with adeno-associated virus (AAV) type 1/ sarcoplasmic reticulum Ca^{2+}-ATPase (SERCA2a) suggests a positive effect on LV function(71), but the therapeutic potential will become apparent as a phase 2b trial is ongoing (clinicaltrials.gov: NCT01643330)(72). Other targets that have been taken forward toward clinical trials include adenylyl cyclase type 6 (clinicaltrials.gov: NCT 00787059) and stromal cell-derived factor 1 (SDF-1) (clinicaltrials.gov: NCT01082094)(70). As more molecular targets associated with HF are discovered more effective gene therapy is expected to emerge(70). Another concept in gene therapy for HF concerns microRNA (miRNA). These are small noncoding RNAs that bind to specific target mRNAs, thereby suppressing protein expression(73,74). The capacity to manipulate miRNA expression and function, together with the fact that their function is heightened under pathophysiological conditions, make them attractive candidates for therapeutic manipulation. Either inhibitors (antimiR) or mimics of miRNA are of interest(73). Several small and large animal studies have targeted relevant miRNA(-families)(73). For example, miRNA-208a (cardiac remodeling), miRNA-21 (cardiac hypertrophy and fibrosis), miRNA-15 (cardiomyocyte apoptosis and regeneration) and miRNA-92a (angiogenesis and regeneration) have been found to play a role in cardiovascular pathology(74–77). Hinkel et al demonstrated improved recovery after ischemia/reperfusion injury by inhibiting miR-92a by LNA-based miRNA inhibitor in a pig

model(74). Challenges in miRNA therapy essentially concern the pleiotrophy and multiplicity of miRNA that needs intensive research, since only target tissue is examined in all studies. Next to that, feasibility of adequate dosing has to be assessed(70).

Exosomes

These small membrane vesicles (40-100nm), endosomal derived and extracellularly released by many cells, are involved in intercellular communication(78,79). Although discovered 30 years ago(80), major interest in exosomes and their function in regenerative medicine recently emerged. In response to injury, extracellular microvesicles are released from activated platelets and apoptotic endothelial cells, suggesting not only therapeutic but also diagnostic value(81). Special attention for exosomes derived from cardiac progenitor cells has originated from the postulated paracrine effects of cell based therapy, mainly regarding the release of growth factors, cytokines and chemokines(78,81). Exosomes derived from cardiomyocyte progenitor cells are proposed to play a role in cardiac protection(78). In mice as well as in a porcine model of ischemia/reperfusion injury, mesenchymal stromal cell-derived exosomes reduced myocardial damage(78,82). While acknowledged to target via transfer of proteins or genetic materials, the role of exosomes in cardiac injury is far from clear(79). Further research on the production and content sorting of exosomes and their effect on target (and non-target) cells is crucial(79,81).

Biomaterials

Another recent topic in regenerative therapy for cardiovascular disease is the use of biomaterials. Multiple scaffolds, naturally derived and synthetic, are used. Therapeutic ability is suggested for MI, prevention of remodeling and in consequence prevention of ischemic heart failure in small and large animal models(83–85). Whilst originally tissue-engineered cardiac patches were of interest, research in the area of injectable biomaterials is rapidly evolving(47,61,83,86,87). The prospective profit of biomaterials is two-sided, either to stimulate endogenous repair and regeneration or to provide a vehicle to support delivery of other therapeutics (e.g. cells, growth factors), generating greater cell retention and survival(47,86). Gelatin microspheres have been shown to be a feasible carrier for cardiomyocyte progenitor cells and growth factors, resulting in improved engraftment and cell survival in mice (Feyen D. Thesis: Strategies to improve cardiac cell therapy. Chapter 8:

Gelatin microspheres as carriers for cardiac progenitor cell and growth factor to the ischemic myocardium, unpublished 2014). Dai et al studied the effect of non-cellular hydrogels versus cell therapy in a rat model of chronic ischemia and showed similar increases in ejection fraction and thereby potential of hydrogels alone(84). No clinical trials have yet been performed with biomaterials. The challenge of this therapy is the delivery, mainly relating to the solubility during the procedure while the hydrogel has to become gel-like after injection in the myocardium.

Combined mechanical support and regenerative therapies

Following unloading of the ventricle a complex network of changes on molecular, cellular, tissue and organ level arises(32,88–94). Although the exact mechanism of reversal of HF during LVAD support is unclear, the effect of ventricular volume and pressure unloading together with improved neurohormonal and cytokine activation are thought to induce reverse remodeling(1,92,95). In a study comparing isolated human myocytes of failing hearts with and without prior LVAD showed increased contractile properties and beta-adrenergic responsiveness after LVAD support(96). Immunohistochemical analysis of the contractile myofilaments after LVAD implantation uncovered improved staining pattern of all thin contractile proteins and titin, however structural myocyte damage was persisting(89). Significant improvement of the proliferation/apoptosis balance by ventricular unloading has been shown in a mouse model of ischemic HF(95). Also, specific changes in gene expression of cytoskeletal proteins after LVAD support have been seen in recovered vs. non-recovered myocardium(91). The beneficial effect on LV function appears to deteriorate over time(2), suggesting that combining mechanical support with other, regenerative, therapeutic strategies like growth hormones, gene therapy or cell therapy might hold the key to better long-term results(92). The unloaded ventricle provides a less hostile milieu and thereby a potentially more appropriate platform for different regenerative therapies. Along the same lines, the combined approach of biventricular pacing and BMMNCs in ischemic HF indicated a significant and clinically relevant improvement in cardiac function in comparison with BMMNCs alone, while CRT showed no impact on perfusion(97). The rationale for this approach is that electrical stimulation might promote cell differentiation.

Preclinical experience

Up to date a representative large animal model of chronic HF with myocardial unloading is lacking. The majority of LVAD studies were performed in healthy animals with only a few studies in chronically failing models(98). Preclinical experience consists of several (b)ovine ischemic HF models, induced by either coronary microembolization, coronary ligation or ameroid constriction(99–103). Non-ischemic HF models include a pressure and volume overload model caused by aortic constriction respectively mitral regurgitation via chordae rupture(98,104). Last-mentioned models have the disadvantage of required thoracotomy, undesirable in case of future device implantation. Other methods like pacing, pharmacotherapeutic induced (doxorubicin), direct shock and cardiotoxins are not reflective of human HF(98). Recreating a model similar to human etiology remains a challenge. To advance innovative and clinically applicable strategies for cardiac regeneration, suitable preclinical research is inevitable. Not only to test combined unloading and regenerative therapies, but also to direct future mechanical support and treatment of earlier stage HF. Thereafter, different regenerative therapies must be evaluated in such a model.

Clinical experience

Combined mechanical unloading and regenerative therapy in clinical setting has only been examined with cell therapy. The results of these studies were systematically reviewed as shown in table 1.(39,40,105–111). A total of 50 patients have been treated with the combinational strategy. The limited data illustrates that in all cases that LVAD was explanted an extracorporal device was used. Usually percutaneous support is initiated when myocardial recovery is expected. However, Sawa et al(105) describe a case where a patient with idiopathic dilated cardiomyopathy did not show enough improvement in LVEF for explantation 7 months after starting MCS. After additional cell transplantation LV improved to a reasonable function that sustained for at least 1.5 years.

All studies, except Ascheim et al, used autologous cells, either bone marrow-derived or skeletal myoblasts, mainly in patients with ischemic cardiomyopathy. The first and only randomized trial with allogeneic mesenchymal precursor cells in ischemic and non-ischemic HF shows encouraging results when it comes to efficacy, but safety regarding sensitization is concerning, especially when the aim is to increase the amount of cells in future studies(111). No results of the combination of SERCA gene therapy and MCS have yet been reported

(clinicaltrials.gov: NCT 000534703). Accordingly, the combination of MCS and cell therapy is promising as both therapies share action mechanisms and might possess synergistic effects(39,40,92,105,107–111). Focusing on this combination provides not only a point of reference to gain more success in bridging to recovery but also the unique opportunity to analyze the myocardium in case of heart transplantation, which can broaden understanding in the process of ventricular reverse remodeling and myocardial recovery. In patients awaiting heart transplantation allogeneic cell therapy should only be considered with great precaution because of immunologic sensitization(111).

Table 1. Clinical experience of LVAD combined with cell therapy

Study type (reference)	N	Etiology CMP	Cell type (and timing)	Clinical outcome	Measured effect
Phase I (111)	20	Ischemic and non-ischemic	Allogeneic MPCs (concomitant)	Increased weaning frequency and duration	Safe/efficacy
Case report (105)	1	Dilated	Autologous skeletal myoblasts (+16 months)	*LVAD explantation*	LVEF increased
Phase I (110)	4	Ischemic	Autologous skeletal myoblasts (concomitant)	*1 LVAD explantation*, 3 non-cardiac deaths	N=2 LVEF increased
Case series (108)	2	Ischemic	Autologous BMMNCs (concomitant)	1 improved perfusion, 1 unknown	Perfusion improved
Case report (107)	1	Ischemic	Autologous skeletal myoblasts (+3 months)	Death +466 days (sepsis)	Increased EF
Case series (109)	10	Ischemic	Autologous BMMNCs (concomitant)	*1 LVAD explantation*, 3 HTx, 2 deaths	N=1 increased EF
Case report (106)	1	Ischemic	Autologous BMMNCs (+99 days)	*LVAD explantation*	Increased EF and perfusion
Phase I (40)	6	Ischemic	Autologous skeletal myoblasts (concomitant)	4 HTx, 3 deaths	Safe/feasible
Phase I (39)	5	Ischemic	Autologous skeletal myoblasts (concomitant)	3 HTx, 1 DT, 1 death	Safe/feasible

CMP, cardiomyopathy; MPCs, mesenchymal progenitor cells; BMMNCs, bone marrow-derived mononuclear cells; HTx, heart transplantation; DT, destination therapy

Future perspective

The rapidly developing field of regenerative therapies enables various combinations with LVAD support (e.g. hydrogel loaded with exosomes or growth factors combined with microspheres). Considering the different etiologies of heart failure, the most pronounced effect of combined cell therapy, biomaterials and mechanical unloading could be expected in patients with ischemic HF. The rationale is that the ischemic myocardium will benefit most from the paracrine effects leading to angiogenesis. The combination with biomaterials might positively enlarge efficacy by higher retention rates, and perhaps through a direct therapeutic effect of the biomaterial. Gene therapy in combination with (biomaterials and) MCS is more probable to enhance myocardial function of patients with dilated cardiomyopathy. The advancements in assist devices will help to uncover the most optimal technology to stimulate recovery and reduce adverse events. Cheng et al suggest that pulsatile flow support might have better results with regard to recovery, due to the less affected vascular reactivity in the presence of a pulse pressure(26). The absence of arterial pulsatility leads to stiff unresponsive arteries(102). Moreover, the development of algorithms for continuous flow-LVADs to generate a pulse pressure is very intriguing, also for the possible influence on adverse events(26). The increasing rate of permanent LVAD support will lead to more clinical data regarding recovery rates and adverse events. However, the small number of patients included in LVAD trials and the lack of an illustrative preclinical model, makes moving forward to clinical application time-consuming. Besides testing of combined therapeutic strategies, preclinical research is also inevitable to gain more understanding of the types of support in the setting of myocardial recovery.

Conclusion.

Since heart transplantation, the gold standard therapy for end-stage HF, is not sufficiently available, other advanced therapeutic approaches are crucial. LVADs provide a bridge for patients awaiting heart transplantation or myocardial recovery. Rates of successful and durable recovery are very low, but this can be stimulated pharmacologically. Better-sustained results could be expected from combining LVADs with regenerative therapies such as gene therapy, biomaterials and cell-based therapies. Especially cell therapy for the treatment of heart disease has been extensively studied, showing promising results. The small number of LVAD patients does not allow clinical testing of the numerous potential

combinations of therapies. A clinically relevant animal model of unloading should be established for preclinical testing of these regenerative approaches. Regarding current experience in the reversal of HF with combined LVAD and cell therapy, future clinical research should focus on placebo-controlled studies in patients undergoing LVAD.

References

1. Levin H, Oz M, Chen J, Packer M, Rose EA, Burkhoff D. Reversal of chronic ventricular dilation in patients with end-stage cardiomyopathy by prolonged mechanical unloading. Circulation (1995) 91(11):2717–20.

2. Maybaum S, Mancini D, Xydas S, Starling RC, Aaronson K, Pagani FD, et al. Cardiac improvement during mechanical circulatory support: a prospective multicenter study of the LVAD Working Group. Circulation (2007) 115(19):2497–505. doi: 10.1161/CIRCULATIONAHA.106.633180

3. Redfield M. Heart Failure - An epidemic of uncertain proportions. N Engl J Med (2002) 347(18):1442–4.

4. Levy D, Kenchaiah S, Larson MG, Benjamin EJ, Kupka MJ, Ho KKL, et al. Long-term trends in the incidence of and survival with heart failure. N Engl J Med (2002) 347(18):1397–402. doi: 10.1056/NEJMoa020265

5. Jonge de N, Vantrimpont PJMJ. Heart failure: chapter 8. Treatment of end-stage heart failure. Netherlands Hear J (2004) 12(12):548–54.

6. De Jonge N, Kirkels JH, Klöpping C, Lahpor JR, Caliskan K, Maat a PWM, et al. Guidelines for heart transplantation. Neth Heart J (2008) 16(3):79–87.

7. Remme WJ, Swedberg K. Guidelines for the diagnosis and treatment of chronic heart failure. Eur Heart J (2001) 22(17):1527–60. doi: 10.1053/euhj.2001.2783

8. Remme WJ, Swedberg K. Comprehensive guidelines for the diagnosis and treatment of chronic heart failure. Task force for the diagnosis and treatment of chronic heart failure of the European Society of Cardiology. Eur J Heart Fail (2002) 4(1):11–22.

9. Mason C, Dunnill P. A brief definition of regenerative medicine. Regen Med (2008) 3:1–5.

10. Du Pré BC, Doevendans PA, van Laake LW. Stem cells for cardiac repair: an introduction. J Geriatr Cardiol (2013) 10(2):186–97. doi: 10.3969/j.issn.1671-5411.2013.02.003

11. Koopman C, Van Dis I, Bots M, Vaartjes I. Feiten en cijfers Hartfalen. Nederlandse Hartstichting (2012).

12. Eurotransplant International Foundation. Annual Report 2013 (2013).

13. Cleveland JC, Naftel DC, Reece TB, Murray M, Antaki J, Pagani FD, et al. Survival after biventricular assist device implantation: an analysis of the Interagency Registry for Mechanically Assisted Circulatory Support database. J Heart Lung Transplant (2011) 30(8):862–9.

14. Liotta D. Early clinical application of assisted circulation. Tex Heart Inst J (2002) 29(3):229–30.

15. Rose EA, Moskowitz AJ, Packer M, Sollano JA, Williams DL, Tierney AR, et al. The REMATCH trial: rationale, design, and end points. Ann Thorac Surg. 1999 Mar;67(3):723–30.

16. Rose EA, Gelijns AC, Moskowitz AJ, Heitjan DF, Stevenson LW, Dembitsky W, et al. Long-term use of a left ventricular assist device for end-stage heart failure. N Engl J Med (2001) 345(20):1435–43.

17. Slaughter MS, Rogers JG, Milano C a, Russell SD, Conte J V, Feldman D, et al. Advanced heart failure treated with continuous-flow left ventricular assist device. N Engl J Med (2009) 361(23):2241–51. doi: 10.1056/NEJMoa0909938

18. Lahpor J, Khaghani A, Hetzer R, Pavie A, Friedrich I, Sander K, et al. European results with a continuous-flow ventricular assist device for advanced heart-failure patients. Eur J Cardiothorac Surg (2010) 37(2):357–61. doi: 10.1016/j.ejcts.2009.05.043

19. Neyt M, Van den Bruel A, Smit Y, De Jonge N, Erasmus M, Van Dijk D, et al. Cost-effectiveness of continuous-flow left ventricular assist devices. Int J Technol Assess Health Care (2013) 29(3):254–60. doi: 10.1017/S0266462313000238

20. Stulak JM, Lee D, Haft JW, Romano M a, Cowger J a, Park SJ, et al. Gastrointestinal bleeding and subsequent risk of thromboembolic events during support with a left ventricular assist device. J Heart Lung Transplant (2014) 33(1):60–4. doi: 10.1016/j.healun.2013.07.020

21. Kirklin JK, Naftel DC, Cantor RS, Myers SL, Clark ML, Collum SC, et al. Quarterly Statistical Report 2014 3rd Quarter. INTERMACS Interagency Registry for Mechanically Assisted Circulatory Support (2014).

22. Kirklin JK, Naftel DC, Pagani FD, Kormos RL, Stevenson LW, Blume ED, et al. Sixth INTERMACS annual report: a 10,000-patient database. J Heart Lung Transplant (2014)33(6):555–64. doi: 10.1016/j.healun.2014.04.010

23. Kirklin JK, Naftel DC, Kormos RL, Pagani FD, Myers SL, Stevenson LW, et al. Interagency Registry for Mechanically Assisted Circulatory Support (INTERMACS) analysis of pump thrombosis in the HeartMate II left ventricular assist device. J Heart Lung Transplant (2014) 33(1):12–22. doi: 10.1016/j.healun.2013.11.001

24. Mehra MR, Stewart GC, Uber PA, PharmD. The vexing problem of thrombosis in long-term mechanical circulatory support. J Heart Lung Transplant (2014) 33(1):1–11. doi: 10.1016/j.healun.2013.12.002

25. Maybaum S, Kamalakannan G, Murthy S. Cardiac recovery during mechanical assist device support. Semin Thorac Cardiovasc Surg (2008) 20(3):234–46. doi: 10.1053/j.semtcvs.2008.08.003

26. Cheng A, Williamitis CA, Slaughter MS. Comparison of continuous-flow and pulsatile-flow left ventricular assist devices: is there an advantage to pulsatility? Ann Cardiothorac Surg (2014)3(6):573–81. doi: 10.3978/j.issn.2225-319X.2014.08.24

27. Mancini DM, Beniaminovitz A, Levin H, Catanese K, Flannery M, DiTullio M, et al. Low Incidence of Myocardial Recovery After Left Ventricular Assist Device Implantation in Patients With Chronic Heart Failure. Circulation (1998) 98(22):2383–9. doi: 10.1161/01.CIR.98.22.2383

28. Simon MA, Kormos RL, Murali S, Nair P, Heffernan M, Gorcsan J, et al. Myocardial recovery using ventricular assist devices: prevalence, clinical characteristics, and outcomes. Circulation (2005) 112(9 Suppl):I32–6. doi: 10.1161/CIRCULATIONAHA.104.524124

29. Yacoub MH. A novel strategy to maximize the efficacy of left ventricular assist devices as a bridge to recovery. Eur Heart J (2001) 22(7):534–40. doi: 10.1053/euhj.2001.2613

30. Birks EJ, Tansley PD, Hardy J, George RS, Bowles CT, Burke M, et al. Left ventricular assist device and drug therapy for the reversal of heart failure. N Engl J Med (2006) 355(18):1873–84. doi: 10.1056/NEJMoa053063

31. Birks EJ, George RS, Firouzi A, Wright G, Bahrami T, Yacoub MH, et al. Long-term outcomes of patients bridged to recovery versus patients bridged to transplantation. J Thorac Cardiovasc Surg (2012) 144(1):190–6. doi: 10.1016/j.jtcvs.2012.03.021

32. Simon MA, Primack BA, Teuteberg J, Kormos RL, Bermudez C, Toyoda Y, et al. Left ventricular remodeling and myocardial recovery on mechanical circulatory support. J Card Fail (2010)16(2):99–105. doi: 10.1016/j.cardfail.2009.10.018

33. Valentova M, von Haehling S. An overview of recent developments in the treatment of heart failure: update from the ESC Congress 2013. Expert Opin Investig Drugs (2014) 23(4):573–8. doi: 10.1517/13543784.2014.881799

34. Dimmeler S, Zeiher AM, Schneider MD. Review series Unchain my heart : the scientific foundations of cardiac repair. J Clin Invest (2005) 115(3):572–83. doi: 10.1172/JCI200524283.572

35. Segers VFM, Lee RT. Stem-cell therapy for cardiac disease. Nature (2008) 451(7181):937–42. doi: 10.1038/nature06800

36. Menasché P, Hagège AA, Vilquin J-T, Desnos M, Abergel E, Pouzet B, et al. Autologous skeletal myoblast transplantation for severe postinfarction left ventricular dysfunction. J Am Coll Cardiol (2003) 41(7):1078–83. doi: 10.1016/S0735-1097(03)00092-5

37.   Dimmeler S, Burchfield J, Zeiher AM. Cell-based therapy of myocardial infarction. Arterioscler Thromb Vasc Biol (2008) 28(2):208–16. doi: 10.1161/ATVBAHA.107.155317

38.   Menasché P. Cardiac cell therapy: lessons from clinical trials. J Mol Cell Cardiol (2011)50(2):258–65. doi: 10.1016/j.yjmcc.2010.06.010

39.   Pagani FD, DerSimonian H, Zawadzka A, Wetzel K, Edge ASB, Jacoby DB, et al. Autologous skeletal myoblasts transplanted to ischemia-damaged myocardium in humans. Histological analysis of cell survival and differentiation. J Am Coll Cardiol (2003) 41(5):879–88. doi: 10.1016/S0735-1097(03)00081-0

40.   Dib N, Michler RE, Pagani FD, Wright S, Kereiakes DJ, Lengerich R, et al. Safety and feasibility of autologous myoblast transplantation in patients with ischemic cardiomyopathy: four-year follow-up. Circulation (2005) 112(12):1748–55. doi: 10.1161/CIRCULATIONAHA.105.547810

41.   Strauer B-E, Yousef M, Schannwell CM. The acute and long-term effects of intracoronary Stem cell Transplantation in 191 patients with chronic heARt failure: the STAR-heart study. Eur J Hear Fail (2010) 12(7):721–9. doi: 10.1093/eurjhf/hfq095

42.   Van der Spoel TI, Jansen Of Lorkeers SJ, Agostoni P, van Belle E, Gyongyosi M, Sluijter JP, et al. Human relevance of pre-clinical studies in stem cell therapy; systematic review and meta-analysis of large animal models of ischemic heart disease. Cardiovasc Res (2011) 91(4):649–58. doi: 10.1093/cvr/cvr113

43.   Koudstaal S. Stamceltherapie voor ischemische hartziekten. Cordiaal (2013) 2: 40–4.

44.   Jeevanantham V, Butler M, Saad A, Abdel-Latif A, Zuba-Surma EK, Dawn B. Adult bone marrow cell therapy improves survival and induces long-term improvement in cardiac parameters: a systematic review and meta-analysis. Circulation (2012) 126(5):551–68. doi: 10.1161/CIRCULATIONAHA.111.086074

45.   Van Ramshorst J, Bax JJ, Beeres SL, Dibbets-Schneider P, Roes SD, Stokkel MP, et al. Intramyocardial Bone Marrow Cell Injection for Chronic Myocardial Ischemia. JAMA (2009)301(19):1997–2004.

46.   Tongers J, Losordo DW, Landmesser U. Stem and progenitor cell-based therapy in ischaemic heart disease: promise, uncertainties, and challenges. Eur Heart J (2011) 32(10):1197–206. doi: 10.1093/eurheartj/ehr018

47.   Radisic M, Christman KL. Materials science and tissue engineering: repairing the heart. Mayo Clin Proc (2013) 88(8):884–98. doi: 10.1016/j.mayocp.2013.05.003

48.   Kurazumi H, Kubo M, Ohshima M, Yamamoto Y, Takemoto Y, Suzuki R, et al. The effects of mechanical stress on the growth, differentiation, and paracrine factor production of cardiac stem cells. PLoS One (2011) 6(12):e28890. doi: 10.1371/journal.pone.0028890

49.   Bergmann O, Bhardwaj RD, Bernard S, Zdunek S, Barnabé-Heider F, Walsh S, et al. Evidence for cardiomyocyte renewal in humans. Science (2009) 324(5923):98–102. doi: 10.1126/science.1164680

50.   Smits AM, van Vliet P, Metz CH, Korfage T, Sluijter JP, Doevendans P a, et al. Human cardiomyocyte progenitor cells differentiate into functional mature cardiomyocytes: an in vitro model for studying human cardiac physiology and pathophysiology. Nat Protoc (2009)4(2):232–43. doi: 10.1038/nprot.2008.229

51.   Senyo S, Wang M, Wu T, Lechene CP. Mammalian heart renewal by preexisting cardiomyocytes. Nature (2013) 493(7432):433–6. doi: 10.1038/nature11682.Mammalian

52.   Bolli R, Chugh AR, D'Amario D, Loughran JH, Stoddard MF, Ikram S, et al. Cardiac stem cells in patients with ischaemic cardiomyopathy (SCIPIO): initial results of a randomised phase 1 trial. Lancet (2011) 378(9806):1847–57. doi: 10.1016/S0140-6736(11)61590-0

53.   Malliaras K, Makkar RR, Smith RR, Cheng K, Wu E, Bonow RO, et al. Intracoronary Cardiosphere-Derived Cells After Myocardial Infarction: Evidence of Therapeutic Regeneration in the Final 1-Year Results of the CADUCEUS Trial (CArdiosphere-Derived aUtologous stem CElls to reverse ventricUlar dySfunction). J Am Coll Cardiol (2014) 63(2):110–22. doi: 10.1016/j.jacc.2013.08.724

54. Gho JMIH, Kummeling GJM, Koudstaal S, Jansen Of Lorkeers SJ, Doevendans PA, Asselbergs FW, et al. Cell therapy, a novel remedy for dilated cardiomyopathy? A systematic review. J Card Fail (2013) 19(7):494–502. doi: 10.1016/j.cardfail.2013.05.006

55. Bellin M, Marchetto MC, Gage FH, Mummery CL. Induced pluripotent stem cells: the new patient? Nat Rev Mol Cell Biol (2012) 13(11):713–26. doi: 10.1038/nrm3448

56. Janssens S. Stem cells in the treatment of heart disease. Annu Rev Med (2010) 61:287–300. doi: 10.1146/annurev.med.051508.215152

57. McElhinney DB, Colan SD, Moran AM, Wypij D, Lin M, Majzoub JA, et al. Recombinant human growth hormone treatment for dilated cardiomyopathy in children. Pediatrics (2004) 114(4):e452–8. doi: 10.1542/peds.2004-0072

58. Castellano G, Affuso F, Di Conza P, Fazio S. The GH/IGF-1 Axis and Heart Failure. Curr Cardiol Rev (2009)5(3):203–15. doi: 10.2174/157340309788970306

59. Urbanek K, Rota M, Cascapera S, Bearzi C, Nascimbene A, De Angelis A, et al. Cardiac stem cells possess growth factor-receptor systems that after activation regenerate the infarcted myocardium, improving ventricular function and long-term survival. Circ Res (2005) 97(7):663–73. doi: 10.1161/01.RES.0000183733.53101.11

60. Ellison GM, Torella D, Dellegrottaglie S, Perez-Martinez C, Perez de Prado A, Vicinanza C, et al. Endogenous cardiac stem cell activation by insulin-like growth factor-1/hepatocyte growth factor intracoronary injection fosters survival and regeneration of the infarcted pig heart. J Am Coll Cardiol (2011) 58(9):977–86. doi: 10.1016/j.jacc.2011.05.013

61. Koudstaal S, Bastings MMC, Feyen DA, Waring CD, van Slochteren FJ, Dankers PYW, et al. Sustained delivery of insulin-like growth factor-1/hepatocyte growth factor stimulates endogenous cardiac repair in the chronic infarcted pig heart. J Cardiovasc Transl Res (2014) 7(2):232–41. doi: 10.1007/s12265-013-9518-4

62. Cittadini A, Grossman JD, Napoli R, Katz SE, Strömer H, Smith RJ, et al. Growth hormone attenuates early left ventricular remodeling and improves cardiac function in rats with large myocardial infarction. J Am Coll Cardiol (1997) 29(5):1109–16.

63. Giusti II, Rodrigues CG, Salles FB, Sant'Anna RT, Eibel B, Han SW, et al. High doses of vascular endothelial growth factor 165 safely, but transiently, improve myocardial perfusion in no-option ischemic disease. Hum Gene Ther Methods (2013) 24(5):298–306. doi: 10.1089/hgtb.2012.221

64. Fazio S, Sabatini S, Capaldo B, Vigorito C, Giordano A, Guida R, et al. A preliminary study of growth hormone in the treatment of dilated cardiomyopathy. N Engl J Med (1996) 334(13):809–14.

65. Isgaard J, Bergh CH, Caidahl K, Lomsky M, Hjalmarson A, Bengtsson B. A placebo-controlled study of growth hormone in patients with congestive heart failure. Eur Heart J (1998) 19(11):1704–11.

66. Acevedo M, Corbalán R, Chamorro G, Jalil J, Nazzal C, Campusano C, et al. Administration of growth hormone to patients with advanced cardiac heart failure : effects upon left ventricular function , exercise capacity , and neurohormonal status. Int J Cardiol (2003) 87:185–91.

67. Spallarossa P, Rossettin P, Minuto F, Caruso D, Cordera R, Battistini M, et al. Evaluation of growth hormone administration in patients with chronic heart failure secondary to coronary artery disease. Am J Cardiol (1999) 84(4):430–3.

68. Smit JW, Janssen YJ, Lamb HJ, van der Wall EE, Stokkel MP, Viergever E, et al. Six months of recombinant human GH therapy in patients with ischemic cardiac failure does not influence left ventricular function and mass. J Clin Endocrinol Metab (2001) 86(10):4638–43. doi: 10.1210/jcem.86.10.7832

69. Kang H-J, Kim H-S, Zhang S-Y, Park K-W, Cho H-J, Koo B-K, et al. Effects of intracoronary infusion of peripheral blood stem-cells mobilised with granulocyte-colony stimulating factor on left ventricular systolic function and restenosis after coronary stenting in myocardial infarction: the MAGIC cell randomised clinical. Lancet (2004) 363(9411):751–6. doi: 10.1016/S0140-6736(04)15689-4

70. Tilemann L, Ishikawa K, Weber T, Hajjar RJ. Gene therapy for heart failure. Circ Res (2012) 110(5):777–93. doi: 10.1161/CIRCRESAHA.111.252981

71. Jessup M, Greenberg B, Mancini D, Cappola T, Pauly DF, Jaski B, et al. Calcium Upregulation by Percutaneous Administration of Gene Therapy in Cardiac Disease (CUPID): a phase 2 trial of intracoronary gene therapy of sarcoplasmic reticulum Ca2+-ATPase in patients with advanced heart failure. Circulation (2011) 124(3):304–13. doi: 10.1161/CIRCULATIONAHA.111.022889

72. Greenberg B, Yaroshinsky A, Zsebo KM, Butler J, Felker GM, Voors AA, et al. Design of a Phase 2b Trial of Intracoronary Administration of AAV1/SERCA2a in Patients With Advanced Heart Failure: The CUPID 2 Trial (Calcium Up-Regulation by Percutaneous Administration of Gene Therapy in Cardiac Disease Phase 2b). JACC Heart Fail (2014) 2(1):84–92. doi: 10.1016/j.jchf.2013.09.008

73. Van Rooij E, Olson EN. MicroRNA therapeutics for cardiovascular disease: opportunities and obstacles. Nat Rev Drug Discov (2012) 11(11):860–72. doi: 10.1038/nrd3864

74. Hinkel R, Penzkofer D, Zühlke S, Fischer A, Husada W, Xu Q-F, et al. Inhibition of microRNA-92a protects against ischemia/reperfusion injury in a large-animal model. Circulation (2013) 128(10):1066–75. doi: 10.1161/CIRCULATIONAHA.113.001904

75. Van Rooij E, Sutherland LB, Liu N, Williams AH, McAnally J, Gerard RD, et al. A signature pattern of stress-responsive microRNAs that can evoke cardiac hypertrophy and heart failure. Proc Natl Acad Sci U S A (2006) 103(48):18255–60. doi: 10.1073/pnas.0608791103

76. Bonauer A, Carmona G, Iwasaki M, Mione M, Koyanagi M, Fischer A, et al. MicroRNA-92a controls angiogenesis and functional recovery of ischemic tissues in mice. Science (2009) 324(5935):1710–3. doi: 10.1126/science.1174381

77. Thum T, Gross C, Fiedler J, Fischer T, Kissler S, Bussen M, et al. MicroRNA-21 contributes to myocardial disease by stimulating MAP kinase signalling in fibroblasts. Nature (2008) 456(7224):980–4. doi: 10.1038/nature07511

78. Vrijsen KR, Sluijter JPG, Schuchardt MWL, van Balkom BWM, Noort WA, Chamuleau SAJ, et al. Cardiomyocyte progenitor cell-derived exosomes stimulate migration of endothelial cells. J Cell Mol Med (2010) 14(5):1064–70. doi: 10.1111/j.1582-4934.2010.01081.x

79. Sahoo S, Losordo DW. Exosomes and cardiac repair after myocardial infarction. Circ Res (2014) 114(2):333–44. doi: 10.1161/CIRCRESAHA.114.300639

80. Harding C, Heuser J, Stahl P. Receptor-mediated endocytosis of transferrin and recycling of the transferrin receptor in rat reticulocytes. J Cell Biol (1983) 97(2):329–39.

81. Sluijter JPG, Verhage V, Deddens JC, van den Akker F, Doevendans PA. Microvesicles and exosomes for intracardiac communication. Cardiovasc Res (2014) 102(2):302–11. doi: 10.1093/cvr/cvu022

82. Lai RC, Arslan F, Lee MM, Sze NSK, Choo A, Chen TS, et al. Exosome secreted by MSC reduces myocardial ischemia/reperfusion injury. Stem Cell Res (2010) 4(3):214–22. doi: 10.1016/j.scr.2009.12.003

83. Johnson TD, Christman KL. Injectable hydrogel therapies and their delivery strategies for treating myocardial infarction. Expert Opin Drug Deliv (2013) 10(1):59–72. doi: 10.1517/17425247.2013.739156

84. Dai W, Kay GL, Kloner RA. The Therapeutic Effect of Cell Transplantation Versus Noncellular Biomaterial Implantation on Cardiac Structure and Function Following Myocardial Infarction. J Cardiovasc Pharmacol Ther (2014) 19(4):350–7. doi: 10.1177/1074248413517746

85. Lam MT, Wu JC. Biomaterial application in cardiovascular tissue repair and regeneration. Expert Rev Cardiovasc Ther (2013) 10(8):1039–49.

86. Christman KL, Vardanian AJ, Fang Q, Sievers RE, Fok HH, Lee RJ. Injectable fibrin scaffold improves cell transplant survival, reduces infarct expansion, and induces neovasculature formation in ischemic myocardium. J Am Coll Cardiol (2004) 44(3):654–60. doi: 10.1016/j.jacc.2004.04.040

87. Bastings MMC, Koudstaal S, Kieltyka RE, Nakano Y, Pape ACH, Feyen DAM, et al. A fast pH-switchable and self-healing supramolecular hydrogel carrier for guided, local catheter injection in the infarcted myocardium. Adv Healthc Mater (2014) 3(1):70–8. doi: 10.1002/adhm.201300076

88. Frazier OH, Benedict CR, Radovancevic B, Bick RJ, Capek P, Springer WE, et al. Improved Left Ventricular Function After Chronic Left Ventricular Unloading. Ann Thorac Surg (1996) 62(3):675–82. doi: 10.1016/S0003-4975(96)00437-7

89. De Jonge N, van Wichen DF, Schipper MEI, Lahpor JR, Gmelig-Meyling FHJ, Robles de Medina EO, et al. Left ventricular assist device in end-stage heart failure: persistence of structural myocyte damage after unloading. An immunohistochemical analysis of the contractile myofilaments. J Am Coll Cardiol (2002) 39(6):963–9

90. Terracciano CMN, Hardy J, Birks EJ, Khaghani A, Banner NR, Yacoub MH. Clinical recovery from end-stage heart failure using left-ventricular assist device and pharmacological therapy correlates with increased sarcoplasmic reticulum calcium content but not with regression of cellular hypertrophy. Circulation (2004) 18;109(19):2263–5. doi: 10.1161/01.CIR.0000129233.51320.92

91. Birks EJ, Hall JL, Barton PJR, Grindle S, Latif N, Hardy JP, et al. Gene profiling changes in cytoskeletal proteins during clinical recovery after left ventricular-assist device support. Circulation (2005) 112(9 Suppl):I57–64. doi: 10.1161/CIRCULATIONAHA.104.526137

92. Ibrahim M, Rao C, Athanasiou T, Yacoub MH, Terracciano CM. Mechanical unloading and cell therapy have a synergistic role in the recovery and regeneration of the failing heart. Eur J Cardiothorac Surg (2012) 42(2):312–8. doi: 10.1093/ejcts/ezs067

93. Schipper MEI, van Kuik J, de Jonge N, Dullens HFJ, de Weger RA. Changes in Regulatory MicroRNA Expression in Myocardium of Heart Failure Patients on Left Ventricular Assist Device Support. J Heart Lung Transplant (2008)27(12):1282–5. doi: 10.1016/j.healun.2008.09.005

94. Lok SI, van Mil A, Bovenschen N, van der Weide P, van Kuik J, van Wichen D, et al. Post-transcriptional regulation of α-1-antichymotrypsin by microRNA-137 in chronic heart failure and mechanical support. Circ Heart Fail (2013) 6(4):853–61. doi: 10.1161/CIRCHEARTFAILURE.112.000255

95. Suzuki R, Li T-S, Mikamo A, Takahashi M, Ohshima M, Kubo M, et al. The reduction of hemodynamic loading assists self-regeneration of the injured heart by increasing cell proliferation, inhibiting cell apoptosis, and inducing stem-cell recruitment. J Thorac Cardiovasc Surg (2007) 133(4):1051–8. doi: 10.1016/j.jtcvs.2006.12.026

96. Dipla K, Mattiello JA, Jeevanandam V, Houser SR, Margulies KB. Myocyte Recovery After Mechanical Circulatory Support in Humans With End-Stage Heart Failure. Circulation (1998) 97(23):2316–22. doi: 10.1161/01.CIR.97.23.2316

97. Pokushalov E, Romanov A, Corbucci G, Prohorova D, Chernyavsky A, Larionov P, et al. Cardiac resynchronization therapy and bone marrow cell transplantation in patients with ischemic heart failure and electromechanical dyssynchrony: a randomized pilot study. J Cardiovasc Transl Res (2011) 4(6):767–78. doi: 10.1007/s12265-011-9283-1

98. Monreal G, Sherwood LC, Sobieski MA, Giridharan GA, Slaughter MS, Koenig SC. Large animal models for left ventricular assist device research and development. ASAIO J (2014) 60(1):2–8. doi: 10.1097/MAT.0000000000000005

99. Goldstein AH, Monreal G, Kambara A, Spiwak AJ, Schlossberg ML, Abrishamchian AR, et al. Partial Support with a Centrifugal Left Ventricular Assist Device Reduces Myocardial Oxygen Consumption in Chronic, Ischemic Heart Failure. J Card Fail (2005) 11(2):142–51. doi: 10.1016/j.cardfail.2004.07.005

100.   Monreal G, Gerhardt M a. Left ventricular assist device support induces acute changes in myocardial electrolytes in heart failure. ASAIO J (2007) 53(2):152–8. doi: 10.1097/MAT.0b013e3180302a8b

101.   Ghodsizad A, Kar BJ, Layolka P, Okur A, Gonzales J, Bara C, et al. Less invasive off-pump implantation of axial flow pumps in chronic ischemic heart failure: survival effects. J Heart Lung Transplant. J Heart Lung Transplant (2011) 30(7):834–7. doi: 10.1016/j.healun.2011.03.012

102.   Bartoli CR, Giridharan GA, Litwak KN, Sobieski M, Prabhu SD, Slaughter MS, et al. Hemodynamic responses to continuous versus pulsatile mechanical unloading of the failing left ventricle. ASAIO J (2010) 56(5):410–6. doi: 10.1097/MAT.0b013e3181e7bf3c

103.   Geens JH, Jacobs S, Claus P, Trenson S, Leunens V, Vantichelen I, et al. Partial mechanical circulatory support in an ovine model of post-infarction remodeling. J Heart Lung Transplant (2013)32(8):815–22. doi: 10.1016/j.healun.2013.05.019

104.   Tuzun E, Bick R, Kadipasaoglu C, Conger JL, Poindexter BJ, Gregoric ID, et al. Modification of a volume-overload heart failure model to track myocardial remodeling and device-related reverse remodeling. ISRN Cardiol (2011) 2011:831062.

105.   Sawa Y, Miyagawa S, Sakaguchi T, Fujita T, Matsuyama A, Saito A, et al. Tissue engineered myoblast sheets improved cardiac function sufficiently to discontinue LVAS in a patient with DCM: report of a case. Surg Today (2012) 42(2):181–4. doi: 10.1007/s00595-011-0106-4

106.   Gojo S, Kyo S, Nishimura S, Komiyama N, Kawai N, Bessho M, et al. Cardiac resurrection after bone-marrow-derived mononuclear cell transplantation during left ventricular assist device support. Ann Thorac Surg (2007)83(2):661–2.

107.   Miyagawa S, Matsumiya G, Funatsu T, Yoshitatsu M, Sekiya N, Fukui S, et al. Combined autologous cellular cardiomyoplasty using skeletal myoblasts and bone marrow cells for human ischemic cardiomyopathy with left ventricular assist system implantation: report of a case. Surg Today (2009) 39(2):133–6. doi: 10.1007/s00595-008-3803-x

108.   Anastasiadis K, Antonitsis P, Argiriadou H, Koliakos G, Doumas A, Khayat A, et al. Hybrid approach of ventricular assist device and autologous bone marrow stem cells implantation in end-stage ischemic heart failure enhances myocardial reperfusion. J Transl Med (2011) 9(1):12. doi: 10.1186/1479-5876-9-12

109.   Nasseri B, Kukucka M, Dandel M, Knosalla C, Potapov E, Lehmkuhl H, et al. Intramyocardial delivery of bone marrow mononuclear cells and mechanical assist device implantation in patients with end-stage cardiomyopathy. Cell Transplant (2007) 16(9):941–9.

110.   Fujita T, Sakaguchi T, Miyagawa S, Saito A, Sekiya N, Izutani H, et al. Clinical impact of combined transplantation of autologous skeletal myoblasts and bone marrow mononuclear cells in patients with severely deteriorated ischemic cardiomyopathy. Surg Today (2011) 41(8):1029–36. doi: 10.1007/s00595-010-4526-3

111.   Ascheim DD, Gelijns AC, Goldstein D, Moye LA, Smedira N, Lee S, et al. Mesenchymal Precursor Cells as Adjunctive Therapy in Recipients of Contemporary LVADs. Circulation (2014) 129:2287–96. doi:10.1161/CIRCULATIONAHA.113.007412

Systematic search LVAD/SCT:

Search detail:

"heart-assist devices"[MeSH Terms] OR ("heart-assist devices"[MeSH Terms] OR ("heart-assist"[All Fields] AND "devices"[All Fields]) OR "heart-assist devices"[All Fields] OR ("heart"[All Fields] AND "assist"[All Fields] AND "device"[All Fields]) OR "heart assist device"[All Fields]) AND ("cell- and tissue-based therapy"[MeSH Terms] OR ("cell-"[All Fields] AND "tissue-based"[All Fields] AND "therapy"[All Fields]) OR "cell- and tissue-based therapy"[All Fields] OR ("cell"[All Fields] AND "therapy"[All Fields]) OR "cell therapy"[All Fields])

In total: 195 results, minus review/animal/Japanese/no combination

→ **9 articles**

Soluble ST2 in end-stage heart failure, before and after support with a left ventricular assist device

C.C.S. Tseng, M.M.H. Huibers, L.H. Gaykema, E. Siera-de Koning,
F.Z. Ramjankhan, A.S. Maisel, N. de Jonge

Abstract

Background

The interleukin-33 (IL-33)/supressor of tumorigenicity 2 (ST2) pathway is suggested to play an important role in fibrosis, remodeling and the progression of heart failure (HF). Increased soluble (sST2) levels are associated with adverse outcome in the average HF population. Less is known about sST2 levels in end-stage HF. Therefore, we studied sST2 levels in end-stage HF and the effect of unloading by left ventricular assist device (LVAD) support on sST2 levels.

Method and results

Serial plasma measurements of sST2 were performed pre-implantation and 1, 3 and 6 months after (LVAD) implantation in 38 patients. sST2 levels were elevated in end-stage HF just prior to LVAD implantation (74.2 ng/ml [IQR 54.7 - 116.9]; normal < 35 ng/ml) and decreased substantially during LVAD support, to 29.5 ng/ml [IQR 24.7 - 46.6]($p < 0.001$). Patients with INTERMACS profile I had significantly higher sST2 levels compared to patients in profile II and III. A moderate correlation was found between sST2 and C-reactive protein ($r = 0.580$, $p < 0.010$).

Conclusion

Levels of sST2 are elevated in end-stage HF patients with variability that suggests multiple inputs to a pro-inflammatory and pro-fibrotic pathway. Cardiogenic shock and increased CRP levels are associated with higher sST2 levels. LVAD support results in a significant drop in sST2 levels with normalization within 3 months post implantation. This suggests that LVAD support leads to lessening of fibrosis and inflammation, which might eventually be used to target medical policy: explantation of the LVAD versus permanent use or cardiac transplantation.

Introduction

The interleukin-33 (IL-33)/suppressor of tumorigenicity 2 (ST2) pathway is part of the IL-1 family and was initially associated with inflammation and immunity. Recently, the IL-33/ST2 pathway has also been suggested to play an important role in the progression of heart failure (HF)(1). It is thought to be a cardio-protective signaling pathway that is activated by cell damage and mechanical stress, through the release of IL-33 from cardiac cells (predominantly stromal). Activation of IL-33 prevents myocardial hypertrophy and fibrosis through interaction of IL-33 and transmembrane bound ST2L(2). The soluble form of ST2 (sST2) acts as a 'decoy' receptor that results in attenuation of the beneficial (myocardial and vascular) effects of IL-33. Increased sST2 levels are associated with an activation of a pro-fibrotic pathway leading to adverse outcomes in the average HF population(1,3). Soluble ST2 has an additive value to natriuretic peptides and superior prognostic performance compared with all other biomarkers (high sensitive troponin T, growth differentiation factor-15, B-type natriuretic peptide (BNP) and N-terminal-proBNP(4). Serial monitoring of sST2 in particular may benefit risk prediction and therapy guidance(5,6). However, most studies are performed in NYHA class II-III heart failure patients and little is known about sST2 in end-stage HF patients (NYHA IV). Left ventricular assist device (LVAD) patients offer an opportunity to investigate sST2 concentrations both during severe end-stage HF as well as during LV unloading. Although sST2 is suggested to be a marker of cardiac fibrosis and remodeling, the association with clinical factors in end-stage heart failure patients has not yet been elucidated. Therefore, the aim of this study was to assess sST2 levels in end-stage heart failure and assess the effect of unloading of the left ventricle by mechanical circulatory support on sST2 levels. Furthermore, we evaluated pre-specified potential determinants of sST2 concentrations in end-stage heart failure patients.

Method

Study population

In this retrospective study 38 consecutive patients were included who received a continuous flow LVAD as bridge to heart transplantation with a support duration of more than 180 days. Exclusion criteria were severe kidney dysfunction, peripheral vasculopathy and also elderly patients. Inclusion was only done if plasma samples of all predefined timepoints were

available. This study was approved by an ethics committee and all patients agreed to collection and banking of blood samples for research purposes at the time of LVAD implant (number 12/387). Reporting of the study conforms to STROBE statement(7).

sST2 measurements

Blood samples were collected within 24 hours prior to LVAD implantation and 1, 3 and 6 months after implantation through a peripheral vein into EDTA-containing tubes. Blood was centrifuged within 6 hours after withdrawal, plasma was collected in aliquots and stored at -80°C. Levels of sST2 were analyzed by double measurements in one batch, using the Presage ST2 ELISA assay according to manufacturer's instructions (Critical diagnostics, San Diego, CA, USA). The assay has an intra- and inter-assay coefficient of variation of 5.1% and 5.2% respectively and a total coefficient of variation ranging from 4.2 to 12.0%.

Clinical parameters

Data regarding HF etiology, INTERMACS profile, blood pressure (BP), HF duration and medication were gathered from the medical file. Diagnostic blood measurements were used for laboratory assessments of BNP (ng/L), CRP (mg/L) and kidney function (eGFR, ml/min/m^2; estimated by MDRD calculation). Echocardiography was used to evaluate right ventricular function (RVF) and left ventricular end diastolic dimension (LVEDD). RVF was classified as poor, moderate, reasonable or good. Categories were paired for analysis: poor and moderate RVF as "<reasonable" and reasonable and good function as ≥reasonable . LVEDD was measured in millimeters. Cardiac output (CO, l/min), right atrial pressure (RAp, mmHg) and pulmonary capillary wedge pressure (PCWP, mmHg) were measured with a Swan-Ganz catheter shortly before LVAD implantation.

Statistical analysis

Continuous data are expressed as medians (interquartile range; IQR, with 25th -75th percentile) and categorical variables as number (%). The overall effect of LVAD implantation on sST2 levels after 6 months was analyzed with the Friedman test. Comparison at different time points was performed with Wilcoxon-signed-rank test, corrected for multiple testing with the Bonferroni method. The distribution of sST2 levels was analyzed for several clinical

154

factors using Mann Whitney U tests. Spearman's correlation was used to calculate correlations. A P-value < 0.05 was considered statistically significant. All analyses were performed with SPSS 21.0 software (SPSS, Inc., Chicago, IL, USA).

Results

Patient characteristics

Baseline patient characteristics are presented in Table 1. The mean age was 50 years (range 17 - 68). Twenty-four patients (63%) were male. The etiology of HF was ischemic in 10 patients (26%) and non-ischemic in 28 patients (74%), with a majority of idiopathic dilated cardiomyopathy. All patients had New York Heart Association (NYHA) class IV. Ten patients (26%) were in INTERMACS profile I ("crash and burn") prior to LVAD implantation, while the majority was in INTERMACS profile II or III (dependent on inotropes with progressive decline resp. clinical stability). Most patients received a HeartMate II (HMII; Abbott, Illinois, United States) device (92%), three patients (8%) received a HVAD (HeartWare; Medtronic, Minneapolis, United States).
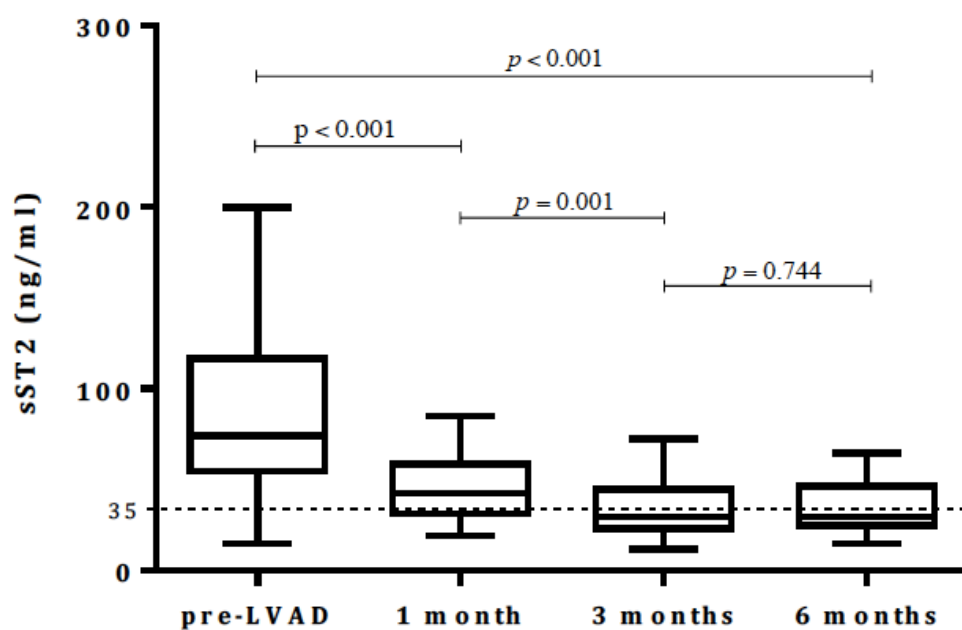
sST2 levels before and after LVAD implantation

Prior to LVAD implantation sST2 was severely elevated (74.2 ng/ml [IQR 54.7 - 116.9 ng/ml]; normal < 35 ng/ml(1)) in the majority of patients (95%). Levels significantly decreased during LVAD support (p < 0.001). In most patients sST2 levels normalized after 6 months (29.5 ng/ml [IQR 24.7 - 46.6 ng/ml]). A maximum drop in sST2 levels was seen after 3 months, without a significant decrease thereafter (**Figure 1**). The great variation of sST2 levels between individuals before LVAD implantation is striking and becomes less prominent during LVAD support.

Table 1. Baseline characteristics

Baseline characteristics	n=38
Age (years)	50 (range 17-68)
Male/female	24 (63%)/14 (37%)
NYHA classification IV	38 (100%)
Heart failure duration (weeks)	220 (range 1-936)
CRT/ICD	23 (61%)
Ischemic /non-ischemic etiology	10 (26%)/ 28 (74%)
Idiopathic dilated	13 (34%)
Hypertrophic	3 (8%)
Other	12 (32%)
Peripartum, myocarditis, tachy	3 (8%)
PLN mutation, familial, non-compaction	6 (16%)
Limb Girdle, hemachromatosis, toxic	3 (8%)
Inotropic medication	30 (79%)
INTERMACS profile I/ II-III	10 (26%)/ 28 (74%)
LVAD	38 (100%)
HeartMate II	35 (92%)
HeartWare	3 (8%)

NYHA, New York Heart Association; CRT, cardiac resynchronization therapy; ICD, implantable cardioverter defibrillator; PLN, phospholamban; INTERMACS, Interagency Registry for Mechanically Assisted Circulatory Support; LVAD, left ventricular assist device

Figure 1. sST2 levels before and during LVAD support

Median sST2 levels before and during LVAD support with IQR (25-75%). The dotted line represents the cut-off value for normal sST2 levels (< 35 ng/ml).

sST2 and clinical factors

To explore the variation of sST2 prior to LVAD implantation various clinical factors were evaluated in relation to sST2 levels (**Table 2**). The distribution of sST2 with regard to patient profile at implant (INTERMACS) showed a significant difference. Patients with INTERMACS profile I had significantly higher sST2 levels compared to patients in profile II and III (p = 0.030; **Figure 2A**).

Figure 2. sST2 in relation to INTERMACS profile and CRP
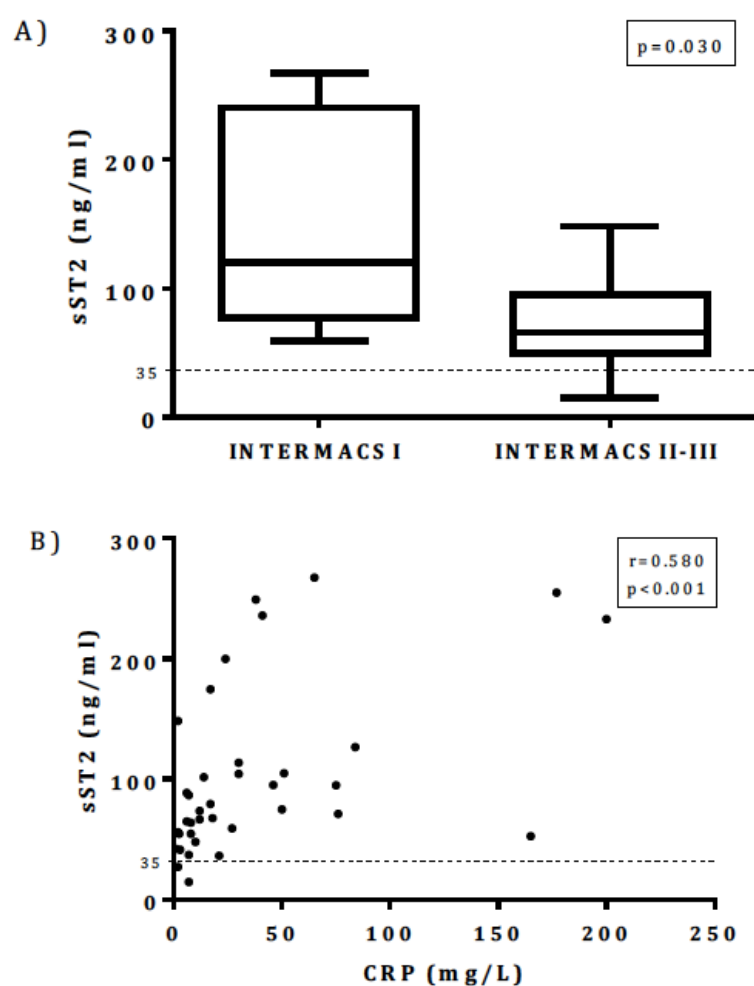
sST2 levels in relation to INTERMACS profile (A) and in correlation with CRP (B). The dotted line represents the cut-off value for normal sST2 levels (< 35 ng/ml).

CRP and sST2 levels showed a moderate positive and significant correlation (r = 0.580, p < 0.010; **Figure 2B**), suggesting higher CRP blood levels in patients with higher sST2 values. No differences in sST2 levels were seen with regard to gender, heart failure etiology (ischemic vs non-ischemic), RV function (≥ reasonable vs < reasonable), kidney function (normal vs

abnormal), inotropic medication (yes vs no) and mineralocorticoid receptor antagonists (yes vs no) (**Table 2**).

Table 2. The relation of sST2 levels and clinical parameters

Clinical parameter		sST2 level (ng/ml)	P-value n=38
Gender	(male / female)	77.1 / 65.8	0.78 [a]
HF etiology	(Ischemic / Nonischemic)	74.2 / 73.5	0.91 [a]
INTERMACS	(**Profile I** / **Profile II-III**)	**120.2 / 65.7**	**0.03** [a]
RV function	(≥Reasonable <Reasonable)	104.3 / 74.8	0.23 [a]
Kidney function	(eGFR≥60 eGFR<60)	64.9 / 74.8	0.19 [a]
Inotropic medication	(Yes / No)	87.7 / 60.8	0.16 [a]
MRA	(Yes / No)	74.8 / 64.9	0.74 [a]
Clinical parameter		**Correlation (r)**	**P-value n=38**
BNP	ng/L	0.19	0.29 [b]
CRP	mg/L	**0.58**	**<0.01** [b]
PCWP	mmHg	0.25	0.19 [b]
RAp	mmHg	0.22	0.28 [b]
LVEDD	mm	0.07	0.72 [b]
Pulse	beats/min	0.02	0.90 [b]
BP syst	mmHg	0.09	0.62 [b]
BP diast	mmHg	0.18	0.32 [b]
CO	(l/min)	-0.07	0.74 [b]
HF duration	weeks	0.14	0.41 [b]

The relation of sST2 levels was analyzed for several clinical factors using Mann Whitney U tests [a] [gender, heart failure etiology (ischemic vs non-ischemic), RV function (≥reasonable vs <reasonable), kidney function (normal vs abnormal), inotropic medication (yes vs no) and mineralocorticoid receptor antagonists (yes vs no)] and nonparametric (Spearman) correlations [b].

HF, heart failure; INTERMACS, Interagency Registry for Mechanically Assisted Circulatory Support; RV, right ventricular; MRA, mineralocorticoid receptor antagonist; BNP, brain natriuretic peptide; CRP, C-reactive protein; PCWP, pulmonary capillary wedge pressure; RAp, right atrial pressure; LVEDD, left ventricular end diastolic dimension; BP, blood pressure; CO, cardiac output;

No significant correlations were found between sST2 levels in end-stage HF and other tested clinical parameters, i.e. heart failure duration, BNP levels and hemodynamic parameters (**Table 2**).

Discussion

This study presents the first reported analysis of sST2 levels in patients with end-stage heart failure before and after LVAD implantation. We demonstrated severely elevated sST2 levels in patients with end-stage heart failure just before LVAD implantation, which decreased to near normal levels during LVAD support. Furthermore, an association between clinical patient profile before LVAD support and sST2 levels was found.

In extension to reported sST2 levels in the NYHA class II and III HF population(1) we found increased sST2 levels in almost all patients prior to LVAD implantation with a wide

distribution of sST2 levels. Despite the diversity of the study population with regard to HF etiology and duration we found significantly higher sST2 levels in patients with INTERMACS profile I vs II-III before LVAD support. This suggests that cardiogenic shock results in higher sST2 levels. As we could not correlate this in our study to hemodynamic data, the inflammatory state coinciding with cardiogenic shock might be responsible for this rise. Moreover, inflammation as an important determinant of sST2 levels corresponds with previous reports on the role of IL-33/ST2 signaling(8,9) and with the moderate positive correlation between sST2 and CRP levels found in this study. The wide variation of sST2 before LVAD implant could not be explained by other clinical factors that have previously been described to affect sST2 levels, like gender, RV function and hemodynamic parameters(10,11). It is not surprising that we could not find a "typical" patient-specific characteristic for the elevated sST2 levels, since sST2 is not merely a reflection of ventricular wall stress, but also of inflammation, active fibrosis and even subendocardial ischemia(12,13). The effect of other related clinical factors on sST2 levels may have been diminished by the impact of cardiogenic shock.

After 6 months of LVAD support sST2 levels were significantly decreased to normal levels in most of the patients (and the distribution narrowed). The biggest drop was seen after 1 month and reached a maximum at 3 months. The decrease in sST2 levels after unloading of the heart suggests that the inflammatory and pro-fibrotic state has dissipated, and in fact reverse remodeling may be occurring. The significant decrease in elevated sST2 levels after unloading of the left ventricle confirms the value of serial ST2 measurements as described previously(14) and indicates a potential role for ST2 as biomarker to monitor therapy, not only in NYHA class II-III patients, but also in patients with end-stage heart failure. However, clinical benefits of sST2 measurements in patients with end-stage heart failure before and after LVAD implantation remain unclear.

By identifying those factors that drive ST2 we may be able to use ST2 as a biomarker to stratify patients and assist in therapy guidance, perhaps even as a response predictor that will help clinicians in decision making. As LVADs become small and more portable, sST2 levels may be used to help profile those patients in whom LVAD discontinuation could be discussed.

Limitations

While there were relatively small numbers of patients in this study, the LVAD effect on sST2 levels was clear. Given the correlation with baseline CRP, sST2 after LVAD implantation may have been influenced by infectious postoperative complications that occurred in 7 patients. Another drawback is the variable timing of hemodynamic measurements prior to LVAD implantation. Unlike eGFR and CRP, measured maximum 48 hours before LVAD, the calculated correlation may not completely represent the hemodynamics on the day of LVAD implantation. BNP levels were also determined at different time frames, within 24 hours to 1 month before LVAD implantation.

The strength of our analysis however lies in the consecutive measurements of sST2 in the same patient, before and after LVAD implantation, eliminating in this way variable results due to variations in patient population.

Conclusion

We extend the reported elevated sST2 levels in class II-III heart failure patients to patients with end-stage heart failure, qualifying for mechanical circulatory support as a bridge to heart transplantation. High sST2 levels predict a worse outcome in patients with conventional treatment. The wide variation in sST2 levels (almost all above the cutpoint of 35 ng/ml) in end-stage heart failure patients delineates the many pathways that feed into the shedding of the decoy receptor sST2. Cardiogenic shock and inflammation (INTERMACS I) are associated with higher levels of sST2. Unloading of the left ventricle by an LVAD results in a rapid decrease of sST2 levels, with complete normalization within 3 months. These findings potentially warrant further research on the role of sST2 as a prognostic and therapeutic marker, not only in moderate heart failure, but also in end-stage heart failure.

References

1.   Bayes-Genis A, Zhang Y, Ky B. ST2 and patient prognosis in chronic heart failure. Am J Cardiol. 2015;115(7 Suppl):64B–9B.

2.   Dieplinger B, Mueller T. Soluble ST2 in heart failure. Clin Chim Acta. 2015;443:57–70.

3.   Broch K, Ueland T, Nymo SH, Kjekshus J, Hulthe J, Muntendam P, et al. Soluble ST2 is associated with adverse outcome in patients with heart failure of ischaemic aetiology. Eur J Heart Fail. 2012;14(3):268–77.

4.   Boer RA De, Daniels LB, Maisel AS, Januzzi Jr JL. State of the Art : Newer biomarkers in heart failure. Eur J Heart Fail. 2015;17:559–69.

5.   Boisot S, Beede J, Isakson S, Chiu A, Clopton P, Januzzi J, et al. Serial sampling of ST2 predicts 90-day mortality following destabilized heart failure. J Card Fail. 2008;14(9):732–8.

6.   Breidthardt T, Balmelli C, Twerenbold R, Mosimann T, Espinola J, Haaf P, et al. Heart failure therapy-induced early ST2 changes may offer long-term therapy guidance. J Card Fail. 2013;19(12):821–8.

7.   Simera I, Moher D, Hoey J, Schulz KF, Altman DG. A catalogue of reporting guidelines for health research. Eur J Clin Invest. 2010;40(1):35–53.

8.   Chen W-Y, Hong J, Gannon J, Kakkar R, Lee RT. Myocardial pressure overload induces systemic inflammation through endothelial cell IL-33. Proc Natl Acad Sci U S A. 2015;112(23):7249–54.

9.   Martinez-Martinez E, Cachofeiro V, Rousseau E, Álvarez V, Calvier L, Fernández-Celis A, et al. Interleukin-33/ST2 system attenuates aldosterone-induced adipogenesis and inflammation. Mol Cell Endocrinol. 2015;411:20–7.

10.   Broch K, Andreassen AK, Ueland T, Michelsen AE, Stueflotten W, Aukrust P, et al. Soluble ST2 reflects hemodynamic stress in non-ischemic heart failure. Int J Cardiol. 2015;179:378–84.

11.   Daniels LB, Clopton P, Iqbal N, Tran K, Maisel AS. Association of ST2 levels with cardiac structure and function and mortality in outpatients. Am Heart J. 2010;160(4):721–8.

12.   Kohli P, Bonaca MP, Kakkar R, Kudinova AY, Scirica BM, Sabatine MS, et al. Role of ST2 in Non–ST-Elevation Acute Coronary Syndrome in the MERLIN-TIMI 36 Trial. Clin Chim Acta. 2012;58(1):257–66.

13.   Pascual-Figal DA, Januzzi JL. The biology of ST2: The international ST2 consensus panel. Am J Cardiol. 2015;115(7):3B–7B.

14.   Wu AHB, Wians F, Jaffe A. Biological variation of galectin-3 and soluble ST2 for chronic heart failure: Implication on interpretation of test results. Am Heart J. 2013;165(6):995–9.

9

The interleukin-33/ST2 pathway is expressed in the failing human heart and associated with pro-fibrotic remodeling of the myocardium

C.C.S. Tseng, M.M.H. Huibers, J. van Kuik, R.A. de Weger, A.Vink, N. de Jonge

Abstract

Background

The interleukin-33 (IL-33)/ suppression of tumorigenicity 2 (ST2) pathway is a potential pathophysiological mediator of cardiac fibrosis. Soluble ST2 (sST2) is one of the main isoforms of ST2 with strong prognostic value in cardiac disease. The exact role of sST2 in cardiac fibrosis is unknown. The aim of this study was 1) to investigate myocardial expression of the IL-33/ST2 pathway in relation to myocardial fibrosis in end-stage heart failure patients and 2) to study whether plasma sST2 is associated with histologically determined cardiac fibrosis.

Method and results

In 38 patients undergoing left ventricular assist device implantation mRNA expression of sST2, total ST2 and IL-33 was measured in cardiac tissue obtained during the implantation. In the same tissue histological fibrosis was digitally quantified and mRNA expression of pro-fibrotic signaling molecules, connective tissue growth factor (CTGF) and transforming growth factor beta 1 (TGFβ1), was measured. In addition, plasma levels of sST2 were determined. Expression levels of IL-33/ST2 pathway factors in myocardial tissue were significantly associated with cardiac fibrosis and the expression levels of CTGF and TGFβ1. Plasma levels of sST2 did not correlate with tissue expression of ST2, the amount of fibrosis or myocardial expression of pro-fibrotic signaling proteins.

Conclusion

The interleukin-33/ST2 pathway is expressed in the failing human heart and its expression is associated with cardiac fibrosis and pro-fibrotic signaling proteins, suggesting a role in pro-fibrotic myocardial remodeling. Soluble ST2 levels in the circulation did not correlate with the amount of cardiac fibrosis or myocardial ST2 expression, however. Therefore, other pathophysiological processes such as inflammation might also substantially affect sST2 plasma levels.

Introduction

Heart failure is a progressive disease with a large burden on public health(1,2). This clinical syndrome is a result of initial injury or stress followed by remodeling of the myocardium leading to changes in size, shape and function of the heart(3,4). Fibrosis is an important component of ventricular remodeling and subsequent cardiac dysfunction(4,5). There is an urgent need for good biomarkers predicting this remodeling process. In contrast to state-of-the-art imaging techniques, biomarkers are considered mechanistically driven and clinically more useful predictors of ventricular remodeling(5).

Suppression of tumorigenicity 2 (ST2) is an interleukin-1 (IL-1) receptor family member, and is a transcriptional product of the IL-1 receptor like-1 (IL1RL1) gene(6). Soluble ST2 (sST2), one of the main isoforms of ST2, is used for risk stratification in heart failure patients(7) and is considered a biomarker of myocardial fibrosis(8). However, the exact role of sST2 and its functional ligand, interleukin-33 (IL-33), in cardiac fibrosis is unexplored(9). The IL-33/ ST2 pathway potentially mediates myocardial inflammation and fibrosis signaling upon biomechanical strain(6,10–12).

We recently demonstrated that end-stage heart failure patients have severely elevated sST2 levels prior to left ventricular assist device (LVAD) support. Within this group of patients we observed a large variation that could not be explained by clinical factors such as heart failure aetiology or duration, and might therefore be explained by the amount of cardiac fibrosis(13). More insight in the relation between fibrosis and ST2 may help to define strategies to predict reverse remodeling and ultimately identify LVAD patients in whom recovery of cardiac function may occur. Therefore, the aim of this study was to assess the association between cardiac fibrosis and IL-33/ST2 signaling in patients with end-stage heart failure just before LVAD implantation. The LVAD bridge to transplantation population provides a unique opportunity to assess both plasma levels and mRNA expression in cardiac tissue in end-stage heart failure. We quantified fibrosis and pro-fibrotic signaling molecules in cardiac biopsies obtained during LVAD implantation. In addition, we assessed myocardial mRNA expression of the IL-33/ST2 pathway and measured sST2 levels in plasma.

Method and materials

Myocardial tissue and serum

From 38 end stage heart failure patients, myocardial tissue was obtained from the apical core biopsy during LVAD implantation. The tissue samples were split in two parts: one part was formalin-fixed and paraffin-embedded for fibrosis quantification and the other part was stored at -80°C for RNA isolation. Serum samples were collected within 24 hours prior to LVAD implantation. All patients approved collection and banking of blood samples and tissue for research purposes and the study was approved by the institutional review board (Medisch Ethische Toetsingscommissie (METC) of the University Medical Center Utrecht, number 12/387).

Fibrosis quantification

The paraffin-embedded samples were sectioned at 4µm thickness. Masson's Trichome stain was performed with an automatic staining system (DakoCytomation Artisan, Glostrup, Denmark). Thereafter, samples were digitalized using an Aperio XT slide scanner (Aperio, Vista, California, United States). For analysis of fibrosis a systematic method for high-resolution digital cardiac fibrosis quantification was used as reported previously(14). The percentage of fibrosis of the total tissue surface area was calculated with the use of Aperio Image Scope v12.1.0.5029 (Aperio, Vista, California, United States).

mRNA expression

RNA was isolated from 20 slides of 10µm of frozen tissue with the RNeasy mini kit (Qiagen Inc, Austin, USA) and synthesis of cDNA was performed with superscript III, oligo-dT and random primers (Invitrogen, Oslo, Norway). QPCR was performed as previously described on the Viia™ 7 Real-Time PCR system (Thermo Fisher Scientific, Massachusetts, USA)(15). The mRNA expression of the IL-33/ST2 pathway and pro-fibrotic signaling proteins was analyzed. The following Taqman primer-probes were used: sST2, total ST2 (**Figure 1**), IL-33, Connective Tissue Growth Factor (CTGF), Transforming growth factor beta 1 (TGFβ1) and GAPDH (as housekeeping gene) (Applied Biosystems, Thermo Fisher Scientific, Massachusetts, USA). Each target was also measured in a calibrator sample (positive control). Each sample was run in duplicate. A maximum ΔCq of 0.5 between duplicates was accepted. Relative quantification (RQ) values were calculated using the comparative Cq method: relative quantity (RQ) = $2^{-\Delta\Delta Ct}$, $\Delta\Delta Cq = \Delta Cq$ (sample) $- \Delta Cq$ (calibrator) and $\Delta Cq = Cq$

(housekeeping) – Cq (sample). Cq values above 35 were interpreted as negative. An estimated ratio (sST2:ST2L) was generated by calculating the percentage of ST2L, from the measured markers sST2 and total ST2 (**Figure 1**). Only patients with RQ sST2 < total ST2 were included in the analysis.

Figure 1. Schematic representation of the interleukin 1 receptor-like 1 (IL1RL) gene
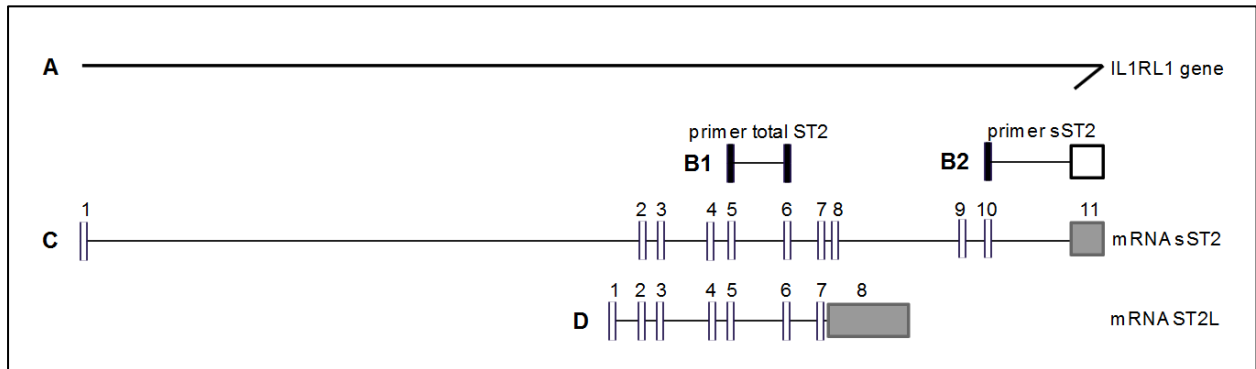
*Schematic representation of the interleukin 1 receptor-like 1 (IL1RL) gene (**A**) and the intron (horizontal line)-exon (vertical stripes) structure of soluble ST2 (sST2, **C**) and ST2 ligand (ST2L, **D**) mRNA . The primer-probe combination for total ST2 (**B1**) will detect sST2 and ST2L (exon 5-6) while primer sST2 (**B2**) is specific for sST2 mRNA (exon 10-11).*

Plasma levels of ST2

Peripheral vein blood EDTA samples were used to determine levels of sST2. After withdrawal blood was centrifuged within 6 hours. Plasma was collected in aliquots and stored at -80°C. The Presage ST2 ELISA assay (Critical diagnostics, San Diego, CA, USA) was used according to manufacturer's instructions to determine sST2 concentrations in one batch(13).

Statistics

Categorical data are expressed as number (%) and continuous data as mean ± SD or median [interquartile range (IQR), 25th -75th percentile]. Correlations were calculated using Pearson (in case of normal distribution) or Spearman (in case of non-parametric distribution) correlation. Comparisons between two groups were performed using a Mann Whitney U test and between more than two groups with a Kruskal Wallis test. Correction for multiple testing was applied when appropriate. Statistical analysis was performed with SPSS version 21 (SPSS Inc. Chicago, IL, USA). A P-value ≤ 0.05 was considered statistically significant.

Results

Patient characteristics

Thirty-eight patients were included in this study. All patients were in New York Heart Association (NYHA) class IV and received an LVAD as bridge to transplantation between January 2010 and October 2013. The majority of patients (74%) had a non-ischemic dilated cardiomyopathy (**Table 1**). Plasma samples and paraffin-embedded tissue of all 38 patients were available. Frozen tissue of 1 patient was not available for research.

Table 1. Patient characteristics.

Characteristic	N=38
Age (years)	50 (range 17-68)
Male/female	24 (63%)/14 (37%)
NYHA classification IV	38 (100%)
Heart failure duration (weeks)	220 (range 1-936)
CRT/ICD	23 (61%)
Aetiology of cardiomyopathy	
Ischemic	10 (26%)
Non-ischemic	27 (71%)
Hypertrophic	1 (3%)
Inotropic medication	30 (79%)
INTERMACS profile I/ II-III	10 (26%)/ 28 (74%)

NYHA, New York Heart Association; CRT, cardiac resynchronization therapy;
ICD, implantable cardioverter defibrillator.

Myocardial fibrosis is related to expression of pro-fibrotic signaling molecules

The amount of fibrosis in myocardial apical tissue (n=38) ranged from 4.0 to 64.4% with a median of 15.2% (IQR 10.1 – 28.3%). **Figure 2A** shows an example of the histology. Patients with ischemic cardiomyopathy had significantly more fibrosis than those with non-ischemic cardiomyopathy ($p = 0.010$, **Figure 2B**). Subsequently, we studied whether the amount of fibrosis and mRNA expression of pro-fibrotic signaling molecules was related to determine whether an ongoing pro-fibrotic process was present (n=37). The quantity of fibrosis was positively correlated with mRNA levels of CTGF and TGFβ1 (**Figure 2C and D**; $r = 0.54$, $p < 0.001$ and $r = 0.49$, $p = 0.004$, respectively). mRNA levels of CTGF and TGFβ1 were strongly positively correlated ($r = 0.68$, $p = 0.002$) as well (**figure S1**).
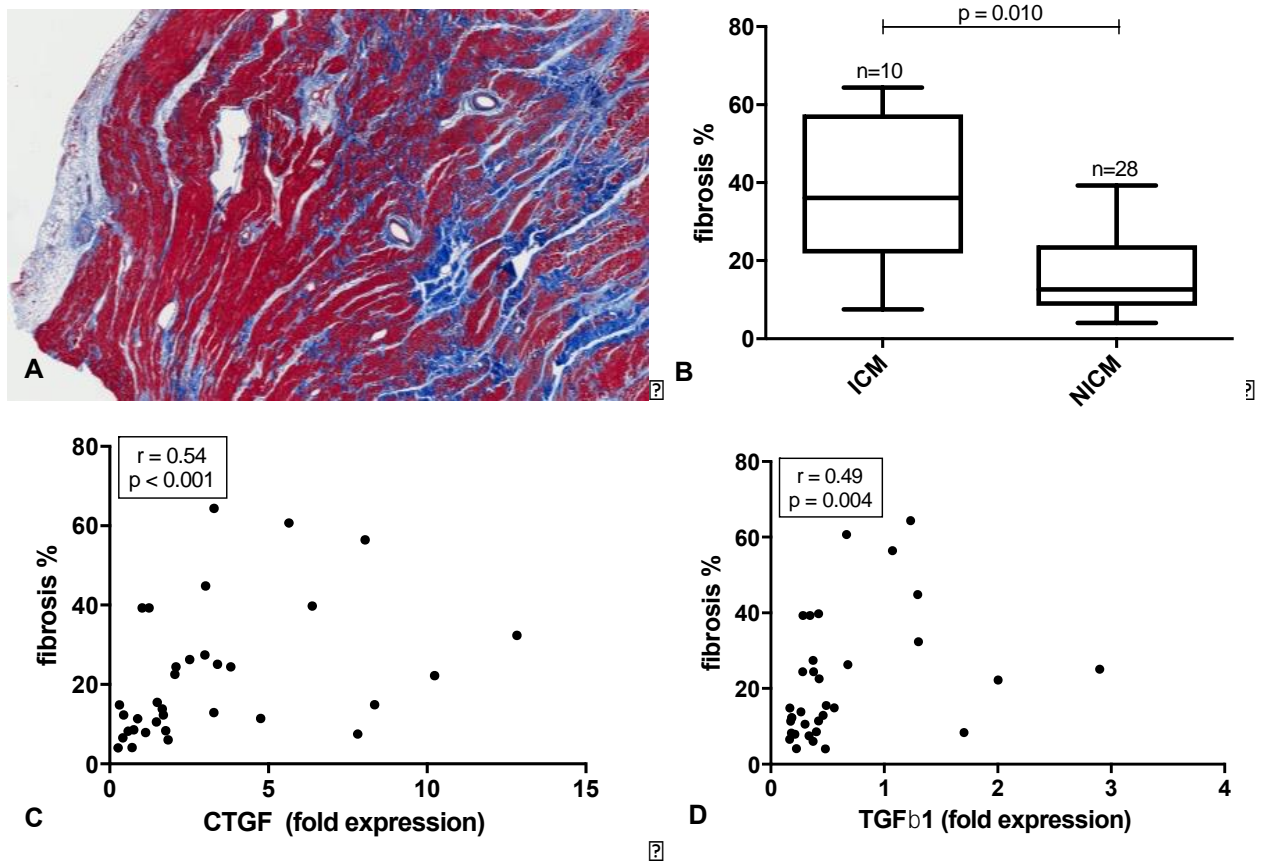
Myocardial expression of the IL-33/ST2 pathway is related to cardiac fibrosis

A strong positive correlation between myocardial mRNA expression (n=37) of sST2 and total myocardial ST2 was observed (r = 0.61, p < 0.001, **Figure S2**). The mRNA expression of IL-33 and sST2 in cardiac tissue showed a moderate positive correlation (r = 0.44, p = 0.010, **Figure S3A**), while IL-33 and total ST2 demonstrated a weak non-significant correlation (r = 0.27, p = 0.121, **Figure S3B**).

To determine whether cardiac fibrosis is associated with cardiac mRNA expression of the IL-33/ST2 pathway, correlations between fibrosis, pro-fibrotic signaling molecules CTGF and TGFβ1, and mRNA expression of sST2, ST2 and IL-33 were calculated (**Table 2**; **Figure S5**).

The mRNA level (n=37) of sST2 was strongly positively correlated to the amount of histological fibrosis (r = 0.43, p = 0.001) and myocardial TGFβ1 mRNA (r = 0.54, p = 0.001;

Figure S5D), but not to CTGF mRNA (r = 0.24, p = 0.177; **Figure S5C**). Statistically significant strong correlations were found between myocardial IL-33 mRNA levels and the amount of fibrosis (r = 0.46, p = 0.007) and pro-fibrotic signaling proteins CTGF and TGFβ1 (r = 0.81, p < 0.001 and r = 0.84, p < 0.001, respectively; **Figure 3C+D**). Total ST2 mRNA was only significantly correlated with TGFβ1 mRNA expression (r = 0.46, p = 0.006; **Table 2 and Figure S5E+F**).

Patients were then divided in categories of fibrosis based on tertiles. The amount of fibrosis from the first tertile (category 1) ranged from 4.00-11.42%, the second tertile (category 2) from 11.43-24.44% and the third tertile (category 3) from 24.45-64.37%. When mRNA expression of sST2, total ST2 and IL-33 was stratified in these fibrosis categories, a significantly different expression was measured in sST2 (p = 0.012, **Figure 3B**) and IL-33 (p = 0.040, **Figure 3C**). A significant difference in fold expression of sST2 and IL-33 was only found between category 1 and 3 (p = 0.004 and p = 0.014 respectively).

Table 2. Correlations of fibrosis and the IL-33/ST2 pathway.

	Fibrosis %		CTGF		TGFβ1	
	digital analysis		mRNA expression		mRNA expression	
	r	p	r	p	r	p
sST2 plasma level	-0.19	0.264	-0.24	0.170	-0.05	0.761
sST2 mRNA expression	**0.43**	**0.011**	0.24	0.180	**0.54**	**0.001**
ST2 (total) mRNA expression	0.21	0.227	0.24	0.177	**0.46**	**0.006**
IL-33 mRNA expression	**0.46**	**0.007**	**0.81**	**<0.001**	**0.84**	**<0.001**

Correlations of fibrosis and the IL-33/ST2 pathway. CTGF, connective tissue growth factor; TGFβ1, transforming growth factor beta 1; sST2, soluble ST2; interleukin-33, IL-33.

sST2 in the circulation is not correlated to myocardial ST2 expression or myocardial fibrosis
As previously demonstrated, the sST2 plasma levels (n=38) were strongly elevated in our cohort compared to levels in healthy individuals with a wide variation (median 74.2 ng/ml [IQR 54.7 - 116.9 ng/ml]; normal < 35ng/ml)(13,16). To study whether these plasma levels are related to the amount of mRNA expression of total ST2 and sST2 in the myocardial tissue, matched plasma and tissue samples from the same patients were used. No

170

significant correlation was found between sST2 plasma levels and myocardial mRNA expression (n=37) of sST2 (r = 0.12, p = 0.505, **Figure S4A**) or total ST2 (r = 0.16, p = 0.371, **Figure S4B**). Also no significant correlation was observed between sST2 plasma levels and the myocardial mRNA expression of IL-33 (r = - 0.09, p = 0.612, **Figure S4C**) or between the ratio of sST2:ST2L (n=32) and sST2 plasma levels (r = 0.01, p = 0.948, **Figure S4D**). The association between the amount of cardiac fibrosis measured with digital analysis and sST2 plasma levels was then determined (n=38). No significant correlation was found (r = - 0.19, p = 0.264, **Table 2**). Next, the correlation between sST2 in plasma and mRNA expression of pro-fibrotic signaling proteins CTGF and TGFβ1 (n=37) was assessed. These factors also did not correlate significantly with sST2 levels in plasma (r = -0.24, p = 0.170,
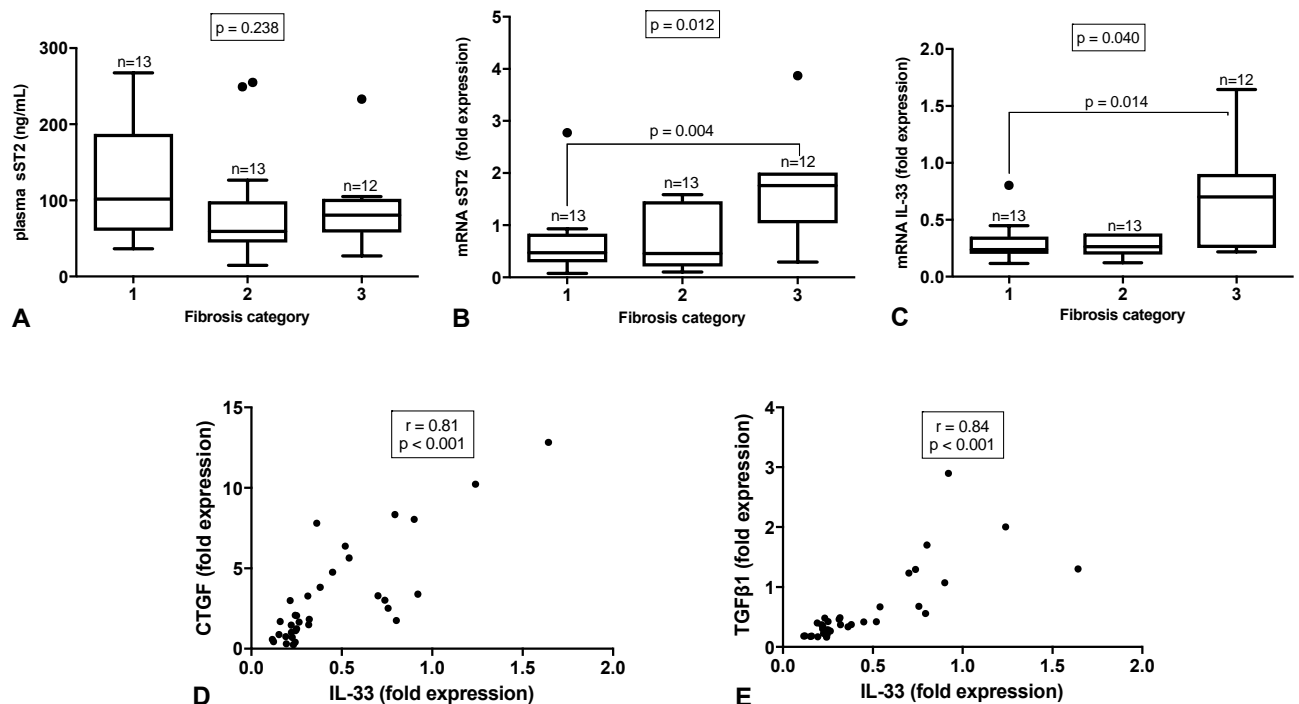
Discussion

This study aimed to assess the association between the IL-33/ST2 pathway and histologically determined myocardial fibrosis in heart failure. The study has 3 important results: first, the IL-33/ST2 pathway is expressed in myocardial tissue of end-stage heart failure patients. Second, its expression is associated with local myocardial fibrosis. Third, plasma levels of sST2 did not correlate with either myocardial expression of this pathway, nor myocardial fibrosis.

We found significant correlations between the myocardial sST2 and IL-33 mRNA expression and the amount of fibrosis, suggesting a potential role of the IL-33/ST2 pathway in cardiac fibrosis. Not only the amount of fibrosis in apical tissue but also the expression of pro-fibrotic signaling molecules CTGF and TGFβ1 was significantly correlated with the IL-33/ST2 pathway factors, implying that there was an active pro-fibrotic remodeling process. Although causality can not be concluded, these data fit the hypothesis that even in end-stage heart failure the IL-33/ST2 pathway is involved in cardiac fibrosis and pro-fibrotic changes of the myocardium(13). The strong correlation between the expression of IL-33 and pro-fibrotic markers was remarkable. While the sST2 mRNA expression significantly correlates with TGFβ1 and not with CTGF, and the IL-33 mRNA expression correlates strongly with TGFβ1 and CTGF, IL-33 mRNA myocardial expression might play a more important role in cardiac fibrosis than myocardial sST2 mRNA expression. Alternatively, CTGF might more specifically regulate fibrosis in the heart as the TGFβ pathway has many other functions besides modulating cardiac fibrosis and CTGF is a downstream modulator of TGFβ1(17).

In this study with end-stage heart failure patients, sST2 plasma levels were not associated with the mRNA expression of sST2, total ST2 or IL-33 in cardiac tissue. We also found a non-significant correlation between the sST2:ST2L mRNA expression ratio and sST2 plasma levels. These results suggest that the heart may not be the main source of sST2 in peripheral blood. This observation is in line with other studies that indicate production of sST2 in, amongst others, vascular endothelial cells(18–20). It also corresponds with the fact that various diseases are associated with high levels of sST2 in plasma(11,21).

Since sST2 plasma levels have major prognostic value in heart failure patients and are suggested to be involved in fibrosis(8,22,23), an association between these two parameters

seemed plausible. However, sST2 plasma levels in this study were not associated with the amount of fibrosis, nor with the expression of pro-fibrotic markers in the heart. These findings indicate that high sST2 levels in the circulation do not positively correlate with fibrosis in myocardial tissue. The lacking association of fibrosis with soluble ST2 in plasma suggests that the levels in circulation are more prominently influenced by other factors than fibrosis in the heart, e.g. chronic overload and inflammatory signals. Although a significant correlation between circulating sST2 and BNP is absent(13), inflammatory signaling due to chronic overload might cause excessive sST2 release in the circulation. This is in accordance with the significant decline in sST2 plasma levels upon LV unloading(13). It is also in line with the concept of chronic heart failure as an inflammatory disease (24) and the role of the IL-1 family in inflammatory signaling(6). Another explanation that sST2 in plasma and fibrosis could not be correlated in this study might be that the overall poor status of patients with end-stage heart failure (INTERMACS profile I-III) is the primary determinant of sST2 levels in plasma, as is suggested by the significantly higher sST2 levels in patients with INTERMACS profile I(13). Perhaps, in patients with less severe decompensated heart failure and without comorbidities that interfere with ST2, plasma levels of sST2 may be more consistent with the amount of cardiac fibrosis. Furthermore, after an acute myocardial infarction, plasma sST2 levels might play a role in the process of fibrosis and remodeling(25). In addition to patients with severe heart failure, it is also of interest to look at determinants of sST2 in the outpatient clinic where patients do not have end-stage heart failure yet, for instance in patients undergoing a biopsy for diagnostic purposes. Besides the presented measurements pre-LVAD, it would be interesting to assess cardiac tissue post-LVAD before heart transplantation and associate fibrosis and the expression of the IL-33/ST2 pathway in this patient population. The effect of the improved neurohormonal milieu due to LV unloading may lead to diminished sST2 expression and reveal stronger associations between plasma sST2 levels and cardiac tissue expression. The presented study emphasizes the importance of cardiac tissue analysis in the exploration of the IL-33/ST2 pathway in cardiac pathophysiology.

Limitations

Limitations of the presented study include the end-stage heart failure population in which

the development and progression of fibrosis may already be advanced to a degree that sST2 expression in the heart or in the circulation is not representative for other stages of heart failure. On the other hand, this population gives the opportunity for additional tissue analysis. Since only the apical core was assessed, this may not fully resemble the whole heart. Another drawback of this study is that inflammation was not assessed. The proposed influence of inflammatory signals on sST2 is an interesting topic for future studies.

Conclusion

Soluble ST2 is a prognostic biomarker in heart failure patients that is suggested to be a marker of cardiac fibrosis. The results of this study show that the interleukin-33/ST2 pathway is expressed in the failing human heart and that its expression is associated with cardiac fibrosis and pro-fibrotic signaling proteins, indeed suggesting a role in pro-fibrotic myocardial remodeling. Levels of sST2 in the circulation were not correlated to cardiac fibrosis or myocardial ST2 expression. Therefore, other pathophysiological processes such as inflammation might also substantially affect sST2 plasma levels.

Acknowledgements

References

1. McMurray JJ, Stewart S. Epidemiology, aetiology, and prognosis of heart failure. Heart. 2000;83:596–602.

2. Ambrosy AP, Fonarow GC, Butler J, Chioncel O, Greene SJ, Vaduganathan M, et al. The global health and economic burden of hospitalizations for heart failure: Lessons learned from hospitalized heart failure registries. J Am Coll Cardiol. 2014;63(12):1123–33.

3. Jessup M, Brozena S. Heart Failure. N Engl J Med. 2003;348(18):2007–18.

4. Burchfield JS, Xie M, Hill JA. Pathological ventricular remodeling: Mechanisms: Part 1 of 2. Circulation. 2013;128(4):388–400.

5. Motiwala SR, Gaggin HK. Biomarkers to Predict Reverse Remodeling and Myocardial Recovery in Heart Failure. Curr Heart Fail Rep. 2016;13(5):207–18.

6. Kakkar R, Lee RT. The IL-33/ST2 pathway: therapeutic target and novel biomarker. Nat Rev Drug Discov. 2008;7(10):827–40.

7. Yancy CW, Jessup M, Bozkurt B, Butler J, Casey DE, Drazner MH, et al. 2013 ACCF/AHA guideline for the management of heart failure: a report of the American College of Cardiology Foundation/American Heart Association Task Force on Practice Guidelines. J Am Coll Cardiol. 2013;62(16):e147-239.

8. Pascual-Figal DA, Lax A, Perez-Martinez MT, del Carmen Asensio-Lopez M, Sanchez-Mas J, on behalf of GREAT Network. Clinical relevance of sST2 in cardiac diseases. Clin Chem Lab Med. 2015;54(1):29–35.

9. Kakkar R, Lee RT. The IL-33/ST2 pathway: therapeutic target and novel biomarker. Nat Rev Drug Discov. 2008;7(10):827–40.

10. Miller AM, Liew FY. The IL-33/ST2 pathway - A new therapeutic target in cardiovascular disease. Pharmacol Ther. 2011;131(2):179–86.

11. Gao Q, Li Y, Li M. The potential role of IL-33 / ST2 signaling in fibrotic diseases. J Leukoc Biol. 2015;98(July):1–8.

12. Caselli C, Amico AD, Ragusa R, Caruso R, Prescimone T, Cabiati M, et al. IL-33 / ST2 Pathway and Classical Cytokines in End-Stage Heart Failure Patients Submitted to Left Ventricular Assist Device Support : A Paradoxic Role for Inflammatory Mediators ? Mediators Inflamm. 2013;

13. Tseng CCS, Huibers MM, Gaykema L, Chamuleau SAJ, de Jonge N. Soluble ST2 Levels in End-Stage Heart Failure and during LVAD Support. J Hear Lung Transplant. 2016;35(4S Abstract Supplement Issue):S12.

14. Gho JMIH, van Es R, Stathonikos N, Harakalova M, te Rijdt WP, Suurmeijer AJH, et al. High Resolution Systematic Digital Histological Quantification of Cardiac Fibrosis and Adipose Tissue in Phospholamban p.Arg14del Mutation Associated Cardiomyopathy. PLoS One. 2014;9(4):e94820.

15. Lok SI, Winkens B, Goldschmeding R, van Geffen AJP, Nous FM a, van Kuik J, et al. Circulating growth differentiation factor-15 correlates with myocardial fibrosis in patients with non-ischaemic dilated cardiomyopathy and decreases rapidly after left ventricular assist device support. Eur J Heart Fail. 2012;14(11):1249–56.

16. Wu AHB, Wians F, Jaffe A. Biological variation of galectin-3 and soluble ST2 for chronic heart failure: Implication on interpretation of test results. Am Heart J. 2013;165(6):995–9.

17. Creemers EE, Pinto YM. Molecular mechanisms that control interstitial fibrosis in the pressure-overloaded heart. Cardiovasc Res. 2011;89(2):265–72.

18. Bartunek J, Delrue L, Van Durme F, Muller O, Casselman F, De Wiest B, et al. Nonmyocardial Production of ST2 Protein in Human Hypertrophy and Failure Is Related to Diastolic Load. J Am Coll Cardiol. 2008;52(25):2166–74.

19. Demyanets S, Kaun C, Pentz R, Krychtiuk KA, Rauscher S, Pfaffenberger S, et al. Components of the interleukin-33/ST2 system are differentially expressed and regulated in human cardiac cells and in cells of the cardiac vasculature. J Mol Cell Cardiol. 2013;60(1):16–26.

20. Pascual-Figal DA, Januzzi JL. The biology of ST2: The international ST2 consensus panel. Am J Cardiol.

2015;115(7):3B–7B.

21. Januzzi JL, Peacock WF, Maisel AS, Chae CU, Jesse RL, Baggish AL, et al. Measurement of the interleukin family member ST2 in patients with acute dyspnea: results from the PRIDE (Pro-Brain Natriuretic Peptide Investigation of Dyspnea in the Emergency Department) study. J Am Coll Cardiol. 2007;50(7):607–13.

22. Januzzi JL, Pascual-Figal D, Daniels LB. ST2 Testing for Chronic Heart Failure Therapy Monitoring: The International ST2 Consensus Panel. Am J Cardiol. 2015;115(7):70B–75B.

23. Bayes-Genis A, Zhang Y, Ky B. ST2 and patient prognosis in chronic heart failure. Am J Cardiol. 2015;115(7 Suppl):64B–9B.

24. Anker SD, von Haehling S. Inflammatory mediators in chronic heart failure: an overview. Heart. 2004;90(4):464–70.

25. Weir RAP, Miller AM, Murphy GEJ, Clements S, Steedman T, Connell JMC, et al. Serum Soluble ST2. A Potential Novel Mediator in Left Ventricular and Infarct Remodeling After Acute Myocardial Infarction. J Am Coll Cardiol. 2010;55(3):243–50.

Supplemental data

Figure S1. The correlation between cardiac mRNA expression of pro-fibrotic markers.
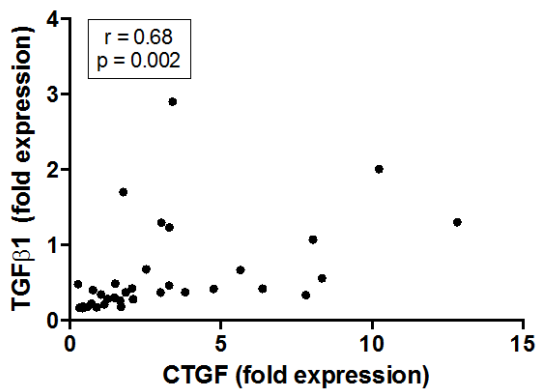
Scatterplot of the correlation between cardiac mRNA expression of connective tissue growth factor (CTGF) and transforming growth factor beta 1 (TGFβ1).

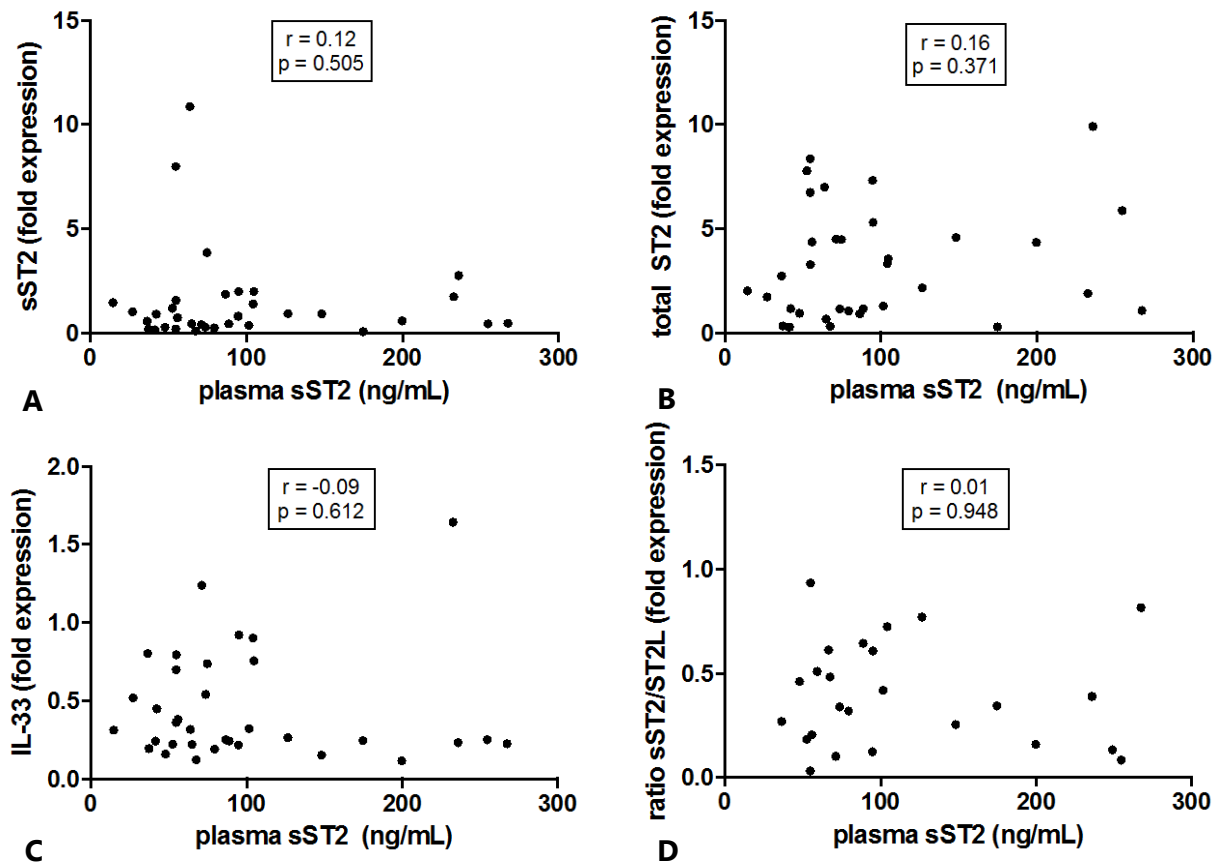**Figure S2. The correlation between cardiac mRNA expression of total ST2 and plasma sST2 levels**
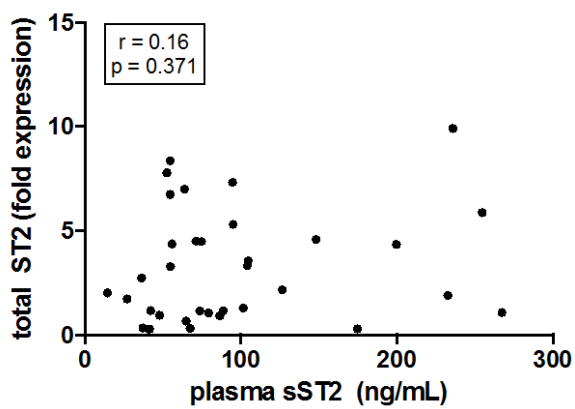
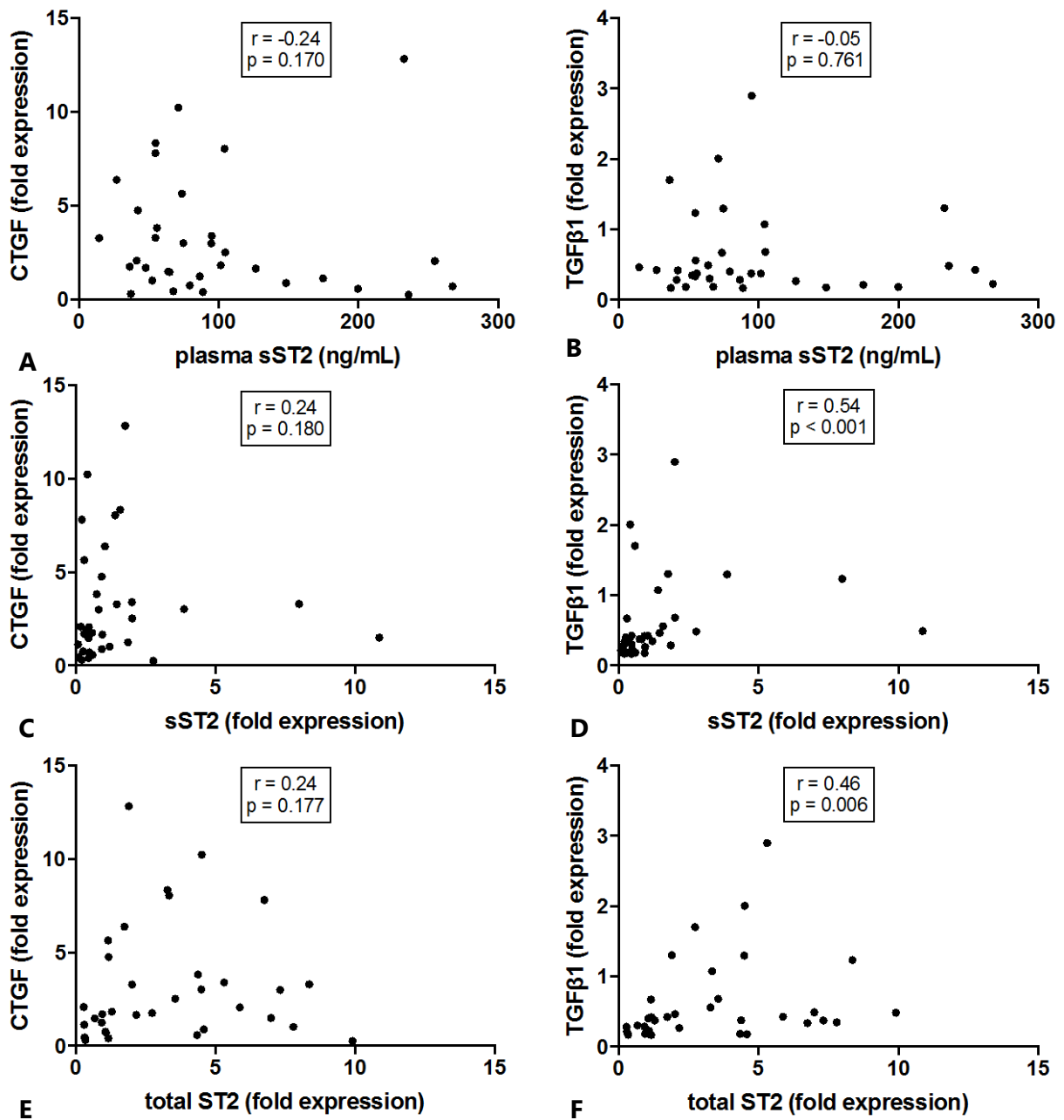*Scatterplot of the correlation between cardiac mRNA expression of total ST2 and plasma sST2 levels*

Figure S3. The correlation between cardiac IL-33 mRNA expression and ST2.
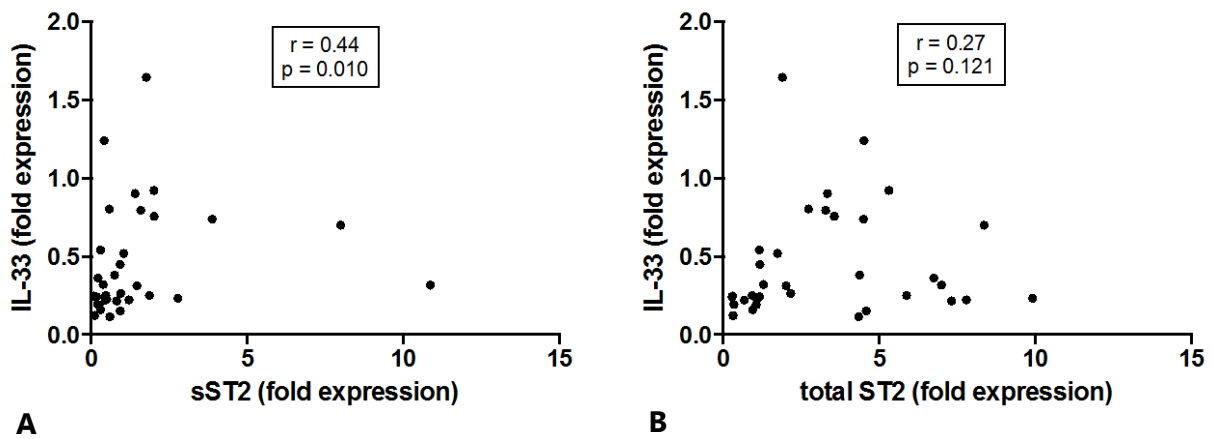
Scatterplots of the correlation between cardiac IL-33 mRNA expression and soluble ST2 (sST2, A) and total ST2 mRNA expression (B).

Figure S4. The correlation between soluble ST2 (sST2) levels in plasma and cardiac mRNA expression of IL-33/ST2 pathway factors

Scatterplots of the correlation of plasma sST2 and sST2 mRNA expression (A), total sST2 mRNA expression (B), IL-33 mRNA expression (C) and the ratio of sST2/ST2L mRNA expression (D)

Figure S5. The correlation between ST2 and cardiac fibrosis markers

Scatterplots of the correlation between soluble ST2 (sST2) in plasma and myocardial expression of connective tissue growth factor (CTGF, A) and transforming growth factor beta 1 (TGFβ1, B). The correlation between myocardial expression of sST2 (C, D) and total ST2 (E,F)and CTGF and TGFβ1.

10

Summary and general discussion

Towards advanced therapy guidance in the failing heart

This thesis discussed limitations of cardiac regenerative therapy and mechanical support, and novel advanced methods to improve heart failure therapy. Part one was aimed at improving cardiac regenerative therapy, while opportunities in the LVAD population were the focus of part two.

PART ONE IMPROVING CARDIAC REGENERATIVE THERAPY

Cell therapy for chronic heart failure

Regeneration of the damaged heart after ischemic injury has been researched extensively over the last 1,5 decade(1–3). The rationale of cell therapy for cardiac regeneration was discussed in **chapter 2**. Bone marrow cells (BMCs) were the first hypothesized cell type to have the potential to differentiate into cardiomyocytes and therefore to have regenerative capacity in the damaged heart. However, the existence of endogenous cardiac stem cells has shifted the thoughts about the mechanism of action. Paracrine effects rather than transdifferentiation of bone marrow-derived stem cells are now suggested to be responsible for clinical effects. **Chapter 2** focused on clinical studies with bone marrow cells (BMCs) for ischemic heart disease. The swift translation to the clinical arena was appraised, alongside limitations and future perspectives. The review article in **chapter 2** shows that cell therapy overall has a borderline significant moderate effect in the clinical setting(1,4–6,7). Although the majority of meta-analyses have demonstrated significant beneficial effects in no-option patients with ischemic heart disease, results have also been conflicting and research quality at times disputable. To aid the field of cardiac regenerative therapy it is important to move back to the bench and reassess hypotheses to find the true impact of cell therapy. We performed a randomized clinical trial with intramyocardial injections of autologous bone marrow derived-mononuclear cells in no-option patients with ischemic heart failure in NYHA class ≥ II. The results of this study were shown in **chapter 3**. After 12 months of follow up no significant difference was seen in left ventricular ejection fraction (LVEF) or stress-inducible ischemia in the cell treated group compared to the placebo group. Patients in this study suffered from chronic heart failure with a poor LVEF and limited ischemia at baseline. Cell therapy may have come too late for these patients, in other words the myocardium may have been too damaged for too long to significantly boost functional and clinical parameters by such a delicate therapy. Although our study did not show any benefit of BMC therapy in

severe chronic ischemic heart failure, the potential of BMC therapy in other patient populations, like acute myocardial infarction patients, may differ. An ongoing trial, BAMI, includes patients for BMC infusion after revascularization (PCI) in acute myocardial infarction patients and is designed to answer the question whether autologous bone marrow-derived cells lower cardiovascular events and mortality in the acute setting.

Besides gaining knowledge about the working mechanisms from previous research, even more questions arose. Up to date, it is not clear which patient population at which timepoint, with which dose might benefit from (which type of) cell therapy. In addition, there might be a specific type of patient that responds best to cell therapy(7,8). Clues for optimization of cell therapy were described in **chapter 2**. With regard to cell source, it has been implied that for instance aging and co-morbidities of the patient may influence the capacity of autologous cell therapy. Therefore, the efficacy of autologous vs allogeneic cells might differ. No differences in these two cell sources were noted in preclinical meta-analyses(9,10), however the hypothesis is not yet elucidated in clinical setting(11). Another clue for more favorable effects of cell therapy, repeated injections, was recently suggested(12,13). As pharmacological treatment for chronic diseases generally requires repeated or chronic dosing, in the same view cell therapy (for chronic heart disease) might generate a greater response when repeated instead of single treatment is given. Some evidence of the effect of repeated injections is found in small animal studies(14) and in a clinical study with refractory angina pectoris patients(12). The REPEAT trial is the first randomized trial that looks at the difference between single and repeated BMC injections. As described in **chapter 2,** other cell types have emerged from basic research during the translation of BMC to clinical trials*.

More research is required to determine the most potent cell for cardiac regeneration and repair. Mesenchymal stem cells (MSCs) are believed to induce major paracrine effect, while cardiac stem cells and induced pluripotent cells are proposed to have the most regenerative capacity(15). Cardiac stem cells have already shown promising results in patients(16,17). A combination of different cell types has demonstrated synergistic effects in a preclinical model(18). Finally, with the paracrine hypothesis in mind, we may not actually need cells for cardiac regeneration. Stimulation of endogenous cardiac stem cells with "cell-less cell therapy" may suffice(19–21).

While the final answers on the optimal therapy still have to follow, it is of utmost importance to find out how to improve retention and delivery accuracy of therapeutics. These crucial advances were the next objectives of the first part of this thesis.

Towards improved cell retention

So, although we have not yet established the optimal therapy cocktail, as a starting point for any kind of therapeutic it is important to retain it in the myocardium. The rapid washout of cells after injection demands novel methods to stimulate retention[22]. Biomaterials are a promising tool to fulfill this goal. An example of a promising biomaterial for minimally invasive injections is the supramolecular hydrogel ureido pyrimidinone (UPy) polyethylene glycol (PEG) (UPy-gel)[20,23]. A unique feature of UPy-gel is its pH-switchable viscosity. In a basic environment (pH > 7.5) the gel behaves like a solution that promptly switches to a gel upon contact with tissue (pH = 7.4). Therefore, UPy-gel is compatible with injection catheters that are used for intramyocardial injections, and increases the retention in the tissue due to the higher viscosity of the gel once it is injected. A protocol for standardized preparation and percutaneous injection of this hydrogel in the myocardium was reported (and visualized) in **chapter 4**. With the use of UPy-gel we aim to increase retention by using an easy injectable substance. We hypothesize that by using UPy-gel as a carrier for biologics in cardiac regenerative therapy[20] retention can be increased and thereby the therapeutic effect, ultimately leading to a better therapy for the patient. As a first step in the exploration of the aforementioned hypothesis *in vivo* visualization of the hydrogel as a proof of increased retention is mandatory. This has however not been established yet. The production of MRI visible UPy-gel was described in **chapter 5**. In this chapter UPy moieties were chemically coupled to Gadolineum (Gd)-DOTA. In release experiments the formed UPy-Gd showed similar characteristics to regular UPy-gel in terms of relaxivity measurements. UPy-Gd (chemically bound) was more able to retain Gd than UPy-gel that was merely mixed with Gd, implying that in-vivo imaging of UPy-Gd indeed would represent retention of UPy-gel. As a proof, an intramuscular injection of UPy-Gd was performed *in vivo* in a porcine model. Imaging of the hydrogel after injection was successfully achieved. This experiment confirmed the possibility of *in vivo* detection of UPy-gel with MRI to assess retention and behavior of this hydrogel over time.

Towards MR-guided therapy delivery

The current clinical standard technique for endomyocardial catheter injections is via electromechanical mapping (EMM) of the LV endocardium with the NOGA®XP system. With this percutaneous EMM approach, described in **chapter 4**, local electrical activity and mechanical movement of the endocardium is measured. Electromagnetic tracking of the cathetertip allows simultaneous acquisition of the 3D locations of the measurements and to create a 3D surface map of the endocardium. EMM allows the user to assess the uni- and bipolar depolarization voltages (UV and BV) and local linear shortening (LLS). Assuming that the infarcted tissue results in lower values, EMM aims to identify the infarction and infarction borderzone. However, EMM does not rely on assessment of true scar (fibrosis). The exact target is therefore not accurately reflected. To assure the most accurate targeting of the borderzone use of LGE MRI seems more suitable. Therefore, integrating additional LGE MRI data during the EMM procedure for advanced treatment planning is a step forward. Fusion of cardiac MRI with X-ray, or the NOGA® and CARTO® system has shown to be beneficial(24–26). To avoid ionizing radiation and data loss by image fusion we established a novel injection method with MR-guidance in **chapter 6.** Instead of bringing the MRI scanner to the catheterization lab, we took the catheterization lab to the MRI scanner. A novel MR-steerable, trackable and biocompatible catheter was developed, and this was combined with a novel catheter visualization and treatment planning approach. For the first time feasibility of real-time active and passive tracked MR-guided intramyocardial injections was shown. In these experiments the hydrogel described in **chapter 5** was injected intramyocardially in the porcine heart. Catheter tracking with both passive visualization and active tracking was feasible and could be used to navigate in real-time to the LV and endocardial targets. Post-injection the hydrogel could be visualized *in vivo*, implicating retention of the injected hydrogel. This advanced delivery approach enables MR tracking and assessment of periprocedural and long-term retention *in vivo*.

Conclusion and Future perspectives

In the first part of this thesis principles and limitations of stem cell research in clinical setting were described, along with the results of our clinical study in no-option chronic ischemic heart failure patients with BMCs. Other cell types for cardiac repair have been suggested throughout the years of stem cell research. All these experimental data will hopefully lead

to the optimal ("cell-less") cell cocktail for cardiac regeneration. Optimizing retention as well as circumventing possible cell death in the ischemic environment with for example cardiac cell-derived exosomes in a hydrogel may provide valuable advances for regenerative therapy. We focused on strategies for intramyocardial injections with an available hydrogel(20,23), discussed and visualized our current delivery method, and established successful modification of the hydrogel for visualization with MRI. Finally, we developed a completely novel injection technique (including a catheter) for accurate navigation of intramycoardial injections with MRI-guidance. We envision a major role for MRI in cardiac interventions since MRI provides advantages such as high spatial resolution, no ionizing radiation and is the gold standard for infarct and function assessment, which with interventional MRI becomes available for treatment planning and guidance during navigation in the heart. Other types of interventions that could benefit from MR-guidance include (atrial and ventricular) ablation procedures, valve replacements, myocardial biopsies, heart catheterizations and interventions in congenital heart disease(27–30).

For regenerative therapy, infarct assessment combined with functional MR-parameters without image fusion and/or data loss may greatly impact treatment planning, target accuracy, visualization of long-term retention of novel therapeutics and eventually therapy efficacy. The combination of UPy-Gd and interventional MRI allows us to gain insight in the mechanisms that could also be useful in the setting of the catheterization lab. For prompt clinical translation and creating a workable setup for interventional MR (for whatever purpose), a more conventional procedure than regenerative therapy should primarily be focused on.

PART TWO EXPLORING OPPORTUNITIES IN END-STAGE HEART FAILURE

Regenerative therapy in the LVAD population

The potential of regenerative therapy in the LVAD population was reviewed in **chapter 7**. While cardiac regenerative therapy is usually infused or injected in a hostile environment, the unloaded heart is suggested to be a better milieu for cells to engraft and survive. Cell therapy was previously combined with cardiac unloading, while other regenerative therapies, such as gene therapy and exosomes, in combination with LVADs have not been studied in clinical setting, however conclusive data is lacking(31). In **chapter 3** no benefit of

BMC therapy was found in patients with chronic ischemic heart failure. The suggestion that no significant effects should be expected of combined LVAD and BMC therapy in this population is supported by histological data of cardiac tissue at time of heart transplantation in these patients. No beneficial effects were seen in vasculature nor fibrosis after BMC injections during LVAD implantation at the time of heart transplantation(32). Of 8 enlisted clinical studies at clinialtrials.gov, one clinical trial with (mesenchymal) cell therapy in LVAD patients has been reported(33). Efficacy of the combined approach cannot be concluded from this study. With regard to other regenerative therapies, a clinical trial that aimed to investigate the combination of SERCA gene therapy was terminated early. The development of a valid large animal model for LV unloading might provide answers with regard to the efficacy of the combined approach albeit that an animal model will never represent the complex etiology of the end-stage HF patients.

A remarkable finding in **chapter 7** was that in all cases of LVAD explantation after combined unloading and cell therapy, an extracorporeal device (ECMO) was used. These temporary devices are mostly used in patients in whom full cardiac recovery is expected. In patients with an LVAD as bridge to transplantation, LVAD explantation due to recovery of cardiac function occurs sporadically(34). Signs of reverse remodeling are seen more frequently than cardiac recovery(35,36). Nonetheless, the mechanism of reverse remodeling and the association with cardiac recovery is unknown(37–40). Changes that occur during unloading on a structural, functional, cellular, molecular and genomic level have been studied, but mechanistic insight in requirements for true cardiac recovery is needed(35,41–43). Despite clinical guidelines for LVAD explantation, evaluating sustained cardiac recovery is difficult(44). Higher rates of cardiac recovery have been reported with adjuvant pharmacological strategies, however the recurrence of heart failure after LVAD removal remained high(45). These data suggest that chronic heart failure is not irreversible and that reverse remodeling might be perceptive to stimulation. As LVADs still cause major adverse events, the ultimate aim is to limit long-term LVAD support and to predict which patients might show substantial and sustained cardiac recovery. The ability to evaluate the effect of the therapy with an easy, non-invasive method could be highly valuable.

Towards biomarker-guided therapy
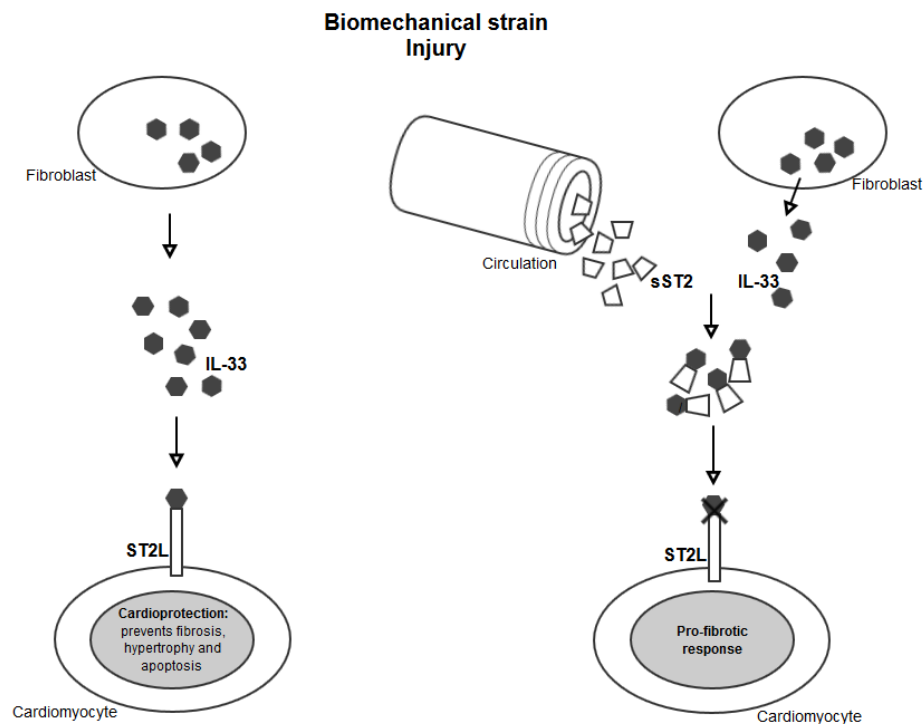
Soluble ST2 in the LVAD population

The ability to evaluate and to eventually predict the response to LVAD therapy in an individual patient is the ultimate way to personalize and, therewith, improve medical care for end stage HF patients. In this way one can predict which patients are prone to cardiac decompensation and hospitalization, and require intensified treatment. Prognostic biomarkers could be an efficient tool for this purpose(46,47). The LVAD population provides an opportunity to test biomarkers and connect these with functional and histological parameters, and changes during mechanical unloading. A promising biomarker in heart disease, soluble ST2 (sST2), was analyzed in end-stage heart failure patients in **chapter 8**, before and during LVAD support. This biomarker is part of the IL-33/ST2 pathway, which is involved in inflammation and fibrosis signaling(48,49). Soluble ST2, one of the main isoforms of ST2, can be measured in plasma. In heart disease sST2 is found to be a predictor of mortality(50) and sST2 can possibly be used to monitor and guide therapy(51–53). In **chapter 8** sST2 plasma levels were measured in end-stage HF patients before and during LVAD support. Before LV unloading severely elevated concentrations of sST2 were found. Interestingly, during unloading sST2 plasma levels significantly dropped to almost normal levels within one month of unloading, reaching a maximum decrease after 3 months. Significantly higher sST2 plasma levels were measured in patients with cardiogenic shock at time of LVAD implantations (INTERMACS profile I) vs patients that were dependent or deteriorating on inotropes (INTERMACS II-III). Also a significant correlation was found between sST2 and CRP levels. We did not find significant correlations between sST2 plasma levels and hemodynamic parameters, HF aetiology or HF duration.

ST2 and cardiac fibrosis

To gain more mechanistic insight in the role of sST2 in heart failure and to evaluate the value of sST2 as marker of cardiac fibrosis (**Figure 1**), we performed tissue analysis of end-stage failing hearts in **chapter 9**. Fibrosis was digitally quantified in apical tissue that was collected during LVAD implantation. In the same tissue mRNA expression was measured for IL-33/ST2 pathway factors as well as two pro-fibrotic markers. Association of sST2 plasma levels and cardiac tissue expression was analyzed. No correlation was found between sST2 plasma levels and mRNA expression of sST2 in cardiac tissue, implying that the heart is not

the major source of circulatory sST2. The mRNA expression of sST2 in myocardial tissue was significantly related to the amount of histological fibrosis, corresponding with the hypothesis that the IL-33/ST2 pathway plays a role in cardiac fibrosis. The mRNA expression of IL-33 was strongly related to pro-fibrotic marker expression. In contrast to mRNA expression, sST2 plasma levels were not related to fibrosis.

Figure 1. Schematic representation of the interleukin-33 (IL-33)/ST2 pathway upon cardiac stress.

The left side depicts the pathway in the absence of soluble ST2 (sST2) in the circulation that results in cardioprotection.
On the right side an excessive amount of sST2 in the circulation abrogates the cardioprotective effect by sequestering IL-33.

These data suggest that sST2 levels in the circulation are more determined by other factors than cardiac fibrosis in end-stage heart failure. Inflammation might significantly influence sST2, as suggested by the association with CRP and INTERMACS profile. Unfortunately, we did not collect data on tissue expression of inflammatory markers. Besides focus on inflammation, further ST2 research with regard to fibrosis should be extended to data collection before LVAD, at time of heart transplant and during biopsies after heart transplant.

Soluble ST2 as therapy guide

Ultimately, for response prediction of therapy in an individual patient so as to personalize treatment, the value of sST2 in clinical decision-making has to be determined. Broadly, three different treatment settings have to be considered: 1) the emergency department, 2) hospital admission and 3) the outpatient clinic. As there are known correlations of sST2 with the development of cardiac symptoms and NYHA class(54,55), elevated levels of sST2 could identify instable patients in the acute setting. Correlations of sST2 with echocardiographic measurements, like left ventricular parameters, left ventricular ejection fraction and reverse remodeling imply potential of sST2 to be a clinical monitor (56,57).

Table 1. Effects of heart failure therapy on sST2 levels

Author	Treatment	Outcome	sST2 potential
Gaggin 2013 (58)	BB	sST2 identifies pts with benefit from uptitrating BB	Therapy guide
Breidthardt 2013(52)	RAAS blockade, BB or diuretics	sST2 identifies pts with benefit from uptitrating BB	Therapy guide
Gaggin 2014 (59)	Standard chronic HF medication	ΔsST2 predicted change in LVF	Response predictor
Lax 2015 (60)	MRAs	Lower expression of sST2	Therapy monitor
Piper 2015(61)	Standard chronic HF medication	ΔsST2 predicted decompensation	Therapy monitor
Tang 2016 (62)	Neseritide	No impact on sST2 levels	None
Xia 2016 (55)	BB	Lower expression of sST2	Therapy monitor

BB, beta-blocker; RAAS, renin-angiotensin-aldosterone system; sST2, soluble ST2

During hospital admission a drop in sST2 levels can be used to evaluate the response to therapy (**Table 1**) and before discharge to assess the risk of recurrence of symptoms and further optimization of medication. In order for sST2 to be an effective clinical monitor serial measurements are essential. This is also relevant in the ambulatory setting where serial sST2 levels can be used to titrate medication and predict cardiac decompensation (**Table 1**). The lack of a uniform method, both in timing and in defining relevant sST2 changes, makes it challenging to determine the best strategy and a standardized method for the current clinic.

Conclusion and Future perspectives

Although signs of reverse remodeling may be present, significant and sustained improvement in LV function for successful LVAD explantation is sporadically seen. Recovery occurs most in non-ischemic heart failure patients with potentially reversible causes. Evidence for cardiac recovery as a result of combining LV unloading and regenerative therapy is absent. Nonetheless, the LVAD population is definitely an interesting study population in which cardiac tissue can be studied before, during and after LVAD implant and more detailed knowledge on the effects of therapy can be gained. Biomarkers provide a non-invasive method that can be useful to monitor treatment and predict therapy response. Plasma levels of a highly prognostic biomarker, soluble ST2, in end-stage heart failure patients that received an LVAD as bridge to transplantation were studied. Severely elevated levels before implantation drastically dropped to normal levels during LVAD support. Although the heart does not seem to be the major source of soluble ST2 in circulation, factors of the IL-33/ST2 pathway are expressed in cardiac tissue and seem associated with cardiac fibrosis. Soluble ST2 thus far fits the criteria of an ideal biomarker for heart failure. Serially measured soluble ST2 might not even be cardiac-specific and more general about inflammation in patients, thereby perhaps the best prognosticator of changes within an individual.

Final remarks

This thesis portrays the road towards advanced therapy guidance in the failing heart. Part one described the path of current cell therapy in ischemic heart failure and associated limitations towards accurate image-guided treatment methods, which may also be useful for other (more conventional) cardiac interventions. Part two provides a starting point for the use of biomarker soluble ST2 in end-stage heart failure patients. More experience and understanding of this biomarker could provide useful tools for clinical decision-making in the individual patient.

References

1. Afzal MR, Samanta A, Shah ZI, Jeevanantham V, Abdel-Latif A, Zuba-Surma EK, et al. Adult Bone Marrow Cell Therapy for Ischemic Heart Disease: Evidence and Insights from Randomized Controlled Trials. Circ Res. 2015;117(6):558–75.

2. Chavakis E, Koyanagi M, Dimmeler S. Enhancing the outcome of cell therapy for cardiac repair: Progress from bench to bedside and back. Circulation. 2010;121(2):325–35.

3. Laflamme MA, Murry CE. Heart regeneration. Nature. 2011;473(7347):326–35.

4. Delewi R, Hirsch A, Tijssen JG, Scha V, Aakhus S, Erbs S, et al. Impact of intracoronary bone marrow cell therapy on left ventricular function in the setting of ST-segment elevation myocardial infarction: a collaborative meta-analysis. Eur Heart J. 2014;35:989–98.

5. Fisher SA, Doree C, Mathur A, Martin-Rendon E. Meta-Analysis of Cell Therapy Trials for Patients with Heart Failure - An Update. Circ Res. 2015;116:1361–77.

6. Jeevanantham V, Butler M, Saad A, Abdel-Latif A, Zuba-Surma EK, Dawn B. Adult bone marrow cell therapy improves survival and induces long-term improvement in cardiac parameters: a systematic review and meta-analysis. Circulation. 2012;126(5):551–68.

7. Rodrigo SF, van Ramshorst J, Mann I, Leong DP, Cannegieter SC, Al Younis I, et al. Predictors of response to intramyocardial bone marrow cell treatment in patients with refractory angina and chronic myocardial ischemia. Int J Cardiol. 2014;175(3):539–44.

8. Zwetsloot PP, Gremmels H, Assmus B, Koudstaal S, Sluijter JPG, Zeiher AM, et al. Responder Definition in Clinical Stem Cell Trials in Cardiology: Will the Real Responder Please Stand Up? Circ Res. 2016;119(4):514–8.

9. Jansen of Lorkeers SJ, Eding JEC, Vesterinen HM, van der Spoel TIG, Sena ES, Duckers HJ, et al. Similar Effect of Autologous and Allogeneic Cell Therapy for Ischemic Heart Disease : Systematic Review and Meta-Analysis of Large Animal Studies. Circ Res. 2015;116:80–6.

10. Zwetsloot PP, Végh A, Jansen of Lorkeers SJ, van Hout GP, Currie GL, Sena ES, et al. Cardiac Stem Cell Treatment in Myocardial Infarction: A Systematic Review and Meta-Analysis of Preclinical Studies. Circ Res. 2016;118(8):1223–32.

11. Hare JM, Fishman JE, Gerstenblith G, DiFede Velazquez DL, Zambrano JP, Suncion VY, et al. Comparison of allogeneic vs autologous bone marrow–derived mesenchymal stem cells delivered by transendocardial injection in patients with ischemic cardiomyopathy: the POSEIDON randomized trial. JAMA. 2012;308(22):2369–79.

12. Mann I, Rodrigo SF, van Ramshorst J, Beeres SL, Dibbets-Schneider P, de Roos A, et al. Repeated Intramyocardial Bone Marrow Cell Injection in Previously Responding Patients With Refractory Angina Again Improves Myocardial Perfusion, Anginal Complaints, and Quality of Life. Circ Cardiovasc Interv. 2015;8(8):1–8.

13. Tokita Y, Tang XL, Li Q, Wysoczynski M, Hong KU, Nakamura S, et al. Repeated Administrations of Cardiac Progenitor Cells Are Markedly More Effective Than a Single Administration: A New Paradigm in Cell Therapy. Circ Res. 2016;119(5):635–51.

14. Guo Y, Wysoczynski M, Nong Y, Tomlin A, Zhu X, Gumpert AM, et al. Repeated doses of cardiac mesenchymal cells are therapeutically superior to a single dose in mice with old myocardial infarction. Basic Res Cardiol. 2017;112(2):18.

15. Shadrin IY, Allen BW, Qian Y, Jackman CP, Carlson AL, Juhas ME, et al. Cardiopatch platform enables maturation and scale-up of human pluripotent stem cell-derived engineered heart tissues. Nat Commun. 2017;8(1).

16. Bolli R, Chugh AR, D'Amario D, Loughran JH, Stoddard MF, Ikram S, et al. Cardiac stem cells in patients with ischaemic cardiomyopathy (SCIPIO): initial results of a randomised phase 1 trial. Lancet. 2011;378(9806):1847–57.

17. Malliaras K, Makkar RR, Smith RR, Cheng K, Wu E, Bonow RO, et al. Intracoronary Cardiosphere-Derived Cells After Myocardial Infarction: Evidence of Therapeutic Regeneration in the Final 1-Year Results of the CADUCEUS Trial (CArdiosphere-Derived aUtologous stem CElls to reverse ventricUlar dySfunction). J Am Coll Cardiol. 2014;63(2):110–22.

18. Natsumeda M, Florea V, Rieger AC, Tompkins BA, Banerjee MN, Golpanian S, et al. A Combination of Allogeneic Stem Cells Promotes Cardiac Regeneration. JACC. 2017;70(20):14–21.

19. van Rooij E, Olson EN. MicroRNA therapeutics for cardiovascular disease: opportunities and obstacles. Nat Rev Drug Discov. 2012;11(11):860–72.

20. Koudstaal S, Bastings MMC, Feyen DA, Waring CD, van Slochteren FJ, Dankers PYW, et al. Sustained delivery of insulin-like growth factor-1/hepatocyte growth factor stimulates endogenous cardiac repair in the chronic infarcted pig heart. J Cardiovasc Transl Res. 2014;7(2):232–41.

21. Wei K, Serpooshan V, Hurtado C, Diez-Cuñado M, Zhao M, Maruyama S, et al. Epicardial FSTL1 reconstitution regenerates the adult mammalian heart. Nature. 2015;

22. van den Akker F, Feyen D a M, van den Hoogen P, van Laake LW, van Eeuwijk ECM, Hoefer I, et al. Intramyocardial stem cell injection: go(ne) with the flow. Eur Heart J. 2016;ehw056.

23. Bastings MMC, Koudstaal S, Kieltyka RE, Nakano Y, Pape ACH, Feyen DAM, et al. A fast pH-switchable and self-healing supramolecular hydrogel carrier for guided, local catheter injection in the infarcted myocardium. Adv Healthc Mater. 2014;3(1):70–8.

24. Dauwe DF, Nuyens D, De Buck S, Claus P, Gheysens O, Koole M, et al. Three-dimensional rotational angiography fused with multimodal imaging modalities for targeted endomyocardial injections in the ischaemic heart. Eur Heart J Cardiovasc Imaging. 2014;15(8):900–7.

25. van Slochteren FJ, van Es R, Koudstaal S, van der Spoel TIG, Sluijter JPG, Verbree J, et al. Multimodality infarct identification for optimal image-guided intramyocardial cell injections. Netherlands Hear J. 2014;22(11):493–500.

26. Caponi D, Corleto A, Scaglione M, Blandino A, Biasco L, Cristoforetti Y, et al. Ablation of atrial fibrillation: Does the addition of three-dimensional magnetic resonance imaging of the left atrium to electroanatomic mapping improve the clinical outcome? Europace. 2010;12(8):1098–104.

27. Hilbert S, Sommer P, Gutberlet M, Gaspar T, Foldyna B, Piorkowski C, et al. Real-time magnetic resonance-guided ablation of typical right atrial flutter using a combination of active catheter tracking and passive catheter visualization in man : initial results from a consecutive patient series. Europace. 2015;

28. Rogers T, Ratnayaka K, Karmarkar P, Campbell-Washburn AE, Schenke WH, Mazal JR, et al. Real-Time Magnetic Resonance Imaging Guidance Improves the Diagnostic Yield of Endomyocardial Biopsy. JACC Basic to Transl Sci. 2016;1(5):376–83.

29. Ratnakaya K, Rogers T, Schenke WH, Mazal JR, Chen MY, Sonmez M, et al. Magnetic Resonance Imaging – Guided Transcatheter Cavopulmonary Shunt. JACC Cardiovasc Interv. 2016;9(9):959–70.

30. Valverde I, Hussain T, Razavi R. Novel imaging techniques for the diagnosis and treatment of congenital heart defects: MR-guided interventions and beyond. Future Cardiol. 2012;8(2):149–52.

31. Tseng CCS, Ramjankhan FZ, de Jonge N, Chamuleau S a J. Advanced Strategies for End-Stage Heart Failure: Combining Regenerative Approaches with LVAD, a New Horizon? Front Surg. 2015;2(April):10.

32. Stempien-Otero A, Helterline D, Plummer T, Farris S, Prouse A, Polissar N, et al. Mechanisms of Bone Marrow-Derived Cell Therapy in Ischemic Cardiomyopathy With Left Ventricular Assist Device Bridge to Transplant. J Am Coll Cardiol. 2015;65(14):1424–34.

33. Ascheim DD, Gelijns AC, Goldstein D, Moye L a, Smedira N, Lee S, et al. Mesenchymal Precursor Cells as Adjunctive

Therapy in Recipients of Contemporary LVADs. Circulation. 2014;129:2287–96.

34. Kirklin JK, Cantor R, Mohacsi P, Gummert J, De By T, Hannan MM, et al. First Annual IMACS Report: A global International Society for Heart and Lung Transplantation Registry for Mechanical Circulatory Support. J Hear lung Transplant. 2016;35(4):407–12.

35. Ambardekar A V, Buttrick PM. Reverse remodeling with left ventricular assist devices: a review of clinical, cellular, and molecular effects. Circ Heart Fail. 2011;4(2):224–33.

36. Bruggink AH, van Oosterhout MFM, de Jonge N, Ivangh B, van Kuik J, Voorbij RH, et al. Reverse remodeling of the myocardial extracellular matrix after prolonged left ventricular assist device support follows a biphasic pattern. J Heart Lung Transplant. 2006;25(9):1091–8.

37. Burkhoff D, Klotz S, Mancini DM. LVAD-induced reverse remodeling: basic and clinical implications for myocardial recovery. J Card Fail. 2006;12(3):227–39.

38. Butler CR, Jugdutt BI. The paradox of left ventricular assist device unloading and myocardial recovery in end-stage dilated cardiomyopathy: Implications for heart failure in the elderly. Heart Fail Rev. 2012;17(4–5):615–33.

39. Mann DL, Burkhoff D. Myocardial expression levels of micro-ribonucleic acids in patients with left ventricular assist devices signature of myocardial recovery, signature of reverse remodeling, or signature with no name? J Am Coll Cardiol. 2011;58(22):2279–81.

40. Marinescu KK, Uriel N, Mann DL, Burkhoff D. Left ventricula assist device-induced reverse remodeling: it's not just about myocardial recovery. Expert Rev Med Devices. 2017;14(1):15–26.

41. Hall JL, Fermin DR, Birks EJ, Barton PJR, Slaughter M, Eckman P, et al. Clinical, Molecular and Genetic Changes in Response to a Left Ventricular Assist Device. J Am Coll Cardiol. 2011;57(6):612–24.

42. Terracciano CMN, Hardy J, Birks EJ, Khaghani A, Banner NR, Yacoub MH, et al. Clinical recovery from end-stage heart failure using left-ventricular assist device and pharmacological therapy correlates with increased sarcoplasmic reticulum calcium content but not with regression of cellular hypertrophy. Circulation. 2004 May 18;109(19):2263–5.

43. Miyagawa S, Toda K, Nakamura T, Yoshikawa Y, Fukushima S, Saito S, et al. Building a bridge to recovery: the pathophysiology of LVAD-induced reverse modeling in heart failure. Surg Today. 2015;

44. Dandel M, Weng Y, Siniawski H, Stepanenko A, Krabatsch T, Potapov E, et al. Heart failure reversal by ventricular unloading in patients with chronic cardiomyopathy: criteria for weaning from ventricular assist devices. Eur Heart J. 2011;32(9):1148–60.

45. Birks EJ, George RS, Hedger M, Bahrami T, Wilton P, Bowles CT, et al. Reversal of severe heart failure with a continuous-flow left ventricular assist device and pharmacological therapy: a prospective study. Circulation. 2011;123(4):381–90.

46. Motiwala SR, Gaggin HK. Biomarkers to Predict Reverse Remodeling and Myocardial Recovery in Heart Failure. Curr Heart Fail Rep. 2016;13(5):207–18.

47. Boer RA De, Daniels LB, Maisel AS, Januzzi Jr JL. State of the Art : Newer biomarkers in heart failure. Eur J Heart Fail. 2015;17:559–69.

48. Kakkar R, Lee RT. The IL-33/ST2 pathway: therapeutic target and novel biomarker. Nat Rev Drug Discov. 2008;7(10):827–40.

49. Gao Q, Li Y, Li M. The potential role of IL-33 / ST2 signaling in fibrotic diseases. J Leukoc Biol. 2015;98(July):1–8.

50. Bayes-Genis A, Zhang Y, Ky B. ST2 and patient prognosis in chronic heart failure. Am J Cardiol. 2015;115(7 Suppl):64B–9B.

51. Januzzi JL, Pascual-Figal D, Daniels LB. ST2 Testing for Chronic Heart Failure Therapy Monitoring: The International

ST2 Consensus Panel. Am J Cardiol. 2015;115(7):70B–75B.

52. Breidthardt T, Balmelli C, Twerenbold R, Mosimann T, Espinola J, Haaf P, et al. Heart failure therapy-induced early ST2 changes may offer long-term therapy guidance. J Card Fail. 2013;19(12):821–8.

53. Villacorta H, Maisel AS. Soluble ST2 Testing: A Promising Biomarker in the Management of Heart Failure. Arq Bras Cardiol. 2016;106(2):145–52.

54. Immanuel S, Mandey NMA, Makmun LH. ST2 Levels Before and After Treatment of NYHA III and IV Heart Failure. Acta Med Indones. 2015;47(4):304–10.

55. Wojtczak-Soska K, Sakowicz A, Pietrucha T, Lelonek M. Soluble ST2 protein in the short-term prognosis after hospitalisation in chronic systolic heart failure. Kardiol Pol. 2014;72(8):725–34.

56. deFilippi C, Daniels LB, Bayes-Genis A. Structural heart disease and ST2: cross-sectional and longitudinal associations with echocardiography. Am J Cardiol. 2015;115(7 Suppl):59B–63B.

57. Lupón J, Gaggin H, de Antonio M, Domingo M, Galán A, Zamora E, et al. Biomarker-assist score for reverse remodeling prediction in heart failure: The ST2-R2 score. Int J Cardiol. 2015;184:337–343.

58. Gaggin HK, Januzzi JL. Biomarkers and diagnostics in heart failure. Biochim Biophys Acta. 2013;1832(12):2442–50.

59. Gaggin HK, Szymonifka J, Bhardwaj A, Belcher A, De Berardinis B, Motiwala S, et al. Head-to-Head Comparison of Serial Soluble ST2, Growth Differentiation Factor-15, and Highly-Sensitive Troponin T Measurements in Patients With Chronic Heart Failure. JACC Hear Fail. 2014;2(1):65–72.

60. Lax A, Sanchez-Mas J, Asensio-Lopez MC, Fernandez-Del Palacio MJ, Caballero L, Garrido IP, et al. Mineralocorticoid receptor antagonists modulate galectin-3 and interleukin-33/ST2 signaling in left ventricular systolic dysfunction after acute myocardial infarction. JACC Heart Fail. 2015;3(1):50–8.

61. Piper S, Sherwood R, Amin-Youssef G, Shah A, McDonagh T. Serial soluble ST2 for the monitoring of pharmacologically optimised chronic stable heart failure. Int J Cardiol. 2015;178:284–291.

62. Tang WHW, Wu Y, Grodin JL, Hsu AP, Hernandez AF, Butler J, et al. Prognostic value of baseline and changes in circulating soluble ST2 levels and the effects of nesiritide in acute decompensated heart failure. JACC Hear Fail. 2016;4(1):68–77.

63. Xia J, Qu Y, Yin C, Xu D. Preliminary study of beta-blocker therapy on modulation of interleukin-33/ST2 signaling during ventricular remodeling after acute myocardial infarction. Cardiol J. 2017;24(2):188–94.

Appendix

Nederlandse samenvatting

Op weg naar geavanceerde begeleiding van therapie in het falende hart

In dit proefschrift werden beperkingen van cardiale regeneratieve therapie en mechanische ondersteuning, en nieuwe geavanceerde methoden bediscussieerd om hartfalen therapie te verbeteren. In deel één lag de focus op het verbeteren van cardiale regeneratieve therapie, terwijl deel twee gericht was op perspectieven in de steunhart (LVAD) populatie.

DEEL EEN - HET VERBETEREN VAN REGENERATIEVE THERAPIE

Celtherapie voor chronisch hartfalen

De rationale van celtherapie voor cardiale regeneratie werd in **hoofdstuk 2** beschreven. Beenmergcellen waren de eerste cellen waarvan differentiatie naar cardiomyocyten, en dus regeneratieve capaciteit, werd verondersteld. Echter worden nu paracriene effecten, en niet transdifferentiatie van stamcellen naar cardiomyocyten, verantwoordelijk geacht voor de klinische effecten van celtherapie. Hoewel de meerderheid van meta-analyses een significant voordeel tonen van celtherapie bij patiënten met ischemische hartziekten zijn veel resultaten ook tegenstrijdig en de kwaliteit van het onderzoek soms discutabel. Om het veld van cardiale regeneratieve therapie een dienst te bewijzen is het belangrijk om een stap terug te doen en hypothesen opnieuw te toetsen om de daadwerkelijke impact van celtherapie te vinden. In **hoofdstuk 3** werden de resultaten van een gerandomiseerde klinische studie met autologe beenmergcellen bij patiënten met ischemisch hartfalen beschreven. De populatie in deze studie had chronisch hartfalen met een slechte ejectiefractie en een beperkte hoeveelheid induceerbare ischemie. Er werd geen significant effect gezien in de linkerventrikel ejectiefractie of de hoeveelheid ischemie in de celtherapie groep vergeleken met de placebogroep. Het hart was wellicht al te lang te ernstig beschadigd om significante verbetering in functionele en klinische parameters te kunnen bewerkstelligen. Ondanks het gebrek aan profijt van celtherapie in onze studie bij ernstig chronisch ischemisch hartfalen, zou de capaciteit van beenmergcellen in andere patiëntpopulaties kunnen verschillen. Wat de meest potente cel(loze) therapie is en in welke populatie is nog onbekend.

Op weg naar verbeterde celretentie

Als beginpunt voor elke mogelijke regeneratieve therapie is de retentie van therapie in het hart van belang. Aangezien cellen na injectie snel worden uitgewassen is er een noodzaak voor nieuwe methoden om retentie te verbeteren. Biomaterialen zijn een veelbelovende manier om dit doel te bereiken. Een potente supramoleculaire hydrogel, ureido pyrimidinone (UPy) polyethyleen glycol (PEG) (UPy-gel), is een kansrijk biomateriaal voor minimaal invasieve injecties in het hart. Een uniek aspect van UPy-gel is de pH-veranderlijke viscositeit. In basische omgeving (pH >7.5) gedraagt de hydrogel zich als een oplossing welke vlot verandert naar een gel wanneer het in contact komt met weefsel (pH = 7.4). Dit maakt UPy-gel compatibel met injectiekatheters die gebruikt worden voor intramyocardiale injecties. Door de hogere viscositeit na injectie in het hart neemt de retentie in het hartweefsel toe. Een protocol voor gestandaardiseerde bereiding en percutane injectie van deze hydrogel in het hart werd gerapporteerd (en gevisualiseerd) in **hoofdstuk 4**. In **hoofdstuk 5** werd een UPy-gel geproduceerd die zichtbaar is met MRI door het koppelen van UPy-gel aan een MRI-zichtbaar molecuul, Gadolinium (Gd). De chemisch gekoppelde hydrogel was beter in staat Gd vast te houden dan UPy gemixt met Gd, wat impliceert dat *in-vivo* UPy-Gd daadwerkelijk retentie van UPy-gel presenteert. De hydrogel kon succesvol worden afgebeeld na injectie. Dit experiment bevestigt de mogelijkheid om UPy-gel *in vivo* te detecteren met MRI om in de toekomst retentie en gedrag van de hydrogel in de loop van tijd te onderzoeken.

Op weg naar MR-geleide therapie

De huidige klinische standaardtechniek voor intramyocardiale katheter injecties is met elektromechanische mapping (EMM) van het linkerventrikel endocard middels het NOGA®XP systeem. Bij deze percutane methode, beschreven in **hoofdstuk 4**, worden lokale elektrische activiteit en mechanische beweging van het endocard gemeten met een katheter om het grensgebied van infarct met viabel weefsel te traceren. Deze methode reflecteert het doelgebied echter mogelijk niet accuraat. Aangezien MRI de gouden standaard is voor het vaststellen van infarctlocatie en grootte, lijkt MRI meer geschikt voor het accuraat weergeven van het doelgebied. Om ioniserende bestraling en dataverlies te voorkomen hebben we een nieuwe methode ontwikkeld met MRI-begeleiding. In **hoofdstuk 6** werd een nieuwe MRI-bestuurbare, traceerbare en biocompatibele katheter ontwikkeld, en werd deze

gecombineerd met een nieuwe methode voor katheter visualisatie en behandelplanning. Voor het eerst werd de haalbaarheid van real-time actief en passief "tracken" van een katheter voor intramyocardiale injecties met begeleiding van MRI aangetoond. Na de injectie kon de (in **hoofdstuk 5** geproduceerde) hydrogel *in vivo* gevisualiseerd worden, wat retentie van de geïnjecteerde hydrogel impliceert. Deze geavanceerde toedieningstechniek maakt MRI-tracking en beoordeling van periprocedurele en lange termijn retentie *in vivo* mogelijk.

DEEL TWEE – HET VERKENNEN VAN MOGELIJKHEDEN BIJ EINDSTADIUM HARTFALEN
Regeneratieve therapie in de LVAD populatie

De potentie van regeneratieve therapie bij patiënten met een LVAD werd besproken in **hoofdstuk 7**. Terwijl cardiale regeneratieve therapie meestal toegediend wordt in een voor cellen vijandige omgeving, wordt gesuggereerd dat het ontladen hart een beter milieu zou zijn voor overleving en "engraftment" van cellen. In klinisch onderzoek is alleen celtherapie, en niet andere regeneratieve therapieën zoals gentherapie of exosomen, gecombineerd met LVAD. Uit verkregen data kunnen echter geen conclusies worden getrokken met betrekking tot effect van de combinatie therapie. Histologische data van hartweefsel van deze patiënten toont op het moment van harttransplantatie geen voordelig effect van beenmergcellen die tijdens de implantatie van een LVAD werden geïnjecteerd, op vascularisatie of fibrose. De ontwikkeling van een valide diermodel voor ontladen van de linker ventrikel zou antwoord kunnen geven op de vraag of de gecombineerde methode van ontladen en regeneratieve therapie effectief is, hoewel een diermodel nooit volledig de complexe etiologie van eindstadium hartfalen nabootst.

Bij patiënten met een LVAD als overbrugging naar harttransplantatie komt explantatie van een LVAD als gevolg van herstel van functie sporadisch voor. Tekenen van herstel, in de zin van omgekeerde remodelering ("reverse remodeling"), worden frequenter gezien. Het mechanisme hiervan en de associatie met cardiaal herstel zijn echter onbekend. Ondanks klinische richtlijnen voor LVAD explantatie is het een uitdaging om werkelijk cardiaal herstel te evalueren. Aangezien LVADs ernstige complicaties kunnen veroorzaken is het uiteindelijke doel om lange termijn ondersteuning met een LVAD te beperken en te voorspellen bij welke patiënten substantieel en blijvend herstel van de hartfunctie verwacht kan worden. De

mogelijkheid om het effect van therapie met een makkelijke, niet-invasieve methode te evalueren kan erg van waarde zijn.

Op weg naar biomarker-geleide therapie

Soluble ST2 in de LVAD populatie

De mogelijkheid om de respons op LVAD therapie te evalueren en uiteindelijk te voorspellen bij de individuele patiënt is de ultieme methode om medische zorg voor eindstadium hartfalen patiënten te personaliseren. Op deze manier kan men voorspellen welke patiënten vatbaar zijn om te decompenseren, opgenomen te worden en intensievere behandeling behoeven. Prognostische biomarkers kunnen efficiënt gereedschap zijn voor dit doel. De LVAD populatie biedt een gelegenheid om biomarkers te testen en deze te verbinden met functionele en histologische parameters, én met veranderingen tijdens mechanisch ontladen. Een veelbelovende biomarker bij hartziekten, soluble ST2 (sST2), werd in **hoofdstuk 8** geanalyseerd bij eindstadium hartfalen patiënten, voor en tijdens ondersteuning met een LVAD. Deze biomarker is deel van de IL-33/ST2 "pathway", welke betrokken is bij inflammatie en fibrose. Bij hartziekten is sST2 in plasma een voorspeller van mortaliteit en mogelijk een therapie-monitor en leidraad. Vóór mechanisch ontladen werden in plasma ernstig verhoogde sST2 waarden gevonden. Opmerkelijk was dat de sST2 waarden na ontladen significant daalden naar bijna normaal. Er werden significant hogere sST2 waarden gemeten bij patiënten met cardiogene shock (INTERMACS profiel I) op het moment van implantatie vs patiënten die afhankelijk waren van inotropie (INTERMACS profiel II-III). Ook werd een significante correlatie gevonden tussen sST2 en CRP waarden. We vonden geen significante correlaties tussen sST2 in plasma en hemodynamische parameters, de oorzaak en/of duur van hartfalen.

ST2 en cardiale fibrose

Om meer inzicht te krijgen in de rol van sST2 bij hartfalen en om de waarde van sST2 als marker van fibrose te beoordelen, werd weefselanalyse verricht bij eindstadium hartfalen in **hoofdstuk 9**. Er werd geen correlatie gevonden tussen sST2 in plasma en mRNA expressie van sST2 in cardiaal weefsel, wat impliceert dat het hart niet de belangrijkste bron is van sST2 in de circulatie. De mRNA expressie van sST2 in cardiaal weefsel was significant gecorreleerd aan de hoeveelheid fibrose bij histologie, corresponderend met de hypothese

dat de IL-33/ST2 "pathway" een rol speelt bij cardiale fibrose. De mRNA expressie van IL-33 was sterk gerelateerd aan expressie van pro-fibrotische markers. In tegenstelling tot mRNA expressie was sST2 in plasma niet gecorreleerd aan fibrose. Deze data impliceren dat sST2 in de circulatie meer beïnvloed wordt door andere factoren dan cardiale fibrose bij eindstadium hartfalen. Mogelijk heeft inflammatie meer invloed op sST2, zoals gesuggereerd wordt door de associatie met CRP en INTERMACS profiel ten tijde van LVAD implantatie. Behalve focus op inflammatie zou toekomstig ST2 onderzoek met betrekking op fibrose zich moeten uitbreiden naar data collectie vóór implantatie van LVAD, op het moment van harttransplantatie en na harttransplantatie (tijdens biopten).

sST2 als therapie gids

Tenslotte moet, om de therapierespons bij de individuele patiënt te voorspellen, de waarde van sST2 in de klinische beslisvorming bepaald worden. Er zijn drie verschillende behandelomgevingen die moeten worden overwogen: 1) spoedeisende hulp, 2) klinische ziekenhuisopname en 3) polikliniek. Verhoogde sST2 waarden zouden instabiele patiënten in de acute setting kunnen identificeren. Tijdens een opname kan een daling van sST2 waarden gebruikt worden om therapierespons te beoordelen, en voor ontslag om het risico op een recidief in te schatten en medicatie verder te optimaliseren. Voor het gebruik van sST2 als effectieve klinische monitor zijn seriële metingen essentieel. Dit is ook relevant in de ambulante setting waarbij seriële sST2 waarden nuttig kunnen zijn om medicatie op te titreren en cardiale decompensatie te voorspellen. Het ontbreken van een uniforme methode, betreft zowel timing als het definiëren van relevante sST2 veranderingen, maakt het bepalen van de beste strategie en een gestandaardiseerde methode voor de huidige kliniek een uitdaging.

Conclusie

Dit proefschrift portretteert de weg naar geavanceerde therapie begeleiding in het falende hart. Deel een beschrijft de route van huidige celtherapie bij ischemisch hartfalen en bijbehorende beperkingen naar accurate beeld-geleide behandelmethoden. Deze nieuwe methoden kunnen ook behulpzaam zijn voor andere (meer conventionele) cardiale interventies. Deel twee verschaft een startpunt voor het gebruik van biomarker sST2 bij

eindstadium hartfalen patiënten. Meer ervaring en begrip van deze biomarker zou nuttig gereedschap kunnen bieden in de klinische besluitvorming bij de individuele patiënt.

List of publications

Tseng CCS, Chamuleau SAJ, de Jonge N, Ramjankhan FZ. *Short-term mechanical support and pharmacotherapy, a new strategy in cardiogenic shock?* Neth Heart J. 2014.

Tseng CCS, Ramjankhan FZ, de Jonge N, Chamuleau SAJ. *Advanced strategies for end-stage heart failure: combining regenerative approaches with LVAD, a new horizon?* Front. Surg. 2015.

Pape ACH*, Bakker MH*, **Tseng CCS**, Bastings MMC, Koudstaal S, Agostoni P, Chamuleau SAJ, Dankers PYW. *An injectable and drug-loaded supramolecular hydrogel for local catheter injection into the pig heart.* J. Vis. Exp. 2015.
* These authors contributed equally to this work

Van der Naald M*, **Tseng** CCS*, Doevendans PAF, Chamuleau SAJ. *Stamceltherapie voor het beschadigde hart.* NTvH 2016.
* These authors contributed equally to this work

Tseng CCS, Huibers MMH, van Kuik J, de Weger RA, Vink A, de Jonge N. *The interleukin-33/ST2 pathway is expressed in the failing human heart and associated with pro-fibrotic remodeling of the myocardium.* J Cardiovasc Transl Res 2017.

Tseng CCS, Huibers MMH, Gaykema LH, Siera-de Koning E, Ramjankhan FZ, Maisel AS, de Jonge N.
Soluble ST2 in end-stage heart failure, before and after support with a left ventricular assist device. Eur J Clin Invest. 2018.

Lewis FC, Cottle BJ, Shone V, Marazzi G, Sassoon D, **Tseng CCS**, Dankers PYW, Chamuleau SAJ, Nadal-Girard B, Ellison-Hughes GM. *Transplantation of allogeneic PW1pos/Pax7neg interstitial cells (PICs) enhance endogenous repair of injured porcine skeletal muscle.* JACC Basic Transl Sci. 2018.

Bakker MH*, **Tseng CCS***, Keizer HM, Seevinck PR, Janssen HM, van Slochteren FJ, Chamuleau SAJ, Dankers PYW. *MRI visualization of injectable ureidopyrimidinone hydrogelators by supramolecular contrast agent labeling.* Adv Health Mat. 2018.
* These authors contributed equally to this work

Dankwoord

In dit dankwoord wil ik mijn dank betuigen aan allen die een bijdrage geleverd hebben aan de totstandkoming van dit proefschrift.

Allereerst mijn promotoren, zonder wie ik dit traject niet had kunnen starten of voltooien. **Prof. Doevendans**, beste Pieter, bedankt voor het vertrouwen om dit promotietraject te starten. De beruchte 4 letters (OK PD) passen helemaal bij jouw begeleidstijl: kort en krachtig. Behalve dat je altijd direct weet wat de volgende stap zou moeten zijn, zal ik ook niet vergeten dat we samen een youtube filmpje keken over hoe sableren nou eigenlijk moet.

Prof. Chamuleau, beste Steven, via jou kreeg ik de kans om in het UMC te werken en onderdeel te worden van de "Champie-groep". Ik bewonder je persisterende enthousiasme en passie binnen en buiten het ziekenhuis. Bedankt voor de ruimte die je mij gaf tijdens dit traject om zelf mijn weg te kiezen, maar ook dat je bijstuurde wanneer ik geen knopen dreigde door te hakken. Ook bedankt voor de enorme hartelijkheid van jou en je gezin die ik tijdens dit traject heb mogen ervaren.

Dan volgen uiteraard mijn co-promotoren in dit dankwoord. **Dr. de Jonge,** beste Nicolaas, jouw deskundigheid en kritische blik hebben mijn onderzoek in opzet en in uiteindelijk resultaat significant verbeterd. Heel veel dank daarvoor. **Dr. van Slochteren**, beste Frebus, ik heb jouw transitie van PhD naar zakenman nog net mogen meemaken. Ik vind het mooi hoe onze tegenstellingen, jouw technische en praktische aanpak versus mijn medische en theoretische aanpak, elkaar uiteindelijk mooi hebben kunnen aanvullen in het MIGRATE project (waarover zo meer).

De leescommissie, **Prof. dr. Bredenoord, Prof. dr. Atsma, Prof. dr. Goldschmeding, Prof. dr. Sluijter** en **Prof. dr. Suyker,** wil ik hartelijk bedanken voor het beoordelen van mijn proefschrift.

Het gehele **MIGRATE consortium** verdient een belangrijke plek in dit boekje: **Peter Seevinck** en **Joost Sluijter** (UMC Utrecht), **Patricia Dankers** (TU Eindhoven), **Jan Weijers** en **Eelco Soeteman** (Netherlands Heart Institute), **Tineke Schaaij** (Hartstichting), **Jouke Smink** en

De **staf van de cardiologie** mag niet ontbreken in dit dankwoord. In het bijzonder, **Pierfranscesco Agostoni** en **Adriaan Kraaijeveld**, bedankt voor jullie inzet en handigheid met katheters om experimentele injecties met of zonder stamcellen te doen bij mensen, varkens en fantomen.

Faiz Ramjankan, bedankt voor jouw LVAD expertise en bereidheid om altijd mee te denken.

Het **stafsecretariaat** en de **R&D** van de cardiologie, bedankt voor jullie hulp en organisatie. In het bijzonder wil ik **Ingrid Meijer** bedanken. Jij hebt het leven van alle Champie-promovendi ten goede doen veranderen. Daarbij ben je een fijn, gezellig en behulpzaam mens.

Mijn vaste stek als onderzoeker begon in de **Appendix** van de **Villa**, een bijzondere plek waar je net niet helemaal bij de Villa hoort maar wel heel dichtbij de koffie zit. Gelukkig mocht ik vlot de echte Villa betreden en heb ik de laatste maanden zelfs mogen genieten van een plek aan het raam. Ik heb hier een hele mooie tijd gehad dankzij mijn mede-Villanen. Te beginnen bij de **Villadies**: **Sanne**, mijn voorbeeld voor een PhD studente die haar zaakjes goed op orde heeft. Maar nog belangrijker, een superleuke collega met wie ik veel gemeen bleek te hebben en waarmee een blik vaak voldoende was. **Iris**, ik ben blij dat jij de villa deed opvrolijken met je opvallende printjes. Wat hebben wij samen veel gelachen en lekker gegeten. Bedankt voor de gezelligheid. **Mira**, jij volgt iets verderop. De andere (oud-)Villanen: **Peter-Paul,** PP, peppie, dank voor je hulp in het lab, met name met de in aluminium-ingepakte spuiten met levensgevaarlijke inhoud. Altijd met een lach, optimisme en veel gezelligheid. We zien elkaar weer in Utrecht. **Ronnie**, Vanessa, Rita (recht door zee), **Gho** (pleinhoppen in Madrid), **Remco** (onze strijd met muziek, nu collega's in het OLVG), **Thomas** (dank voor mijn scratchy bijnaam), **Thijs** (droogste woordgrappen ooit), en samen met "strain echo" **Bas** (Jiskefet), **Dirk** (bulderlach), **Einar** (ik zal "arcometeencee" nooit vergeten), **Steven** (MIGRATE opvolger). Tot slot, niet-Villanen maar wel Champie-PhDers, **Wouter G** (mede-fantoombouwer) en **Rosemarijn** (wat gezellig dat we elkaar zowel in als buiten het ziekenhuis toch steeds weer tegenkomen!).

Alle andere onderzoekers uit het Nest, het Q en bij de Medische Fysiologie wil ik ook bedanken voor de gezelligheid.

De **Prof. Sluijter-groep**, bedankt voor het wegwijs maken in het lab en jullie betrokkenheid bij mijn onderzoek tijdens jullie meetings.

Ook wil ik via deze weg studenten **Lisanne**, **Eline** en **Lonneke** bedanken voor hun enthousiasme en hulp.

Buiten het UMC Utrecht en het MIGRATE consortium zijn er een aantal mensen die niet mogen ontbreken in dit dankwoord. Mijn **collegae** in het **OLVG**, wat een gezelligheid en goede sfeer is er binnen de assistentengroep van de interne geneeskunde. Bedankt hiervoor, ook aan opleiders **Marcel Weijmer** en **Yves Smet** voor mijn succesvolle eerste wintersportervaring.

Uiteraard wil ook dank betuigen aan alle vrienden, vriendinnen en familie die me altijd hebben bijgestaan en voor de soms nodige afleiding hebben gezorgd. Ik zal jullie, om het niet te uitgebreid te maken, niet één voor één noemen. **Team awesome**, dank voor de vele kilometers die we samen door weer en wind hebben gerend, waarmee het hoofd even leeg kon worden gemaakt. Op naar de hele marathon!

Dan zijn nu mijn paranimfen aan de beurt.
Mira mira, Miertje biertje, buuf, mijn mede-Amsterdammer in de Villa (al vind jij dat sinds mijn verhuizing niet meer het geval). Jouw komst in de Villa was een aanwinst, ook voor de Champie-groep. Je bent een echte aanpakker, collegiaal, perfectionistisch, de nieuwe Trial police en voorvechter van goed dierexperimenteel onderzoek. Maar je bent vooral ook een heel gezellig en hartelijk mens met wie ik kan genieten van lekker eten (en/of een flesje Rioja). Succes met de afronding van je promotie en het vervolg in Enschede!

Aafke, Baaf, Achmed, na de geneeskunde studie zijn we dezelfde weg ingeslagen, via ANIOS in de periferie en de academie naar een promotietraject. Zodoende hebben we vele uren, zuchtend en steunend, beide achter de laptop geprobeerd in de vrije uren ons promotietraject af te ronden. Intussen kennen we alle goede werkplekken in Amsterdam (OBA, volkshotel, Belcampo, Drovers Dog, hotel Zoku, Caffénation, Kanarieclub) waar we met een hapje en een drankje het harde werken konden afsluiten. Zonder jouw aanwezigheid was dit traject een stuk zwaarder geweest, dus heel veel dank daarvoor. Voor

jou nu ook de laatste loodjes, dus nog even volhouden! Ik ben vereerd jou straks bij te mogen staan op de grote dag.

O & M & O: **Odessa**, grote zus, een beter voorbeeld kan ik me niet indenken. Dank voor je interesse in waar ik mee bezig ben en dat ik altijd bij je terecht kan. **Maikel**, je bent een aanvulling in ons gezin. Dankzij jou (en Odessa) zijn we nog een familielid rijker: **Olivia**, liefste Liv, wat ben je een fantastisch en prachtig wezen. Ondanks je jonge leeftijd heeft jouw komst al veel impact teweeg gebracht. Ik kan niet wachten jouw eerste en alle volgende stappen mee te maken.

Lieve **Nadia** & **Henk**: Dank voor jullie onvoorwaardelijke steun. Nad, jij hebt me geleerd altijd mijn dromen na te jagen en nooit op te geven, vooral als het tegen zit. Bedankt voor je wijze en opbeurende woorden als dat even nodig was.

Anthony, de meest significante uitkomst van dit promotietraject. Wie had gedacht dat onze ontmoeting bij de running junkies zoveel zou opleveren. Mijn promotietraject gaf ons de ruimte om onze gezamenlijke passies (reizen, eten en hardlopen) in hoge intensiteit te kunnen ervaren. Ook nu het hectische leven in de kliniek begonnen is, blijf je met veel begrip, geduld, humor en liefde mijn allerbeste maatje. Ik kijk uit naar onze toekomst samen.

Curriculum Vitae

Cheyenne Tseng werd op 2 maart 1987 geboren te Amsterdam. In haar vroege jeugd raakt zij al geïntrigeerd door de geneeskunde. Na het behalen van haar diploma aan het Vossius Gymnasium te Amsterdam begon zij aan de geneeskunde opleiding aan de Vrije Universiteit van Amsterdam. Tijdens het laatste co-assistentschap cardiologie in het Spaarne ziekenhuis te Hoofddorp ontstaat een grote interesse voor de cardiologie. Om die reden begon zij aan haar eerste baan als arts-assistent cardiologie in hetzelfde ziekenhuis. Na dit jaar was de keuze voor de cardiologie een feit. Om meer academische ervaring op te doen startte zij hierna als arts-assistent in het UMC Utrecht, waar zij na een jaar een PhD-traject onder leiding van Steven Chamuleau en Pieter Doevendans mocht beginnen.

Sinds april 2017 is Cheyenne in het UMC Utrecht begonnen aan de opleiding tot cardioloog onder supervisie van Hans Kirkels en Steven Chamuleau. Momenteel volgt zij de vooropleiding Interne Geneeskunde in het OLVG West onder leiding van Marcel Weijmer.